

Copyright  
by  
Soumik Das  
2020

**The Dissertation Committee for Soumik Das Certifies that this is the approved  
version of the following Dissertation:**

**Evaluation and Design of Surfactant Formulations for Wettability  
Alteration**

**Committee:**

---

Roger T. Bonnecaze, Supervisor

---

Quoc P. Nguyen, Co-Supervisor

---

Gary T. Rochelle

---

Nathaniel Lynd

---

Claribel Acevedo

**Evaluation and Design of Surfactant Formulations for Wettability  
Alteration**

**by**

**Soumik Das**

**Dissertation**

Presented to the Faculty of the Graduate School of

The University of Texas at Austin

in Partial Fulfillment

of the Requirements

for the Degree of

**Doctor of Philosophy**

**The University of Texas at Austin**

**May 2020**

## **Dedication**

To my parents, Narayani and Saroj Kumar Das, and brother, Souvik Das



## **Acknowledgements**

I would like to start by thanking my advisor Dr. Roger Bonnecaze for being the best mentor and teacher that one could hope for. His enthusiasm, constant optimism and celebration of small achievements kept me motivated whenever I was stranded in my research. Despite his busy schedule, he was always available to guide and help me. I have thoroughly enjoyed our “short” meetings and discussions on a wide range of research and non-research related topics. His nuggets of wisdom have contributed immensely to my overall development as a person and as a professional.

I would also like to thank Dr. Quoc Nguyen for being a terrific co-advisor and mentor. I would always be indebted to him for introducing and guiding me to this research topic. His supervision and guidance were very helpful in designing and setting up experiments. I would also like to thank him for letting me use his laboratory to carry out many of my experiments. I have learnt a lot on how to approach a particular problem and analyze results from both Dr. Bonnecaze and Dr. Nguyen. Overall, it has been an honor and a pleasure to work with them.

I would like to thank Dow Chemical for their funding and providing me with the opportunity to work for this project. Special thanks to Dr. Amit Katiyar, Dr. Pramod Patil, Dr. Neeraj Rohilla, Dr. Wanglin Yu, Dr. Claribel Acevedo, Dr. Joydeep Mukherjee, Dr. Norm Byrne and Dr. Biplab Mukherjee for their valuable input in the research, organizing

the monthly meetings and site visits, and helping me transition to an industry sponsored project. The dissertation wouldn't be in its current shape without their contribution.

I have thoroughly enjoyed my time as a member of the Bonnacaze group. I would like to thank Dr. Ben Huntington, Dr. Mohammadreza Shafiei, Dr. Shruti Jain, Tianfei Liu and Dr. Fardin Khabaz for being the absolute best colleagues, lunch and dinner partners, and buddies in numerous scientific and philosophical discussions. Special thanks also to Fardin for his guidance and help with the molecular dynamics simulations. I have also greatly enjoyed the company of Xilan Zhu, Yang Ban, Steven Stanley, Dr. Ali Shahmohammadi, Dr. Meghali Chopra, Dr. Akhilesh Jain, Dr. Talha Arshad, Dr. Mark Ferraro and Dr. Michael Clements and would like to thank them for their companionship. I would also like to thank past and present members of Nguyen group – Litan Li, Tyler Seay, Sean Brame, Motaz Taha, Dr. Oualid Mbarki, Taylor Morris and Lei Liu for their help with the experiments. I would specially like to thank Litan and Sean for being wonderful companions during our travels. Special thanks to Dr. Juan Camilo Gonzalez-Rivera for being a great friend and partner in meals, sports, games and numerous discussions.

I would like to thank my friends in Austin who have made my time in UT even more enjoyable – Akshay Kamath, Allen Fernandes, Arijit Paladhi, Pratik Kakkar, Edwin Thomas, Dr. Ankur Kumar, Dr. Chola Bhargava Dandamudi, Harish Potti, Srijith Balakrishnan, Mukul Bhattacharya and Gopindra Nair. I would also like to thank my friends who have helped me constantly in many ways even though they were not in Austin – Subhabrata Das, Sunit Kumar Swain, Dr. Sabyasachi Chatterjee, Sidhant Kumar Singh,

Harsha Putta, Srivigna Ganapathineedi, Nalini Srivastava, Ravi Agrawal, Raunak Ramakrishnan and Kumar Karthik Immaneni. I would also like to thank Netflix, Hulu, HBO and Amazon Prime for providing me with the timely relaxation and escape from work whenever things got stressful.

Finally, I would like to thank my parents and my elder brother for their love, support, encouragement and everything they have done and sacrificed for me.

## **Abstract**

# **Evaluation and Design of Surfactant Formulations for Wettability Alteration**

Soumik Das, Ph.D.

The University of Texas at Austin, 2020

Supervisors: Roger T. Bonnecaze, Quoc P. Nguyen

Only about 35% of oil is recovered from carbonate reservoirs through primary and secondary flooding because of oil wet surfaces and unfavorable capillary pressures. Surfactants, with their dual hydrophobic and hydrophilic nature have been known to improve oil recovery significantly by lowering oil-water interfacial tension and by altering wettability of surfaces. However, the process of selecting an efficient surfactant for wettability alteration is dependent on several factors, including mineral type, porosity, temperature, salinity, nature of adsorbed oil, molecular structure and surfactant adsorption. Core-flood experiments usually used for evaluating surfactants tend to be time-consuming and provide very little information on the actual mechanism of surfactant action. A fast evaluation scheme is hence required to measure surfactant performances corresponding to the above mentioned parameters.

The current work focusses on macro and molecular scale analysis of surfactants to understand relevant structure-property relationships and mechanism of wettability alteration. Surfactants are first evaluated and screened through a series of phase behavior, contact angle and oil-film experiments. The experimental observations have been used to

correlate parameters like molecular structure, temperature and brine salinity to macroscopic properties like wettability alteration, adsorption and capillary driving force. Oil-film experiments have been used to understand the surfactant-aided wettability alteration.

The role of surfactant adsorption in wettability alteration is investigated by static adsorption experiments. Adsorption isotherms are measured for different surfactant hydrophilicities at different temperatures and surfactant cloud point is used to develop a thermodynamic model explaining the universal surfactant behavior. Along with experiments, molecular dynamics simulations are also performed to understand the mechanism of aggregative adsorption of the nonionic surfactants.

To address the issue of high temperature, high salinity applications, mixed surfactant formulations of nonionic surfactants and anionic hydrotropes are developed. Detailed investigations are performed to understand the role of hydrotrope structure, concentration and temperature on the mechanism of aqueous stabilization and adsorption and their effect on wettability alteration.

Overall, the current work first establishes a macro and molecular-scale understanding of the phenomenon of surfactant-assisted wettability alteration and associated structure-property relationships. While shorter surfactant hydrophilic units and high temperatures are found to exhibit better wettability alteration, in fact it is proximity to surfactant cloud point which is the determining thermodynamic descriptor. Improved wettability alteration is correlated with surfactant adsorption which occurs in an aggregative manner. It also means there is a tradeoff between surfactant adsorption and wettability alteration. Using this knowledge, surfactant formulations are developed to observe and predict enhanced oil recoveries from representative porous media.

## Table of Contents

List of Tables .....	xiii
List of Figures .....	xv
Chapter 1: Introduction.....	1
1.1. Oil Recovery in Carbonate Reservoirs .....	1
1.2. Surfactant-Induced Wettability Alteration.....	1
1.3. Background .....	4
1.4. Dissertation Outline .....	19
References.....	21
Chapter 2: Wettability Alteration of Calcite by Nonionic Surfactants .....	28
2.1 Introduction .....	28
2.2. Overview of Approach.....	30
2.3. Materials.....	31
2.4. Methodology .....	32
2.5. Results and Discussions .....	35
2.6. Conclusions .....	61
References.....	62
Chapter 3. Universal Scaling of Adsorption of Nonionic Surfactants on Carbonates using Cloud Point Temperatures .....	66
3.1 Introduction .....	66
3.2. Materials.....	70
3.3. Methodology .....	71
3.4. Results and Discussion.....	77
3.5. Conclusions .....	93

<b>REFERENCES</b> .....	95
Chapter 4: Wettability alteration and Adsorption of Mixed Nonionic and Anionic Surfactants on Carbonates.....	102
4.1. Introduction .....	102
4.2. Materials.....	106
4.3. Methodology .....	107
4.4. Results.....	114
4.5. Discussions .....	126
4.6. Conclusions .....	138
<b>REFERENCES</b> .....	141
Chapter 5: Molecular Dynamics Simulations of Aqueous Nonionic Surfactants on a Carbonate Surface .....	147
5.1. Introduction .....	147
5.2. Methodology .....	150
5.3. Results.....	156
5.4. Discussion .....	165
5.4. Conclusions .....	169
References.....	171
Chapter 6: Wettability Alteration and Spontaneous Imbibition by Single and Mixed Surfactants in Carbonates .....	177
6.1. Introduction .....	177
6.2. Materials.....	181
6.3. Methodology .....	182
6.4. Results and Discussions .....	185
6.5. Conclusions .....	201

References .....	203
Chapter 7: Concluding Remarks .....	207
7.1. Conclusions .....	207
7.2. Suggested Future work.....	211
References .....	216
Appendices.....	219
Appendix A: Phase Behavior .....	219
Appendix B: Estimation of incremental oil recovery and surfactant requirements in a reservoir .....	222
Bibliography .....	223
Vita .....	242



## List of Tables

Table 1.1. Common Chemical EOR Techniques .....	2
Table 1.2. Examples of different surfactant types along with their structures <sup>46</sup> .....	8
Table 2.1. List of nonionic surfactants evaluated in the study. CMC values are reported at 25°C. ....	32
Table 2.2. Phase behavior results -            - No microemulsion phase,            - Separate microemulsion,            - Slight three-phase separation            - Wax like deposition. The columns indicate brine salinity (% NaCl by weight). ....	38
Table 2.3: Cloud points of nonionic surfactants measured in 12% NaCl, 0.2% CaCl <sub>2</sub> brine.....	40
Table 2.4. Activation energies extracted from timescale values for the evaluated surfactants.....	54
Table 3.1: List of nonionic surfactants evaluated in the study. CMC values are reported at 25°C for 12% NaCl, 0.2% CaCl <sub>2</sub> brine.....	70
Table 3.2: Weight-average micelle sizes reported for 1000 ppm and 4000 ppm NP-x and SAE-x at 25°C and 50°C.....	80
Table 3.3. Volumes of surfactant molecules used to calculate $N_{agg}$ . The volume includes additional volume because of water molecules in the micelle. <sup>55-</sup> <sup>56</sup> .....	80
Table 3.4: Maximum adsorptions and estimated surface coverages for SAE-x and NP-x.....	83
Table 4.1: List of nonionic surfactants evaluated in the study. ....	107
Table 4.2: List of anionic co-surfactants evaluated in the study.....	107

Table 5.1. Nonionic surfactant evaluated in the study. Experimental CMC values are reported at 25°C. <sup>18</sup> .....	151
Table 5.2: Force-field parameters for Buckingham Potential - $E = Ae^{-r/\rho} - \frac{C}{r^6}$ .....	154
Table 5.3: Force-field parameters for Leonard-Jones Potential - $E = 4\varepsilon \left[ \left( \frac{\sigma}{r} \right)^{12} - \left( \frac{\sigma}{r} \right)^6 \right]$ .....	154
Table 5.4. Micelle aggregation numbers, radius of gyration squared, number of hydrogen-bonded water molecules per surfactant and adsorption well features for SAE-15 and SAE-40.....	158
Table 5.5. Estimation of the partition coefficient and comparison with experimentally measured adsorptions for SAE-15 and SAE from ref. 19. ....	167
Table 6.1: List of nonionic surfactants evaluated in the study. ....	181
Table 6.2: List of anionic cosurfactants evaluated in the study.....	181
Table 6.3. Core properties, experimental conditions, and results for spontaneous imbibition experiments.....	194
Table A1. Structure and specification of additional nonionic surfactants.....	219
Table A2. Phase behavior results -        - No microemulsion phase,        - Separate microemulsion,        - Slight three-phase separation        - Wax like deposition .....	220

## List of Figures

Figure 1.1 Oil-water distribution in reservoirs of different wettabilities (Fundamentals of wettability – Schlumberger, 2007) <sup>1</sup> .....	5
Figure 1.2. Schematic representations of surfactant molecules. ....	7
Figure 1.3. Depiction of oil drop contact angle in a) water-wet b) neutral-wet and c) oil-wet surface <sup>1</sup> .....	9
Figure 1.4. Initial and final oil drop states at 25°C and brine salinity of 12% NaCl, 0.2% CaCl <sub>2</sub> for a) no surfactant b) SAE-12 c) SAE -15 d) SAE-20 e) SAE-40 f) NP-15.SAE and NP stand for Secondary alcohol ethoxylate and nonyl-phenol ethoxylate respectively. The numbers denote the number of hydrophilic ethoxylate groups. The oil drops bead up in the presence of surfactants implying a change in wetting behavior from an initial oil-wet to an eventual water-wet or intermediate-wet surface.....	10
Figure 1.5. a) Schematic representation of the growth of ionic surfactant aggregates for various regions of the adsorption isotherm. In region I, the surfactant adsorbs mainly by electrostatic interactions between the surfactant headgroup and the charged sites on the mineral surface. In region II, an increase in adsorption occurs because of hydrophobic interactions between new surfactants with adsorbed ones. Region III marks the saturation of active sites with hydrophobic interactions dominating adsorption mechanism. An adsorption plateau is observed in region IV. <sup>54</sup> b) Adsorption of dodecyl sulfate on alumina displaying the different regions and the aggregation numbers. <sup>55</sup> .....	12

Figure 1.6. a) Typical adsorption isotherms of nonionic surfactants of different hydrophilicities on water-silica surface. Schematic of adsorption of nonionic surfactants is also shown with the orientation of molecules at the surface. At low surface coverages adsorption is driven mainly by Van der Waals interaction between surfactant and the surface. Within a very small bulk concentration, an increase in the adsorption is observed because of pre-aggregate formations driven by surfactant-surfactant hydrophobic interactions. These aggregates increase in size and form micellar structures as the adsorption and surface coverage increases. Adsorption decreases with an increase in hydrophilicity of surfactant headgroups from 4 EO units to 8 EO units.<sup>56</sup> b) Schematic of surface aggregates as a function of surfactant hydrophilicity.<sup>56</sup> Aggregates are smaller and farther apart for more hydrophilic surfactants. .... 14

Figure 1.7. Effect of addition of co-surfactants on the cloud point of nonionic surfactants. The nonionic surfactant selected is secondary alcohol ethoxylate (SAE) with 15 EO units. The co-surfactant is an anionic molecule of different sizes – LM (low molecular weight), MM2 (medium molecular weight), MM (medium molecular weight with higher charge density), HM (high molecular weight), VM (very high molecular weight). The concentration of SAE-15 is kept constant at 4000 ppm whereas two different concentrations – 2000 ppm and 4000 ppm of co-surfactant is used. The system salinity is 12% NaCl and 0.2% CaCl<sub>2</sub> ..... 16

Figure 1.8. Typical oil recoveries through spontaneous imbibition in the presence of surfactants. In this case, spontaneous imbibition is gravity-driven and hence oil is generated mostly from the top surface of the core. ....	18
Figure 1.9. Oil recovery plots from spontaneous imbibition experiments on chalk cores using the cationic surfactant – cetrimonium bromide(CTAB) at two different temperatures. <sup>7</sup> .....	18
Figure 2.1. a) Cut and polished calcite plate. b) Calcite aged in crude oil. c) Schematic of contact angle experiment. d) Schematic representation of oil-film over a calcite surface. ....	34
Figure 2.2. Phase behavior results at 50°C for a) SAE-12 b) SAE-15 c) SAE-20 and d) NP-40 .....	37
Figure 2.3. Phase behavior results at 80°C for a) SAE-12 b) SAE-15 c) SAE-20 and d) NP-40. ....	37
Figure 2.4. Initial and final oil drop states at 25°C and brine salinity of 12% NaCl, 0.2% CaCl <sub>2</sub> for a) no surfactant b) SAE-12 c) SAE -15 d) SAE-20 e) SAE-40 f) NP-15 g) NP-40 and h) NP-50.....	39
Figure 2.5. Final contact angles for a) NP-x and b) SAE-x at different temperatures. The light blue bar is for NP-12 at 45°C.....	42
Figure 2.6. Final contact angle vs hydrophile chain length for SAE and NP surfactants at a) 25°C b) 40°C and c) 50°C. The half-filled circle denotes an experiment done at 45°C. ....	44
Figure 2.7. Final contact angles vs brine salinity at a) 25°C. b) Final contact angles for SAE-12 and SAE-15 at 25°C, 40°C and 50°C as a function of brine salinity .....	45

Figure 2.8. Effect of $SO_4^{2-}$ addition to 12% NaCl brine at 40°C for a) No surfactant b) SAE-20 c) SAE-40 and d) NP-40.....	46
Figure 2.9. Final contact angle vs $SO_4^{2-}$ concentration at 12% NaCl brine at 40°C.....	46
Figure 2.10. Evolution of contact angle with time for a) SAE-15 b) SAE-20 and c) SAE-40. Contact angle evolution is shown for three different temperatures.....	48
Figure 2.11. Evolution of contact angle with time for a) NP-15 b) NP-40 and c) NP-50. Contact angle evolution is shown for three different temperatures. ....	49
Figure 2.12. Effect of surfactant size on contact angle evolution – Contact angle vs time for a) SAE-x at 50°C and b) NP-x at 40°C. ....	50
Figure 2.13. Extracted timescales from contact angle measurements for a) SAE-x and b) NP-x at 25°C, 40°C and 50°C.....	52
Figure 2.14. Arrhenius plots of timescale vs 1/T for a) SAE-x and b) NP-x surfactants..	53
Figure 2.15. Images from oil-film experiments at 12% NaCl salinity at 50°C. Colored images show the top view and black-white images show the side view for a) No surfactant at t = 0 b) No surfactant at t = 120 mins c) SAE-15 at t = 0 d) SAE-15 at t = 25 mins e) SAE-15 at t = 60 mins f) NP-40 at t = 0 g) NP-40 at t = 10 mins and h) NP-40 at 60 mins .....	56
Figure 2.16. Images from oil-patch experiment with 12% NaCl salinity at 50°C. Colored images show the top view and black-white images show the side view for a) No surfactant at t = 0 b) No surfactant at t = 15 hrs. c) NP-40 at t = 0 d) NP-40 at t = 10 mins e) NP-40 at 50 mins. f) Initial g) Intermediate and h) Final states of an oil-film experiments done with a “defective” aged surface. Note the artificial striations in f) .....	57

Figure 2.17. Schematic of the proposed mechanism of wettability alteration. Blue spirals represent the hydrophilic moiety of the surfactants. a) Initial oil-wet surface with micro-defects. b) Hydrophilic zone formed by surfactant coating c) Oil “sweeping” as shown in green arrows - by surfactant and water. ....	60
Figure 3.1. Measurement of CMC using surface tension values measured in air .....	71
Figure 3.2: a) Chromatogram obtained from HPLC-ELSD analysis of SAE-x. b) Typical calibration plots for SAE-x surfactants. ....	75
Figure 3.3: a) Typical absorption spectra for NP-x surfactant. b) First derivative absorption spectra for NP-x and the corresponding c) calibration curve. ....	76
Figure 3.4. Micelle size distributions for SAE-x .....	78
Figure 3.5. Micelle size distributions for NP-x.....	79
Figure 3.6: Adsorption isotherms of a) NP-15 b) NP-30 c) NP-40 d) SAE-15 e) SAE-30 and f) SAE-40 .....	82
Figure 3.7: Micelle aggregation number as a function of concentration for NP-15 at 50°C. Inset shows the dependence of adsorption on the micelle aggregation number.....	85
Figure 3.8. Micelle growth potential vs T .....	87
Figure 3.9: a) Maximum molar adsorption of surfactants as a function of CPTD. b) Universal behavior of adsorption of nonionic surfactants. The maximum adsorption of surfactants is plotted in mg/m <sup>2</sup> against the cloud point-temperature difference (CPTD) .....	89
Figure 3.10. Variation of $\frac{N_{wc}}{D_{mc}^2}$ vs surfactant molecular weight. The dotted line represents the function $\frac{N_{agg,c}}{D_{m,c}^2} \sim \frac{1}{M_w}$ .....	90

Figure 3.11: Final contact angle on oil-wet calcite is plotted against maximum adsorption. Contact angles are measured in the aqueous phase. Contact angles greater than 90° represent an oil-wet state. Final contact angles almost linearly decrease with an increase in adsorption signifying a positive correlation between wettability alteration and adsorption. .... 92

Figure 4.1. Onset of clouding upon heating solutions of nonionic surfactants ..... 108

Figure 4.2. Typical drop images used for IFT measurements. a) Shape of an inverted oil drop inside surfactant solution. b) Drop of surfactant solution in air ... 108

Figure 4.3. IFT vs total surfactant concentration in 2/1 by mass mixture of SAE-15/LM at 70°C. The vertical dotted line represents the CMC of the solution. .... 109

Figure 4.4. Measured CMCs of SAE-15, LM, HM and SAE-15+LM, SAE-15+HM mixtures at different compositions. The CMCs correspond to two different temperatures – 50°C and 70°C..... 110

Figure 4.5. Micelle-size of surfactant systems - SAE-15, SAE-15+LM and SAE-15+HM obtained from DLS measurements. .... 111

Figure 4.6a) Side-view of an oil patch on calcite. The drop spreads on the calcite indicating that the patch is aged..... 112

Figure 4.6b) Side-view of an oil patch after treatment with surfactant solution. The patch beads up indicating wettability alteration by the surfactant. .... 112

Figure 4.7. Typical absorbance plots from UV-Vis measurements of co-surfactant solutions..... 113

Figure 4.8. Cloud point values for a) SAE-9 and b) SAE-15 with co-surfactants at two different concentrations. .... 114

Figure 4.9. Oil/Surfactant IFT values for a) SAE-9 and b) SAE-15 + Co-surfactants ... 115



Figure 4.10. Final contact angles for a) brine and b) 4000 ppm LM c) SAE-9 + LM (4000 ppm:4000 ppm) and d) SAE-15 + LM (4000 ppm: 4000 ppm) at 70°C.....	117
Figure 4.11. Bar plots showing final contact angles in mixed surfactant systems containing a) SAE-9 and b) SAE-15.....	117
Figure 4.12. Adsorption isotherms of SAE-15+LM mixtures at 70°C. a) Adsorption of SAE-15 versus the bulk SAE-15 concentration. b) Adsorption of LM versus the bulk LM concentration. The dotted lines represent the maximum adsorption of SAE-15 in single surfactant system at 50°C.....	121
Figure 4.13. Adsorption isotherms of SAE-15+LM at 90°C. a) Adsorption of SAE-15 versus the bulk SAE-15 concentration. b) Adsorption of LM versus the bulk LM concentration. The dotted lines represent the maximum adsorption of SAE-15 in single surfactant system at 50°C. ....	122
Figure 4.14. Adsorption isotherms of SAE-15+HM at 70°C. a) Adsorption of SAE-15 versus the bulk SAE-15 concentration. b) Adsorption of HM versus the bulk HM concentration. The dotted lines represent the maximum adsorption of SAE-15 in single surfactant system at 50°C. ....	124
Figure 4.15. Adsorption isotherms of SAE-15+HM mixtures at 90°C. a) Adsorption of SAE-15 versus the bulk SAE-15 concentration. b) Adsorption of HM versus the bulk HM concentration. The dotted lines represent the maximum adsorption of SAE-15 in single surfactant system at 50°C.....	125
Figure 4.16. Oil/Surfactant IFT for a) SAE-9 and b) SAE-15 + Co-surfactants plotted against CPTD.....	127
Figure 4.17. Final contact angle as a function of Cloud Point Temperature Difference for single and mixed-surfactant systems. ....	129

Figure 4.18. Capillary driving force for different mixed surfactant systems as a function of the system temperature for a) SAE-9 and b) SAE-15. The dotted lines represent the zero capillary force corresponding to a switch between oil-wet and water-wet state. .... 130

Figure 4.19. Driving force as a function of Cloud Point Temperature Difference for single and mixed-surfactant systems. Lines are meant to be guides to the eye. .... 131

Figure 4.20. Molar fraction of SAE-15 in the adsorbed aggregates versus total molar adsorption for SAE-15+LM mixtures at a) 70°C, b) 90°C and for SAE-15+HM mixtures at c) 70°C and d) 90°C. The solid lines in a) and c) correspond to bulk molar fraction of SAE-15 in a 2/1 mixture of SAE-15/co-surfactant by mass. The dotted lines in the plots correspond to molar fraction of SAE-15 in a 1/1 mixture of SAE-15/co-surfactant by mass. .... 134

Figure 4.21. Schematic explaining the two different modes of aqueous stabilization for SAE-15+LM and SAE-15+HM systems. LM molecules remain mostly near the periphery of the SAE-15 micelles and stabilize through a solubilization mechanism. HM molecules form mixed micelles and these charged micelles are responsible for aqueous stabilization. In both cases, the mixed aggregates adsorb on the carbonate surface. .... 136

Figure 4.22. Maximum adsorption of SAE-x plotted against the system CPTD. Filled circles correspond to single surfactant systems of SAE-15, SAE-30 and SAE-40. The non-circular symbols are for the mixed systems of SAE-15+LM (red filled and empty squares) and SAE-15+HM (green filled and empty diamonds). The lines are guides for the eyes only. The lines show the offset in adsorption for mixed surfactant systems..... 137

Figure 4.23. a) Final contact angle and b) Capillary driving force versus maximum adsorption of SAE-x in single and mixed systems. Filled circles correspond to single surfactant systems of SAE-15, SAE-30 and SAE-40. The non-circular symbols are for the mixed systems of SAE-15+LM (red filled and empty squares) and SAE-15+HM (green filled and empty diamonds). Lines are guides for the eyes only. .... 139

Figure 5.1. a) Randomly distributed 100 SAE-15 and 120,000 water molecules used for surfactant-water simulations. Water molecules are shown in cyan-colored points. b) Randomly distributed 100 SAE-15 molecules to study adsorption on calcite (shown in red). The blue and green spheres represent the surfactant hydrophile and hydrophobe, respectively..... 152

Figure 5.2. a) SAE-15 micelle formation after 100 ns of simulations at 50°C with 100 surfactant molecules. b) Asphericity of SAE-x micelles. Smaller the asphericity, closer the micelle is to a spherical structure. .... 157

Figure 5.3. Final simulation state for a) Single molecule of SAE-15 + water + calcite and b) 100 molecules of SAE-15+water+calcite at 50°C. Both images correspond to the minimum energy positions discussed in Sec 5.3.2..... 159

Figure 5.4. a) MD trajectory of single SAE-15 molecule. b) MD trajectories for 100 molecule micelle of SAE-15 for two different initial positions. .... 160

Figure 5.5. Adsorption free energy profiles at infinite dilution for a) SAE-15 and b) SAE-40 at 50°C.....	162
Figure 5.6. Adsorption free energy profiles for a) SAE-15 and b) SAE-40 micelles at 50°C.....	163
Figure 5.7. Adsorption free energy profiles for a) SAE-15 and b) SAE-40 micelles at 25°C.....	164
Figure 5.8. Density profiles of water and surfactant micelle as a function of separation from the calcite surface. ....	168
Figure 6.1. Cloud point values for a) SAE-9 and b) SAE-15 with co-surfactants.....	186
Figure 6.2. Oil/Surfactant IFT values for a) SAE-9 and b) SAE-15 + Co-surfactants ...	187
Figure 6.3. Final contact angles for a) Brine and b) 4000 ppm LM c) SAE-9 + LM (4000 ppm:4000 ppm) and d) SAE-15 +LM (4000 ppm: 4000 ppm) at 70°C.....	188
Figure 6.4. Bar plots showing final contact angles in mixed surfactant systems containing a) SAE-9 and b) SAE-15. Initial contact angles are typically between 160°-170°.....	189
Figure 6.5. Capillary driving force for a) SAE-9 and b) SAE-15 containing systems....	190
Figure 6.6. Adsorption of SAE-15 at different temperatures for a) single surfactant and mixed-systems with b) 1/1 mixture (by mass) with LM and c) 1/1 mixture (by mass) with HM. d) Maximum adsorption of SAE-15 as a function of system CPTD .....	191
Figure 6.7. a) Initial and b) final contact angles of brine on outer surface of oil-aged Indiana limestone. c) Initial and d) final contact angles corresponding to 4000 ppm SAE-15.....	193

Figure 6.8. a) Oil recovery plots for brine solutions. b) Typical oil recoveries in the presence of surfactants. Oil is generated mostly from the top surface of the core. ....	195
Figure 6.9. Oil recovery plots for a) single SAE-15 at 50°C and b) mixed systems containing SAE-15 and co-surfactants at 90°C .....	195
Figure 6.10. Oil recovery plots for system containing SAE-9 and co-surfactants at 50°C and 90°C. ....	197
Figure 6.11. Oil recovery plots for systems containing 1% $\text{SO}_4^{2-}$ . ....	197
Figure 6.12. Plot of fractional oil recovery vs dimensionless time for different spontaneous imbibition experiments.....	199
Figure 6.13. Ultimate oil recoveries as a function of initial water saturations .....	200
Figure 6.14. a) Maximum oil recoveries plotted against system CPTD for different single and mixed-surfactant systems. b) Ultimate oil recoveries rescaled by capillary driving force plotted against CPTD. The dotted line is a guide for the eye only.....	201
Figure A1. Phase behaviors of a) BG-10 and b) RW-150 at 50°C .....	220
Figure A2. Initial and final contact angles at 25°C for a) BG-10 and b) RW-150 .....	221

## **Chapter 1: Introduction**

### **1.1. OIL RECOVERY IN CARBONATE RESERVOIRS**

More than half of world's oil reserves are present in naturally fractured carbonate formations.<sup>1</sup> Wettability of a rock-brine-oil system determines both the distribution and permeability of each fluid inside the reservoir.<sup>2</sup> The wetting fluid generally occupies the small pores while the non-wetting fluid tends to reside in the larger ones forming connected pathways. Carbonate reservoirs tend to be oil-wet because of the adsorption of acidic and surface-active components present in crude oil onto the typically positively charged rock surface.<sup>3,4</sup> The unfavorable capillary forces originating from the oil-wetting nature inside these reservoirs prevent spontaneous water imbibition. Using primary and secondary oil recovery techniques, which relies on increasing reservoir pressure, most of the recoverable oil is displaced before water breakthrough and only about 30-40% of total oil in place is obtained. The residual oil remains trapped as a discontinuous phase separated by the brine. Fractures present in such reservoirs compound the problem as injected water often takes a fractured route from the injection well to the production well without significant oil displacements. The low oil recovery rates, hence, prompted the development of tertiary techniques which aim at extracting the trapped residual oil.

### **1.2. SURFACTANT-INDUCED WETTABILITY ALTERATION**

Chemical Enhanced Oil Recovery (EOR) falls under the category of tertiary oil recovery techniques. This involves injection of various chemicals into the reservoir to aid the process of oil extraction. These chemicals include polymers, surface-active chemicals, gas, alkali or different combinations of the above. Table 1.1 outlines a brief summary of pros and cons associated with these chemicals.

Table 1.1. Common Chemical EOR Techniques

Method	Advantage	Disadvantage
Polymer	Better mobility control, fracture blocking	Lower incremental oil recovery
Surfactant flooding	IFT reduction and wettability alteration	High surfactant requirement, Adsorption loss
Alkali flooding	IFT reduction	Poor mobility control
Supercritical CO <sub>2</sub> flooding	Improved mobility control	Limited reservoir applicability

Introduction of surfactants in a reservoir system can improve oil recovery by reducing the oil-water interfacial tension (IFT) and by changing the wettability of the rock surface. An ultra-low IFT lowers capillary forces and improves oil mobilization by the formation of oil-in-water microemulsion. Along with IFT reduction, surfactant induced wettability alteration has been identified as a key mechanism to improve oil recovery,<sup>5-10</sup> particularly where spontaneous imbibition is the dominant physical process.<sup>5, 7-10</sup> Many studies have pointed out to the presence of an optimum wettability state of a reservoir at which the oil recovery rate is the maximum.<sup>11-13</sup> This optimum wettability, which arises because of oil snap-off at strongly water-wet conditions, can be obtained in the most efficient way by a proper selection and design of surfactants and the corresponding wettability alteration process. Since wettability alteration can act independently of IFT reduction, it becomes imperative to have a good understanding of this process. Several core-level and single-pore-level experimental<sup>5-7, 14-23</sup> and computational studies<sup>24-34</sup> are available, demonstrating the beneficial effects of different surfactant systems on oil recovery from surfaces involving sandstone, calcite, etc. It is, however, worth mentioning that surfactant action in its fundamental sense happens at a molecular scale. Key aspects of this type of wettability

alteration involve the electrostatic and covalent interactions of surfactant molecules with the rock surface and the ability of the surfactants to modify the brine-rock interfacial energy. As such a molecular level study which correlates critical macroscopic parameters to the molecular entities is crucial to bridge the enormous length-scale gaps of the two systems of interest. Recently there have been some molecular level studies aimed at studying surfactant influence on oil-film for surfaces like quartz<sup>35-37</sup> and calcite<sup>38-41</sup>. These studies have provided insights into how interactions between surfactants and substrate enable formation of water channels critical for oil detachment.

The surfactant-substrate interactions determine the extent of surfactant adsorption which is a critical factor determining the efficiency of surfactants. Excess adsorption translates to surfactant loss in a localized region and the consequent unavailability in regions far from the injection point. At the same time high adsorption is also correlated to better wettability alteration in contact angle studies.<sup>42</sup> Studying the nature and extent of adsorption as a function of surfactant structure thus becomes imperative to strike the optimum balance between adsorption and wettability alteration.

In an oil reservoir, there are several factors which can impact the decision-making process to optimize surfactant chemistry. This includes rock type, reservoir brine chemistry and temperature, pH, permeability, and nature of oil to list a few. Consequently, different surfactant formulations are required to adjust to the conditions and maintain desirable oil recoveries. This becomes particularly important for high-temperature and high-salinity reservoirs where many surfactants either perform poorly or exhibit phase separation. A special class of compounds known as hydrotropes has been known to alleviate the issue of phase separation and have the potential to be considered for surfactant formulations in such cases. Such a study will ensure optimum surfactant chemistries for a wide range of reservoir conditions.



Finally, it is necessary to perform laboratory scale experiments to quantify oil recoveries associated with different surfactant formulations. Spontaneous imbibition tests done on oil-wet cores can deliver critical information on how wettability alteration and adsorption is related to ultimate oil recoveries. Along with determining surfactant selection, these studies also serve as a tool to scale laboratory imbibition performance to a reservoir level.

The present work is a step towards linking surfactant molecular factors to macroscopic parameters determining wettability and the eventual oil recoveries from a porous medium.

### **1.3. BACKGROUND**

#### **1.3.1. Wettability**

The classic definition of wettability is that it is the tendency of a fluid to spread or adhere to a surface in the presence of other immiscible fluids. From a reservoir standpoint, wettability can be broadly of three types – water-wet, oil-wet or heterogeneous wet as shown in Fig. 1.1 Purely water and oil wet reservoirs are rare as reservoirs generally tend to exhibit different wetting behavior in different regions. This heterogeneity is captured in two different forms – fractional wet, where there are pockets of regions exhibiting different wettability than the rest and mixed wet, where invading oil has managed to displace water from some of the surfaces but exists mostly in the larger pores surrounded by the aqueous phase.

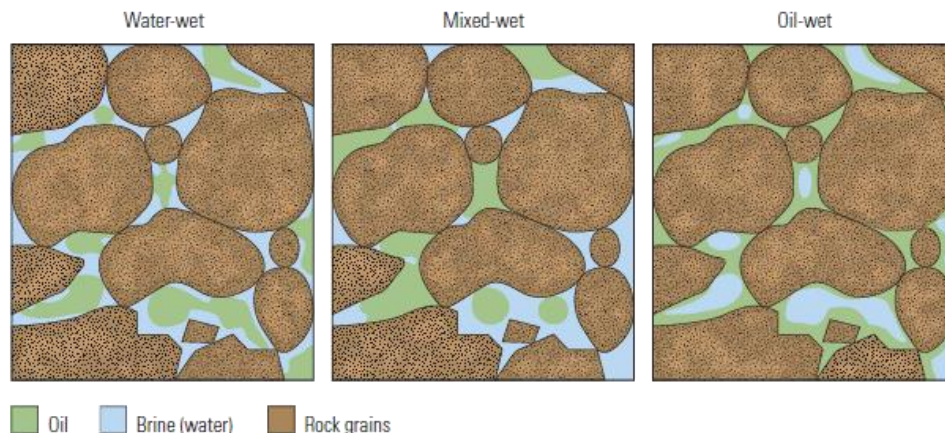


Figure 1.1 Oil-water distribution in reservoirs of different wettabilities (Fundamentals of wettability – Schlumberger, 2007)<sup>1</sup>

Reservoir wettability is determined by a combination of different factors. Important among them are the oil composition, brine and mineral chemistry, temperature and pressure. Different mechanisms have been proposed over the years trying to explain the switch from originally water-wet mineral surface to oil and mixed wet conditions. Polar compounds in resins and asphaltenes behave as wettability altering agents because of their amphiphilic nature. Low solubility in oil phase often results in precipitation of these compounds with a resulting change in wettability. Water-wet mineral surfaces inside reservoirs always have a thin coating of brine over them. Polar and charged components present in the crude oil can accumulate near the brine-oil interface. The resulting ionic interactions with the mineral surface often lead to removal of the water film and subsequent adsorption onto the surface, making them more oil-wet.

### 1.3.2. Surfactants

Surfactants are amphiphilic molecules which comprise of both hydrophilic and hydrophobic parts. Because of this duality, surfactants tend to be surface-active and can

alter the interfacial properties of a multi-component system. According to standard surfactant description, the hydrophilic group is termed as the head and the hydrophobic group as the tail. Based on the nature of charge on the hydrophilic heads the surfactants can be broadly classified as

- Anionic surfactants having negatively charged head groups like sulfates and phosphates of fatty acids
- Cationic surfactants having positively charged head groups like quaternary ammonium salts of fatty acids
- Nonionic surfactants with neutral head groups like ethoxylated alcohols
- Zwitterionic surfactants having both positive and negative charges like betaines and sulfobetaines.

These surfactant types are shown in Fig. 1.2. Table 1.2 shows typical examples of different types of surfactants. The behavior and effectiveness of ionic surfactants are determined by the electrostatic interactions with the substrate to a large extent. Anionic surfactants undergo high adsorption on positively charged carbonate surfaces.<sup>43-44</sup> Cationic surfactants are believed to form ion-pair complexes with negatively charged adsorbed oil molecules<sup>6, 45</sup> and this entails requirement of high surfactant concentration for maximum effectiveness<sup>19</sup>. The lack of charged moieties in nonionic surfactants provides several benefits – suitability to different surface types, compatibility with other surfactants and insensitivity to electrolytes. The most common type of nonionic surfactant is one with oxyethylene or ethoxylate oligomers as the polar head. Because of the hydrogen-bonding between oxyethylene groups and water, these surfactants also display interesting temperature-dependent physicochemical properties. In the subsequent chapters, the major focus will be on wettability alteration using nonionic surfactants.

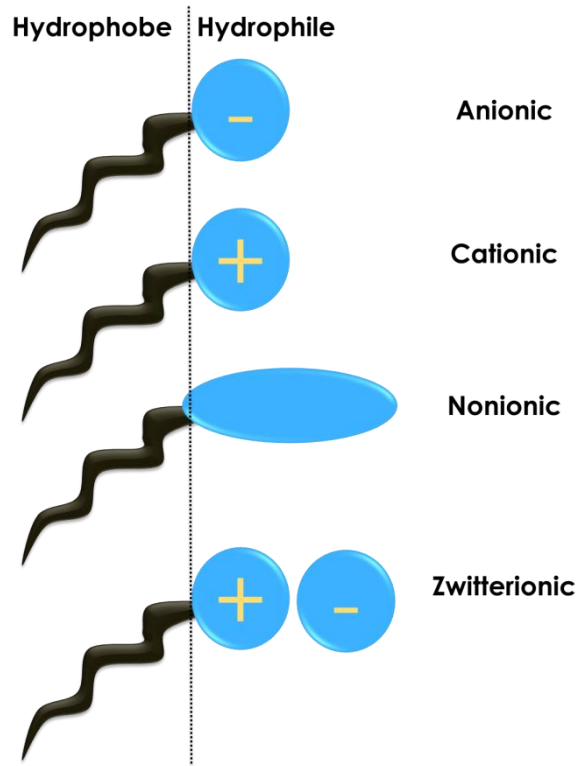
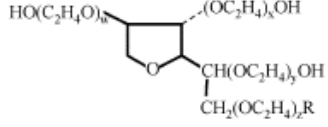


Figure 1.2. Schematic representations of surfactant molecules.

Table 1.2. Examples of different surfactant types along with their structures<sup>46</sup>

Class	Examples	Structures
Anionic	Na stearate	$\text{CH}_3(\text{CH}_2)_{16}\text{COO}^-\text{Na}^+$
	Na dodecyl sulfate	$\text{CH}_3(\text{CH}_2)_{11}\text{SO}_4^-\text{Na}^+$
	Na dodecyl benzene sulfonate	$\text{CH}_3(\text{CH}_2)_{11}\text{C}_6\text{H}_4\text{SO}_3^-\text{Na}^+$
Cationic	Laurylamine hydrochloride	$\text{CH}_3(\text{CH}_2)_{11}\text{NH}_3^+\text{Cl}^-$
	Trimethyl dodecylammonium chloride	$\text{C}_{12}\text{H}_{25}\text{N}^+(\text{CH}_3)_3\text{Cl}^-$
	Cetyl trimethylammonium bromide	$\text{CH}_3(\text{CH}_2)_{15}\text{N}^+(\text{CH}_3)_3\text{Br}^-$
Non-ionic	Polyoxyethylene alcohol	$\text{C}_n\text{H}_{2n+1}(\text{OCH}_2\text{CH}_2)_m\text{OH}$
	Alkylphenol ethoxylate	$\text{C}_9\text{H}_{19}-\text{C}_6\text{H}_4-(\text{OCH}_2\text{CH}_2)_n\text{OH}$
	Polysorbate 80	$\text{HO}(\text{C}_2\text{H}_4\text{O})_n$
	$w + x + y + z = 20$ $\text{R} = (\text{C}_{17}\text{H}_{33})_w\text{COO}$	
	Propylene oxide-modified polymethylsiloxane (EO = ethyleneoxy, PO = propyleneoxy)	$(\text{CH}_3)_3\text{SiO}((\text{CH}_3)_2\text{SiO})_n(\text{CH}_3\text{SiO})_m\text{Si}(\text{CH}_3)_3$ $ \text{CH}_2\text{CH}_2\text{CH}_2\text{O}(\text{EO})_m(\text{PO})$
Zwitterionic	Dodecyl betaine	$\text{C}_{12}\text{H}_{25}\text{N}^+(\text{CH}_3)_2\text{CH}_2\text{COO}^-$
	Lauramidopropyl betaine	$\text{C}_{11}\text{H}_{23}\text{CONH}(\text{CH}_2)_3\text{N}^+(\text{CH}_3)_2\text{CH}_2\text{COO}^-$
	Cocoamido-2-hydroxypropyl sulfobetaine	$\text{C}_n\text{H}_{2n+1}\text{CONH}(\text{CH}_2)_3\text{N}^+(\text{CH}_3)_2\text{CH}_2\text{CH}(\text{OH})\text{CH}_2\text{SO}_3^-$

### 1.3.3. Wettability Measurements

Wettability characterization of reservoir systems is usually done using one of the following processes:

- Contact angle measurement
- The Amott method
- The USBM method

The main focus in the following sections will be on using contact angle measurement as a tool to evaluate surfactants.

### 1.3.3.1. Contact Angle

This is the simplest way to measure the wettability of a surface. A finite contact angle is observed whenever a liquid drop is placed on a solid surface. The value of the contact angle, which is measured from the denser phase, gives a quantitative measure of the wettability. For an oil-water-surface system, a contact angle less than  $90^\circ$  represents a water-wet surface whereas contact angles greater than  $90^\circ$  are indicative of an oil-wet surface. Different wettability states and the corresponding contact angles are shown in Fig. 1.3.

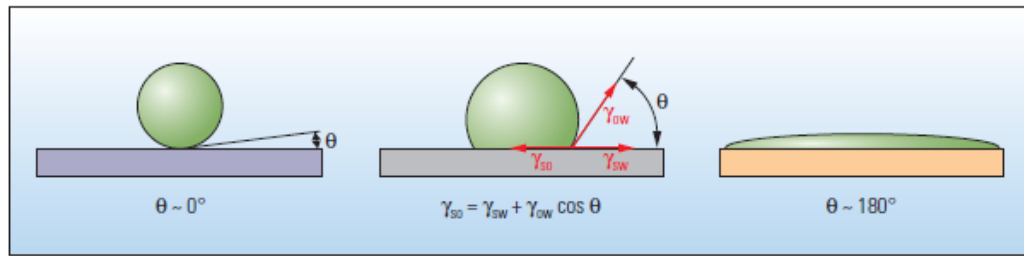


Figure 1.3. Depiction of oil drop contact angle in a) water-wet b) neutral-wet and c) oil-wet surface<sup>1</sup>

Contact angles are related to the different interfacial energies by the Young-Laplace equation,

$$\gamma_{so} = \gamma_{sw} + \gamma_{ow} \cos \theta, \quad (1)$$

where  $\gamma_{so}$ ,  $\gamma_{sw}$  and  $\gamma_{ow}$  represent the solid-oil, solid-water and oil-water surface energies respectively.  $\theta$  is the contact angle associated with the system. Contact angles are a function of the surface physical properties like roughness, electric charge and porosity in addition to the surface chemistry and proper care should be taken to report and interpret these values. Contact angles can be measured either from a static sessile drop or from a dynamic setting involving either a dynamic sessile drop or a moving plate (Wilhelmy plate

method). Figure 1.4 depicts typical wettability alteration performance of nonionic surfactants as obtained through contact angle measurements on an initial oil-wet surface.<sup>47</sup>

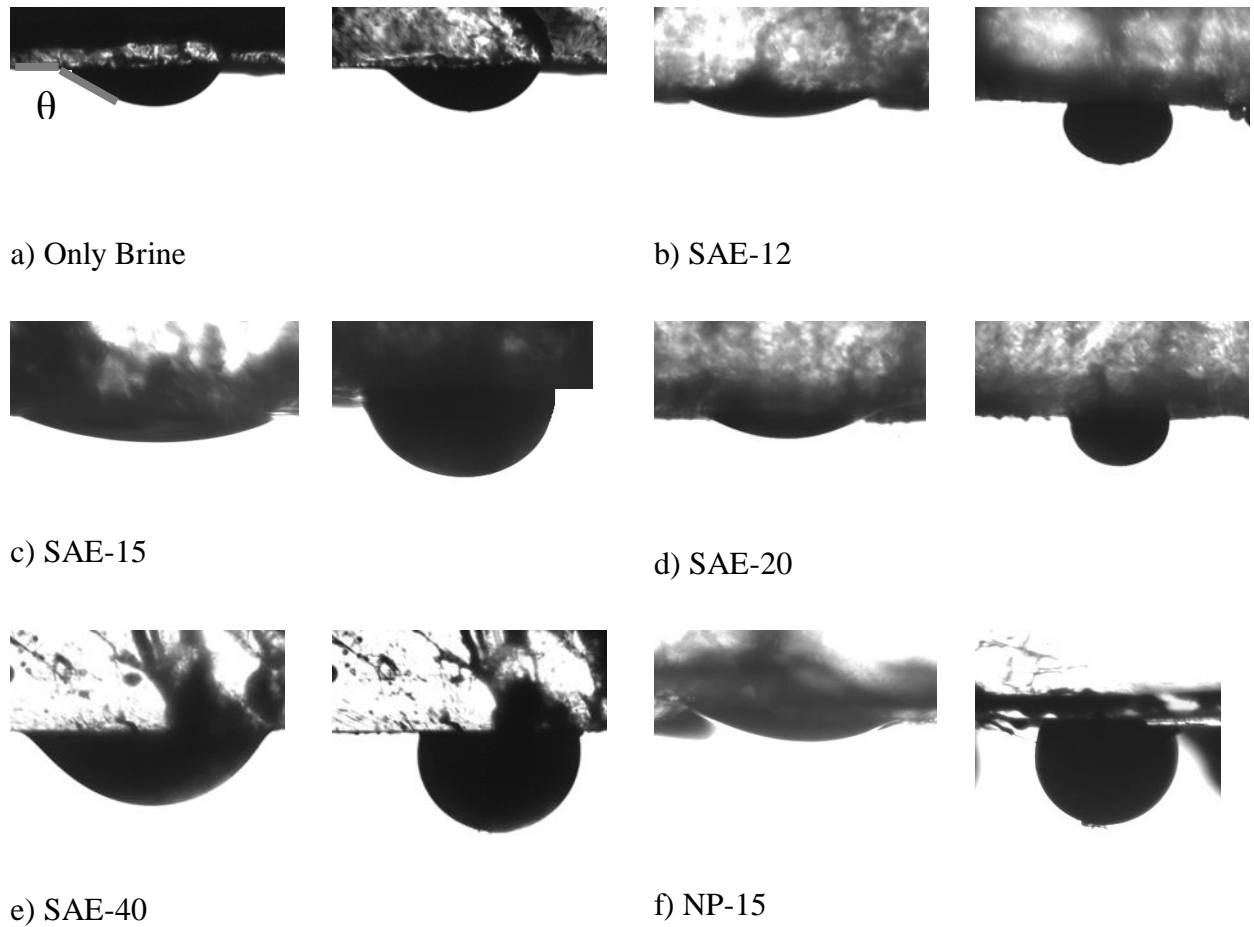


Figure 1.4. Initial and final oil drop states at 25°C and brine salinity of 12% NaCl, 0.2% CaCl<sub>2</sub> for a) no surfactant b) SAE-12 c) SAE -15 d) SAE-20 e) SAE-40 f) NP-15. SAE and NP stand for Secondary alcohol ethoxylate and nonyl-phenol ethoxylate respectively. The numbers denote the number of hydrophilic ethoxylate groups. The oil drops bead up in the presence of surfactants implying a change in wetting behavior from an initial oil-wet to an eventual water-wet or intermediate-wet surface.

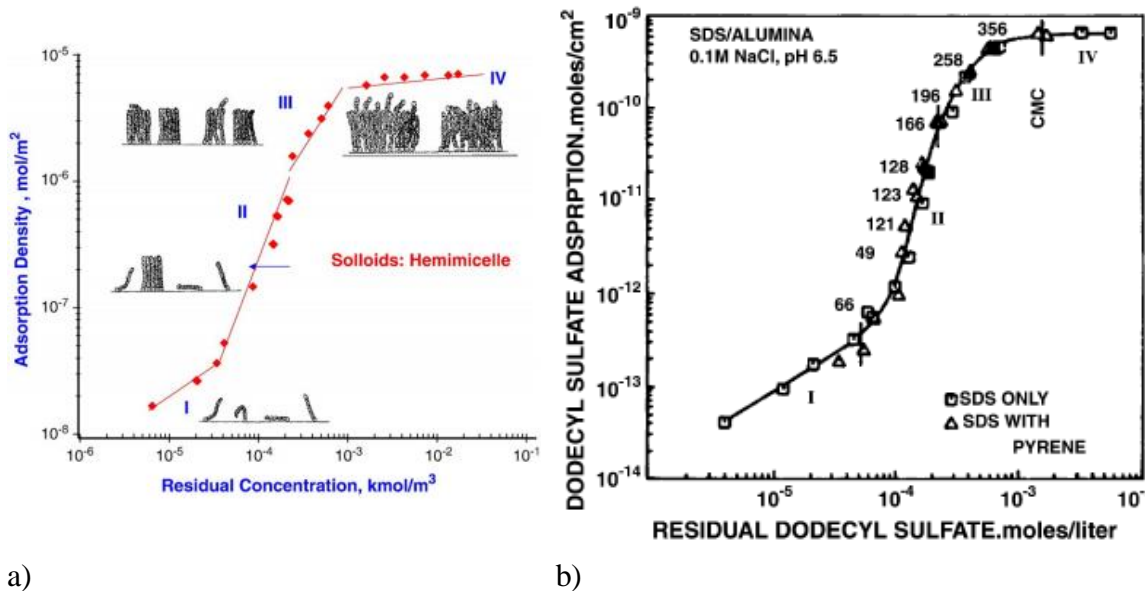
#### 1.3.4. Adsorption of Surfactants

Adsorption is the process of exchange or transfer of molecules from bulk solution to an interface. This phenomenon is critical in the process of wettability alteration and oil recovery. Analysis of surfactant adsorption can provide information on extent of surface coverage and the nature of surfactant orientation during the process. The adsorption of surfactants is a strong function of the substrate type, nature of surfactants, aqueous bulk phase chemistry and the temperature of the system. It is imperative to know about the surfactant-substrate interactions responsible for adsorption and obtain representative adsorption isotherms.

The adsorption of ionic surfactants depends on the surface charge or the zeta potential which in turn is dependent on the ionic strength of the bulk solution.<sup>48</sup> Anionic surfactants thus have low adsorption on silica surfaces, which acquire a negative zeta potential over a large pH range.<sup>49</sup> On the other hand, they exhibit high adsorption on positively charged carbonate surfaces.<sup>43-44</sup> Cationic surfactants typically have a lower adsorption on carbonates.<sup>50</sup> But the presence of silica and clay in carbonates can significantly increase the adsorption of cationic surfactants.<sup>51-53</sup> Ionic surfactants typically adsorb via direct electrostatic interactions between individual molecules and the surface resulting in a typical monolayer to admicelle transition which is marked by an eventual plateau in the adsorption isotherm (Fig. 1.5).<sup>54-55</sup>

Because of the lack of charged moieties in nonionic surfactants, a different adsorption mechanism is observed. Surfactant-bulk and lateral hydrophobic interactions among surfactant molecules seem to drive surface aggregation in such systems. Adsorption of nonionic surfactants like polyoxyethylene alkyl ethers on silica surface, have been investigated in detail.<sup>56-66</sup> Aggregative adsorption have been predicted which starts in a narrow concentration region before the critical micelle concentration.<sup>61-62</sup>

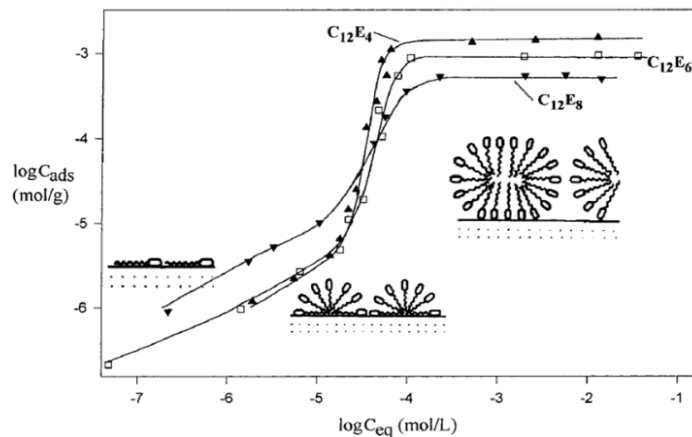




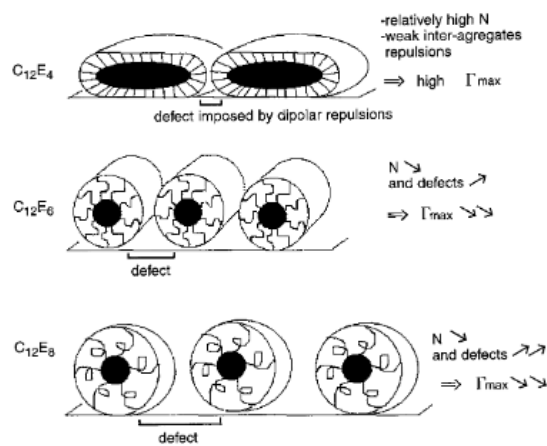
a) Schematic representation of the growth of ionic surfactant aggregates for various regions of the adsorption isotherm. In region I, the surfactant adsorbs mainly by electrostatic interactions between the surfactant headgroup and the charged sites on the mineral surface. In region II, an increase in adsorption occurs because of hydrophobic interactions between new surfactants with adsorbed ones. Region III marks the saturation of active sites with hydrophobic interactions dominating adsorption mechanism. An adsorption plateau is observed in region IV.<sup>54</sup> b) Adsorption of dodecyl sulfate on alumina displaying the different regions and the aggregation numbers.<sup>55</sup>

The extent of adsorption and the aggregate sizes decreased with increasing head group size.<sup>56, 59-64</sup> A primary adsorption mechanism involving hydrogen bonding between hydrophilic component of the surfactant and the silanol groups, and a secondary process, which requires lateral interactions between the hydrophobe components, is hypothesized to be responsible for aggregate formation.(Fig. 1.6)<sup>56</sup> Nonionic surfactants also exhibit temperature-dependent physicochemical properties and consequently temperature-dependent adsorption has been reported in the past.<sup>67-68</sup> Similarly, adsorption on carbonates was found to depend on surfactant hydrophilicity and a decrease in adsorption was observed for more hydrophilic surfactants.<sup>69-70</sup>

Molecular dynamics (MD) simulations can be a powerful tool to study the interactions at an atomistic level – which can be difficult to obtain from experiments. The adsorptions of different ionic surfactants on mineral surfaces have been studied using MD in the past.<sup>35-41</sup> These studies highlighted the importance of surfactant-substrate electrostatic interactions as well as surfactant-surfactant hydrophobic interactions responsible for different adsorption regimes as explained above. The mechanism of surfactant adsorption can be understood by investigating the energetics associated with surfactant-bulk and surfactant-substrate interactions. Adsorption free energies have been measured for different surfactant-substrate systems in the past.<sup>71-72</sup> The solvent and substrate contributions towards the adsorption free energy can also be determined from these simulations. Using this approach, interesting features like – locally favorable adsorption zone and long-range barrier to adsorption of surfactant aggregates have been reported for multiple systems.<sup>71-72</sup>



a)



b)

Figure 1.6. a) Typical adsorption isotherms of nonionic surfactants of different hydrophilicities on water-silica surface. Schematic of adsorption of nonionic surfactants is also shown with the orientation of molecules at the surface. At low surface coverages adsorption is driven mainly by Van der Waals interaction between surfactant and the surface. Within a very small bulk concentration, an increase in the adsorption is observed because of pre-aggregate formations driven by surfactant-surfactant hydrophobic interactions. These aggregates increase in size and form micellar structures as the adsorption and surface coverage increases. Adsorption decreases with an increase in hydrophilicity of surfactant headgroups from 4 EO units to 8 EO units.<sup>56</sup> b) Schematic of surface aggregates as a function of surfactant hydrophilicity.<sup>56</sup> Aggregates are smaller and farther apart for more hydrophilic surfactants.

### **1.3.5. Mixed-surfactant Formulations for Wettability Alteration**

Nonionic surfactants tend to phase separate at a critical temperature which prevents their direct application in high-temperature, high-salinity systems. The temperature at which this happens is known as the cloud point and this cloud point can be increased by adding appropriate molecules, which enhances the aqueous stability of the nonionic surfactants. These molecules, known as hydrotropes, are typically short ionic surfactants which form charged micelles with nonionic surfactants to delay the surfactant aggregation necessary for phase separation.

Figure 1.7 shows the effect of incorporation of an anionic hydrotrope on the cloud point of nonionic surfactants. Appropriate selection of hydrotrope allows operating at a temperature significantly higher than what is possible for just the nonionic surfactant. Currently, very few studies exist on the systematic analysis and evaluation of mixed surfactants.<sup>16,73-74</sup> Along with aqueous stability, a detailed study of these mixed surfactants is thus essential to understand their wettability alteration and adsorption behavior. From Fig. 1.7, it can also be seen that the structure and concentration of the hydrotrope affects the solution behavior, and it is imperative to understand its role on wettability alteration.

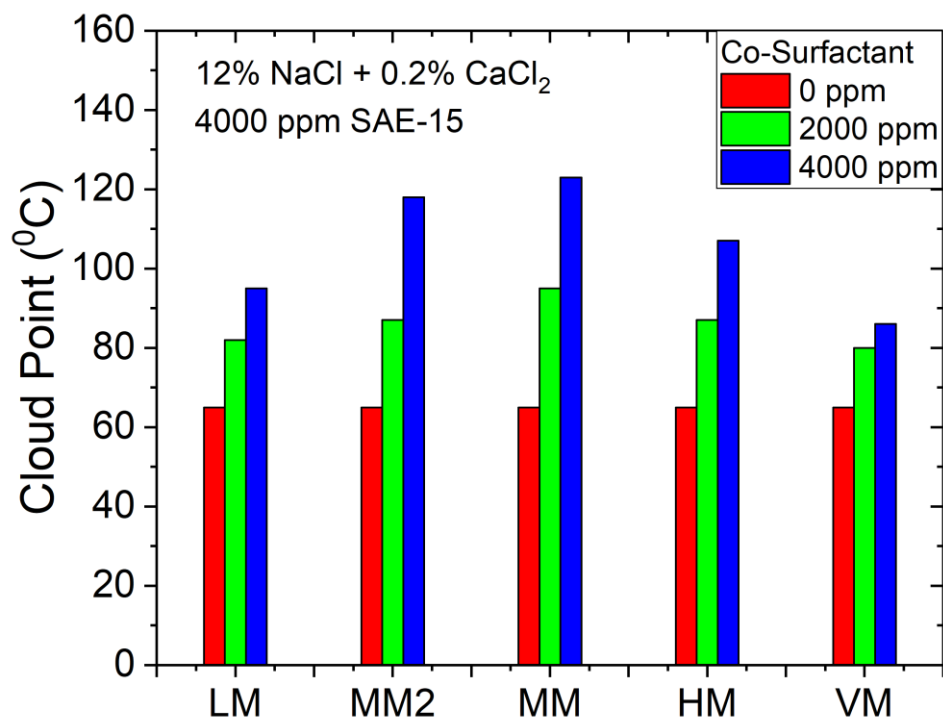


Figure 1.7. Effect of addition of co-surfactants on the cloud point of nonionic surfactants. The nonionic surfactant selected is secondary alcohol ethoxylate (SAE) with 15 EO units. The co-surfactant is an anionic molecule of different sizes – LM (low molecular weight), MM2 (medium molecular weight), MM (medium molecular weight with higher charge density), HM (high molecular weight), VM (very high molecular weight). The concentration of SAE-15 is kept constant at 4000 ppm whereas two different concentrations – 2000 ppm and 4000 ppm of co-surfactant is used. The system salinity is 12% NaCl and 0.2% CaCl<sub>2</sub>

### **1.3.6. Spontaneous Imbibition Tests for Wettability Alteration**

Spontaneous imbibition experiments are laboratory scale tests done to evaluate surfactant formulations by measuring incremental oil recoveries from oil-aged porous media. Typical porous media include short cores which are used as representatives for the actual reservoir. Along with wettability alteration measurements, these tests have been done extensively in the past to study the effect of surfactant-induced wettability alteration. For a successful imbibition process, the surfactant needs to alter the wettability of the oil-wet surface to water-wet. This ensures there is a positive capillary driving force necessary to promote imbibition of the displacing aqueous phase inside the porous media. The aqueous phase displaces the oleic phase which translates to ultimate oil recoveries. Along with a low contact angle, a low-moderate oil-water interfacial tension (IFT) is also essential for a high capillary driving force.

Different surfactants have been evaluated in spontaneous imbibition experiments in the past. Along with the type of surfactant, other factors like rock permeability, initial water saturation, temperature also play a crucial role in determining the extent as well as the rate of oil recovery through spontaneous imbibition.<sup>75-76</sup> Figures 1.8 and 1.9 shows typical oil recovery in a spontaneous imbibition experiment and the associated oil recovery curve. These imbibition experiments constitute a critical step for surfactant evaluation necessary before conducting pilot plant tests and as such scaling laws have also been developed to scale the imbibition rate and oil recoveries from the laboratory to reservoir scale.<sup>77-79</sup>



Figure 1.8. Typical oil recoveries through spontaneous imbibition in the presence of surfactants. In this case, spontaneous imbibition is gravity-driven and hence oil is generated mostly from the top surface of the core.

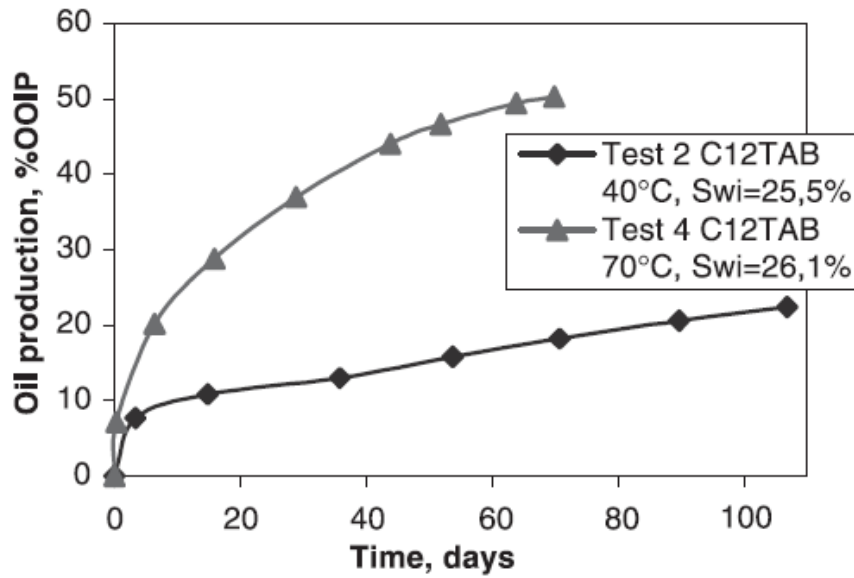


Figure 1.9. Oil recovery plots from spontaneous imbibition experiments on chalk cores using the cationic surfactant – cetrimonium bromide (CTAB) at two different temperatures.<sup>7</sup>

#### **1.4. DISSERTATION OUTLINE**

Primary and secondary oil recovery techniques produce about 20-30% of oil from carbonate-based reservoirs. The low oil production and the fact that more than half of world's oil reserves are carbonate-based, call for development of tertiary oil recovery methods. Surfactants with their amphiphilic nature have been known to alter interfacial properties responsible for these lower oil recoveries. This dissertation investigates different families of nonionic surfactants with the goal of developing surfactant formulations for enhanced oil recovery through wettability alteration. It studies the effect of surfactant structure, composition, brine salinity and temperature on adsorption and wettability alteration on carbonate surfaces. It also aims to predict oil recoveries associated with different surfactant systems by combining results from spontaneous imbibition experiments with wettability alteration behavior. The outline for rest of the dissertation is as follows:

In Chapter 2, wettability alteration on carbonate surface is studied for different nonionic surfactants as a function of brine salinity and temperature. Kinetic studies are performed to obtain activation energies associated with wettability alteration. Complementary oil-film studies are also performed together with the kinetic study to propose a conceptual model explaining the wettability alteration phenomena.

In Chapter 3, the adsorption of surfactants on carbonate surface is investigated to understand its role on wettability alteration. A detailed evaluation of the surfactant structure and system temperature on adsorption is performed. The concepts of packing factor and surface coverage are used to understand the nature of surfactant adsorption. At the same time a universal adsorption behavior associated with an intrinsic thermodynamic property (CPTD – Cloud point temperature difference) is developed to predict surfactant adsorption.



The correlation between surfactant adsorption and wettability alteration is also established in this chapter.

In Chapter 4, the applicability of nonionic surfactants is extended to high temperature systems by incorporating different co-surfactants. The wettability alteration and adsorption associated with these mixed systems at high temperatures are studied in detail. The concept of CPTD is applied to mixed systems to predict the capillary driving forces and to compare their performances with single surfactant systems. The effect of the co-surfactant structure on the mechanism of aqueous stabilization and surface aggregation is also discussed.

In Chapter 5, molecular dynamics simulations are performed for select nonionic surfactants to understand the mechanism of adsorption on carbonate surfaces. Using appropriate sampling methods, the adsorption energies corresponding to monomer and aggregative adsorption are obtained. The energy landscape gives a complete picture of the adsorption process and agrees qualitatively with experimental findings. The role of surfactant hydrophilicity and system temperature is also analyzed in this study.

In Chapter 6, oil recoveries from oil-wet porous media are investigated by performing spontaneous imbibition tests in small carbonate cores. Both single and mixed surfactant formulations are used in this study. The effect of surfactant composition, brine salinity, capillary driving force, surfactant adsorption and initial water saturation on oil recovery is studied in detail. Rate studies are also done to collapse oil recovery curves and to scale laboratory scale results to reservoir level. Finally using a combination of capillary driving force and CPTD, an attempt has been made to predict oil recoveries for these systems.

In Chapter 7, important conclusions from different chapters are summarized and recommendations for future works are presented

## REFERENCES

1. Schlumberger Market Analysis, **2007**.
2. Salathiel, R. A. Oil recovery by surface film drainage in mixed-wettability rocks. *Journal of Petroleum Technology*, **1973**, 25(10), 1-216.
3. Buckley, J. S., Liu, Y., & Monsterleet, S. Mechanisms of wetting alteration by crude oils. *SPE journal*, **1998**, 3(01), 54-61.
4. Al-Maamari, R. S., & Buckley, J. S. Asphaltene precipitation and alteration of wetting: the potential for wettability changes during oil production. *SPE Reservoir Evaluation & Engineering*, **2003**, 6(04), 210-214.
5. Strand, S., Standnes, D. C., & Austad, T. Spontaneous imbibition of aqueous surfactant solutions into neutral to oil-wet carbonate cores: Effects of brine salinity and composition. *Energy & fuels*, **2003**, 17(5), 1133-1144.
6. Standnes, D. C., & Austad, T. Wettability alteration in carbonates: Interaction between cationic surfactant and carboxylates as a key factor in wettability alteration from oil-wet to water-wet conditions. *Colloids and Surfaces A: Physicochemical and Engineering Aspects*, **2003**, 216(1-3), 243-259.
7. Austad, T., & Standnes, D. C. Spontaneous imbibition of water into oil-wet carbonates. *Journal of Petroleum Science and Engineering*, **2003**, 39(3-4), 363-376.
8. Austad, T. and Milter, J. Spontaneous imbibition of water into low permeable chalk at different wettabilities using surfactants. In *International Symposium on Oilfield Chemistry*, Society of Petroleum Engineers, **1997**.
9. Standnes, D.C., Nogaret, L.A., Chen, H.L. and Austad, T. An evaluation of spontaneous imbibition of water into oil-wet carbonate reservoir cores using a nonionic and a cationic surfactant. *Energy & Fuels*, 16(6), **1997**, pp.1557-1564.
10. Spinler, E.A., Zornes, D.R., Tobola, D.P. and Moradi-Araghi, A. Enhancement of oil recovery using a low concentration of surfactant to improve spontaneous and forced imbibition in chalk. In *SPE/DOE Improved Oil Recovery Symposium*. Society of Petroleum Engineers, **2000**.
11. Amott, E., 1959. Observations relating to the wettability of porous rock.
12. Jadhunandan, P.P. and Morrow, N.R., 1995. Effect of wettability on waterflood recovery for crude-oil/brine/rock systems. *SPE reservoir engineering*, 10(01), pp.40-46.

13. Anderson, G.A., 2006. *Simulation of chemical flood enhanced oil recovery processes including the effects of reservoir wettability* (Doctoral dissertation, University of Texas at Austin).
14. Gupta, R. and Mohanty, K.K., 2007, January. Temperature effects on surfactant-aided imbibition into fractured carbonates. In *SPE Annual Technical Conference and Exhibition*. Society of Petroleum Engineers.
15. Seethepalli, A., Adibhatla, B. and Mohanty, K.K., 2004, January. Wettability alteration during surfactant flooding of carbonate reservoirs. In *SPE/DOE symposium on improved oil recovery*. Society of Petroleum Engineers.
16. Sharma, G. and Mohanty, K., 2013. Wettability alteration in high-temperature and high-salinity carbonate reservoirs. *SPE Journal*, 18(04), pp.646-655.
17. Hirasaki, G. and Zhang, D.L., 2004. Surface chemistry of oil recovery from fractured, oil-wet, carbonate formations. *Spe Journal*, 9(02), pp.151-162.
18. Xie, X., Liu, Y., Sharma, M. and Weiss, W.W., 2009. Wettability alteration to increase deliverability of gas production wells. *Journal of Natural Gas Science and Engineering*, 1(1-2), pp.39-45.
19. Wu, Y., Shuler, P., Blanco, M., Tang, Y. and Goddard, W.A., 2006. A Study of Wetting Behavior and Surfactant EOR in Carbonates With Model Components. Paper SPE 99612 presented at the SPE. In *DOE Symposium on Improved Oil Recovery, Tulsa*.
20. Tiberg, F., Zhmud, B., Hallstenson, K. and Von Bahr, M., 2000. Capillary rise of surfactant solutions. *Physical Chemistry Chemical Physics*, 2(22), pp.5189-5196.
21. Starov, V.M., Zhdanov, S.A. and Velarde, M.G., 2004. Capillary imbibition of surfactant solutions in porous media and thin capillaries: partial wetting case. *Journal of colloid and interface science*, 273(2), pp.589-595.
22. Starov, V.M., 2004. Spontaneous rise of surfactant solutions into vertical hydrophobic capillaries. *Journal of colloid and interface science*, 270(1), pp.180-186.
23. Unsal, E., Broens, M. and Armstrong, R.T., 2016. Pore scale dynamics of microemulsion formation. *Langmuir*, 32(28), pp.7096-7108.
24. Adibhatla, B. and Mohanty, K.K., 2006, January. Oil recovery from fractured carbonates by surfactant-aided gravity drainage: laboratory experiments and mechanistic simulations. In *SPE/DOE Symposium on Improved Oil Recovery*. Society of Petroleum Engineers.

25. Kalaei, M.H., Green, D. and Willhite, G.P., 2013. A new dynamic wettability-alteration model for oil-wet cores during surfactant-solution imbibition. *SPE Journal*, 18(05), pp.818-828.
26. Delshad, M., Najafabadi, N.F., Anderson, G.A., Pope, G.A. and Sepehrnoori, K., 2006, January. Modeling wettability alteration in naturally fractured reservoirs. In *SPE/DOE Symposium on Improved Oil Recovery*. Society of Petroleum Engineers.
27. Delshad, M., Najafabadi, N.F. and Sepehrnoori, K., 2009, January. Scale Up Methodology for Wettability Modification in Fractured Carbonates. In *SPE Reservoir Simulation Symposium*. Society of Petroleum Engineers.
28. Hammond, P.S. and Unsal, E., 2012. A dynamic pore network model for oil displacement by wettability-altering surfactant solution. *Transport in porous media*, 92(3), pp.789-817.
29. Lenormand, R., Touboul, E. and Zarcone, C., 1988. Numerical models and experiments on immiscible displacements in porous media. *Journal of fluid mechanics*, 189, pp.165-187.
30. DiCarlo, D.A., 2006. Quantitative network model predictions of saturation behind infiltration fronts and comparison with experiments. *Water resources research*, 42(7).
31. Hammond, P.S. and Unsal, E., 2009. Spontaneous and forced imbibition of aqueous wettability altering surfactant solution into an initially oil-wet capillary. *Langmuir*, 25(21), pp.12591-12603.
32. Hammond, P.S. and Unsal, E., 2010. Forced and spontaneous imbibition of surfactant solution into an oil-wet capillary: the effects of surfactant diffusion ahead of the advancing meniscus. *Langmuir*, 26(9), pp.6206-6221.
33. Hammond, P.S. and Unsal, E., 2011. Spontaneous imbibition of surfactant solution into an oil-wet capillary: wettability restoration by surfactant–contaminant complexation. *Langmuir*, 27(8), pp.4412-4429.
34. Zhmud, B.V., Tiberg, F. and Hallstensson, K., 2000. Dynamics of capillary rise. *Journal of colloid and interface science*, 228(2), pp.263-269.
35. Yan, H. and Yuan, S., 2016. Molecular dynamics simulation of the oil detachment process within silica nanopores. *The Journal of Physical Chemistry C*, 120(5), pp.2667-2674.
36. Liu, Q., Yuan, S., Yan, H. and Zhao, X., 2012. Mechanism of oil detachment from a silica surface in aqueous surfactant solutions: molecular dynamics simulations. *The Journal of Physical Chemistry B*, 116(9), pp.2867-2875.

37. Li, X., Xue, Q., Wu, T., Jin, Y., Ling, C. and Lu, S., 2015. Oil detachment from silica surface modified by carboxy groups in aqueous cetyltriethylammonium bromide solution. *Applied Surface Science*, 353, pp.1103-1111.
38. Lu, G., Zhang, X., Shao, C. and Yang, H., 2009. Molecular dynamics simulation of adsorption of an oil-water-surfactant mixture on calcite surface. *Petroleum Science*, 6(1), pp.76-81.
39. Yuan, S., Wang, S., Wang, X., Guo, M., Wang, Y. and Wang, D., 2016. Molecular dynamics simulation of oil detachment from calcite surface in aqueous surfactant solution. *Computational and Theoretical Chemistry*, 1092, pp.82-89.
40. Li, X., Xue, Q., Zhu, L., Jin, Y., Wu, T., Guo, Q., Zheng, H. and Lu, S., 2016. How to select an optimal surfactant molecule to speed up the oil-detachment from solid surface: a computational simulation. *Chemical Engineering Science*, 147, pp.47-53.
41. Durán-Álvarez, A., Maldonado-Domínguez, M., González-Antonio, O., Durán-Valencia, C., Romero-Ávila, M., Barragán-Aroche, F. and López-Ramírez, S., 2016. Experimental–Theoretical Approach to the Adsorption Mechanisms for Anionic, Cationic, and Zwitterionic Surfactants at the Calcite–Water Interface. *Langmuir*, 32(11), pp.2608-2616.
42. Das, S., Katiyar, A., Rohilla, N., Nguyen, Q., Bonnecaze, R.T., Adsorption of nonionic surfactants on carbonates. Under Review
43. Ma, K., Cui, L., Dong, Y., Wang, T., Da, C., Hirasaki, G. J., & Biswal, S. L. Adsorption of cationic and anionic surfactants on natural and synthetic carbonate materials. *Journal of colloid and interface science*, 2013, 408, 164-172.
44. Fletcher, P. D., Savory, L. D., Clarke, A., & Howe, A. M. Model Study of Enhanced Oil Recovery by Flooding with Aqueous Solutions of Different Surfactants: How the Surface Chemical Properties of the Surfactants Relate to the Amount of Oil Recovered. *Energy & Fuels*, 2016, 30(6), 4767-4780.
45. Jarrahan, K., Seiedi, O., Sheykhani, M., Sefti, M. V., & Ayatollahi, S. Wettability alteration of carbonate rocks by surfactants: a mechanistic study. *Colloids and Surfaces A: Physicochemical and Engineering Aspects*, 2012, 410, 1-10.
46. Holmberg, K., JoËnsson, B., Kronberg, B. and Lindman, B., 2002. SURFACTANTS AND POLYMERS IN AQUEOUS SOLUTION.
47. Das, S., Nguyen, Q., Patil, P.D., Yu, W. and Bonnecaze, R.T., 2018. Wettability alteration of calcite by nonionic surfactants. *Langmuir*, 34(36), pp.10650-10658.

48. Zhang, R. and Somasundaran, P., 2006. Advances in adsorption of surfactants and their mixtures at solid/solution interfaces. *Advances in colloid and interface science*, 123, pp.213-229.
49. Thibaut, A., Misselyn-Bauduin, A.M., Grandjean, J., Broze, G. and Jérôme, R., 2000. Adsorption of an aqueous mixture of surfactants on silica. *Langmuir*, 16(24), pp.9192-9198.
50. Ahmadall, T., Gonzalez, M.V., Harwell, J.H. and Scamehorn, J.F., 1993. Reducing surfactant adsorption in carbonate reservoirs. *SPE reservoir engineering*, 8(02), pp.117-122.
51. Bastrzyk, A.P.I.S.E., Polowczyk, I., Szelag, E. and Sadowski, Z., 2012. Adsorption and co-adsorption of PEO-PPO-PEO block copolymers and surfactants and their influence on zeta potential of magnesite and dolomite. *Physicochemical Problems of Mineral Processing*, 48(1), p.2012.
52. Rosen, M.J. and Li, F., 2001. The adsorption of gemini and conventional surfactants onto some soil solids and the removal of 2-naphthol by the soil surfaces. *Journal of colloid and interface science*, 234(2), pp.418-424.
53. Ivanova, N.I., Volchkova, I.L. and Shchukin, E.D., 1995. Adsorption of nonionic and cationic surfactants from aqueous binary mixtures onto the solid/liquid interface. *Colloids and Surfaces A: Physicochemical and Engineering Aspects*, 101(2-3), pp.239-243.
54. Somasundaran, P. and Zhang, L., 2006. Adsorption of surfactants on minerals for wettability control in improved oil recovery processes. *Journal of Petroleum Science and Engineering*, 52(1-4), pp.198-212.
55. Chandar, P., Somasundaran, P. and Turro, N.J., 1987. Fluorescence probe studies on the structure of the adsorbed layer of dodecyl sulfate at the alumina—water interface. *Journal of colloid and interface science*, 117(1), pp.31-46.
56. Desbene, P.L., Portet, F. and Treiner, C., 1997. Adsorption of pure nonionic alkylethoxylated surfactants down to low concentrations at a silica/water interface as determined using a HPLC technique. *Journal of Colloid and Interface Science*, 190(2), pp.350-356.
57. Curbelo, F.D., Santanna, V.C., Neto, E.L.B., Dutra Jr, T.V., Dantas, T.N.C., Neto, A.A.D. and Garnica, A.I., 2007. Adsorption of nonionic surfactants in sandstones. *Colloids and Surfaces A: Physicochemical and Engineering Aspects*, 293(1-3), pp.1-4.

58. Caruso, F., Serizawa, T., Furlong, D.N. and Okahata, Y., 1995. Quartz crystal microbalance and surface plasmon resonance study of surfactant adsorption onto gold and chromium oxide surfaces. *Langmuir*, 11(5), pp.1546-1552.
59. Levitz, P.E., 2002. Adsorption of non ionic surfactants at the solid/water interface. *Colloids and Surfaces A: Physicochemical and Engineering Aspects*, 205(1-2), pp.31-38.
60. Levitz, P., 1991. Aggregative adsorption of nonionic surfactants onto hydrophilic solid/water interface. Relation with bulk micellization. *Langmuir*, 7(8), pp.1595-1608.
61. Tiberg, F., 1996. Physical characterization of nonionic surfactant layers adsorbed at hydrophilic and hydrophobic solid surfaces by time-resolved ellipsometry. *Journal of the Chemical Society, Faraday Transactions*, 92(4), pp.531-538.
62. Tiberg, F., Joensson, B., Tang, J.A. and Lindman, B., 1994. Ellipsometry studies of the self-assembly of nonionic surfactants at the silica-water interface: equilibrium aspects. *Langmuir*, 10(7), pp.2294-2300.
63. Levitz, P., Van Damme, H. and Keravis, D., 1984. Fluorescence decay study of the adsorption of nonionic surfactants at the solid-liquid interface. 1. Structure of the adsorption layer on a hydrophilic solid. *The Journal of Physical Chemistry*, 88(11), pp.2228-2235.
64. Levitz, P. and Van Damme, H., 1986. Fluorescence decay study of the adsorption of nonionic surfactants at the solid-liquid interface. 2. Influence of polar chain length. *The Journal of Physical Chemistry*, 90(7), pp.1302-1310.
65. Portet, F., Desbene, P.L. and Treiner, C., 1997. Adsorption isotherms at a silica/water interface of the oligomers of polydispersed nonionic surfactants of the alkylpolyoxyethylated series. *Journal of colloid and interface science*, 194(2), pp.379-391.
66. Gellan, A. and Rochester, C.H., 1985. Adsorption of n-alkylpolyethylene glycol nonionic surfactants from aqueous solution on to silica. *Journal of the Chemical Society, Faraday Transactions 1: Physical Chemistry in Condensed Phases*, 81(9), pp.2235-2245.
67. Partyka, S., Zaini, S., Lindheimer, M. and Brun, B., 1984. The adsorption of nonionic surfactants on a silica gel. *Colloids and surfaces*, 12, pp.255-270.
68. Corkill, J.M., Goodman, J.F. and Tate, J.R., 1966. Adsorption of nonionic surface-active agents at the graphon/solution interface. *Transactions of the Faraday Society*, 62, pp.979-986.
69. Kuno, H. and Abe, R., 1961. The adsorption of polyoxyethylated nonylphenol on calcium carbonate in aqueous solution. *Kolloid-Zeitschrift*, 177(1), pp.40-44.

70. Akers, R.J. and Riley, P.M., 1974. Adsorption of polyoxyethylene alkyl-phenols onto calcium carbonate from aqueous solution. *J. Colloid Interface Sci.*(United States), 48(1).
71. Xu, Z., Yang, X. and Yang, Z., 2008. On the mechanism of surfactant adsorption on solid surfaces: Free-energy investigations. *The Journal of Physical Chemistry B*, 112(44), pp.13802-13811.
72. Kurapati, Y. and Sharma, S., 2018. Adsorption Free Energies of Imidazolium-Type Surfactants in Infinite Dilution and in Micellar State on Gold Surface. *The Journal of Physical Chemistry B*, 122(22), pp.5933-5939.
73. Patil, P.D., Rohilla, N., Katiyar, A., Yu, W., Falcone, S., Nelson, C. and Rozowski, P., 2018, March. Surfactant based EOR for tight oil reservoirs through wettability alteration: novel surfactant formulations and their efficacy to induce spontaneous imbibition. In *SPE EOR Conference at Oil and Gas West Asia*. Society of Petroleum Engineers.
74. Alvarez, J.O. and Schechter, D.S., 2017. Wettability alteration and spontaneous imbibition in unconventional liquid reservoirs by surfactant additives. *SPE Reservoir Evaluation & Engineering*, 20(01), pp.107-117.
75. Zhou, X., Morrow, N.R. and Ma, S., 2000. Interrelationship of wettability, initial water saturation, aging time, and oil recovery by spontaneous imbibition and waterflooding. *Spe Journal*, 5(02), pp.199-207.
76. Hamouda, A. and Karoussi, O., 2008. Effect of temperature, wettability and relative permeability on oil recovery from oil-wet chalk. *Energies*, 1(1), pp.19-34.
77. Mattax, C.C. and KYTE, J.R., 1962. Imbibition oil recovery from fractured, water-drive reservoir. *Society of Petroleum Engineers Journal*, 2(02), pp.177-184.
78. Cuiec, L., Bourbiaux, B. and Kalaydjian, F., 1994. Oil recovery by imbibition in low-permeability chalk. *SPE Formation Evaluation (Society of Petroleum Engineers)*;(United States), 9(3).
79. Zhang, X., Morrow, N.R. and Ma, S., 1996. Experimental verification of a modified scaling group for spontaneous imbibition. *SPE Reservoir Engineering*, 11(04), pp.280-285.



## Chapter 2: Wettability Alteration of Calcite by Nonionic Surfactants\*

### 2.1 INTRODUCTION

More than 60% of world's oil reserves are held within carbonate formations.<sup>1</sup> Wettability of such rock-brine-oil systems determines both the distribution and relative permeability of each fluid inside the reservoirs.<sup>2</sup> The wetting fluid generally occupies the small pores while the non-wetting fluid tends to reside in the larger ones forming connected pathways. One of the major features of carbonates is their inherent oil-wetness which is believed to be due to the adsorption of acidic components present in crude oil onto the rock surface.<sup>3,4</sup> Because of the oil-wetting nature, the capillary forces inside these reservoirs prevent spontaneous water imbibition. Typical water flood recovery for fractured carbonate reservoir is less than 40 % of original oil in place (OOIP). Unfavorable capillary forces ensure that residual oil remains trapped as a discontinuous phase separated by the brine. The low oil recovery rates demand development of tertiary techniques which can extract the trapped residual oil.

Surfactants can improve oil recovery by lowering the oil-water capillary forces and by changing the wettability of the reservoir rock. Standnes and co-workers investigated the effect of both cationic and anionic surfactants on oil recovery from oil-wet chalk and dolomite cores.<sup>5-7</sup> The ability of the cationic surfactants to form ion-pairs with negatively charged adsorbed oil molecules was put forth as a possible reason to explain their excellent performance. They also reported improved oil recovery at higher temperature and with increased sulfate concentration.<sup>8</sup> Core-flood experiments with anionic surfactants have

---

\* Much of this chapter has appeared in Das, S., Nguyen, Q., Patil, P.D., Yu, W. and Bonnacaze, R.T. 2018 "Wettability alteration of calcite by nonionic surfactants," *Langmuir* **34**(36) 10650-10658. S.D. designed and performed the experiments, analyzed the data and wrote the manuscript.

reported recovering close to 60% of original oil through a combination of capillary and gravity effects.<sup>9-11</sup> The lowering of oil-water interface tension (IFT) is believed to be the crucial factor for these anionic surfactants. Zhang et al<sup>12</sup>. provided significant insights into capillary and emulsification driven natural imbibition mechanisms. Anionic surfactants were reported to enhance the imbibition process mainly by an emulsification process. Contact angle experiments have been done in the past as a qualitative tool to understand surfactant performance in alternating mineral surface wettability. Final contact angle values were reported for different anionic and nonionic surfactants on calcite,<sup>13-18</sup> quartz and mica.<sup>19-20</sup> Microfluidic experiments<sup>22-24</sup> studying spontaneous imbibition of surfactant solutions inside hydrophobic capillaries<sup>25-27</sup> and dynamics visualization of different flow regimes<sup>22-25, 28</sup> have been performed to study the pore-level mechanisms of diffusion and adsorption. Adhibhatla and Mohanty simulated the effect of wettability alteration on spontaneous imbibition by correlating the phase permeabilities to the contact angle.<sup>29</sup> Kalaei et al. used this concept to form a wettability alteration model in which the contact angle varies with surfactant concentration.<sup>30</sup> Delshad et al. modeled the wettability alteration using a scaling factor estimated from the ratio of adsorbed surfactant concentration to the total surfactant concentration.<sup>31-32</sup> Zhmud et al.<sup>33</sup> presented a detailed theoretical analysis of the capillary rise of surfactant solutions, which was then expanded by Hammond and Unsal<sup>34-36</sup> to model the two known mechanisms of wettability alteration, namely – the coating and cleaning mechanism. According to their model there is a critical surfactant concentration limit for the coating mechanism to work. The cleaning mechanism promoted oil displacement at all surfactant concentrations. Recently, Hammond and Unsal also developed a dynamic pore-network model to predict oil recovery in porous media by the use of surfactants.<sup>37</sup> They were able to reproduce the displacement patterns obtained in previous works.<sup>14, 25</sup>

For ionic surfactants, the electrostatic interactions with other components dominate their behavior and effectiveness to a large extent. Anionic surfactants typically suffer from detrimentally high adsorption on positively charged carbonate surfaces.<sup>19, 38</sup> Cationic surfactants are believed to operate under an ion-pair mechanism forming complexes with negatively charged adsorbed oil molecules.<sup>6, 17</sup> While, this leads to better wettability alteration, it also implies requirement of high surfactant concentration for effectiveness.<sup>14</sup> In fact requirement of cationic surfactant concentration as high as 1-2.5 wt% has been reported<sup>6</sup>. The absence of charged head groups in nonionic surfactants make them suitable for multiple surfaces. The most common type of nonionic surfactant is one with oxyethylene or ethoxylate oligomers as the polar head. The performance of these surfactants to alter wettability typically lie somewhere in between the two cationic and anionic surfactants.<sup>17</sup> These surfactants show an additional interesting feature of temperature-dependent physicochemical properties. Indeed, wettability alteration in nonionic systems has been found to be enhanced significantly by increasing the temperature.<sup>15</sup>

## **2.2. OVERVIEW OF APPROACH**

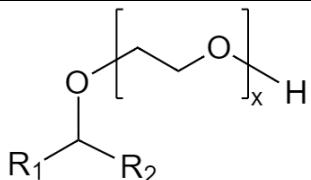
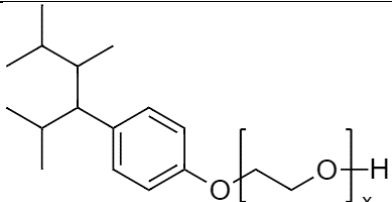
The presence of large number of surfactants makes it imperative to devise a rapid evaluation technique to measure surfactant efficiency in making surfaces water-wet. A systematic way of characterizing surfactants based on their hydrophobic and hydrophilic components is necessary to predict wetting performances and identify critical parameters for surfactant selection and design. In this work, a series of nonionic surfactants belonging to different hydrophobe families is selected for evaluation. A simple three-step evaluation process is designed to extract maximum information about structure-property relationships and details about possible mechanism of surfactant action. Surfactants are first tested using

a phase behavior experiment to confirm the presence/absence of microemulsion formation at different operating temperatures and brine salinities. A sessile drop contact angle experiment is then done to measure the evolution of contact angle with time for the different surfactant systems. Temperatures and brine salinities are varied to study their effect on the wettability change. Quantitative experimental observations are efficiently summarized by a few thermodynamic and kinetic parameters. The process of wettability alteration involves overcoming energy barriers. The concept of activation energy is introduced to understand the energetics involved and gain significant insights into the nature of the rate limiting steps. A qualitative oil-film stability experiment is then done to study the behavior of wettability alteration in oil-wet surfaces in the presence of surfactant solutions. Together with the kinetic study, results from the oil-film tests are then used to propose a simple conceptual model explaining wettability alteration in the presence of surfactants.

### **2.3. MATERIALS**

Table 2.1 lists the surfactants used in this study along with their molecular structures and their CMC values. All the surfactants were provided by The Dow Chemical Company. The two groups of surfactants evaluated in the current study are secondary alcohol ethoxylates represented by the notation SAE-x and nonylphenol ethoxylates represented by NP-x. The hydrophilic components in both groups are repeating units of ethylene oxide. The hydrophobe units are secondary alcohol and nonylphenol for SAE-x and NP-x respectively. Calcite plates (Iceland Spar) obtained from Wards Natural Sciences were used as a representative carbonate surface. Crude oil used in the experiments was obtained from a carbonate oil formation. Sodium chloride and calcium chloride (Fisher) were used as received.

Table 2.1. List of nonionic surfactants evaluated in the study. CMC values are reported at 25°C.

Surfactant name	Structure	Specification (x)	CMC(ppm)
SAE-x (Secondary alcohol ethoxylate)		12	104
		15	162
		20	315
		30	558
		40	1314
NP-x (Nonylphenol ethoxylate)		12	85
		15	90
		30	157
		40	232
		50	256

## 2.4. METHODOLOGY

### 2.4.1. Brine/Surfactant/Oil Phase Behavior

Brine-surfactant-oil mixtures exhibit rich and complex phase behavior depending upon the temperature and brine salinity. Both of these factors determine the solubility of surfactants in aqueous or oleic phase. At low brine salinity and low temperatures surfactants tend to have high aqueous phase solubility and any microemulsion formation will reside in this phase (Winsor I system). At high salinities and temperatures the situation reverses and any microemulsion will be in the oil phase (Winsor II system). At intermediate conditions surfactants might form a separate microemulsion phase in equilibrium with both excess oleic and aqueous phases (Winsor III system). The presence of a microemulsion phase indicates a low oil-water IFT in the system. Following steps were followed to carry out these experiments:

- Brine solutions of different salinities are prepared by varying NaCl concentration. The CaCl<sub>2</sub> concentration is kept constant at 0.2% by weight. Different brine compositions ranging from 0.1% - 12% NaCl are used.

- Surfactant is added to the brine (surfactant concentration  $>$  CMC or about 4000ppm) and then 2mL of the surfactant-brine solution is placed in a pipette.
- Equal volume of oil is added to the pipette and the pipette is then sealed.
- The contents of the pipette are then mixed thoroughly over a period of time.
- After mixing the pipette is allowed to rest at the required temperature. Periodic mixing and observations are done to check on phase behavior.

#### **2.4.2. Contact Angle Experiments**

Evaluation of surfactants using contact angle comprised of two separate procedures:

##### a) Calcite plate preparation

- Calcite plates (3cm x 3cm x 1cm) are first cut from calcite blocks by breaking across the cleavage planes and then cleaned using ethyl alcohol.
- These calcites are then placed inside crude oil at 120°C and aged for 2-3 days.
- After this the plates are removed from crude oil and excess oil is dripped off by gravity. They are then kept at 100°C for 3 days following which a uniform oil wet surface is formed.

##### b) Contact angle measurement

- A quartz cell is filled with surfactant brine solution and placed inside an environmental chamber set at a desired temperature.
- An oil-aged calcite plate is then placed inside the solution with the aged surface facing down.
- Oil drops are placed on this surface using a syringe with inverted needle.
- The shape of the oil drop is then monitored using a high magnification camera and the contact angle extracted from the images.

- These measurements were done at three different temperatures – 25°C, 40°C and 50°C and at three different brine salinities – 0.5%, 6% and 12% NaCl with 0.2% CaCl<sub>2</sub>.

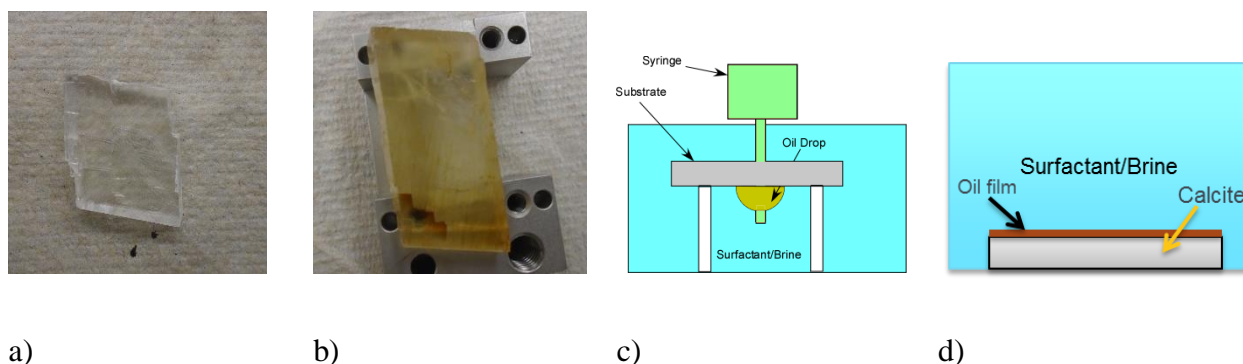


Figure 2.1. a) Cut and polished calcite plate. b) Calcite aged in crude oil. c) Schematic of contact angle experiment. d) Schematic representation of oil-film over a calcite surface.

The ageing of calcite in crude oil alters the water-wet surface to an oil-wet one. Polar compounds in resins and asphaltenes behave as wettability altering agents because of their amphiphilic nature.<sup>3-4</sup> The presence of thin water-film on calcite surface can enable accumulation of polar and charged components present in crude oil near the oil-water interface. The resulting ionic interactions with the mineral surface often lead to removal of the water film and subsequent adsorption onto the surface, making them oil-wet.

### 2.4.3. Oil Film Experiments

For the oil film experiments, a similar procedure to age the calcite plates is followed as before. However, the excess oil is now allowed to evaporate at a temperature of 100°C rather than being dripped off so that a relatively thick layer is available for observation. After ageing the plates are kept in surfactant/brine solutions and the surface is monitored to check for the oil-film decomposition. One such plate is shown in Fig. 2.15a.

In order to confirm the mechanism of oil detachment, two additional experiments are performed. For the first, oil-aged plates are prepared as described for the oil-film experiments. Once, prepared artificial striations are introduced on the film using a sharp pin, making sure that the film layer has been disturbed to expose the bare calcite. Representative image can be seen in Fig. 2.16f.

For the second confirmation experiment, a bare calcite plate is first cleaned and a drop of oil was placed at the center of the plate as a patch. The calcite surface is then allowed to age at an elevated temperature of 120°C for 48 hours. At the end, a calcite surface exhibiting mixed wettability is obtained.

## **2.5. RESULTS AND DISCUSSIONS**

### **2.5.1 Phase Behavior**

Figures 2.2 and 2.3 show examples of phase behavior for select surfactants at different salinities and at two different temperatures - 80°C and 50°C. At 80°C for SAE-12 and SAE-15, separate microemulsion phases are clearly visible for intermediate salinities. At high salinities, a solid wax like layer of similar appearance often forms at the oil-water interface, like at 10% NaCl + SAE-15. The difference from a microemulsion can be understood from the fact that these solid depositions can only be removed through vigorous shaking. For SAE-20 a slight microemulsion formation was observed at about 6% salinity. No microemulsion phases were observed for NP-40 and higher surfactants from the same family. At a lower temperature of 50°C, the extent of microemulsion formation is reduced significantly. SAE-12 showed a slight yellowish oil-water interface at the highest salinity. An excess oil-phase corresponding to surfactants being in the aqueous phase was observed for all other surfactants at this temperature. Table 2.2 displays the phase behavior results for all the surfactants analyzed. Since most of the surfactants didn't exhibit prominent



microemulsion formation at 50°C, all of them were used for the next set of contact angle evaluations. Two additional nonionic surfactants were also evaluated and their results are shown in Appendix 1.

### **2.5.2. Contact Angle**

Figure 2.4 shows the initial and final contact angles, for selected surfactants at 25°C and a brine salinity of 12% NaCl, 0.2% CaCl<sub>2</sub>. The contact angles are measured from the denser aqueous phase as shown in Fig. 2.4a. In all cases the initial contact angle is around 150-165°, indicating an initially oil-wet surface. In the absence of surfactant, there was no detectable change in contact angle (Fig. 2.4a). Upon addition of surfactants, the final contact angles decreased, indicating an increase in the hydrophilicity of the original oil-wet surface.

As mentioned previously the properties of nonionic surfactants depend on temperature of the system. It is known that these surfactant solutions start becoming “cloudy” on being heated beyond a certain temperature. The temperature at which this happens is referred to as the cloud point. It is a consequence of decreased hydration of oxyethylene chains with increase in temperature. Table 2.3 shows the cloud points of the surfactants studied at the selected brine salinity.

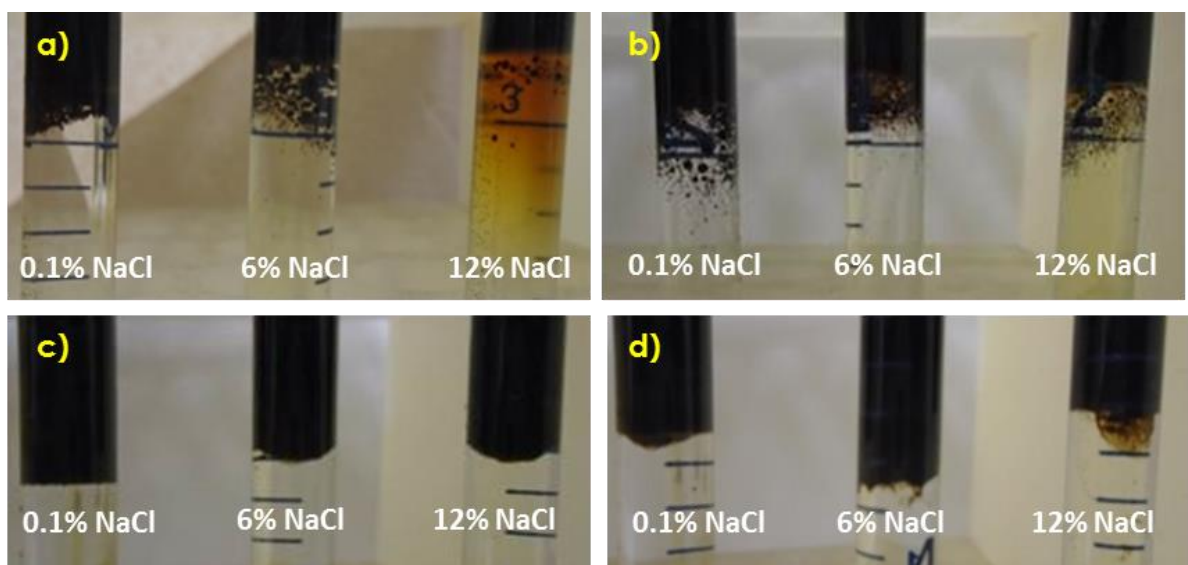


Figure 2.2. Phase behavior results at 50°C for a) SAE-12 b) SAE-15 c) SAE-20 and d) NP-40

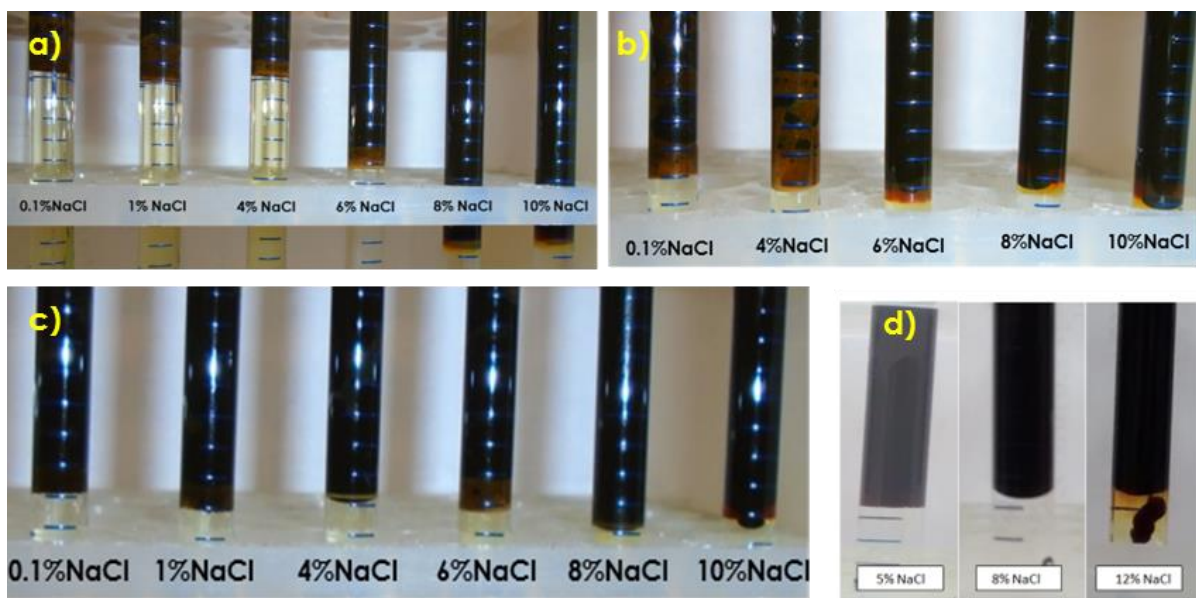






Figure 2.3. Phase behavior results at 80°C for a) SAE-12 b) SAE-15 c) SAE-20 and d) NP-40.

Table 2.2. Phase behavior results -  - No microemulsion phase,  - Separate microemulsion,  - Slight three-phase separation  - Wax like deposition. The columns indicate brine salinity (% NaCl by weight).

Surfactant	1%		2%	3%	4%	5%	6%		8%	10%	12%	
SAE-12	80°C		50°C	50°C	80°C	80°C	80°C	50°C	80°C	80°C	80°C	50°C
SAE-15	80°C	50°C	80°C	80°C	80°C	80°C	80°C	50°C	80°C	80°C	80°C	50°C
SAE-20	80°C	50°C	80°C	-	80°C	80°C	80°C	50°C	80°C	80°C	80°C	50°C
SAE-40	80°C	50°C	60°C	60°C	80°C	80°C	80°C	50°C	80°C	80°C	80°C	80°C
NP-40	-		-	-	-	80°C	80°C	50°C	80°C	-	80°C	50°C
NP-50	80°C		-	-	-	80°C	80°C	50°C	80°C	80°C	80°C	50°C
NP-70	-		60°C	60°C	60°C	80°C	80°C	50°C	80°C	-	80°C	50°C

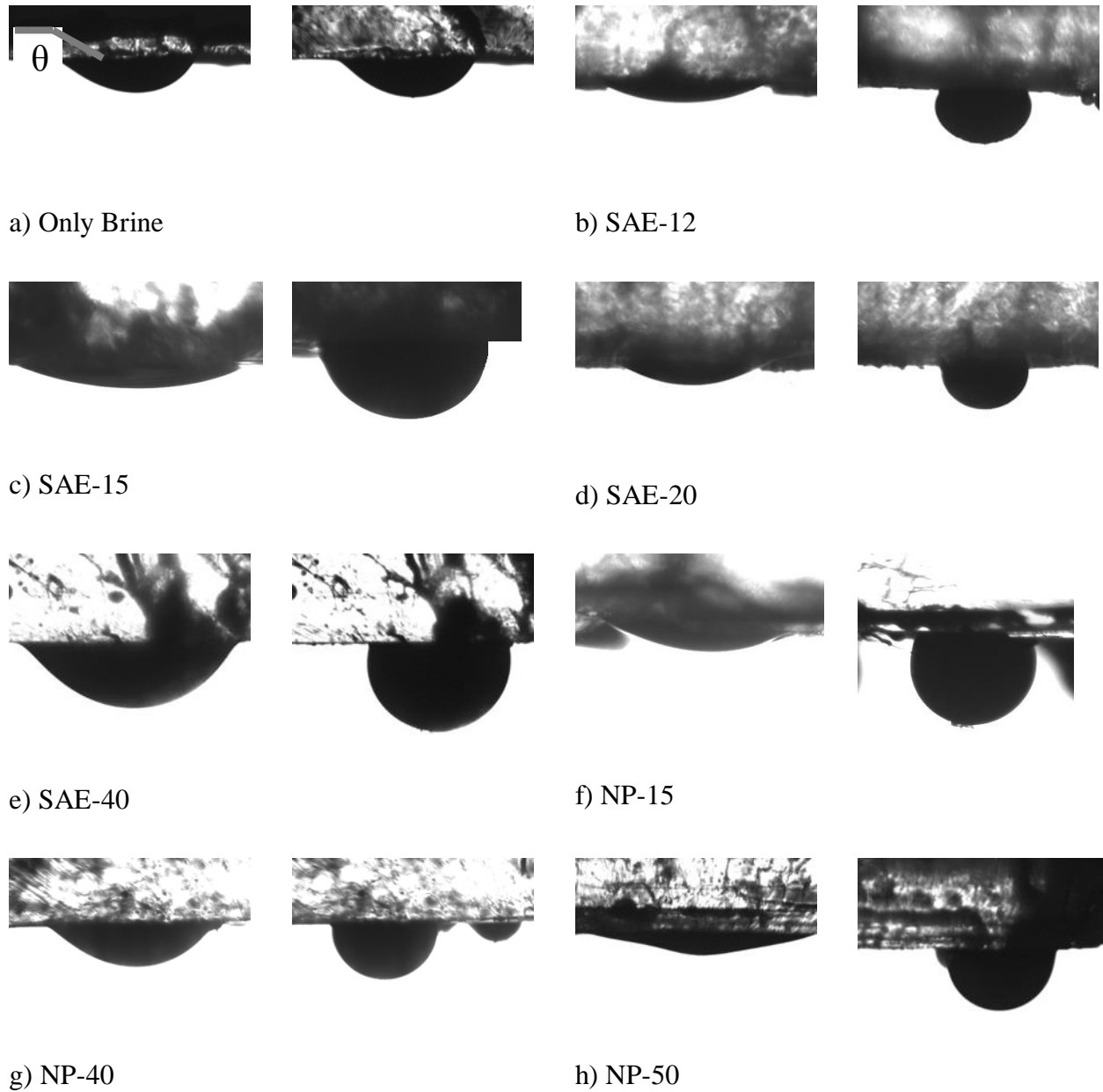


Figure 2.4. Initial and final oil drop states at 25°C and brine salinity of 12% NaCl, 0.2% CaCl<sub>2</sub> for a) no surfactant b) SAE-12 c) SAE -15 d) SAE-20 e) SAE-40 f) NP-15 g) NP-40 and h) NP-50

Table 2.3: Cloud points of nonionic surfactants measured in 12% NaCl, 0.2% CaCl<sub>2</sub> brine.

No. of EO units(x)	Cloud point of SAE-x (°C)	Cloud point of NP-x (°C)
12	55	52
15	66	69
20	77	-
30	85	78
40	79	80
50	-	77

Figure 2.5 shows bar plots of the final contact angles obtained for a series of SAE and NP surfactants with varying lengths of ethoxylate groups. For both families of surfactants, the final contact angles decrease as the temperature is increased. This behavior can be explained by the decrease in solubility of nonionic surfactants in water with a concomitant increase in adsorption over the oil-wet surface and a better wettability alteration<sup>41</sup>. The cloud point values can be used as a reference for the solubilities of the surfactants. Similar behavior has been observed in the past for wettability alteration involving nonionic surfactants.<sup>15</sup>

Figures 2.6a-c depicts the final contact angle in the system as a function of the hydrophilic length of surfactants for the alcohol ethoxylate and NP families of surfactants at different temperatures. In each case the final contact angle tends to increase as the hydrophilic portion of the surfactant is increased. This equates to a low wettability alteration in the system. The rather suppressed change going from 12 EO surfactant to 15

EO surfactant, in both the cases, can be attributed to the close proximity of the two surfactants in the homologue series and significant overlap in their molecular composition. The extent of wettability alteration depends upon the capacity of the surfactant molecules to adsorb onto the oil-wet surface. This adsorption capacity is expected to decrease with increasing hydrophilicity and corresponding solubility in the aqueous phase, giving rise to higher final contact angles. Subsequently, it can be said that wettability alteration improves by increasing the hydrophobicity of a surfactant. From SAE-30 to SAE-40 and NP40-NP50 a deviation from the usual trend is observed. The final contact angle values for SAE-40 are lower than SAE-30. NP-50 shows a slightly smaller contact angle values than NP-40. It has been found that the cloud point of similar oxyethylene based nonionic surfactants first increases with increasing EO units, reaches a maximum around EO =30-40 and then decreases upon further increase of EO units.<sup>42</sup> This is true from our measurements of cloud points also.

At low and intermediate temperatures NP surfactants perform better than alcohol ethoxylate surfactants with the same number of hydrophilic groups. The difference becomes less prominent at higher temperatures. This implies that for the specific crude oil analyzed in the study, the final wettability change is rather indistinguishable between the secondary alcohol and nonylphenol hydrophobe groups and is mainly determined by the number of hydrophilic units present in the molecules. For NP-12 the highest temperature at which the experiment is done is 45°C to avoid going beyond the cloud point.

The effect of salinity on wettability alteration was studied by repeating the contact angle experiments at different salinities. In most surfactants the effect of increasing salinity had a negligible effect on the final contact value as can be seen in Fig. 2.7a. Similar observations were made at higher temperatures also for SAE-15 and SAE-20.

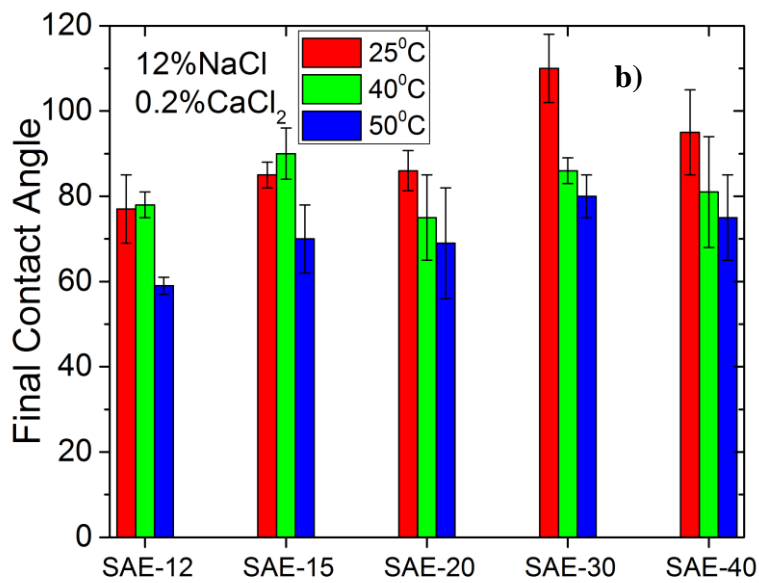
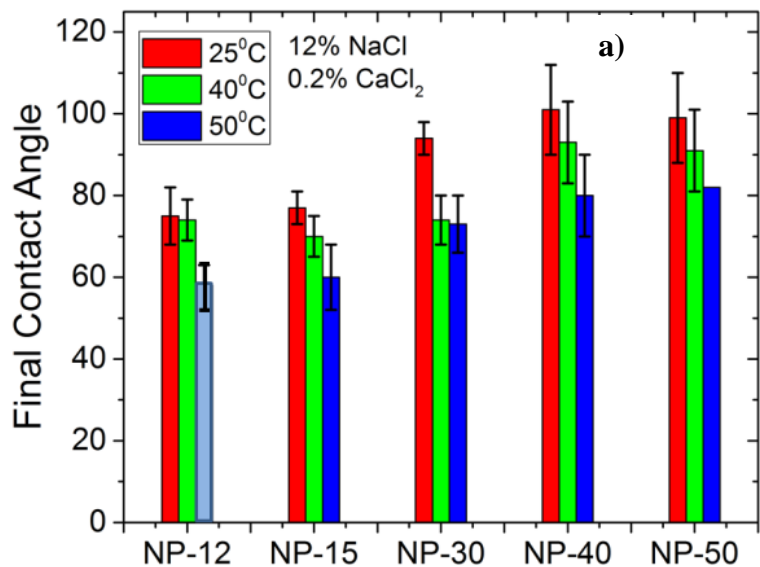


Figure 2.5. Final contact angles for a) NP-x and b) SAE-x at different temperatures. The light blue bar is for NP-12 at 45°C

SAE-12 showed deviations from the usual trend at intermediate salinities. The final contact angles for SAE-12 and SAE-15 at different salinities and temperatures are shown in Fig. 2.7b.

Wettability alteration has been found to be dependent on the brine salinity and in particular to the concentration of potential-determining divalents.<sup>8,39-40</sup> Sulfate and calcium ions have been found to be effective in changing oil-wet chalk to preferential water-wet, particularly at high temperatures.<sup>40</sup> Sulfates have been known to influence charge distribution on mineral surfaces. In case of carbonate surfaces, the sulfates can reduce the positive charge density which can lead to increased surface accumulation of cations like  $\text{Ca}^{2+}$ ,  $\text{Mg}^{2+}$ . These cations can remove adsorbed carboxylates by forming ion-pairs with them thus altering the wettability. Sulphates can also simply promote carboxylate desorption via a single displacement mechanism on the positively charged carbonate surface. In order to study this contact angle experiments were done for two different sulfates concentration, 0.5% and 2% by weight, at 40°C for the different surfactants. Fig. 2.8 shows the change in the shape of the drops because of the presence of sulfates and Fig. 2.9 shows the final contact angles for different sulfate concentrations. It can be seen from the figures that irrespective of surfactant type,  $\text{SO}_4^{2-}$  enhances the wettability alteration and the enhancement increases with an increase in the  $\text{SO}_4^{2-}$  concentration.



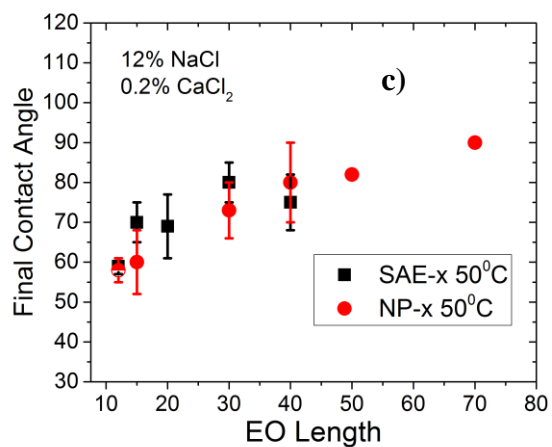
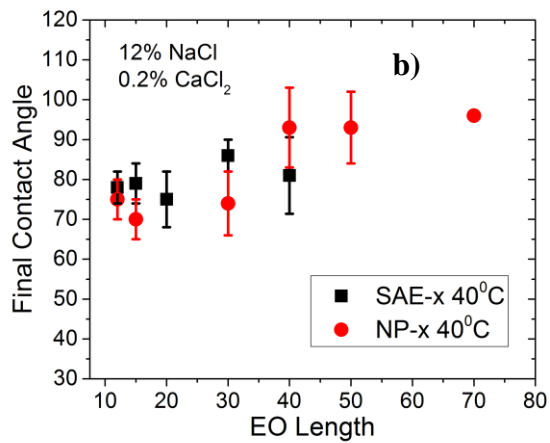
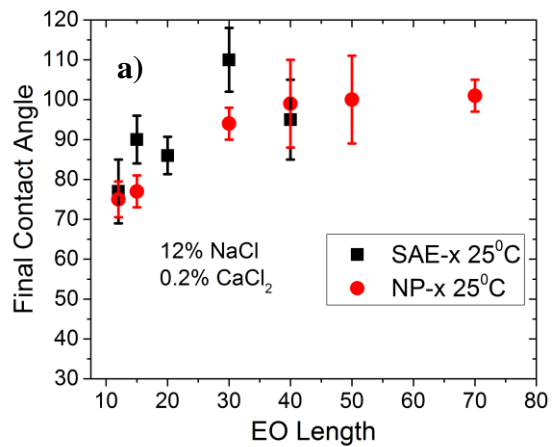


Figure 2.6. Final contact angle vs hydrophile chain length for SAE and NP surfactants at a) 25°C b) 40°C and c) 50°C. The half-filled circle denotes an experiment done at 45°C.

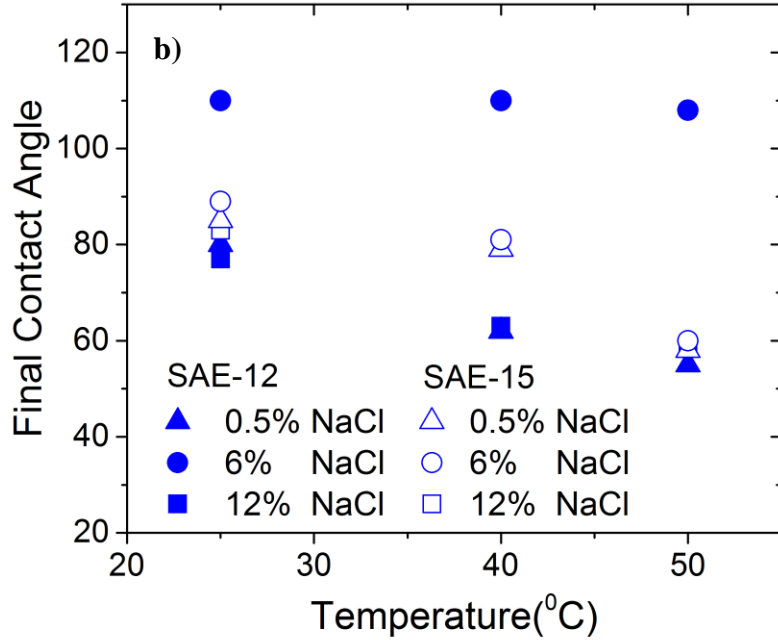
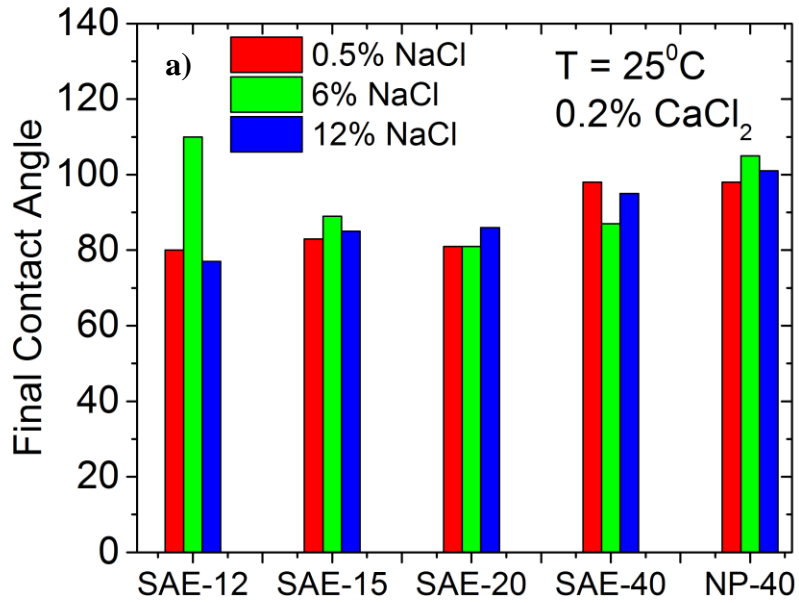


Figure 2.7. Final contact angles vs brine salinity at a)  $25^{\circ}\text{C}$ . b) Final contact angles for SAE-12 and SAE-15 at  $25^{\circ}\text{C}$ ,  $40^{\circ}\text{C}$  and  $50^{\circ}\text{C}$  as a function of brine salinity

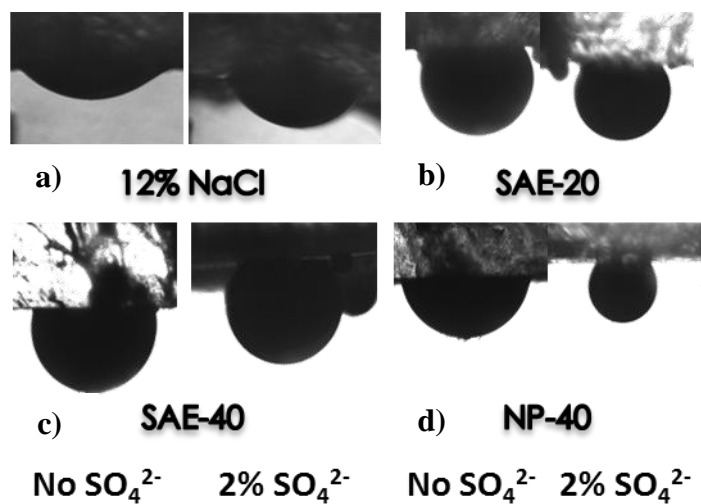


Figure 2.8. Effect of  $SO_4^{2-}$  addition to 12% NaCl brine at 40°C for a) No surfactant b) SAE-20 c) SAE-40 and d) NP-40

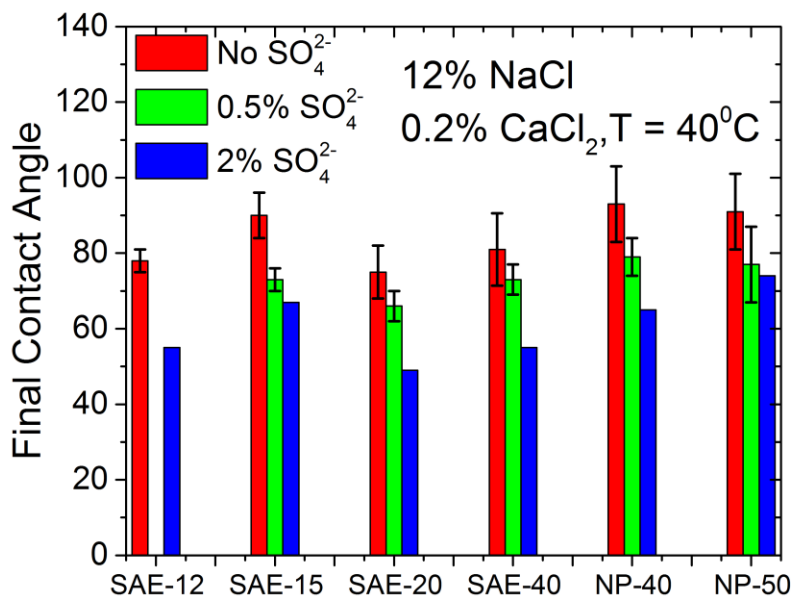


Figure 2.9. Final contact angle vs  $SO_4^{2-}$  concentration at 12% NaCl brine at 40°C

In order to decipher a mechanism explaining surfactant action to improve wettability alteration, contact angle data are collected at regular intervals until equilibrium is reached. The change of contact angle with time at different temperatures is plotted for different surfactants in Figs. 2.10 and 2.11. The plots in Fig. 2.10a-c depict the transient contact angle measurements for SAE-15, SAE-20 and SAE-40 at 25°C, 40°C and 50°C respectively. Fig. 2.11a-c similarly represent the transient behavior of NP-15, NP-40 and NP-50 the three temperatures. It can be seen from the plots that most of the change in contact angle happens in the first 5-10 minutes, after which the contact angle slowly decays to its equilibrium value. The two different timescales are easily observed in these two plots. It is also evident from the plots that the evolution of contact angle occurs at a faster rate as the temperature is increased from 25°C to 50°C. In order to understand the dependence of contact angle evolution on surfactant structure contact angle is plotted for different EO units at same temperature. Figs. 2.12a-b depict such transient contact angle measurements for SAE-x at 50°C and NP-x at 40°C respectively. For the alcohol ethoxylate series of surfactants, there is a monotonic trend observed in the plot; contact angle evolves faster for surfactant molecules with smaller hydrophilic units. The trend is, however, not so evident for the NP family, in which the presence of an aromatic phenol group gives rise to a non-monotonic evolution behavior with an increase in the hydrophilic units.

In order to quantify the evolution of contact angle, a first order decay equation,

$$\theta = \theta_{\infty} + [\theta_0 - \theta_{\infty}] \exp(-t/\tau) \quad , \quad (1)$$

is then used to fit the contact angle data with time and extract the values of time-constants,  $\tau$  for each of the surfactants. Here  $\theta$  is the measured contact angle as a function of time  $t$ .  $\theta_0$  and  $\theta_{\infty}$  are the initial and final contact angles respectively. The fitted curves for the two surfactant classes are shown in Fig. 2.12a and Fig. 2.12b.

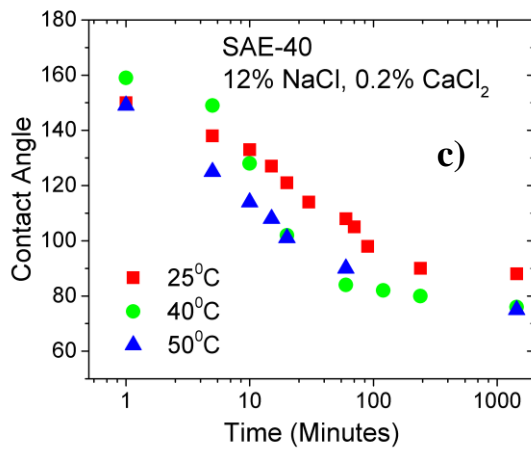
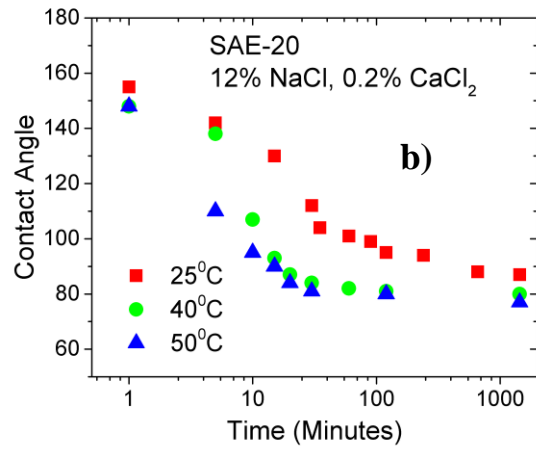
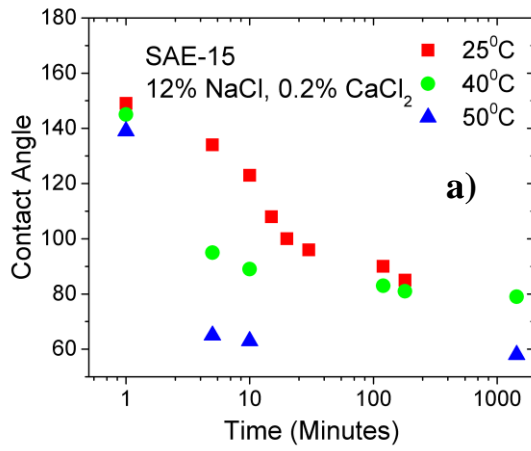


Figure 2.10. Evolution of contact angle with time for a) SAE-15 b) SAE-20 and c) SAE-40. Contact angle evolution is shown for three different temperatures.

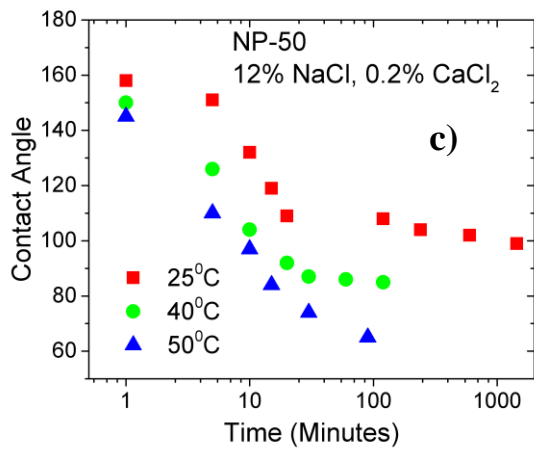
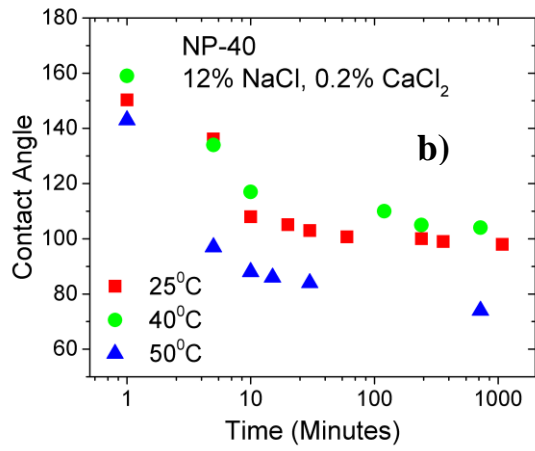
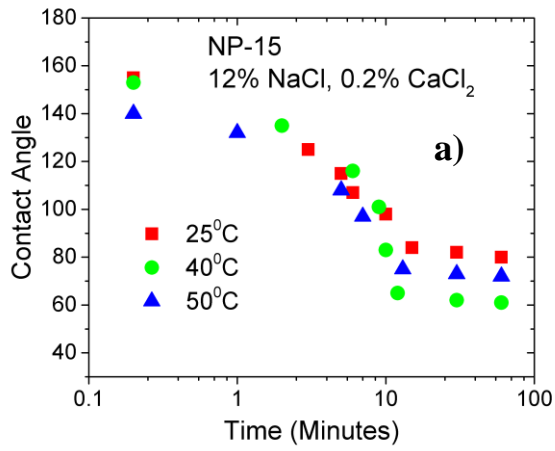


Figure 2.11. Evolution of contact angle with time for a) NP-15 b) NP-40 and c) NP-50. Contact angle evolution is shown for three different temperatures.

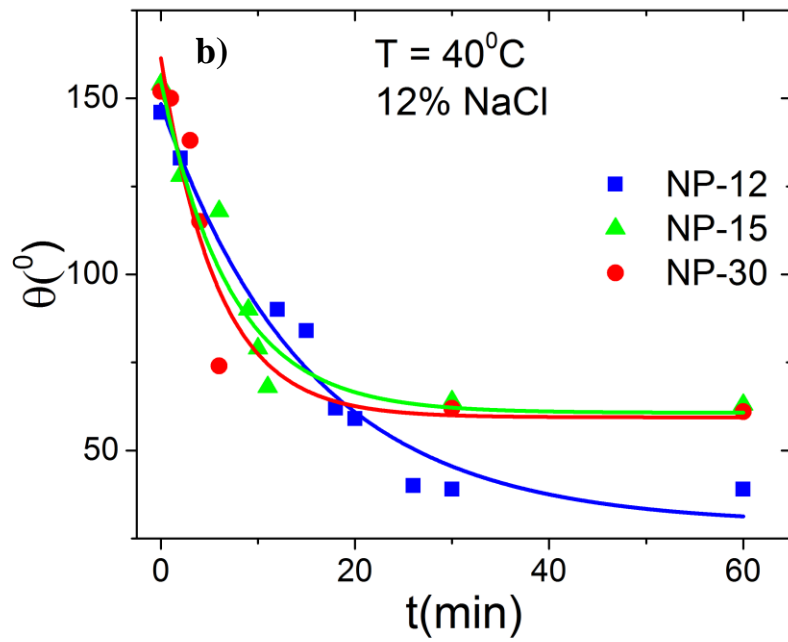
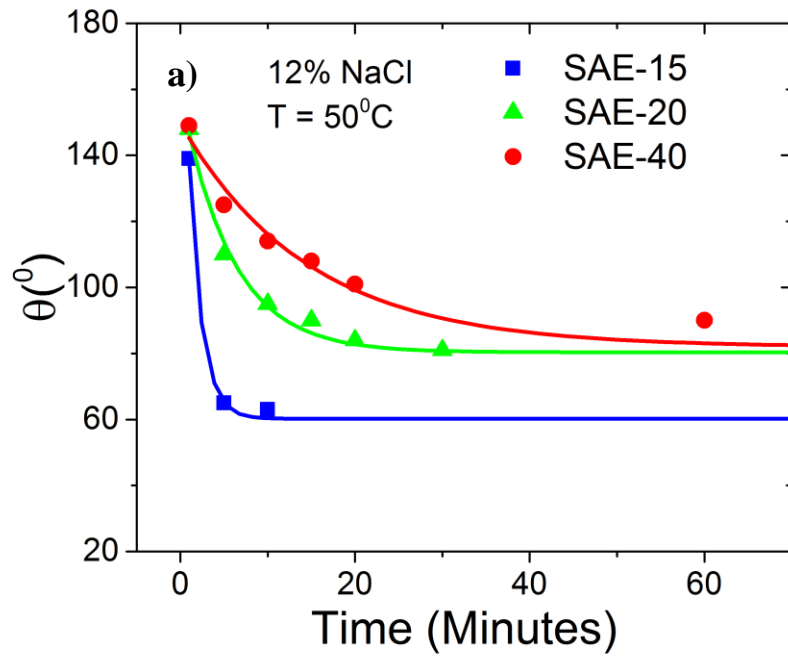


Figure 2.12. Effect of surfactant size on contact angle evolution – Contact angle vs time for a) SAE-x at 50°C and b) NP-x at 40°C.

The fitted time-constants for the two groups of surfactants at different temperatures are shown in the bar plots in Fig. 2.13a-b. The time-constants are found to increase with an increase in hydrophilic units for alcohol ethoxylate series while the variation is much more muted for NP surfactants with shorter hydrophilic chains. A clear monotonic trend is also observed as the time-constants decrease with temperature for all surfactants. This particular trend is akin to an activated process and can help point out the principal mechanism for wettability alteration in a drop setup. Time-constants for each surfactant are extracted at different temperatures by collecting the dynamic contact angle data at three different temperatures.

The corresponding time-constant vs temperature plots are shown in scatter plots in Fig. 2.14a and Fig. 2.14b. It is clear from the plots that contact angle reaches steady state faster at higher temperatures. The activation energies associated with each surfactant is then estimated by fitting the time-constant values in an Arrhenius plot,

$$\tau = \tau_0 \exp\left(\frac{E_a}{RT}\right) \quad (2)$$

as shown in Figs. 2.14a and 2.14b. The individual activation energies  $E_a$  are reported in Table 2.4. Further discussion about the kinetic studies is done in following sections.



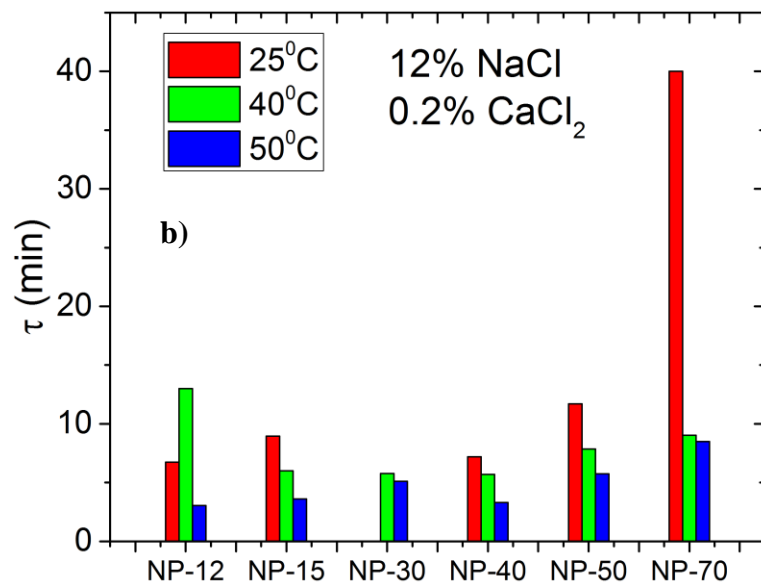
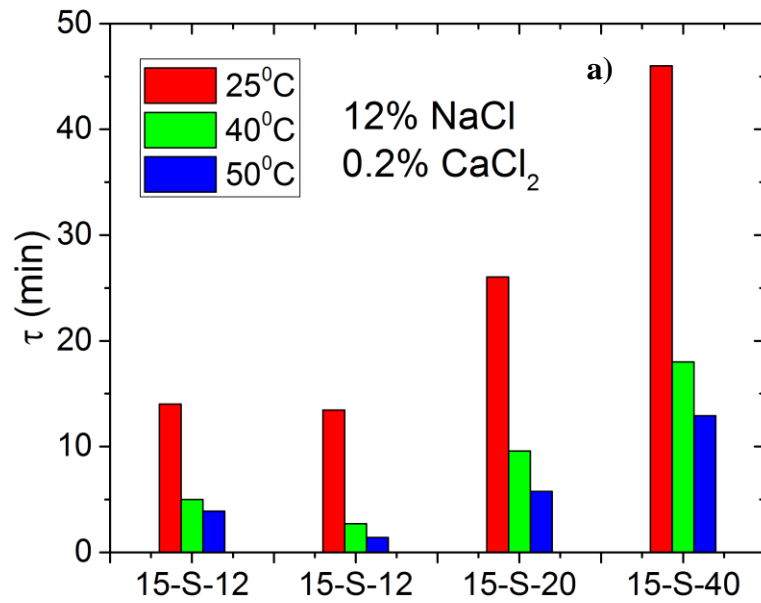


Figure 2.13. Extracted timescales from contact angle measurements for a) SAE-x and b) NP-x at 25°C, 40°C and 50°C.

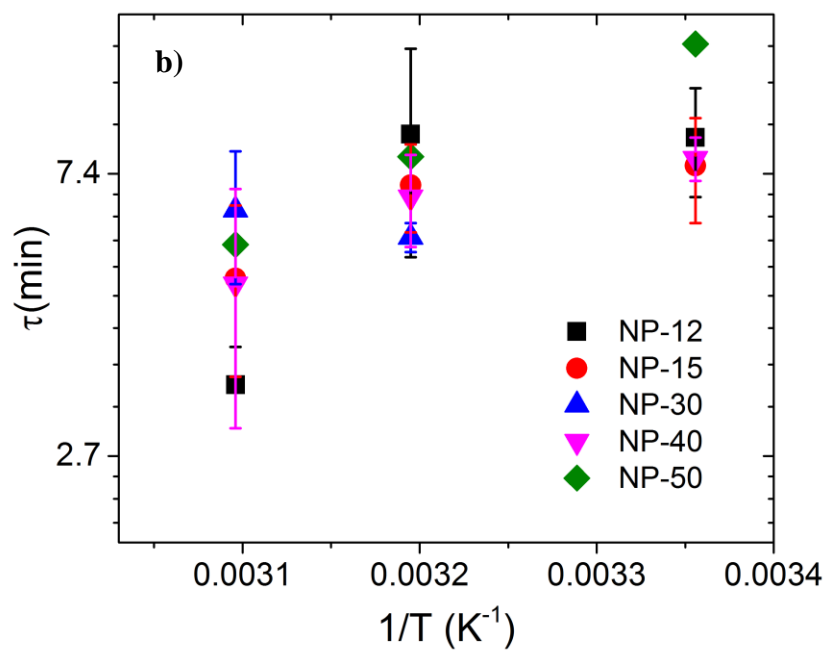
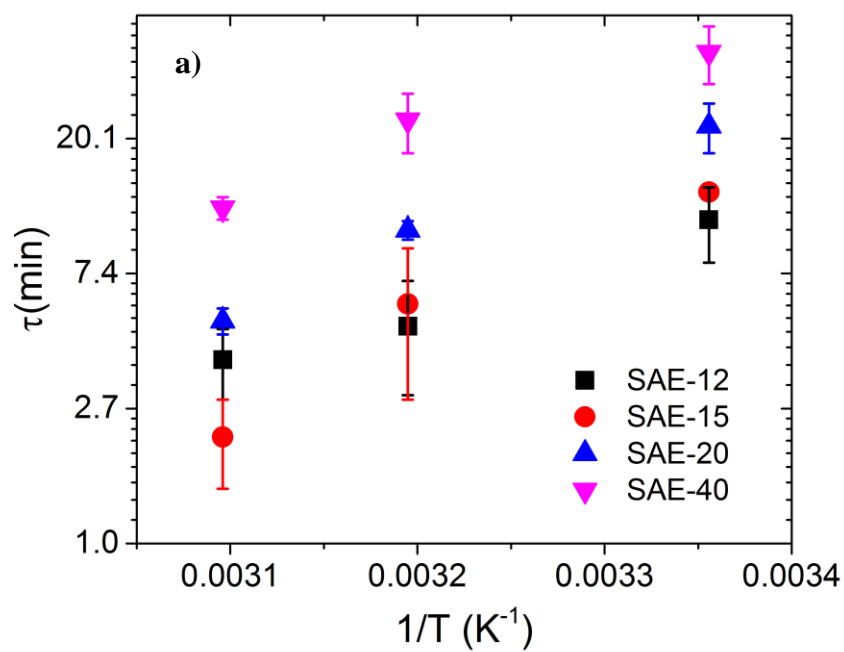


Figure 2.14. Arrhenius plots of timescale vs  $1/T$  for a) SAE-x and b) NP-x surfactants

Table 2.4. Activation energies extracted from timescale values for the evaluated surfactants.

EO length (x)	E <sub>a</sub> (kcal/mol)	
	NP-x	SAE-x
12	6.1 ± 2	8.2 ± 3
15	2.9 ± 0.3	13.6 ± 4
20	-	10.9 ± 1.4
30	4 ± 1	-
40	3.3 ± 1	8.6 ± 2
50	5.4 ± 0.3	-

### 2.5.3. Oil Film Experiments

Fig. 2.15 shows the top and side views of an oil-aged calcite plate for different surfactants. The topmost figure corresponds to the case when there is no surfactant present. No significant change in the oil-film is observed in this case as can be seen from the undisturbed top and side views. The effect of surfactant addition is clear in the next set of images. From the oil-film images corresponding to SAE-15 and NP-40, it seems the oil layer starts retreating across the surface with a gradual decrease in the oil coverage. This process typically takes place over an hour and after that oil is found in a beaded up state on the surface with bare calcite exposed in multiple regions. Molecular simulations involving cationic surfactant, oil and mineral substrates have shown that after the initial hydrophobic interaction-based aggregation of the surfactant molecules on the oil-water interface, the surfactant molecules are able to destroy the ordered arrangement of oil molecules on the substrate.<sup>43-44</sup> This then enables water molecules to enter the oil/substrate interface leading

to the formation of water channels, which slowly widens over time leading to oil detachment. One could expect similar behavior for nonionic surfactants.

Oil detachment from calcite can also occur if the surfactant molecules can access the contact line through surface “defects”. These defects can be thought to be analogous to mixed-wet surfaces present in many oil reservoirs and also in reservoirs with high water saturation. To confirm this hypothesis these defects can be artificially added onto the oil-wet surface. Two additional experiments were carried out – one where the state of an oil patch was monitored in the presence of surfactants and other where defects were manually added to the oil layer and the resulting behavior was observed. The results can be seen in Fig. 2.16. Brine solution in itself didn’t have any effect on the oil patch as can be seen from the topmost images in the figure. In presence of NP-40 at 50°C, the oil patch started retracting and eventually ended up in a beaded state. In the next experiment, line defects were added onto the oil layer and it was found that the oil layer started retracting along these defects very prominently. The top view at 10 mins for NP-40 clearly shows four separate oil groups which have been formed because of the added defects.



Figure 2.15. Images from oil-film experiments at 12% NaCl salinity at 50°C. Colored images show the top view and black-white images show the side view for a) No surfactant at t = 0 b) No surfactant at t = 120 mins c) SAE-15 at t = 0 d) SAE-15 at t = 25 mins e) SAE-15 at t = 60 mins f) NP-40 at t = 0 g) NP-40 at t = 10 mins and h) NP-40 at 60 mins

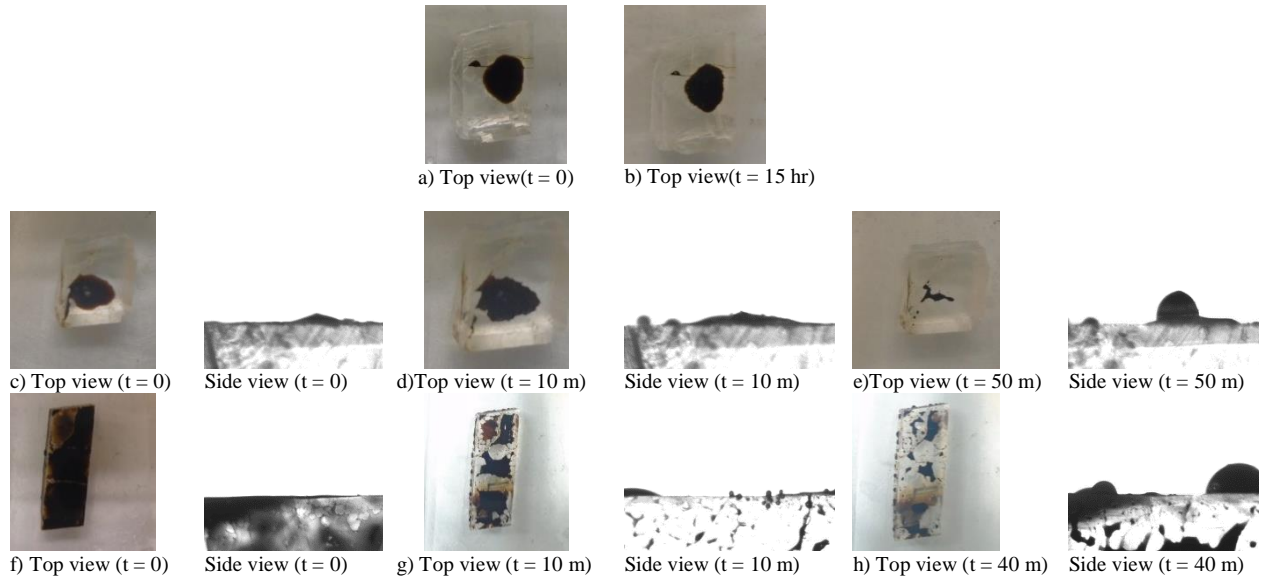


Figure 2.16. Images from oil-patch experiment with 12% NaCl salinity at 50°C. Colored images show the top view and black-white images show the side view for a) No surfactant at t = 0 b) No surfactant at t = 15 hrs. c) NP-40 at t = 0 d) NP-40 at t = 10 mins e) NP-40 at 50 mins. f) Initial g) Intermediate and h) Final states of an oil-film experiments done with a “defective” aged surface. Note the artificial striations in f)

Important conclusions can be inferred from the activation energy values and the time-scales involved in the evolution of contact angles. The activation energies associated with the self-diffusion of typical concentrated nonionic surfactants are in the order of 26-40kcal/mol<sup>45</sup>, which is significantly larger than the values reported here. This along with the fact that all the solutions are well-mixed prior to each experiment eliminates any diffusion-controlled process being responsible for the wettability alteration. Another possible explanation for the change in contact angle of the drops is a viscous spreading mechanism, the expression for which was derived by Tanner.<sup>46</sup> The scaling equation for this flow can be obtained from the thin-film lubrication approximation

$$\frac{dR}{dt} = \frac{h^2}{3\mu} \frac{\partial}{\partial x} \left( \gamma \frac{\partial^2 h}{\partial x^2} \right) \quad (3)$$

Typical time-scale values for such a process are given by

$$\Delta t \sim \frac{\mu \Delta R (\Delta x)^3}{\gamma_{ow} h^3} \quad (4)$$

where  $\gamma_{ow}$  is the oil-water interfacial tension,  $R$  is the typical radius associated with the drop during the change and  $\mu$  is the viscosity. This value is of the order of 0.01 to 1 s and is significantly smaller than the timescales obtained from the experiments. In the absence of diffusion and viscous driven mechanism, interfacial adsorption is the most likely explanation kinetic limitation for the wettability alteration. This proceeds by a combination of coating and sweeping mechanism as described below. Initially, the hydrophobic moiety of surfactants adsorb on hydrophobic surfaces with their head groups pointing towards the solution. This generates a temporary hydrophilic surface on account of surfactant coating which promotes favorable interaction with the water molecules near the surface as shown in Fig. 2.17a. The dangling hydrophilic components reduce the water-calcite surface energy near the three-phase contact line. Water aided by the surfactant molecules on the nearby hydrophobic locations then displaces or “sweeps” the oil away exposing the solid surface underneath. This is made possible by the very strong hydrophilic zone created by the adsorbed surfactants near the defects as shown in Fig. 2.17b-c. The final contact angle and the activation energy values corroborate with the above mechanism. Activation energy values seem to be fairly constant over the length of hydrophilic chains evaluated in the study for both the surfactants. The values however differ for the two hydrophobe classes. This points to a more hydrophobic-interaction dominated energy barrier. Initially surfactant adsorption on the surface is driven mainly by the hydrophobic interactions between the oil-wet surface and the hydrophobic chains. Once near the surface, as the oil is swept away, more of the substrate gets exposed to water and the hydrophilic interactions with calcite and water molecules increase and start dominating. Thermodynamically

speaking, the water-calcite surface energy decreases with the adsorption of surfactants which leads to the receding of three-phase contact line. This enhanced water-calcite interaction explains the similar final contact angle values reported at the highest temperature for both the surfactants when the hydrophile lengths are the same and when the effect of the hydrophobic energy barrier is the least. The exact nature of the energy barrier however needs further evaluation. It can be either due to surfactant-hydrophobic layer interaction, or the sweeping process or a combination of both. The case of 12 EO units for both SAE and NP seem to be an exception. It can be seen that the final contact angle is independent of the hydrophobe group at all temperatures. Another observation from the contact angle experiments is that the final contact angle value increases with an increase in the hydrophilicity of the surfactant. Both these behaviors can be explained by a combination of surfactant interactions in the bulk and on the surface. Surface activity of the surfactants reduces as the hydrophilicity is increased owing to better hydration by the water molecules. For SAE-12 and NP-12, this means higher availability of surfactants near the three-phase interface leading to higher decrease in water-calcite surface energy. It would seem that the hydrophobic energy barrier is least consequential for 12 EO units. However, this is not the case for molecules with larger hydrophilic units. Also, as the surfactant molecules accumulate in the strong hydrophilic zone near the defects, the hydrophilic repulsions between the polar head groups increase and become a significant factor for the molecules with bulkier hydrophile groups. The final wettability state is then determined by the effective surfactant-water-surface interactions instead of being a monotonic function of its hydrophilicity. These effective interactions are investigated in the following chapters through a combination of adsorption experiments and molecular dynamics simulations.



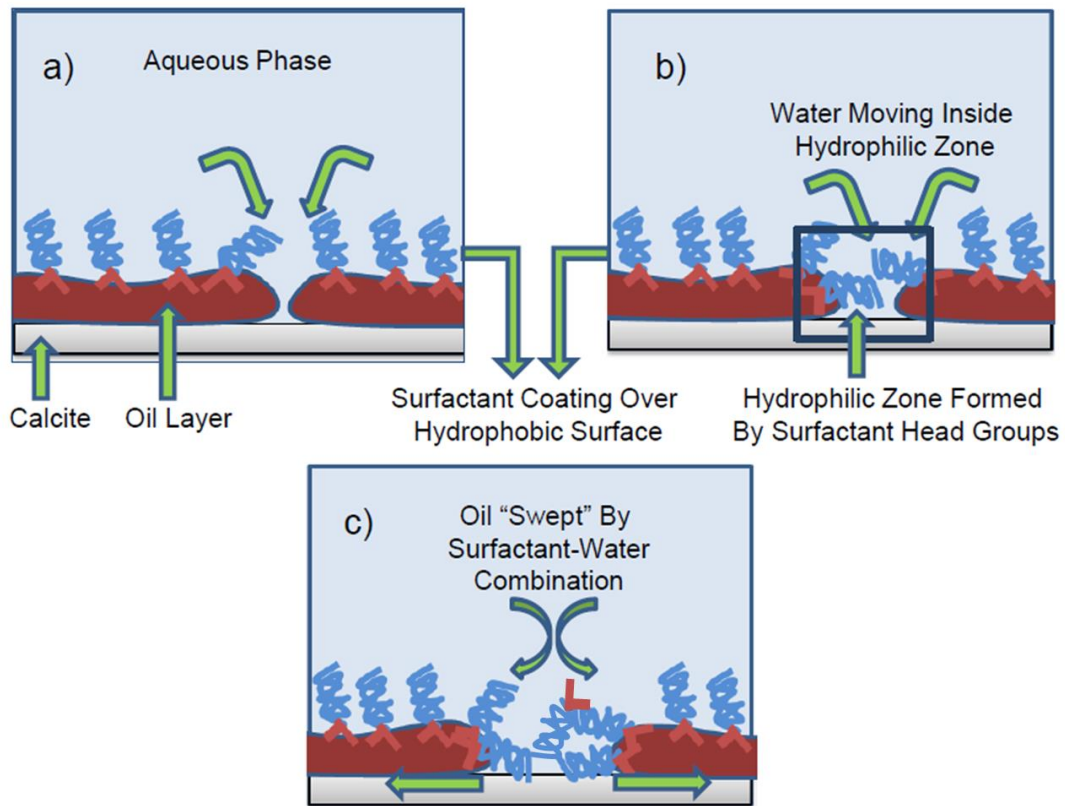


Figure 2.17. Schematic of the proposed mechanism of wettability alteration. Blue spirals represent the hydrophilic moiety of the surfactants. a) Initial oil-wet surface with micro-defects. b) Hydrophilic zone formed by surfactant coating c) Oil "sweeping" as shown in green arrows - by surfactant and water.

## 2.6. CONCLUSIONS

Nonionic surfactants of two distinct groups have been evaluated in the study to measure their wettability alteration properties on oil-aged calcite surface. The hydrophilic groups were varied to study the effect of surfactant hydrophilicity along with the nature of hydrophobe. Wettability alteration is found to depend significantly on the surfactant structure. The final contact angle decreases with decrease in surfactant hydrophilicity as well as with an increase in temperature, implying better wettability alteration at these conditions. Kinetic analysis of the experiments revealed enhanced wettability alteration rates at higher temperatures. The time-scales for different surfactants were then used to extract the activation energy or the energy barrier associated with the wettability alteration process. Together with a series of qualitative oil-film experiments, these energy values were then used to generate a simple model explaining the mechanism of surfactant action. A combination of coating and sweeping mechanism is proposed for the same. The current work is an important step in the direction of evaluation and design of nonionic surfactants for wettability alteration of carbonate surfaces. Similar methodology, in principal, can also be implemented to study wettability alteration and cleaning of any mineral oxide surfaces in the presence of surfactants. Wettability alteration is dependent on the molecular structure and the temperature of the system. These factors determine the extent of surfactant adsorption which needs investigation. Surfactant interactions with different interfaces are actually driven by molecular-scale processes. A complete understanding of mechanism of wettability alteration can hence be obtained from adsorption experiments complemented with suitable atomistic simulations. These are discussed in the following chapters.

## REFERENCES

1. Schlumberger Market Analysis, **2007**.
2. Salathiel, R. A. Oil recovery by surface film drainage in mixed-wettability rocks. *Journal of Petroleum Technology*, **1973**, 25(10), 1-216.
3. Buckley, J. S., Liu, Y., & Monsterleet, S. Mechanisms of wetting alteration by crude oils. *SPE journal*, **1998**, 3(01), 54-61.
4. Al-Maamari, R. S., & Buckley, J. S. Asphaltene precipitation and alteration of wetting: the potential for wettability changes during oil production. *SPE Reservoir Evaluation & Engineering*, **2003**, 6(04), 210-214.
5. Strand, S., Standnes, D. C., & Austad, T. Spontaneous imbibition of aqueous surfactant solutions into neutral to oil-wet carbonate cores: Effects of brine salinity and composition. *Energy & fuels*, **2003**, 17(5), 1133-1144.
6. Standnes, D. C., & Austad, T. Wettability alteration in carbonates: Interaction between cationic surfactant and carboxylates as a key factor in wettability alteration from oil-wet to water-wet conditions. *Colloids and Surfaces A: Physicochemical and Engineering Aspects*, **2003**, 216(1-3), 243-259.
7. Austad, T., & Standnes, D. C. Spontaneous imbibition of water into oil-wet carbonates. *Journal of Petroleum Science and Engineering*, **2003**, 39(3-4), 363-376.
8. Zhang, P., & Austad, T. Wettability and oil recovery from carbonates: Effects of temperature and potential determining ions. *Colloids and Surfaces A: Physicochemical and Engineering Aspects*, **2006**, 279(1-3), 179-187.
9. Adibhatla, B., & Mohanty, K. K. Oil recovery from fractured carbonates by surfactant-aided gravity drainage: laboratory experiments and mechanistic simulations. *SPE Reservoir Evaluation & Engineering*, **2008**, 11(01), 119-130.
10. Seethepalli, A., Adibhatla, B., & Mohanty, K. K. Wettability alteration during surfactant flooding of carbonate reservoirs. In *SPE/DOE Symposium on Improved Oil Recovery*. Society of Petroleum Engineers, **2004**.
11. Hirasaki, G., & Zhang, D. L. Surface chemistry of oil recovery from fractured, oil-wet, carbonate formations. *Spe Journal*, **2004**, 9(02), 151-162.
12. Zhang, J., Nguyen, Q. P., Flaaten, A., & Pope, G. A. Mechanisms of enhanced natural imbibition with novel chemicals. *SPE reservoir evaluation & engineering*, **2009**, 12(06), 912-920.

13. Sofla, S. J. D., Sharifi, M., & Sarapardeh, A. H. Toward mechanistic understanding of natural surfactant flooding in enhanced oil recovery processes: the role of salinity, surfactant concentration and rock type. *Journal of Molecular Liquids*, (2016), 222, 632-639.
14. Wu, Y., Shuler, P. J., Blanco, M., Tang, Y., & Goddard, W. A. A study of wetting behavior and surfactant EOR in carbonates with model compounds. In *SPE/DOE Symposium on Improved Oil Recovery*. Society of Petroleum Engineers, 2006.
15. Gupta, R., & Mohanty, K. Temperature effects on surfactant-aided imbibition into fractured carbonates. *SPE Journal*, 2010, 15(03), 588-597.
16. Sharma, G., & Mohanty, K. Wettability alteration in high-temperature and high-salinity carbonate reservoirs. *SPE Journal*, 2013, 18(04), 646-655.
17. Jarrahan, K., Seiedi, O., Sheykhan, M., Sefti, M. V., & Ayatollahi, S. Wettability alteration of carbonate rocks by surfactants: a mechanistic study. *Colloids and Surfaces A: Physicochemical and Engineering Aspects*, 2012, 410, 1-10.
18. Fletcher, P. D., Savory, L. D., Woods, F., Clarke, A., & Howe, A. M. Model study of enhanced oil recovery by flooding with aqueous surfactant solution and comparison with theory. *Langmuir*, 2015, 31(10), 3076-3085.
19. Fletcher, P. D., Savory, L. D., Clarke, A., & Howe, A. M. Model Study of Enhanced Oil Recovery by Flooding with Aqueous Solutions of Different Surfactants: How the Surface Chemical Properties of the Surfactants Relate to the Amount of Oil Recovered. *Energy & Fuels*, 2016, 30(6), 4767-4780.
20. Bera, A., Ojha, K., Kumar, T., & Mandal, A. Mechanistic study of wettability alteration of quartz surface induced by nonionic surfactants and interaction between crude oil and quartz in the presence of sodium chloride salt. *Energy & Fuels*, 2012, 26(6), 3634-3643.
21. Zhang, R., Qin, N., Peng, L., Tang, K., & Ye, Z. Wettability alteration by trimeric cationic surfactant at water-wet/oil-wet mica mineral surfaces. *Applied Surface Science*, 2012, 258(20), 7943-7949.
22. Schneider, M. H., & Tabeling, P. Lab-on-chip methodology in the energy industry: wettability patterns and their impact on fluid displacement in oil reservoir models. *American Journal of Applied Sciences*, 2011, 8(10), 927.
23. Joseph, J., Gunda, N. S. K., & Mitra, S. K. On-chip porous media: Porosity and permeability measurements. *Chemical Engineering Science*, 2013, 99, 274-283.

24. Howe, A. M., Clarke, A., Mitchell, J., Staniland, J., Hawkes, L., & Whalan, C. Visualising surfactant enhanced oil recovery. *Colloids and Surfaces A: Physicochemical and Engineering Aspects*, **2015**, 480, 449-461.
25. Tiberg, F., Zhmud, B., Hallstenson, K., & Von Bahr, M. Capillary rise of surfactant solutions. *Physical Chemistry Chemical Physics*, **2000**, 2(22), 5189-5196.
26. Starov, V. M., Zhdanov, S. A., & Velarde, M. G. Capillary imbibition of surfactant solutions in porous media and thin capillaries: partial wetting case. *Journal of colloid and interface science*, **2004**, 273(2), 589-595.
27. Starov, V. M. Spontaneous rise of surfactant solutions into vertical hydrophobic capillaries. *Journal of colloid and interface science*, **2004**, 270(1), 180-186.
28. Unsal, E., Broens, M., & Armstrong, R. T. Pore Scale Dynamics of Microemulsion Formation. *Langmuir*, **2016**, 32(28), 7096-7108.
29. Adibhatla, B., & Mohanty, K. K. Oil recovery from fractured carbonates by surfactant-aided gravity drainage: laboratory experiments and mechanistic simulations. *SPE Reservoir Evaluation & Engineering*, **2008**, 11(01), 119-130.
30. Kalaei, M. H., Green, D., & Willhite, G. P. A new dynamic wettability-alteration model for oil-wet cores during surfactant-solution imbibition. *SPE Journal*, **2013**, 18(05), 818-828.
31. Delshad, M., Najafabadi, N. F., Anderson, G. A., Pope, G. A., & Sepehrnoori, K. Modeling wettability alteration in naturally fractured reservoirs. *In SPE/DOE Symposium on Improved Oil Recovery*. Society of Petroleum Engineers, **2006**.
32. Delshad, M., Najafabadi, N. F., & Sepehrnoori, K. Scale Up Methodology for Wettability Modification in Fractured Carbonates. *In SPE Reservoir Simulation Symposium*. Society of Petroleum Engineers, **2009**.
33. Zhmud, B. V., Tiberg, F., & Hallstenson, K. (2000). Dynamics of capillary rise. *Journal of colloid and interface science*, 228(2), 263-269.
34. Hammond, P. S., & Unsal, E. (2009). Spontaneous and forced imbibition of aqueous wettability altering surfactant solution into an initially oil-wet capillary. *Langmuir*, 25(21), 12591-12603.
35. Hammond, P. S., & Unsal, E. Forced and spontaneous imbibition of surfactant solution into an oil-wet capillary: the effects of surfactant diffusion ahead of the advancing meniscus. *Langmuir*, **2010**, 26(9), 6206-6221.

36. Hammond, P. S., & Unsal, E. Spontaneous Imbibition of Surfactant Solution into an Oil-Wet Capillary: Wettability Restoration by Surfactant–Contaminant Complexation. *Langmuir*, **2011**, 27(8), 4412-4429.
37. Hammond, P. S., & Unsal, E. A dynamic pore network model for oil displacement by wettability-altering surfactant solution. *Transport in porous media*, **2012**, 92(3), 789-817.
38. Ma, K., Cui, L., Dong, Y., Wang, T., Da, C., Hirasaki, G. J., & Biswal, S. L. Adsorption of cationic and anionic surfactants on natural and synthetic carbonate materials. *Journal of colloid and interface science*, **2013**, 408, 164-172.
39. Zhang, P., Tweheyo, M. T., & Austad, T. Wettability alteration and improved oil recovery by spontaneous imbibition of seawater into chalk: Impact of the potential determining ions  $\text{Ca}^{2+}$ ,  $\text{Mg}^{2+}$ , and  $\text{SO}_4^{2-}$ . *Colloids and Surfaces A: Physicochemical and Engineering Aspects*, **2007**, 301(1-3), 199-208.
40. Strand, S., Høgnesen, E. J., & Austad, T. Wettability alteration of carbonates—Effects of potential determining ions ( $\text{Ca}^{2+}$  and  $\text{SO}_4^{2-}$ ) and temperature. *Colloids and Surfaces A: Physicochemical and Engineering Aspects*, **2006**, 275(1-3), 1-10.
41. Steinby, K., Silveston, R., & Kronberg, B. The effect of temperature on the adsorption of a nonionic surfactant on a PMMA latex. *Journal of colloid and interface science*, **1993**, 155(1), 70-78.
42. Shigeta, K., Olsson, U., & Kunieda, H. Correlation between micellar structure and cloud point in long poly (oxyethylene)<sub>n</sub> oleyl ether systems. *Langmuir*, **2001**, 17(16), 4717-4723.
43. Liu, Q., Yuan, S., Yan, H., & Zhao, X. Mechanism of oil detachment from a silica surface in aqueous surfactant solutions: molecular dynamics simulations. *The Journal of Physical Chemistry B*, **2012**, 116(9), 2867-2875.
44. Li, X., Xue, Q., Wu, T., Jin, Y., Ling, C., & Lu, S. Oil detachment from silica surface modified by carboxy groups in aqueous cetyltriethylammonium bromide solution. *Applied Surface Science*, **2015**, 353, 1103-1111.
45. Kato, T., Terao, T., & Seimiya, T. Intermicellar migration of surfactant molecules in entangled micellar solutions. *Langmuir*, **1994**, 10(12), 4468-4474.
46. Tanner, L. H. The spreading of silicone oil drops on horizontal surfaces. *Journal of Physics D: Applied Physics*, **1979**, 12(9), 1473.

## **Chapter 3. Universal Scaling of Adsorption of Nonionic Surfactants on Carbonates using Cloud Point Temperatures**

### **3.1 INTRODUCTION**

Surfactants are amphiphilic molecules comprised of hydrophilic and hydrophobic parts. Because of this duality, they tend to be surface-active and can alter the interfacial properties of a multiphase system. This makes them an important ingredient in industrial applications like detergency, lubricants, inks, adhesives and emulsifiers. Introduction of surfactants in a hydrocarbon reservoir can improve oil recovery by reducing the oil-water interfacial tension (IFT) and by changing the wettability of the rock surface from oil wet to water wet.<sup>1-7</sup> An ultra-low IFT lowers capillary forces and improves oil mobilization by the formation of oil-in-water microemulsion.<sup>1-4</sup> Surfactant induced wettability alteration has also been identified as a key mechanism to improve oil recovery<sup>5-7</sup>, particularly where spontaneous imbibition is the dominant physical process.<sup>7-10</sup> To this end, several studies have been done to study wettability alteration and its effect on oil recovery on different mineral substrates. Wettability alteration refers to changing the contact angle at the three phase oil-water-rock contact line. Typically, one wants to change the contact angle from oil-wet to water-wet, or contact angles that reflect a preference for water over oil on the surface of the rock. Wettability can be evaluated by measuring the water-oil contact angle on the substrate and surfactants with lower contact angle value ( $< 80^\circ$ ) have been correlated to higher oil recoveries.<sup>6-9</sup> Along with the contact angle, a moderate to low O/W IFT (1 – 10 mN/m) is ideal for a strong imbibition force for spontaneous imbibition.

A principal factor determining the efficiency of surfactants in wettability alteration of oil reservoirs is the amount that adsorbs on the mineral surfaces. Very high adsorption means more surfactant is needed for wettability alteration and higher cost that may translate to undesirable economics. It is imperative to know about the surfactant-substrate

interactions responsible for adsorption and obtain representative adsorption isotherms for the analysis and design of wettability alteration in oil reservoirs. Here we study the adsorption of nonionic surfactants and present a correlation to predict it based on the temperature and structure of the surfactant.

The dependence of adsorption on water and surface chemistry, surfactant structure has been studied extensively for anionic and cationic surfactants.<sup>11-13</sup> Because of their charges, adsorption of ionic surfactants is determined largely by the surface charge or the zeta potential, which in turn is dependent on the ionic strength of the bulk solution<sup>14</sup> and the charges on the surfactant molecules. Consequently anionic surfactants have been found to have low adsorption on silica surfaces, which acquire a negative zeta potential over a large pH range.<sup>15</sup> On the other hand, anionic surfactants have been found to have a prohibitively high adsorption on positively charged carbonate surfaces.<sup>11, 16</sup> Cationic surfactants typically have a lower adsorption on carbonates than their anionic counterparts<sup>17</sup>; their adsorption, however, was found to depend significantly on the source of the carbonate.<sup>11, 18</sup> In fact higher adsorptions of cationic surfactants on carbonates have often been reported compared to anionic ones.<sup>19, 20</sup> Mechanisms explaining surfactant aggregate formation and adsorption kinetics have also been developed for these surfactants<sup>21-29</sup> particularly on silica adsorbents.<sup>27-28</sup>

Nonionic surfactants typically exhibit a different adsorption mechanism that depends on their structure and their interactions with the bulk phase. These surfactants, particularly, polyoxyethylene alkyl ethers on silica surface, have been investigated by several authors in the past.<sup>30-40</sup> Tiberg et al.<sup>35, 36</sup> studied the structure of adsorbed layers as well as the kinetics of adsorption on different surfaces. While monolayer adsorption was put forward as the mechanism for hydrophobic surfaces, aggregates of the surfactant in the form of micelles or bilayers were shown to form on hydrophilic surfaces. The process of



adsorption of surfactant aggregates on the surface starts in a narrow concentration region before the critical micelle concentration and surface aggregates are present even at small surface coverages. Brinck et al.<sup>29</sup> portrayed a picture of adsorption in which surfactant micelles exchange monomers, predominantly with surface aggregates, present in a thin sub-surface layer which is determined by the surface-surfactant interactions. A single layer of aggregates of nonionic surfactants were proposed to explain the adsorption behavior and kinetics on gold and silica surfaces.<sup>43-45</sup> The effect of surfactant structure on the extent of adsorption was also studied.<sup>30, 33-38</sup> It was found that both surface excesses and surface aggregate sizes decreased with increasing head group size and inter-micellar repulsions were put forth as a possible explanation. Desbene et al.<sup>30</sup> varied the degree of ethoxylation of the molecules and proposed that the adsorption behavior is determined by a combination of primary and secondary adsorption mechanisms which in turn depends on the length of the ethoxylated chain. While the primary mechanism involves hydrogen bonding between hydrophilic component of the surfactant and the silanol groups, the secondary process, which requires lateral interactions between the hydrophobe components, is responsible for aggregate formation and induces a large increase in adsorption. Additionally, nonionic surfactants show an interesting feature of temperature-dependent physicochemical properties and consequently temperature-dependent adsorption has been reported in the past.<sup>41, 42</sup> Studies of adsorption of nonionic surfactants on carbonate surfaces have been relatively fewer in comparison to silica surfaces.<sup>46-49</sup> Adsorption on carbonates was studied at different temperatures and it was found that the adsorption was independent of brine composition for dolomite surface.<sup>46</sup> Kuno et al.<sup>47</sup> and Akers et al.<sup>48</sup> evaluated the adsorption of polyoxyethylene alkyl-phenols on chalk surfaces and found that the extent of adsorption depends on the surfactant hydrophilicity. A decrease in adsorption was observed for more hydrophilic surfactants.

The general consensus is that nonionic surfactants reach adsorption plateau around the CMC and have a weak polar interaction with substrates. Because of the weak nature of interactions, adsorption typically takes place in the form of patchy micellar or hemimicellar aggregates. A comprehensive review on this adsorption phenomena can be found in multiple works.<sup>14, 33, 50-51, 53</sup>

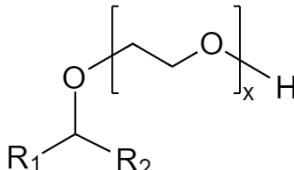
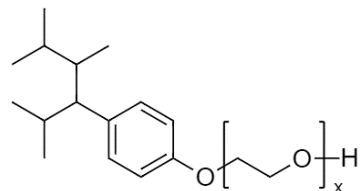
In a previous study, two families of nonionic surfactants with different hydrophobic units were evaluated on their wettability alteration properties through a series of contact-angle experiments on oil-wet calcite.<sup>54</sup> Wettability alteration, changing the rock from oil-wet to water wet and reducing the contact angle, was found to be enhanced by surfactants with shorter hydrophilic groups and higher temperatures. An increased adsorption under those conditions was hypothesized to be the underlying cause and it is imperative to understand the correlation between adsorption and wettability alteration. A detailed evaluation of molecular structure and the effect of temperature on adsorption are required to extend applicability to different system conditions.

Here, the phenomenon of adsorption of the above mentioned nonionic surfactants on carbonate surface is investigated through series of static adsorption experiments. The concepts of packing parameter and surface coverage are used to understand the nature of adsorption. Adsorption is correlated to an intrinsic thermodynamic parameter to generate a universal adsorption curve that can be used as a predictive tool for surfactant selection. A theoretical justification is provided for this universal behavior.

### 3.2. MATERIALS

Table 3.1 lists the surfactants studied with their molecular structures. All surfactants were provided by The Dow Chemical Company. The two families studied are secondary alcohol ethoxylates represented by SAE-x and nonylphenol ethoxylates represented by NP-x. The hydrophilic component in both cases is repeating units of ethylene oxide. The hydrophobe units in SAE-x are short alkyl chains represented by R<sub>1</sub> and R<sub>2</sub>. For NP-x, the hydrophobe a nonylphenol group. Indiana limestone is used as the representative carbonate surface for adsorption experiments. It is obtained from Kocurek (TX, USA) and sieved with 200-400 mesh, washed and dried before experiments. HPLC grade water (Fisher Scientific) was used to make all the solutions.

Table 3.1: List of nonionic surfactants evaluated in the study. CMC values are reported at 25°C for 12% NaCl, 0.2% CaCl<sub>2</sub> brine.

Surfactant name	Structure	Specification (x)	CMC (mM)	Cloud Point (°C)
SAE-x (Secondary alcohol ethoxylate)		15	0.16	66
		30	0.10	85
		40	0.49	79
NP-x (Nonylphenol ethoxylate)		15	0.06	69
		30	0.05	79
		40	0.09	77

### 3.3. METHODOLOGY

#### 3.3.1. Critical Micelle Concentration

Interfacial tension (IFT) measurements were performed to determine the CMCs of individual surfactants. The inverted pendant drop technique was used to measure the surfactant-air interfacial tensions. Surfactant solutions were first heated to the desired temperature following which drops were introduced in an environmental chamber set at the same temperature using a syringe with inverted needle. The shape of the surfactant drop was monitored using a high magnification camera and the IFT values were extracted from the images using the Pendant drop plug-in in ImageJ. The IFT values corresponding to SAE-15 at 25°C is shown in Figure 3.1. The CMC is determined using the technique shown in the plot. The CMCs measured at 25°C are reported in Table 3.1. CMCs for the surfactants varied typically within 10-20% for the range of temperatures of the current study.

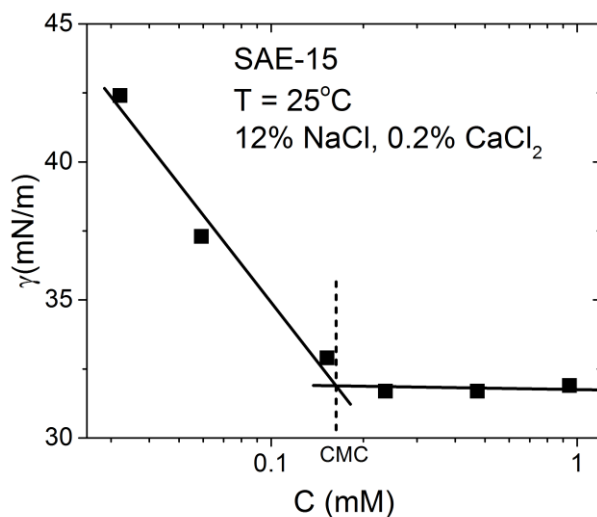


Figure 3.1. Measurement of CMC using surface tension values measured in air

### **3.3.2. Cloud Point Measurements**

Surfactant solutions were prepared in glass vials and placed in an oven and heated for 20 minutes at a given temperature. The temperature was increased by 1° at each step and shaken gently to observe the formation of a white opaque phase in the solutions. The onset of opacity was reported as the cloud point temperature. Table 3.1 shows the cloud point temperatures measured for 4000 ppm surfactant solutions in 12% NaCl, 0.2% CaCl<sub>2</sub> brine.

### **3.3.3. Dynamic Light Scattering (DLS)**

Dynamic light scattering with non-invasive backscatter optics is used to measure the micelle sizes of surfactants. Measurements were carried out in a Malvern Zetasizer Nano ZS. These measurements were done for SAE-15, SAE-40, NP-15 and NP-40. For NP-15, the surfactant concentration was varied from 100 ppm to 4000 ppm to determine the average size of the micelles as a function of concentration and temperature. For other surfactants, measurements were done at concentrations of 1000 ppm and 4000 ppm. In order to study the variation of micelle size with temperature, measurements were done at two different temperatures 25°C and 50°C. Each measurement was repeated three times to get an average size.

### **3.3.4. Adsorption Experiments**

Static adsorption tests were carried out for different surfactants at three different temperatures 25°C, 40°C and 50°C. Indiana limestone particles were used a representative carbonate surface in the experiments. Limestone particles were first sieved using 200 and 400 mesh sieves (30 – 70 µm) to get a uniform distribution of particle sizes. The sieved particles were then washed and rinsed three times to remove any unwanted organic matter present in the samples. After washing the particles were dried in an oven at a temperature

of 100°C for three days, following which they were used in the experiments. The brine salinity used in the experiments is 12% NaCl and 0.2% CaCl<sub>2</sub> by weight. One part of the brine was separated and equilibrated with selected mass of prepared limestone particles at the required temperature for one day. This takes care of any change in brine composition because of substrate dissolution. After equilibration the brine solution was separated and used to form surfactant solutions of different strengths (100 ppm to 4000 ppm). Calibration curve corresponding to surfactant concentration was then prepared. The second part of the initial brine was then used to prepare surfactant solutions of different mass concentrations. 10 ml of surfactant solution was then added to 2.75 gm of limestone particles. The ratio of limestone to mass of brine was kept the same as the ratio in the first case. After adding the solutions, the tubes were placed in a horizontal position inside a shaker to ensure proper mixing. This mixing process was done for 24 hours following which the contents are allowed to settle without shaking for additional 24 hours. The supernatant surfactant solution was then separated, while inside the shaker, to analyze the concentration. The adsorption amount is obtained from a simple mass balance

$$\Gamma = m_{sol} (C_0 - C_{eq}) / Sm_c \quad (1)$$

where  $m_{sol}$ ,  $C_0$ ,  $C_{eq}$ ,  $S$  and  $m_c$  are mass of the surfactant solution, initial surfactant concentration, final surfactant concentration, BET surface area of limestone and mass of limestone used in the experiment, respectively.

### 3.3.5. Measurement of BET Surface Area

BET surface area analysis was performed using a Micromeritics Accelerated Surface Area & Porosimetry instrument (ASAP 2420). The sample was out-gassed at 300°C while under vacuum prior to analysis. The BET surface area for the limestone particles was found to be 0.84 m<sup>2</sup>/gm.

### 3.3.6. Measurement of Surfactant Concentration

The concentration of SAE-x surfactants was determined by High Performance Liquid Chromatography (HPLC) with an Evaporative Light Scattering Detector (ELSD). The Agilent 1260 Infinity II Series HPLC and Model 385 ELSD were used for the analysis. A Zorbax Eclipse plus C8 (3 x 150 mm, 3.5  $\mu$ m) column was used for chromatographic separation. The mobile phase consists of acetonitrile and water. Initially, the acetonitrile fractional flow was 5% and then gradually increased to 100% over 9 minutes and held for 6 minutes. The flow rate of the total mobile phase was 0.62 mL/min. The column was set at a temperature of 40°C. For all experiments, the sample injection volume was 16  $\mu$ L. Each run was followed by a post-run of 95% acetonitrile and 5% water for 9 minutes. A blank sample of HPLC grade water was run after every 8 runs. The above steps ensured that there was no carryover of surfactants from previous runs. Typical elution chromatograms of SAE-15 are shown as obtained in Figure 3.2a. The width of the peak is associated with the distribution of hydrophilic units in the molecule. This result indicates that the surfactant has a range of EO groups for a given hydrophobic tail length. The area under the chromatogram was integrated for different surfactant concentrations. The area was then plotted against the known concentration to get a calibration curve for each surfactant from which unknown concentrations were extracted. A representative calibration plot is shown in Figure 3.2b.

The UV-Vis spectroscopy technique was used to measure the concentration of NP-x surfactants. This was made possible because of the presence of the aromatic group in the NP surfactants. A Cary UV-Vis instrument in single-front mode was used for the experiments. Figure 3.3a depicts the absorbance spectrum for NP-15 at different concentrations. Two absorbance peaks are observed corresponding to the wavelengths of 220nm and 277 nm. At high concentrations, the instrument displayed a limited sensitivity

to the absorbance at 226 nm. The absorbance peak near 277nm was hence picked for the purpose of analysis. In order to ensure a constant baseline signal and to remove any unwanted contribution to absorption signal, the first derivative technique was used to prepare calibration curves for the surfactants and determine unknown concentrations. The first derivative of the absorbance plotted against the wavelength is shown in Figure 3.3b. The process of taking a derivative eliminates any constant signal interference at all wavelengths. The plots show a peak corresponding to 286.5nm for all samples. This peak value is then used for the subsequent calibration and analysis purposes. Figure 3.3c shows a typical calibration curve obtained by using this method. Separate calibration plots were prepared for each separate experiment for both SAE-x and NP-x.

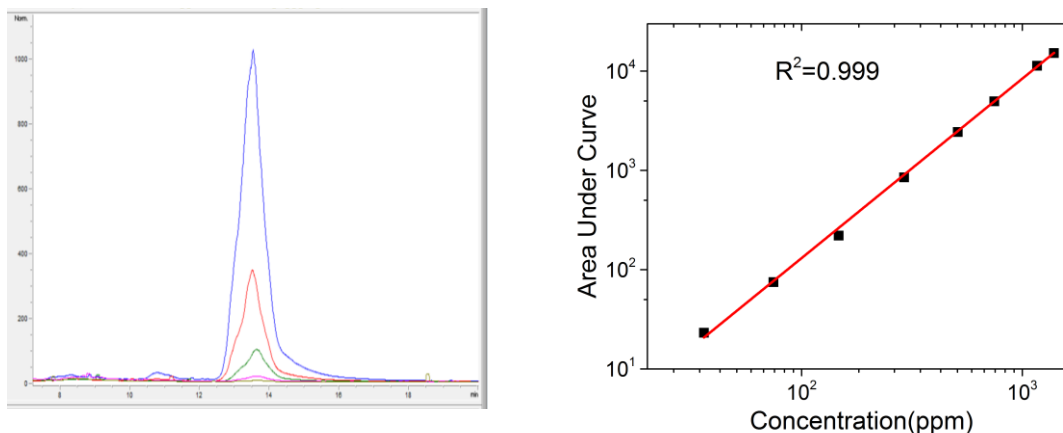


Figure 3.2: a) Chromatogram obtained from HPLC-ELSD analysis of SAE-x. b) Typical calibration plots for SAE-x surfactants.



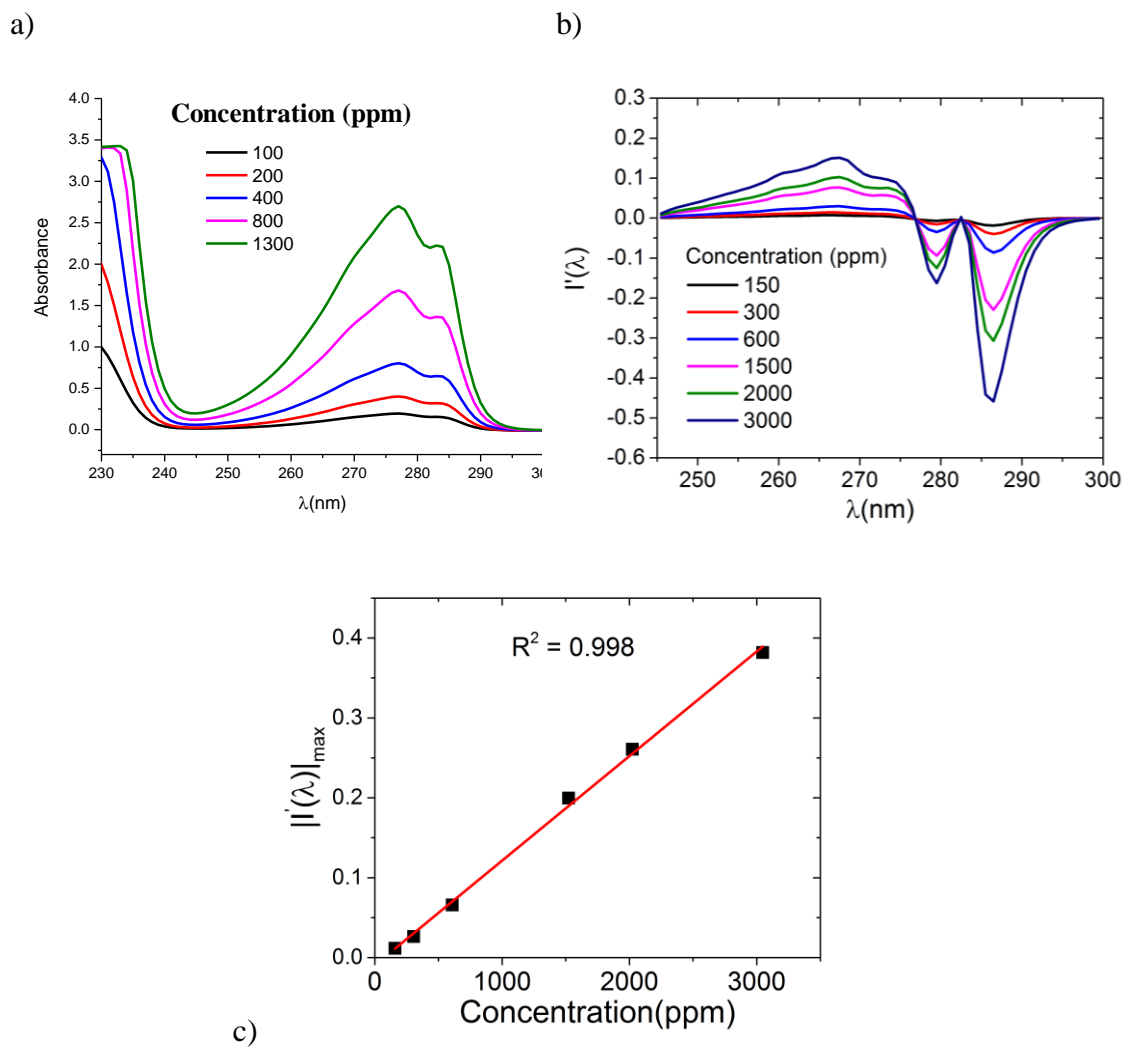


Figure 3.3: a) Typical absorption spectra for NP-x surfactant. b) First derivative absorption spectra for NP-x and the corresponding c) calibration curve.

### 3.4. RESULTS AND DISCUSSION

#### 3.4.1. Micelle Size Measurement

Figures 3.4 and 3.5 show typical micelle size distributions of the SAE-x and NP-x micelles. The weight averaged micelle sizes  $D_m$  of NP-15, NP-40 and SAE-15, SAE-40 at two different concentrations (1000 ppm and 4000 ppm) and two temperatures (25°C and 50°C) are shown in Table 3.2. The measured micelle sizes typically lie between 11 – 14 nm. Micelle size increases with the number of hydrophilic units, which can be attributed to the increase in the size of surfactant monomers. Micelle size tends to be relatively independent of the type of hydrophobe. Micelles also increase in size as the temperature is increased and this growth is more prominent at higher concentrations – an increase in size from 11 nm to 14 nm can be seen for 4000 ppm SAE-15 and NP-15. A limited micelle growth is observed for a 4000 ppm surfactant concentration of SAE-40 and NP-40 at 50°C.

The aggregation number can be determined from the micelle size,  $D_m$ , and the volume of a hydrated surfactant monomer inside a micelle  $V_s$  using the relation

$$N_{agg} = \frac{\pi D_m^3}{6V_s}. \quad (2)$$

The values of  $V_s$  used for the calculation<sup>55-56</sup> are shown in Table 3.3. The extracted values of  $N_{agg}$  are shown in Table 3.2.  $N_{agg}$  decreases with an increase in EO number for both SAE and NP surfactants. This is because while there is a modest increase of  $D_m$ ,  $V_s$  increases significantly with the EO number. On the other hand,  $N_{agg}$  increases with temperature. The decreased hydration of surfactant molecules at high temperatures increases their tendency to form aggregates, which increases the size of the micelles. The effect of  $N_{agg}$  on adsorption is discussed in detail in the following sections.

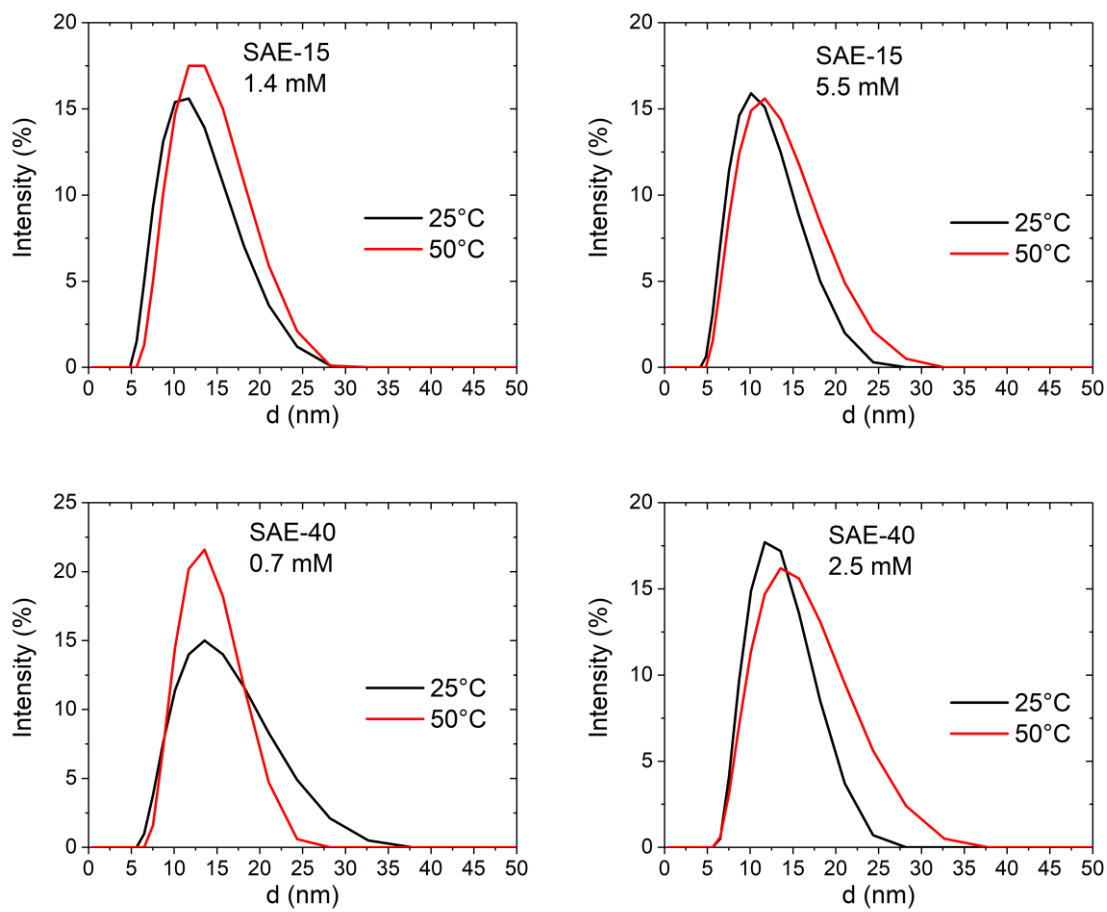


Figure 3.4. Micelle size distributions for SAE-x

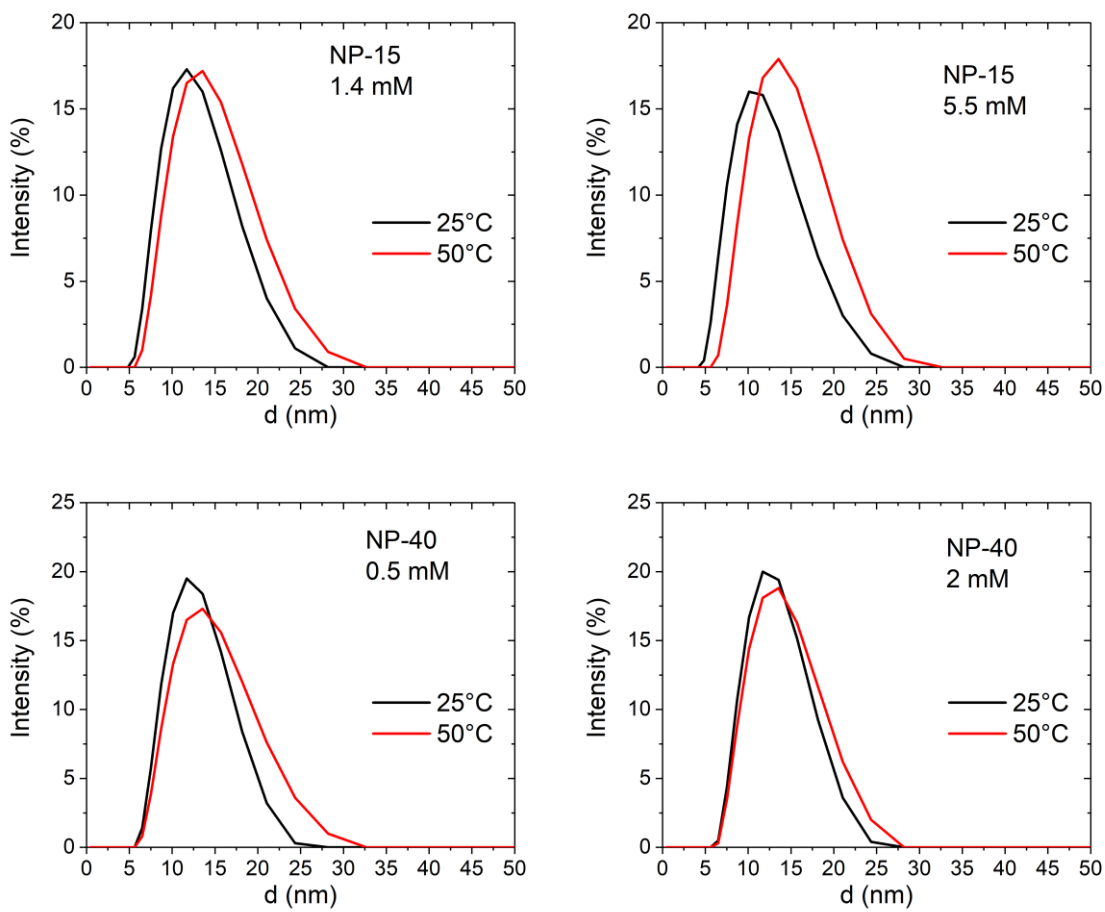


Figure 3.5. Micelle size distributions for NP-x

Table 3.2: Weight-average micelle sizes reported for 1000 ppm and 4000 ppm NP-x and SAE-x at 25°C and 50°C.

	1000 ppm						4000 ppm					
	25°C			50°C			25°C			50°C		
	$D_m$ (nm)	PDI	$N_{agg}$	$D_m$ (nm)	PDI	$N_{agg}$	$D_m$ (nm)	PDI	$N_{agg}$	$D_m$ (nm)	PDI	$N_{agg}$
NP-15	11.7	0.13	215	12.5	0.15	255	11.8	0.10	215	14.1	0.26	366
NP-40	12.5	0.09	109	13.3	0.13	131	12.9	0.07	120	13.6	0.10	141
SAE-15	11.1	0.07	190	12.5	0.10	277	11.2	0.08	199	13.8	0.16	372
SAE-40	13.3	0.08	134	13.5	0.12	141	13.5	0.06	140	14.2	0.15	163

Table 3.3. Volumes of surfactant molecules used to calculate  $N_{agg}$ . The volume includes additional volume because of water molecules in the micelle.<sup>55-56</sup>

Surfactant	$V_s$ (Å <sup>3</sup> )
SAE-15	3688
SAE-30	6985
SAE-40	9184
NP-15	3990
NP-30	7171
NP-40	9369

### 3.4.2. Adsorption Isotherms

Figure 3.6 shows the adsorption isotherms for NP-x and SAE-x at the three different temperatures. In case of NP surfactants, adsorption of each surfactant increases rapidly with the bulk concentration and then levels off. The CMC values of the surfactants are shown by the dotted lines. In most cases an adsorption plateau happens around the surfactant CMC. At 25°C, a maximum adsorption of 0.7  $\mu\text{mol}/\text{m}^2$  is observed for NP-15 (Fig. 6a). When temperature is increased to 40°C, a rise in adsorption is observed from the first plateau at 0.6  $\mu\text{mol}/\text{m}^2$  to about 1  $\mu\text{mol}/\text{m}^2$ . Similar behavior is observed at 50°C where adsorption increases from 0.8  $\mu\text{mol}/\text{m}^2$  to 1.3  $\mu\text{mol}/\text{m}^2$ . For NP-30 (Fig. 6b) the maximum adsorptions are 0.2  $\mu\text{mol}/\text{m}^2$ , 0.3  $\mu\text{mol}/\text{m}^2$  and 0.6  $\mu\text{mol}/\text{m}^2$  at 25°C, 40°C and 50°C

respectively. The corresponding values for NP-40 (Fig. 6c) are  $0.1 \mu\text{mol}/\text{m}^2$ ,  $0.1 \mu\text{mol}/\text{m}^2$  and  $0.4 \mu\text{mol}/\text{m}^2$ .

The adsorption isotherms for SAE-15 (Fig. 6d) are similar to NP-15. At  $25^\circ\text{C}$ , a single adsorption plateau is observed at  $0.6 \mu\text{mol}/\text{m}^2$ . Once again, as the temperature is increased, an upward trend in adsorption is observed. The maximum adsorption for SAE-15 is  $0.8 \mu\text{mol}/\text{m}^2$  and  $1 \mu\text{mol}/\text{m}^2$  at  $40^\circ\text{C}$  and  $50^\circ\text{C}$ , respectively. For SAE-30 (Fig. 6e) the maximum adsorptions are  $0.1 \mu\text{mol}/\text{m}^2$ ,  $0.2 \mu\text{mol}/\text{m}^2$  and  $0.3 \mu\text{mol}/\text{m}^2$  at  $25^\circ\text{C}$ ,  $40^\circ\text{C}$  and  $50^\circ\text{C}$ , respectively. The maximum adsorption values for SAE-40 (Fig. 6f) are  $0.1 \mu\text{mol}/\text{m}^2$ ,  $0.3 \mu\text{mol}/\text{m}^2$  and  $0.4 \mu\text{mol}/\text{m}^2$ . Because of the high CMC, the levelling of adsorption near the CMC can be seen prominently for SAE-40.

### 3.4.2. Molecular interpretation of adsorption isotherms

Below a critical surfactant concentration, most surfactant molecules are expected to remain parallel to the surface aided by favorable interactions with calcium and carbonate groups.<sup>30</sup> Adsorption via this mechanism would mean a higher adsorption for surfactants with more EO groups. This is found to be true in the case of adsorption of nonionic surfactants on silica when the concentrations are below the CMC.<sup>30</sup> In practice wettability alteration is done at surfactant concentrations well above the CMC.<sup>54, 66</sup> At these concentrations, the adsorption of surfactants with fewer EO groups is higher. This indicates that at high concentrations, relevant for wettability alteration, aggregates of the surfactants similar to micelles adsorb onto the surface.<sup>38, 57</sup>

From a molecular point of view, the structure of adsorbed surfactant aggregates can be predicted using the concept of packing parameter introduced by Israelachvili et al.<sup>58</sup> The packing parameter is defined as

$$P = \frac{V}{a_0 l}, \quad (3)$$

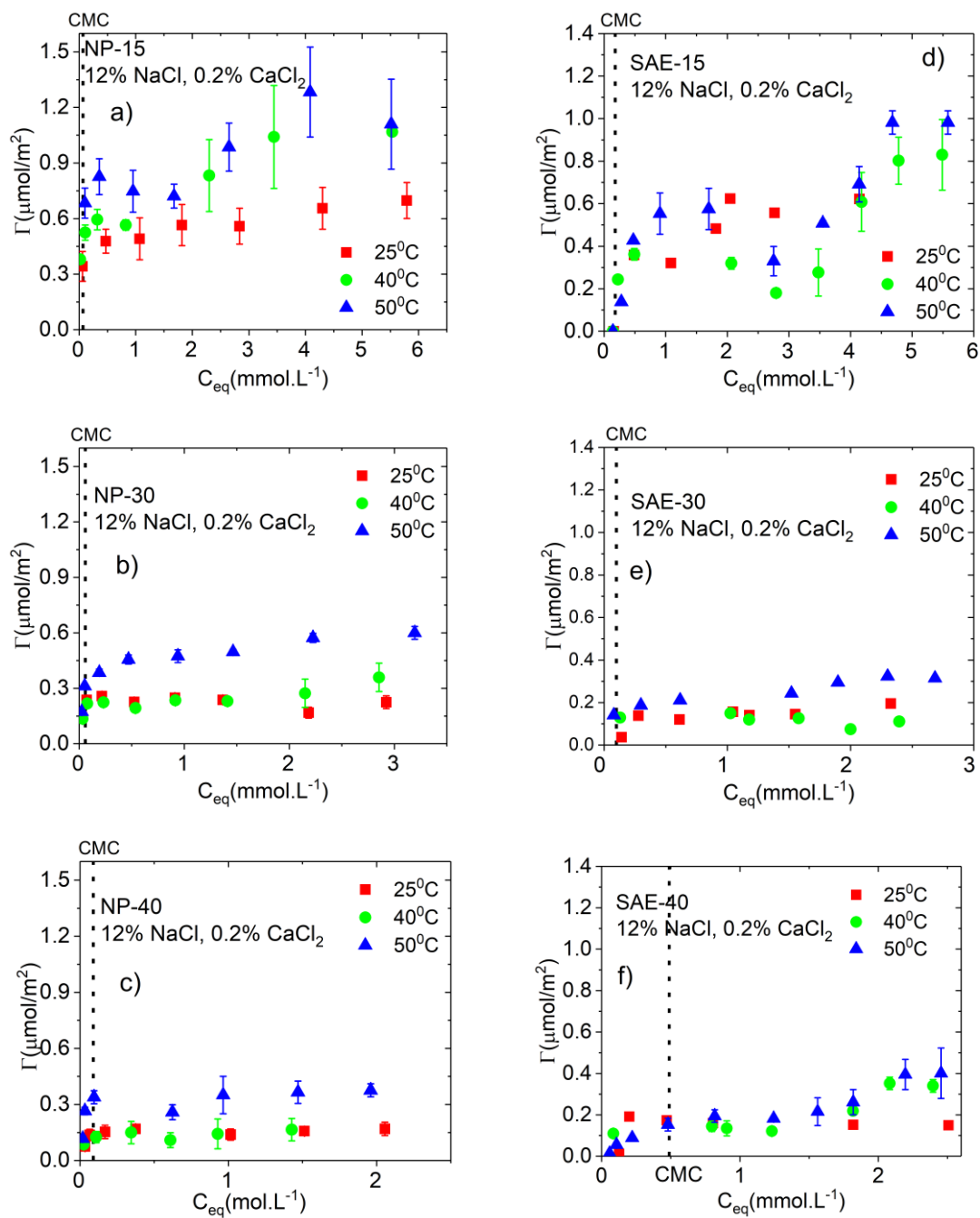


Figure 3.6: Adsorption isotherms of a) NP-15 b) NP-30 c) NP-40 d) SAE-15 e) SAE-30 and f) SAE-40

where  $V$  is surfactant hydrophobe volume,  $a_0$  is the optimum hydrophilic cross-section area and  $l$  is the hydrophobe chain length. For values of  $P$  less than about  $1/3$ , the micelles are spherical. In previous works, the aggregates of similar EO containing surfactants were expectedly found to depend on the length of the hydrophilic units –spherical for EO units several mers or more in length.<sup>35, 59</sup> The packing parameter values for the current system of surfactants are below  $1/3$ . As such adsorption for the more hydrophilic surfactants is expected to take place in the form of interspersed patches of monolayer and spherical aggregates.

Table 3.4 lists the maximum adsorption observed for each surfactant at three different temperatures. At a given temperature, this adsorption decreases as the number of EO units is increased.

Table 3.4: Maximum adsorptions and estimated surface coverages for SAE-x and NP-x

Surfactant	25°C		40°C		50°C	
	$\Gamma_{\max}$ ( $\mu\text{mol}/\text{m}^2$ )	$\phi$	$\Gamma_{\max}$ ( $\mu\text{mol}/\text{m}^2$ )	$\phi$	$\Gamma_{\max}$ ( $\mu\text{mol}/\text{m}^2$ )	$\phi$
SAE-15	0.6	0.17	0.8	0.22	1.0	0.23
SAE-30	0.1	0.06	0.2	0.06	0.3	0.17
SAE-40	0.1	0.10	0.3	0.21	0.4	0.24
NP-15	0.7	0.19	1.0	0.28	1.3	0.29
NP-30	0.2	0.14	0.3	0.20	0.6	0.32
NP-40	0.1	0.13	0.1	0.14	0.4	0.28

This can be explained by considering the micellar nature of adsorbed aggregates. For the given surfactants, surface aggregates behave very similar to bulk micelles.<sup>38, 57</sup> Hence an estimate of adsorption can be obtained from the following relation

$$\Gamma \sim \frac{N_{agg}}{A_{ads}}, \quad (4)$$

where  $A_{ads}$  is the area associated with each adsorbed micelle and  $N_{agg}$  is the micelle aggregation number available in Table 3.2. The decrease in  $N_{agg}$  with an increase in EO number is thus responsible for the observed lower adsorption.



For each surfactant, the maximum adsorption increases with temperature. This can be explained by considering the surfactant-water interactions. With increasing temperature, these interactions become weaker because of dehydration of the polyoxyethylene chains. This in turn promotes intermolecular hydrophobic interactions and makes surface aggregation more favorable for the surfactants. This behavior is similar to the observed increase in micelle aggregation number with temperature. The combination of two effects – reduced surfactant-water interactions and increased tendency of aggregation, thus leads to higher adsorptions at higher temperatures.

A distinct trend of higher adsorption at high concentrations is observed for surfactants with shorter ethoxylated chains at higher temperatures. This rise in adsorption is quite evident for NP-15 and SAE-15 beyond 40°C. The micelle size of smaller surfactants like SAE-15 and NP-15 increase significantly with temperature. The increase in the size of micellar aggregates and consequently in the micelle aggregation number is believed to be responsible for the observed increase in adsorption. Figure 3.7 shows the plot of micelle aggregation number of NP-15 at different concentrations at a fixed temperature (50°C). The nature of this plot is very similar to the adsorption isotherm of NP-15 at the same temperature. Given that, surface aggregates behave very similar to bulk micelles,<sup>38, 57</sup> it can be established that there is a correlation between the appearances of higher adsorption with the increase in micelle size.

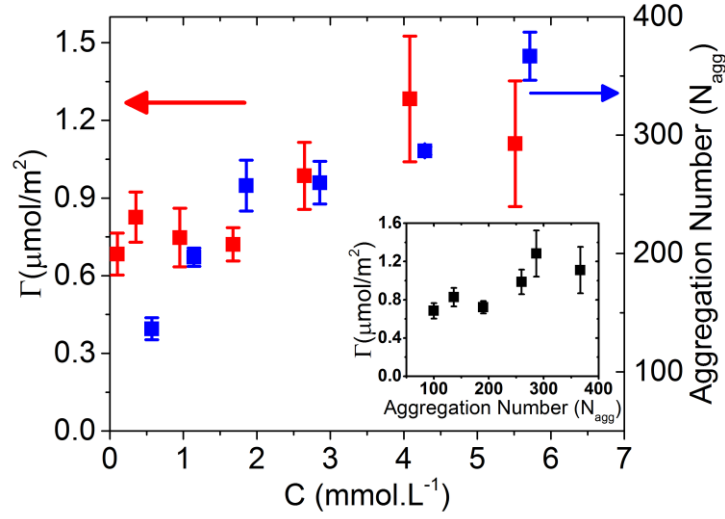


Figure 3.7: Micelle aggregation number as a function of concentration for NP-15 at 50°C. Inset shows the dependence of adsorption on the micelle aggregation number

### 3.4.3. Surface Coverage

The fraction of the surface covered by adsorbed micelles  $\phi$  can be computed from

$$\phi = \frac{\Gamma_{\max} A_{\text{mic}} N_A}{N_{\text{agg}} M_W} \quad (5)$$

Here  $\Gamma_{\max}$  is the maximum adsorption in mg/m<sup>2</sup>,  $A_{\text{mic}} = \pi D_m^2/4$  is the projected area of a micelle,  $N_{\text{agg}}$  is the aggregation number,  $M_W$  is the average molecular weight of the surfactant and  $N_A$  is the Avogadro's number.

Table 3.4 lists the predicted coverage values for different surfactants at different temperatures. The lowest coverages predicted are 6% for SAE-30 surfactant while the maximum coverage of around 30% is observed for NP surfactants, respectively. The surface coverage values are typically found to decrease with an increase in hydrophilicity. SAE-30 seems to behave unexpectedly in this regard exhibiting very low adsorption and correspondingly a lower surface coverage than SAE-40. The coverages also increase at

higher temperatures indicating enhanced surfactant adsorption. The surface coverage values indicate a sparse and patchy adsorption consistent with previous findings from literature.<sup>30, 57</sup>

#### 3.4.4. Universal Adsorption Behavior

In general adsorption increases as the temperature approaches the cloud point of the surfactant. Similarly, the change in contact angle or wettability alteration was also observed to be larger closer to the cloud point. This suggests that the proximity to the cloud point may offer a parameter that captures the effects of the structure of the surfactant and the temperature. Here we present a theory and evidence to support this hypothesis.

The cloud point for nonionic surfactants is the lower consolute (critical) temperature where phase separation is induced. Below and up to this critical temperature, the weight-averaged micelle aggregation number has been predicted to depend on the surfactant mole fraction  $X$  according to

$$N_{agg} = 2\sqrt{KX} \quad , \quad (6)$$

where  $K = \exp\left(\frac{\Delta\mu}{k_B T}\right)$  and  $\Delta\mu$  represents the free-energy for micellar formation.<sup>60-62</sup> From measurements of the micelle size and aggregation number, we can extract  $\Delta\mu/k_B$  and find that it varies linearly with  $T$  as shown in Fig. 8. Such behavior has been found previously.<sup>60-61</sup> This allows aggregation number to be written in terms of critical temperature  $T_c$  as

$$N_{agg} = 2\sqrt{K_c X} \exp\left[\frac{\alpha}{2}\left(\frac{1}{T} - \frac{1}{T_c}\right)\right] \quad , \quad (7)$$

where  $K_c$  is measured at  $T_c$  and  $\alpha$  is a constant which can be determined from the plot in Fig. 8. Under the assumption that surface aggregates behave similar to bulk micelles,<sup>38, 57</sup>

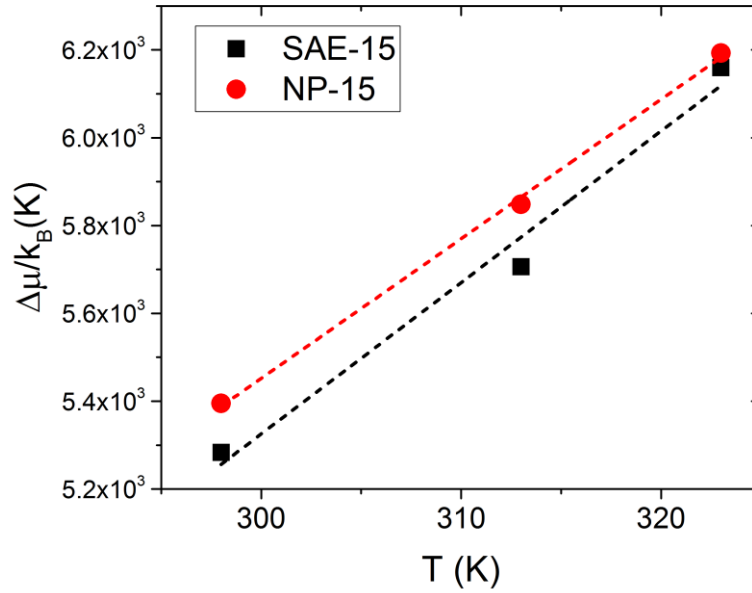


Figure 3.8. Micelle growth potential vs T

the energy of interaction between surfactant aggregates, and substrate is proportional to the projected area of aggregates, the adsorption energy can be written as

$$\Delta G_{ads} = \frac{\pi D_m^2}{4} \varepsilon_a, \quad (8)$$

where  $\varepsilon_a$  is the free energy related to adsorption site density and a free energy change associated with displacement of adsorbed water molecule by the surfactant.<sup>34</sup> Using (6), (7) and (8) the adsorption energy can then be written as

$$\Delta G_{ads} = \Delta G_o \exp \left[ \frac{\alpha}{3} \left( \frac{1}{T} - \frac{1}{T_c} \right) \right], \quad (9)$$

where

$$\Delta G_o = \frac{(12V_s)^{2/3} (K_c X)^{1/3} \varepsilon_a}{4}. \quad (10)$$

The adsorption energy corresponding to maximum adsorption at a given concentration and temperature,  $\Gamma_{max}$  can be summarily written as

$$\Delta G_{ads} \sim k_B T \ln \Gamma_{\max} . \quad (11)$$

Using (9) and (11), the maximum adsorption is then given by

$$\Gamma_{\max} \sim \exp \left[ \left( \frac{\Delta G_o}{k_B T} \right) \exp \frac{\alpha}{3} \left( \frac{1}{T} - \frac{1}{T_c} \right) \right] . \quad (12)$$

While exact value of  $\varepsilon_a$  is difficult to determine, a simplified form of (12) can be developed by understanding how it varies with temperature. It has been found that adsorption of organic molecules with polar components on hydrated carbonates involve overcoming a free energy barrier which decreases with temperature.<sup>63</sup> This can be attributed to two factors – weaker water-carbonate interactions thus rendering more active sites available for adsorption, and a favorable surfactant solvation entropic contribution near the surface.<sup>63,64</sup> As a simple approximation, a linear dependence of  $\varepsilon_a$  with temperature can hence be assumed. It will be found later that this approximation works quite well for this system. Typical values of  $\varepsilon_a$  give rise to  $\frac{\Delta G_o}{k_B T} \sim O(-1)$ .<sup>34</sup> Micelle size measurements at different

temperatures give  $\frac{\alpha}{3} \left( \frac{1}{T} - \frac{1}{T_c} \right) \sim O(-10^{-2})$  to  $O(-10^{-1})$  for the current family of nonionic surfactants. This allows (12) to be approximated as

$$\Gamma_{\max} = \Gamma_c \left[ 1 + \beta (T_c - T) \right] , \quad (13)$$

where  $\Gamma_c$  is the adsorption at cloud point and  $\beta$  is a negative constant. Figure 3.9a plots the maximum molar adsorption of these surfactants as a function of

$$CPTD = T_c - T , \quad (14)$$

for each system tested, where  $T_c$  is the cloud-point temperature of the surfactant solution and  $T$  is the experimental temperature.

The plot agrees qualitatively with (13) as a linear decrease in adsorption is observed as the system moves away from the cloud point. However, surfactants with 15

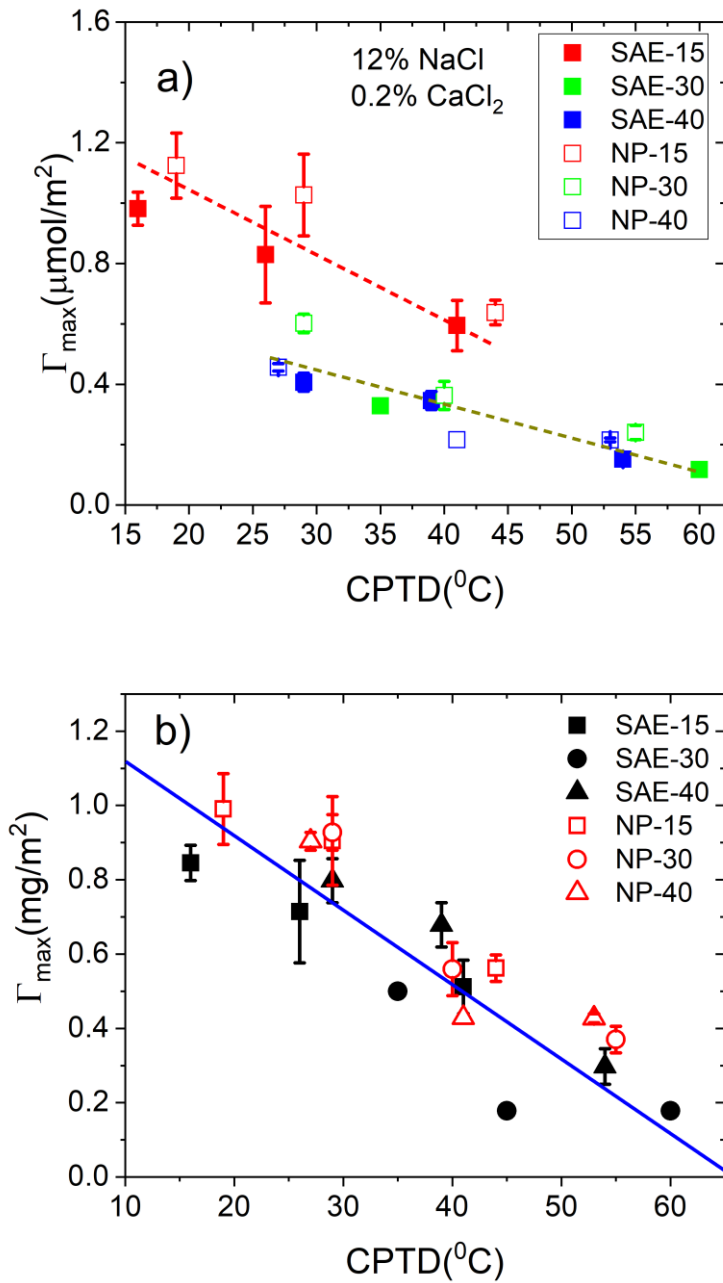


Figure 3.9: a) Maximum molar adsorption of surfactants as a function of CPTD. b) Universal behavior of adsorption of nonionic surfactants. The maximum adsorption of surfactants is plotted in  $\text{mg}/\text{m}^2$  against the cloud point-temperature difference (CPTD)

EO groups (red filled and empty squares) exhibit a higher  $\Gamma_c$  and steeper rate of decrease compared to the larger surfactants with 30 and 40 EO groups (blue and green squares). A better collapse of the experimental data and a more universal behavior could be possible by investigating  $\Gamma_c$  in detail. Near the cloud point, where surfactant adsorption is very high  $\Gamma_c$  can be estimated to be proportional to  $N_{agg,c}/D_{m,c}^2$ , where  $N_{agg,c}$  and  $D_{m,c}$  refer to the aggregation number and micelle size at the cloud point. At the same time  $N_{agg,c}/D_{m,c}^2$  has an inverse relationship with the molecular weight of the surfactant (Fig. 10). This means a universal behavior is expected when (13) is written on a mass basis according to

$$\Gamma_{w,max} = \Gamma_{w,c} [1 + \beta(T_c - T)], \quad (15)$$

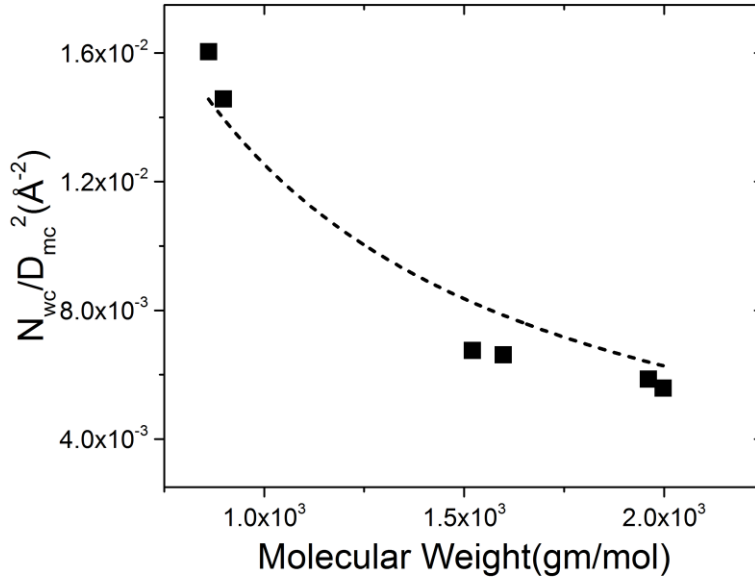


Figure 3.10. Variation of  $\frac{N_{wc}}{D_{mc}^2}$  vs surfactant molecular weight. The dotted line represents

the function  $\frac{N_{agg,c}}{D_{m,c}^2} \sim \frac{1}{M_w}$

Figure 3.9b exhibits this universal collapse of maximum mass-based adsorption. The universal behavior is quite apparent from the plot. The maximum adsorption is found to vary linearly with CPTD if the surfactant hydrophobe is the same. Even with a different hydrophobe, the differences are only minor; signifying the dominating effect of hydrophilic components as far as adsorption is concerned. As can be seen from the plot, the adsorption increases as one moves nearer to the cloud point. This can be obtained either with a more hydrophobic surfactant at a given temperature or by increasing the temperature for a given surfactant – effectively encompassing the two observations from the experiments. The small scatter in the data can be attributed to limited information on temperature dependence of hydrated surfactant volume and aggregate shape near the cloud point. Nevertheless, this plot serves as a powerful tool to predict adsorption behavior with respect to an intrinsic thermodynamic property of the surfactant.

The predicted relationship is expected to hold for families of nonionic surfactants up to their cloud point temperatures. In the current study the cloud point temperatures, at a high brine salinity of 12% NaCl, 0.2% CaCl<sub>2</sub>, were around 70°C – 80°C, which meant these surfactants could not be used directly at higher temperatures without phase separation. The surfactant-bulk and surfactant-carbonate interactions are expected to behave differently beyond phase separation, which should lead to a different adsorption behavior. The brine salinity used in the study is a good representative of high salinity reservoirs. The cloud point of these surfactant solutions is also determined by the brine salinity. Any change in the salinity will thus be reflected upon the adsorption through the adsorption-CPTD relationship. This relationship is expected to hold true if the brine components do not change the mechanism of adsorption, significantly.



### 3.4.5. Adsorption and Wettability Alteration

The relationship between surfactant adsorption and wettability alteration can be inferred by combining the results from contact angle experiments done with these surfactants in a previous study.<sup>54</sup> These contact angle measurements were performed on an initially oil-wet calcite surface. Along with the contact angle values, activation energy calculations and oil-film experiments suggested that the adsorbed surfactants determined final wettability state by accessing the bare calcite near the receding three phase contact line. This means that the extent of wettability alteration is determined mainly by the calcite-surfactant interactions. Figure 3.11 plots the final contact angle values for the selected surfactant systems against the corresponding maximum adsorption.

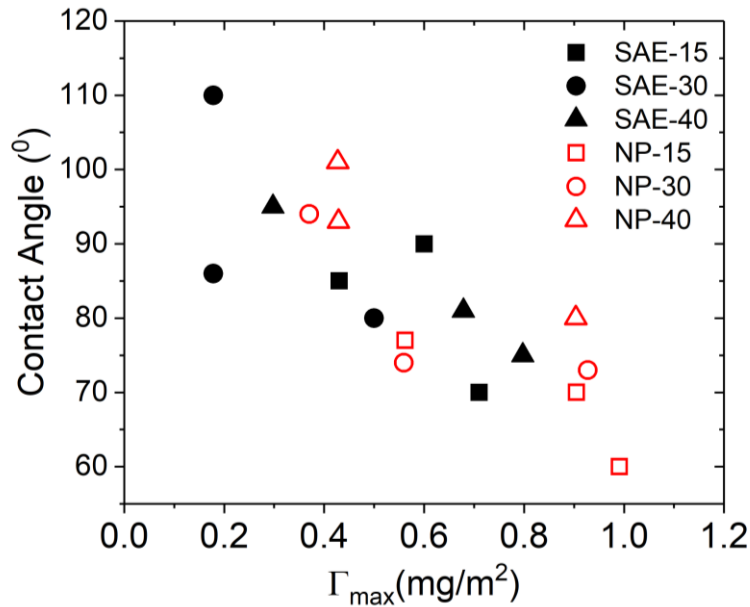


Figure 3.11: Final contact angle on oil-wet calcite is plotted against maximum adsorption. Contact angles are measured in the aqueous phase. Contact angles greater than  $90^\circ$  represent an oil-wet state. Final contact angles almost linearly decrease with an increase in adsorption signifying a positive correlation between wettability alteration and adsorption.

The plot confirms the hypothesis of better wettability alteration at high adsorption and this behavior is independent of the surfactant structure. The cases where the final calcite surfaces are still oil-wet (Contact Angle  $> 90^\circ$ ) correspond to lower adsorptions and vice-versa.

### 3.5. CONCLUSIONS

Secondary alcohol ethoxylate and nonyl phenol ethoxylate surfactants have been found to be effective in altering the wettability of an oil-wet carbonate surface to water-wet.<sup>54</sup> An increase in wettability alteration performance was observed for these families of surfactants as the number of hydrophilic units was reduced and with an increase in temperatures. It was hypothesized that an enhanced adsorption is responsible for this behavior and it is important both from a fundamental and economic point of view to understand the mechanism and estimate the extent of surfactant adsorption for such an application. Along with substrate type, temperature is an important parameter which needs to be considered for reservoir applications and this is also addressed in the current study.

Static adsorption experiments were performed to obtain representative adsorption isotherms for different surfactant hydrophilicities and temperatures. Similar to previous observations,<sup>35-36</sup> adsorption isotherms display a sharp increase in the adsorbed amount within a very small bulk concentration range followed by a constant adsorption plateau. Surfactant adsorption increases with a decrease in surfactant hydrophilicity and with an increase in system temperature. These two factors have been combined into the parameter CPTD which incorporates the thermodynamic property of cloud point of a nonionic surfactant. A universal behavior of higher adsorption is observed as a surfactant nears its cloud point and a thermodynamic explanation is provided for the same. Compared to

existing models of aggregative adsorption, this model provides a simple way to predict the adsorption of nonionic surfactants.<sup>34</sup>

At higher temperatures, an upward drift in adsorption is observed, particularly for the more hydrophobic surfactants. This has been attributed to the increase in micelle size with temperature. Based on the values of the packing parameters, a micellar aggregative mechanism is proposed. This is also seen in similar experiments performed on silica substrates.<sup>29, 30, 35-36</sup> Surface-coverages, estimated using maximum adsorption and micellar sizes, offer a picture of sparsely distributed micellar aggregates on the surface. Combining the wettability results,<sup>54</sup> it can be confirmed that the degree of wettability alteration is proportional to surfactant adsorption.

While adsorption of similar surfactants on silica has been linked to hydrophilicity in the past,<sup>30</sup> a universal correlation of adsorption and wettability alteration to an intrinsic surfactant characteristic, that combines the effect of both surfactant structure and temperature, has not been done till date. The relative dearth of works on carbonate surfaces<sup>46-49</sup> combined with the fact that most oil reservoirs tend to be carbonate formations<sup>65</sup> highlight the significance of these findings. A molecular level understanding of adsorption energetics is necessary to understand aggregative adsorption, and this is a part of ongoing study.

In summary, the effects of structure of nonionic surfactant on adsorption have been determined, with shorter hydrophilic units adsorbing more on calcite at a given temperature. A successful method has been presented to collapse all the adsorption data for different nonionic surfactants on a universal curve based on the temperature relative to the cloud point. A theory is presented to support this. Finally, a universal trade-off curve for the wettability alteration (final contact angle) for an initially oil-wet carbonate surface versus the adsorption is shown. These results and the methodology for correlating the data

is of great importance for practical implementation of wettability alteration in a carbonate oil reservoir.

## REFERENCES

1. Adibhatla, B., & Mohanty, K. K. Oil recovery from fractured carbonates by surfactant-aided gravity drainage: laboratory experiments and mechanistic simulations. *SPE Reservoir Evaluation & Engineering*, **2008**, 11(01), 119-130.
2. Seethepalli, A., Adibhatla, B., & Mohanty, K. K. Wettability alteration during surfactant flooding of carbonate reservoirs. In *SPE/DOE Symposium on Improved Oil Recovery*. Society of Petroleum Engineers, **2004**.
3. Hirasaki, G., & Zhang, D. L. Surface chemistry of oil recovery from fractured, oil-wet, carbonate formations. *SPE Journal*, **2004**, 9(02), 151-162.
4. Zhang, J., Nguyen, Q. P., Flaaten, A., & Pope, G. A. Mechanisms of enhanced natural imbibition with novel chemicals. *SPE reservoir evaluation & engineering*, **2009**, 12(06), 912-920.
5. Strand, S., Standnes, D. C., & Austad, T. Spontaneous imbibition of aqueous surfactant solutions into neutral to oil-wet carbonate cores: Effects of brine salinity and composition. *Energy & fuels*, **2003**, 17(5), 1133-1144.
6. Standnes, D. C., & Austad, T. Wettability alteration in carbonates: Interaction between cationic surfactant and carboxylates as a key factor in wettability alteration from oil-wet to water-wet conditions. *Colloids and Surfaces A: Physicochemical and Engineering Aspects*, **2003**, 216(1-3), 243-259.
7. Austad, T., & Standnes, D. C. Spontaneous imbibition of water into oil-wet carbonates. *Journal of Petroleum Science and Engineering*, **2003**, 39(3-4), 363-376.
8. Austad, T. and Milter, J. Spontaneous imbibition of water into low permeable chalk at different wettabilities using surfactants. In *International Symposium on Oilfield Chemistry*, Society of Petroleum Engineers, **1997**.
9. Standnes, D.C., Nogaret, L.A., Chen, H.L. and Austad, T. An evaluation of spontaneous imbibition of water into oil-wet carbonate reservoir cores using a nonionic and a cationic surfactant. *Energy & Fuels*, 16(6), **1997**, pp.1557-1564.

10. Spinler, E.A., Zornes, D.R., Tobola, D.P. and Moradi-Araghi, A. Enhancement of oil recovery using a low concentration of surfactant to improve spontaneous and forced imbibition in chalk. In *SPE/DOE Improved Oil Recovery Symposium*. Society of Petroleum Engineers, **2000**.
11. Ma, K., Cui, L., Dong, Y., Wang, T., Da, C., Hirasaki, G. J., & Biswal, S. L. Adsorption of cationic and anionic surfactants on natural and synthetic carbonate materials. *Journal of colloid and interface science*, **2013**, 408, 164-172.
12. Muherei, M.A., Junin, R. and Merdhah, A.B.B. Adsorption of sodium dodecyl sulfate, Triton X100 and their mixtures to shale and sandstone: a comparative study. *Journal of Petroleum Science and Engineering*, **2009**, 67(3-4), pp.149-154.
13. Tagavifar, M., Jang, S.H., Sharma, H., Wang, D., Chang, L.Y., Mohanty, K. and Pope, G.A., 2018. Effect of pH on adsorption of anionic surfactants on limestone: Experimental study and surface complexation modeling. *Colloids and Surfaces A: Physicochemical and Engineering Aspects*, 538, pp.549-558.
14. Zhang, R. and Somasundaran, P., 2006. Advances in adsorption of surfactants and their mixtures at solid/solution interfaces. *Advances in colloid and interface science*, 123, pp.213-229.
15. Thibaut, A., Misselyn-Bauduin, A.M., Grandjean, J., Broze, G. and Jérôme, R., 2000. Adsorption of an aqueous mixture of surfactants on silica. *Langmuir*, 16(24), pp.9192-9198.
16. Fletcher, P. D., Savory, L. D., Clarke, A., & Howe, A. M. Model Study of Enhanced Oil Recovery by Flooding with Aqueous Solutions of Different Surfactants: How the Surface Chemical Properties of the Surfactants Relate to the Amount of Oil Recovered. *Energy & Fuels*, **2016**, 30(6), 4767-4780.
17. Ahmadall, T., Gonzalez, M.V., Harwell, J.H. and Scamehorn, J.F., 1993. Reducing surfactant adsorption in carbonate reservoirs. *SPE reservoir engineering*, 8(02), pp.117-122.
18. Bastrzyk, A.P.I.S.E., Polowczyk, I., Szelag, E. and Sadowski, Z., 2012. Adsorption and co-adsorption of PEO-PPO-PEO block copolymers and surfactants and their influence on zeta potential of magnesite and dolomite. *Physicochemical Problems of Mineral Processing*, 48(1), p.2012.

19. Rosen, M.J. and Li, F., 2001. The adsorption of gemini and conventional surfactants onto some soil solids and the removal of 2-naphthol by the soil surfaces. *Journal of colloid and interface science*, 234(2), pp.418-424.
20. Ivanova, N.I., Volchkova, I.L. and Shchukin, E.D., 1995. Adsorption of nonionic and cationic surfactants from aqueous binary mixtures onto the solid/liquid interface. *Colloids and Surfaces A: Physicochemical and Engineering Aspects*, 101(2-3), pp.239-243.
21. Ananthapadmanabhan, K.P. and Somasundaran, P., 1983. Mechanism for adsorption maximum and hysteresis in a sodium dodecylbenzenesulfonate/kaolinite system. *Colloids and Surfaces*, 7(2), pp.105-114.
22. Blokhuis, A.M., Høiland, H., Gjerde, M.I. and Ersland, E.K., 1996. Adsorption of sodium dodecyl sulfate on kaolin from different alcohol–water mixtures. *Journal of colloid and interface science*, 179(2), pp.625-627.
23. Koopal, L.K., Lee, E.M. and Böhmer, M.R., 1995. Adsorption of cationic and anionic surfactants on charged metal oxide surfaces. *Journal of colloid and interface science*, 170(1), pp.85-97.
24. Viswanathan, K.V. and Somasundaran, P., 1987. Adsorption of ethoxylated sulfonates on kaolinite and alumina. *Colloids and surfaces*, 26, pp.19-41.
25. Li, N., Zhang, G., Ge, J., Luchao, J., Jianqiang, Z., Baodong, D. and Pei, H., 2011. Adsorption behavior of betaine-type surfactant on quartz sand. *Energy & Fuels*, 25(10), pp.4430-4437.
26. Durán-Álvarez, A., Maldonado-Domínguez, M., González-Antonio, O., Durán-Valencia, C., Romero-Ávila, M., Barragán-Aroche, F. and López-Ramírez, S., 2016. Experimental–Theoretical Approach to the Adsorption Mechanisms for Anionic, Cationic, and Zwitterionic Surfactants at the Calcite–Water Interface. *Langmuir*, 32(11), pp.2608-2616.
27. Shah, K., Chiu, P., Jain, M., Fortes, J., Moudgil, B. and Sinnott, S., 2005. Morphology and Mechanical Properties of Surfactant Aggregates at Water–Silica Interfaces: Molecular Dynamics Simulations. *Langmuir*, 21(12), pp.5337-5342.
28. Bera, A., Kumar, T., Ojha, K. and Mandal, A., 2013. Adsorption of surfactants on sand surface in enhanced oil recovery: Isotherms, kinetics and thermodynamic studies. *Applied Surface Science*, 284, pp.87-99.

29. Brinck, J., Jönsson, B. and Tiberg, F., 1998. Kinetics of nonionic surfactant adsorption and desorption at the silica– water interface: One component. *Langmuir*, 14(5), pp.1058-1071.
30. Desbene, P.L., Portet, F. and Treiner, C., 1997. Adsorption of pure nonionic alkylethoxylated surfactants down to low concentrations at a silica/water interface as determined using a HPLC technique. *Journal of Colloid and Interface Science*, 190(2), pp.350-356.
31. Curbelo, F.D., Santanna, V.C., Neto, E.L.B., Dutra Jr, T.V., Dantas, T.N.C., Neto, A.A.D. and Garnica, A.I., 2007. Adsorption of nonionic surfactants in sandstones. *Colloids and Surfaces A: Physicochemical and Engineering Aspects*, 293(1-3), pp.1-4.
32. Caruso, F., Serizawa, T., Furlong, D.N. and Okahata, Y., 1995. Quartz crystal microbalance and surface plasmon resonance study of surfactant adsorption onto gold and chromium oxide surfaces. *Langmuir*, 11(5), pp.1546-1552.
33. Levitz, P.E., 2002. Adsorption of nonionic surfactants at the solid/water interface. *Colloids and Surfaces A: Physicochemical and Engineering Aspects*, 205(1-2), pp.31-38.
34. Levitz, P., 1991. Aggregative adsorption of nonionic surfactants onto hydrophilic solid/water interface. Relation with bulk micellization. *Langmuir*, 7(8), pp.1595-1608.
35. Tiberg, F., 1996. Physical characterization of non-ionic surfactant layers adsorbed at hydrophilic and hydrophobic solid surfaces by time-resolved ellipsometry. *Journal of the Chemical Society, Faraday Transactions*, 92(4), pp.531-538.
36. Tiberg, F., Joansson, B., Tang, J.A. and Lindman, B., 1994. Ellipsometry studies of the self-assembly of nonionic surfactants at the silica-water interface: equilibrium aspects. *Langmuir*, 10(7), pp.2294-2300.
37. Levitz, P., Van Damme, H. and Keravis, D., 1984. Fluorescence decay study of the adsorption of nonionic surfactants at the solid-liquid interface. 1. Structure of the adsorption layer on a hydrophilic solid. *The Journal of Physical Chemistry*, 88(11), pp.2228-2235.
38. Levitz, P. and Van Damme, H., 1986. Fluorescence decay study of the adsorption of nonionic surfactants at the solid-liquid interface. 2. Influence of polar chain length. *The Journal of Physical Chemistry*, 90(7), pp.1302-1310.

39. Portet, F., Desbene, P.L. and Treiner, C., 1997. Adsorption isotherms at a silica/water interface of the oligomers of polydispersed nonionic surfactants of the alkylpolyoxyethylated series. *Journal of colloid and interface science*, 194(2), pp.379-391.
40. Gellan, A. and Rochester, C.H., 1985. Adsorption of n-alkylpolyethylene glycol non-ionic surfactants from aqueous solution on to silica. *Journal of the Chemical Society, Faraday Transactions 1: Physical Chemistry in Condensed Phases*, 81(9), pp.2235-2245.
41. Partyka, S., Zaini, S., Lindheimer, M. and Brun, B., 1984. The adsorption of non-ionic surfactants on a silica gel. *Colloids and surfaces*, 12, pp.255-270.
42. Corkill, J.M., Goodman, J.F. and Tate, J.R., 1966. Adsorption of non-ionic surface-active agents at the graphon/solution interface. *Transactions of the Faraday Society*, 62, pp.979-986.
43. Gutig, C., Grady, B.P. and Striolo, A., 2008. Experimental Studies on the Adsorption of Two Surfactants on Solid– Aqueous Interfaces: Adsorption Isotherms and Kinetics. *Langmuir*, 24(9), pp.4806-4816.
44. Shi, L., Ghezzi, M., Caminati, G., Lo Nostro, P., Grady, B.P. and Striolo, A., 2009. Adsorption isotherms of aqueous C12E6 and cetyltrimethylammonium bromide surfactants on solid surfaces in the presence of low molecular weight coadsorbents. *Langmuir*, 25(10), pp.5536-5544.
45. Stålgren, J.J.R., Eriksson, J. and Boschkova, K., 2002. A comparative study of surfactant adsorption on model surfaces using the quartz crystal microbalance and the ellipsometer. *Journal of colloid and interface science*, 253(1), pp.190-195.
46. Jian, G., Puerto, M.C., Wehowsky, A., Dong, P., Johnston, K.P., Hirasaki, G.J. and Biswal, S.L., 2016. Static adsorption of an ethoxylated nonionic surfactant on carbonate minerals. *Langmuir*, 32(40), pp.10244-10252.
47. Kuno, H. and Abe, R., 1961. The adsorption of polyoxyethylated nonylphenol on calcium carbonate in aqueous solution. *Kolloid-Zeitschrift*, 177(1), pp.40-44.
48. Akers, R.J. and Riley, P.M., 1974. Adsorption of polyoxyethylene alkyl-phenols onto calcium carbonate from aqueous solution. *J. Colloid Interface Sci.*(United States), 48(1).



49. Barati, A., Najafi, A., Daryasafar, A., Nadali, P. and Moslehi, H., 2016. Adsorption of a new nonionic surfactant on carbonate minerals in enhanced oil recovery: experimental and modeling study. *Chemical Engineering Research and Design*, 105, pp.55-63.
50. Tiberg, F., Brinck, J. and Grant, L., 1999. Adsorption and surface-induced self-assembly of surfactants at the solid–aqueous interface. *Current opinion in colloid & interface science*, 4(6), pp.411-419.
51. Paria, S. and Khilar, K.C., 2004. A review on experimental studies of surfactant adsorption at the hydrophilic solid–water interface. *Advances in colloid and interface science*, 110(3), pp.75-95.
52. Zhang, R. and Somasundaran, P., 2005. Aggregate formation of binary nonionic surfactant mixtures on hydrophilic surfaces. *Langmuir*, 21(11), pp.4868-4873.
53. Somasundaran, P. and Krishnakumar, S., 1997. Adsorption of surfactants and polymers at the solid-liquid interface. *Colloids and Surfaces A: physicochemical and engineering aspects*, 123, pp.491-513.
54. Das, S., Nguyen, Q., Patil, P.D., Yu, W. and Bonnecaze, R.T., 2018. Wettability alteration of calcite by nonionic surfactants. *Langmuir*, 34(36), pp.10650-10658.
55. Urbina-Villalba, G., Reif, I., Márquez, M.L. and Rogel, E., 1995. Theoretical study on the structure and interfacial areas of nonyl phenol ethoxylated surfactants. *Colloids and Surfaces A: Physicochemical and Engineering Aspects*, 99(2-3), pp.207-220.
56. El Eini, D.I.D., Barry, B.W. and Rhodes, C.T., 1976. Micellar size, shape, and hydration of long-chain polyoxyethylene nonionic surfactants. *Journal of Colloid and Interface Science*, 54(3), pp.348-351.
57. Lee, E.M., Thomas, R.K., Cummins, P.G., Staples, E.J., Penfold, J. and Rennie, A.R., 1989. Determination of the structure of a surfactant layer adsorbed at the silica/water interface by neutron reflection. *Chemical physics letters*, 162(3), pp.196-202.
58. Israelachvili, J.N., 1976. Mitchell, DJ.; Ninham, BWJ Chem. Soc. *Faraday Trans. II*, 72, pp.1525-1568.

59. Somasundaran, P., Snell, E.D., Fu, E. and Xu, Q., 1992. Effect of adsorption of non-ionic surfactant and non-ionic—anionic surfactant mixtures on silica—liquid interfacial properties. *Colloids and surfaces*, 63(1-2), pp.49-54.
60. Blankschtein, D., Thurston, G.M. and Benedek, G.B., 1986. Phenomenological theory of equilibrium thermodynamic properties and phase separation of micellar solutions. *The Journal of chemical physics*, 85(12), pp.7268-7288.
61. Thurston, G.M., Blankschtein, D., Fisch, M.R. and Benedek, G.B., 1986. Theory of thermodynamic properties and phase separation of micellar solutions with lower consolute points. *The Journal of chemical physics*, 84(8), pp.4558-4562.
62. Brown, W., Johnsen, R., Stilbs, P. and Lindman, B., 1983. Size and shape of nonionic amphiphile (C12E6) micelles in dilute aqueous solutions as derived from quasielastic and intensity light scattering, sedimentation, and pulsed-field-gradient nuclear magnetic resonance self-diffusion data. *The Journal of Physical Chemistry*, 87(22), pp.4548-4553.
63. Valiya Parambathu, A., Wang, L., Asthagiri, D. and Chapman, W.G., 2019. Apolar behavior of hydrated calcite {1 0-1 4} surface assists in naphthenic acid adsorption. *Energy & Fuels*.
64. Xu, Z., Yang, X. and Yang, Z., 2008. On the mechanism of surfactant adsorption on solid surfaces: free-energy investigations. *The Journal of Physical Chemistry B*, 112(44), pp.13802-13811.
65. Schlumberger Market Analysis, **2007**.

## **Chapter 4: Wettability alteration and Adsorption of Mixed Nonionic and Anionic Surfactants on Carbonates**

### **4.1. INTRODUCTION**

Surfactants improve oil recovery by lowering oil-water capillary forces and by changing wettability of reservoir surfaces.<sup>1-7</sup> Lowering of oil-water (O/W) interfacial tension (IFT) to ultra-low values ( $< 10^{-3}$  mN/m) promotes spontaneous emulsification which significantly improves oil mobilization.<sup>1-4</sup> Surfactant-induced wettability alteration is also a key mechanism to improve oil recovery.<sup>5-7</sup> This is particularly important in fractured and oil-wet carbonates. The change in wettability from oil to water-wet can lead to higher oil recoveries by allowing spontaneous imbibition of the aqueous phase inside the porous media.<sup>7-10</sup> Several studies have been done to study wettability alteration and its effect on oil recovery on different mineral substrates.<sup>1-14</sup> The water-oil contact angle on the substrate gives an indication of the wettability in the system. Surfactants that give rise to lower contact angles ( $< 80^\circ$ ) have been correlated to higher oil recoveries.<sup>6-9</sup> The desirable properties of a surfactant for wettability alteration are low contact angles, a moderate to low O/W IFT (1 – 10 mN/m), low adsorption on the rock, and operation at elevated temperatures of the reservoir. In this paper we evaluate all four of these metrics for mixed-surfactant systems consisting of secondary alcohol ethoxylates and anionic cosurfactants.

In an oil reservoir there are several factors that can impact the decision-making process to optimize surfactant chemistry. These include rock-type, reservoir brine chemistry and temperature, pH, permeability, and nature of oil. Consequently, different surfactant formulations are required to adjust to the reservoir conditions and maintain desirable oil recoveries. Previously, two families of nonionic surfactants, with repeating units of oxyethylene groups as the hydrophilic moiety, were evaluated on their wettability alteration properties through a series of contact-angle experiments on oil-wet calcite.<sup>15</sup>

Wettability alteration was found to be enhanced by surfactants with shorter hydrophilic groups and at higher temperatures. An increased adsorption under those conditions was determined to be the underlying cause.<sup>16</sup>

Nonionic surfactant solutions exhibit phase separation beyond a temperature known as the cloud point. It is a consequence of decreased hydration of oxyethylene chains with an increase in temperature, and this prevents use of nonionic surfactants at high temperature. The cloud point and hence the operating temperature of nonionic surfactants can be increased by incorporating molecules that can improve their aqueous stability at high temperatures. These molecules, known as hydrotropes, are typically ionic surfactants that form charged mixed micelles of the nonionic surfactant and the hydrotrope. The mixed micelles precipitate at higher temperatures increasing the cloud point.

Different organic molecules have been evaluated in the past, named cloud point boosters (CPBs). They were classified as ionic or nonionic based on the presence or not of charges. Alkanols and polyalkylene glycols are a few popular nonionic CPBs. Charged phospholipids and long chain fatty acids are ionic CPBs. While the nonionic CPBs are effective only at molar concentrations, ionic CPBs are effective even at millimolar concentrations. This makes ionic surfactants a more suitable candidate for surfactant formulations for oil reservoirs. A few surfactant formulations for high-temperature and high-salinity reservoir applications have been developed for nonionic surfactants in the past.<sup>18</sup> Using appropriate additives the cloud point of nonionic surfactant solutions in high brine salinities were raised to around 120°C. Similar elevations in cloud points were also reported in systems of nonionic and cationic surfactants.<sup>19</sup>

There have been few studies evaluating the effect of surfactant mixtures on wettability alteration in mineral substrates. Mixtures of nonionic and cationic surfactants were evaluated in qualitative contact angle measurements on calcite and systems which

exhibited wettability alteration to final weakly water-wet state were used in spontaneous imbibition experiments.<sup>19</sup> Similar contact angle tests were also performed with mixed surfactant formulations on a hydrophobic parafilm surface.<sup>18</sup> Significant decrease in contact angle upon surfactant addition along with oil recoveries up to 31% above the brine recovery in core-flooding experiments were reported.

The adsorption of nonionic/ionic surfactants on solid substrates has been found to exhibit synergistic or antagonistic interactions depending on the nature of the charges involved. Intermolecular interactions between the different surfactants, lateral hydrophobic interactions especially for nonionic surfactants and the molecule-substrate interactions together determine the eventual adsorption of these mixtures. Three different combinations of surfactant mixtures were identified based on whether the ionic/nonionic component acts as an active and/or a passive adsorption species.<sup>48</sup> Competition for adsorption sites has been found in the case in which both act as active adsorption species. At equal mixing ratio, however ionic species adsorb more because of stronger electrostatic interactions. When the ionic surfactants have identical charges as that of the substrate, their adsorption is significantly increased in the presence of nonionic surfactants. The lateral hydrophobic interactions between the two groups of molecules act as an anchor for ionic surfactants to co-adsorb on the substrate. The adsorption of passive nonionic surfactants can also be significantly increased in the presence of active ionic surfactants.<sup>50-51</sup> The mechanisms of adsorption of these mixtures have been investigated for select cases. Ionic surfactants typically adsorb via direct electrostatic interactions between individual molecules and the surface resulting in a typical monolayer to admicelle transition which is marked by an eventual plateau in the adsorption isotherm. For nonionic surfactants, an aggregative or micellar adsorption is believed to be the key mechanism. Rises in adsorption at higher concentrations and temperatures have been observed which corresponds to the growth in

the adsorbed aggregates.<sup>16</sup> The extent of adsorption for such systems is found to depend both on surfactant hydrophilicity and the temperature – both of which can be combined into the parameter, Cloud point temperature difference,

$$\text{CPTD} = \text{CP} - T, \quad (1)$$

which incorporates the thermodynamic property of cloud point of a nonionic surfactant.<sup>16</sup> A universal behavior of higher adsorption has also been observed as a surfactant nears its cloud point.

A detailed study of mixed surfactants and their evaluations of wettability alteration as a function of individual surfactant composition and temperature is not present currently. In addition, the adsorption of surfactants in such dual systems and the corresponding correlation to wettability alteration has not been done to date. Here, anionic hydrotropes are first evaluated on their capacity to enhance aqueous stabilities of nonionic surfactants. These surfactants will be henceforth referred to as co-surfactants. The cloud point temperatures of the mixed surfactant systems are reported for different co-surfactants and at different compositions. The effect of molecular structure of both the primary and co-surfactant in determining the aqueous stability is then discussed. One of the main applications for these mixed systems is as stable, high-temperature wettability-altering agents. Hence, depending on the cloud point of the formulations, different mixed-surfactant systems are then used for wettability alteration analyses on mixed-wet carbonate surface. This includes both contact angle and oil/water interfacial tension (IFT) measurements to determine the overall capillary driving force responsible for spontaneous imbibition inside porous media. The adsorption in both single and mixed-surfactant systems is then investigated through static adsorption experiments on carbonate surfaces. A probable mechanism of adsorption has been inferred from these adsorption studies. Like in single-surfactant systems,<sup>16</sup> the parameter of CPTD has been used to correlate the different aspects

of aqueous stability, driving force and adsorption to put forward a case for universal behavior in surfactant based wettability-altering systems.

#### **4.2. MATERIALS**

Tables 4.1 and 4.2 list the surfactants studied with their molecular structures. All surfactants were provided by The Dow Chemical Company. The family of nonionic surfactant studied is secondary alcohol ethoxylates represented by SAE-x. The hydrophilic and hydrophobic components in this family are repeating units of ethylene oxide and secondary alcohol comprised of short alkyl chains  $R_1$  and  $R_2$  respectively. In the current study, nonionic surfactants corresponding to 9 and 15 hydrophilic units were used. The co-surfactants are families of anionic surfactants, differentiated by their molecular sizes. Calcite plates (Iceland Spar) obtained from Wards Natural Sciences were used as a representative carbonate surface for wettability alteration experiments. Crude oil used in the experiments was obtained from a carbonate oil formation. Indiana limestone is used as the representative carbonate surface for adsorption experiments. It was obtained from Kocurek Industries (TX, USA) and sieved with 200-400 mesh, washed and dried before carrying out any experiments. The surface area of the limestone particles is determined to be  $0.84 \text{ m}^2/\text{gm}$  by the Brunauer–Emmett–Teller (BET) method.

Table 4.1: List of nonionic surfactants evaluated in the study.

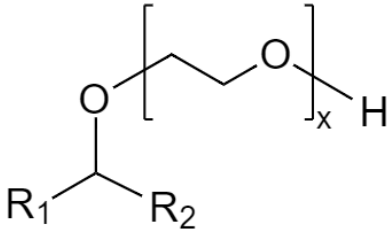
Structure	Surfactant name	Specification (x)
	SAE-x (Secondary alcohol ethoxylate)	9
		15

Table 4.2: List of anionic co-surfactants evaluated in the study.

Surfactant name	Specification
LM	Low molecular weight
MM	Medium molecular weight (Higher degree of sulfonation)
MM2	Medium molecular weight
HM	High molecular weight
VM	Very high molecular weight

Sodium chloride and calcium chloride (Fisher) were used as received. HPLC grade water (Fisher Scientific) was used to make all the solutions.

### 4.3. METHODOLOGY

#### 4.3.1. Cloud Point Measurements

Surfactant solutions were prepared in glass vials and placed in an oven and heated for 20 minutes at a given temperature. The temperature was increased by 1° at each step



and shaken gently to observe the formation of a white opaque phase in the solutions. The onset of opacity was reported as the cloud point temperature (Figure 4.1).



Figure 4.1. Onset of clouding upon heating solutions of nonionic surfactants

#### 4.3.2. Interfacial Tension Measurements

The inverted pendant drop technique was used to measure the oil-brine and oil-surfactant interfacial tensions (IFT). A quartz cell was filled with surfactant brine solution and placed inside an environmental chamber set at a desired temperature. Oil drops were introduced in the solution using a syringe with inverted needle. The shape of the oil drop was monitored using a high magnification camera (Figure 4.2) and the IFT

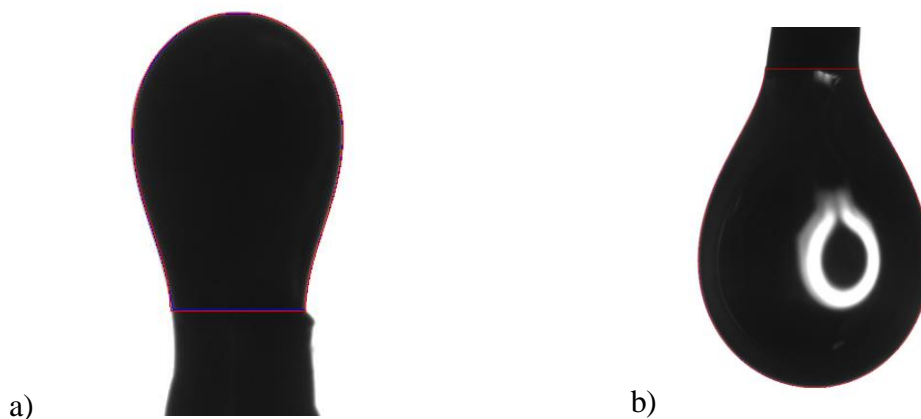


Figure 4.2. Typical drop images used for IFT measurements. a) Shape of an inverted oil drop inside surfactant solution. b) Drop of surfactant solution in air

values were extracted from the images using the Pendant drop plug-in in ImageJ.

### 4.3.3. Critical Micelle Concentrations (CMC)

Air-surfactant IFT measurements were used to determine the CMCs of different single and mixed surfactant systems. The regular pendant drop method as shown in figure 4.2b was used for these measurements. The IFT values were measured at different surfactant concentrations and the CMC was extracted from IFT vs concentration plot as shown in Figure 4.3. CMCs measured for SAE-15, LM and HM surfactants are shown in Figure 4.4. A brine salinity of 12% NaCl and 0.2% CaCl<sub>2</sub> was used for all the measurements. The measurements were performed at two different temperatures – 50°C and 70°C.

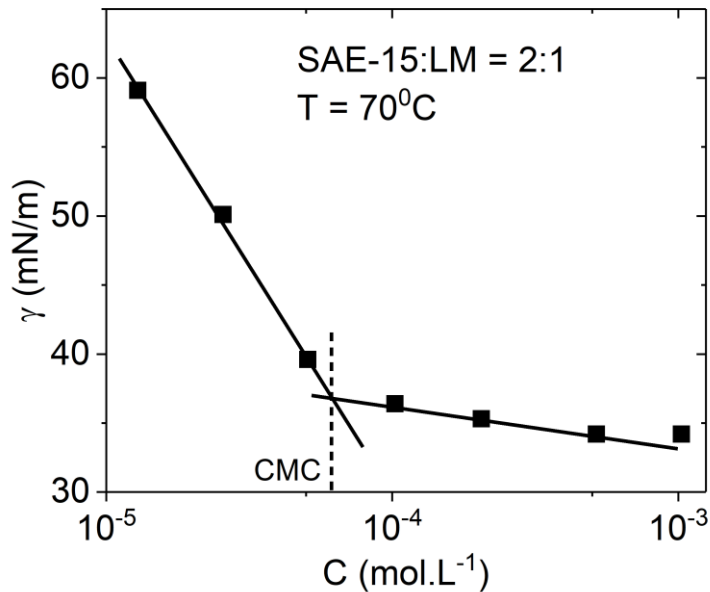


Figure 4.3. IFT vs total surfactant concentration in 2/1 by mass mixture of SAE-15/LM at 70°C. The vertical dotted line represents the CMC of the solution.

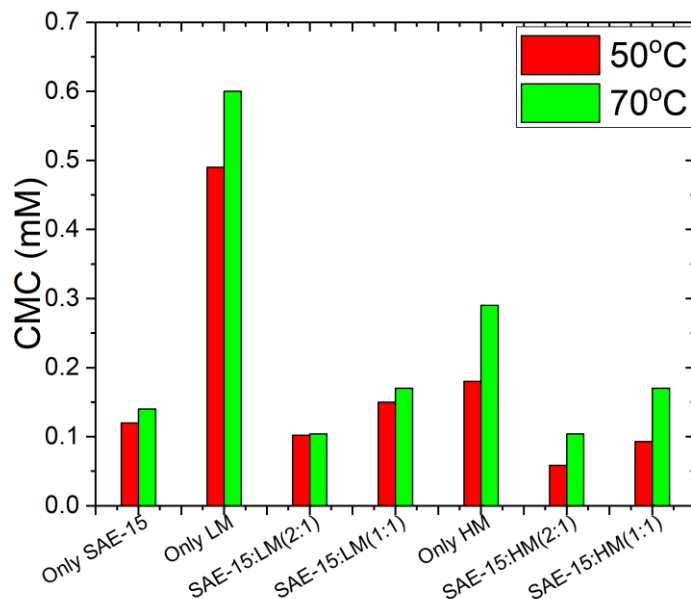


Figure 4.4. Measured CMCs of SAE-15, LM, HM and SAE-15+LM, SAE-15+HM mixtures at different compositions. The CMCs correspond to two different temperatures – 50°C and 70°C.

#### 4.3.4. Micelle size measurements

Dynamic light scattering with non-invasive backscatter optics is used to measure the micelle sizes of surfactants. Measurements were carried out in a Malvern Zetasizer Nano ZS. Measurements were done for SAE-15+LM and SAE+HM systems. The brine salinity was the same as before. Two different concentrations – 4000 ppm SAE-15/2000 ppm co-surfactant and 4000 ppm SAE-15/4000 ppm co-surfactant were used in the measurements. The temperature was varied between 50°C to 90°C whenever possible. The micelle sizes for these systems are shown in the bar plot in Figure 4.5.

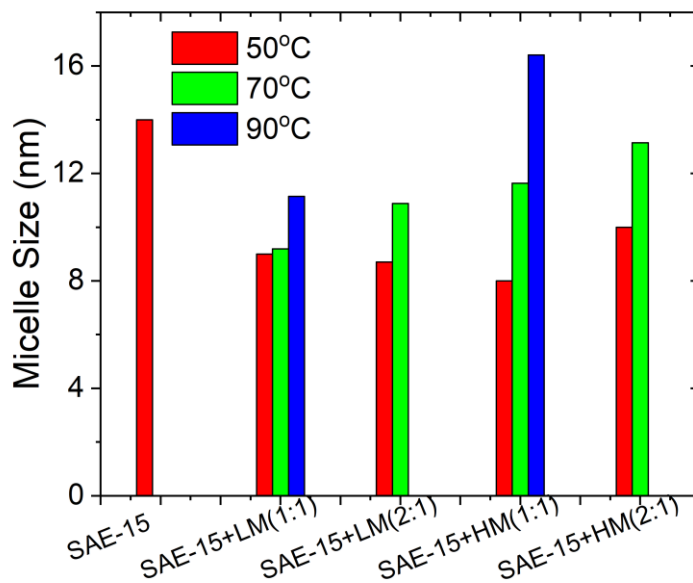


Figure 4.5. Micelle-size of surfactant systems - SAE-15, SAE-15+LM and SAE-15+HM obtained from DLS measurements.

#### 4.3.5. Contact Angle Measurements

Calcite plates (3cm x 3cm x 1cm) were first cut from calcite blocks by breaking across the cleavage planes, cleaned using ethyl alcohol and subsequently dried at 120°C. Following this, a small drop of oil (~ 1mm size) was placed on the calcite. The drop was then allowed to age the calcite at 70°C for 3 days. During the ageing process, the drop was kept covered to minimize evaporation. A uniform oil-patch was formed at the end of ageing which was placed inside a quartz cell containing surfactant-brine solutions. The temperature was regulated by an environmental chamber. The shape of the drops was monitored using a high magnification camera and the contact angles extracted using the ImageJ software. Figure 4.6 shows the side views of an aged oil-patch on calcite before and after treatment with surfactant solutions.



Figure 4.6a) Side-view of an oil patch on calcite. The drop spreads on the calcite indicating that the patch is aged.

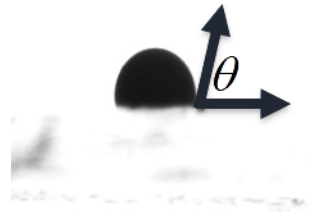


Figure 4.6b) Side-view of an oil patch after treatment with surfactant solution. The patch beads up indicating wettability alteration by the surfactant.

#### 4.3.6. Adsorption Experiments

Batch adsorption experiments were carried out for the surfactants at 70°C and 90°C. Indiana limestone particles were used as the representative carbonate surface for these experiments. A constant brine salinity of 12% NaCl and 0.2% CaCl<sub>2</sub> was used for all the experiments. Prior to each experiment, the brine was equilibrated with a given mass of limestone at the experimental temperature for a day. This ensured that the brine composition remained same for both the calibration and experimental samples. One part of this brine was then used to prepare calibration samples in the concentration range of 100 – 4000 ppm. Another part was used to prepare the surfactant solutions for adsorption experiments. Along with surfactant mixtures, pure co-surfactants were also used for this study. 10 mL of these surfactant solutions were added to 2.75 g of prepared limestone particles in centrifuge tubes and placed in an oven. The mixture was shaken periodically for 24 hours and then allowed to settle without shaking for additional 24 hours. Following this, the supernatant solution was separated to analyze the equilibrium bulk surfactant concentration.

#### 4.3.7. Measurement of Surfactant Concentration

The concentrations of solutions containing only co-surfactants were analyzed using the UV-Vis spectroscopy method. A Cary UV-Vis instrument in single-front mode was used to observe absorbance peaks corresponding to 210 nm and 236 nm (Figure 4.7). Separate calibration curves were prepared for each experiment.

Surfactant concentrations in mixed systems were analyzed using the NMR technique. Samples were first prepared by pipetting 500 $\mu$ l of sample into a vial with 100 $\mu$ l of Deuterium Oxide/TSP (3-(Trimethylsilyl)propionic-2,2,3,3-d<sub>4</sub> acid, sodium salt) standard solution (TSP 1 $\mu$ mol/100 $\mu$ L). The samples were shaken and vortexed to ensure homogeneity. The samples were analyzed by <sup>1</sup>H NMR using a Bruker AVANCE 400 MHz NMR spectrometer.

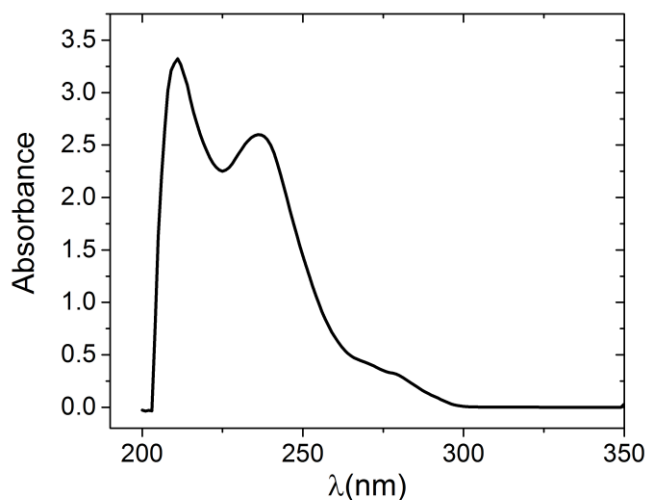


Figure 4.7. Typical absorbance plots from UV-Vis measurements of co-surfactant solutions.

<sup>1</sup>H NMR analysis was performed using the water suppression experiment. 66,000 data points were used with a sweep width of 6,400 Hz. Separate calibration curves were

prepared for each experiment prior to determining the unknown concentrations. The adsorption is obtained from a simple mass balance

$$\Gamma = m_{sol} (C_0 - C) / Sm_c, \quad (2)$$

where  $m_{sol}$ ,  $C_0$ ,  $C$ ,  $S$  and  $m_c$  are mass of the surfactant solution, initial surfactant concentration, final surfactant concentration, BET surface area of limestone and mass of limestone used in the experiment respectively.

#### 4.4. RESULTS

##### 4.4.1. Aqueous Stability and Cloud Point Measurements

Cloud point measurements were carried out for both SAE-9 and SAE-15 as the primary component along with the co-surfactants. A brine salinity of 12% NaCl and 0.2% CaCl<sub>2</sub> was used and the primary component concentration was kept fixed at 4000 ppm. Co-surfactant concentrations of 2000 ppm and 4000 ppm were used to observe the effect of co-surfactant composition. Figures 4.8 shows the cloud point values for different

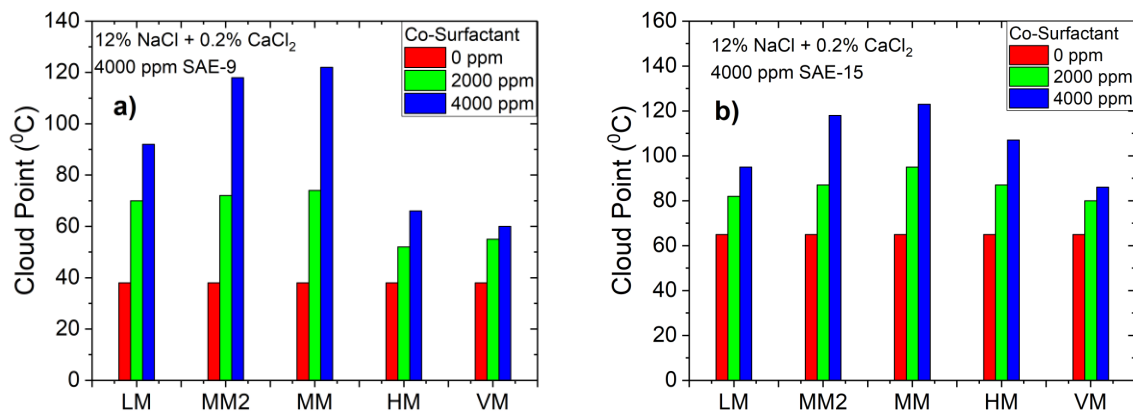


Figure 4.8. Cloud point values for a) SAE-9 and b) SAE-15 with co-surfactants at two different concentrations.

systems studied. Cloud points of solutions with only the primary component are 39°C and 65°C for SAE-9 and SAE-15 respectively. The cloud points increase significantly with addition of co-surfactants. For SAE-9 the highest increase corresponds to MM with a cloud point of 125°C. MM also gives the highest cloud point of 122°C for SAE-15. VM co-surfactant is associated with the lowest cloud point elevation in both the systems.

#### 4.4.2. O/W IFT Measurements

O/W IFTs were measured using the pendent drop technique at three different temperatures 50°C, 70°C and 90°C whenever admissible by the system cloud point. Figure 4.9 shows the IFT values measured for selected mixed surfactant systems.

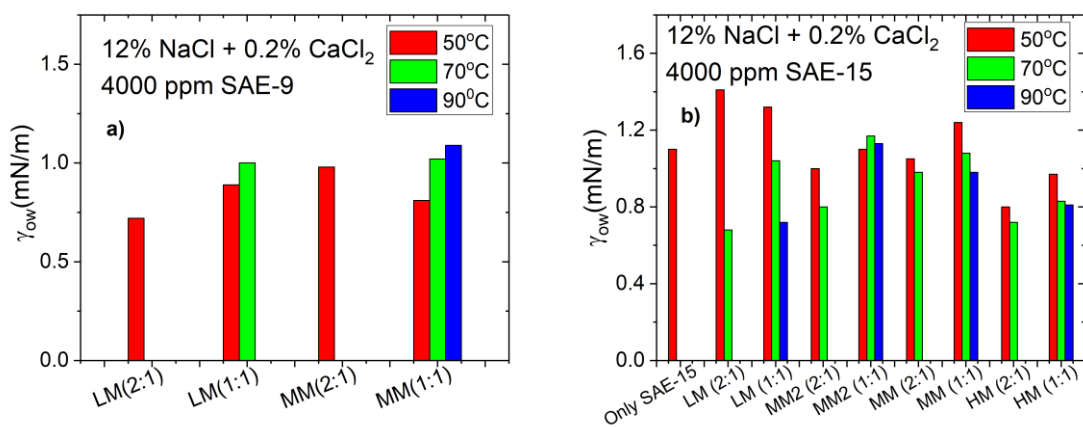


Figure 4.9. Oil/Surfactant IFT values for a) SAE-9 and b) SAE-15 + Co-surfactants

The primary component concentration is again fixed at 4000 ppm and the co-surfactant concentration is varied between 2000 ppm (SAE-15/Co-Surfactant – 2:1) and 4000 ppm (SAE-15/Co-Surfactant – 1:1). For SAE-9 containing systems, the IFT values varied between 0.8 – 1.1 mN/m whereas for SAE-15 containing systems the IFT values were between 0.7 – 1.4 mN/m. These values indicate that the O/W IFTs are high enough to



eliminate any microemulsion formation and consequently any emulsification-driven process can be neglected.

#### **4.4.3. Wettability Alteration**

Contact angle measurements were used as an indicator for wettability alteration for these mixed surfactant systems. The concentrations and temperatures used for these experiments were same as those used in IFT measurements. Initial contact angles measured in the aqueous phase were around 160-170°. Figure 4.10 shows the final (equilibrium) contact angles measured in brine and single component LM, respectively, at 70°C. The high contact angles ( $\sim 160^\circ$ ) indicate that brine and co-surfactant by themselves do not alter the wettability of these systems. This also indicates that any wettability alteration observed in the mixed systems is solely because of the primary nonionic surfactant. The effect of primary component in mixed system can be seen in Figs. 4.10c and 4.10d which show the final contact angle for SAE-9 + LM (1:1) and SAE-15 + LM (1:1) at 70°C. The oil patch beads up giving a final contact angle  $< 90^\circ$  indicating wettability alteration.

The final contact angles for surfactant mixtures are plotted in Fig 4.11. The contact angles reported are the average of at least three separate measurements. At 50°C, SAE-9+LM systems reported a contact angle value of about 68° and 78° for 2:1 and 1:1 SAE-9/LM mixtures, respectively. This indicates an increase in contact angle or decrease in wettability alteration as the percentage of co-surfactant is increased in the mixture.

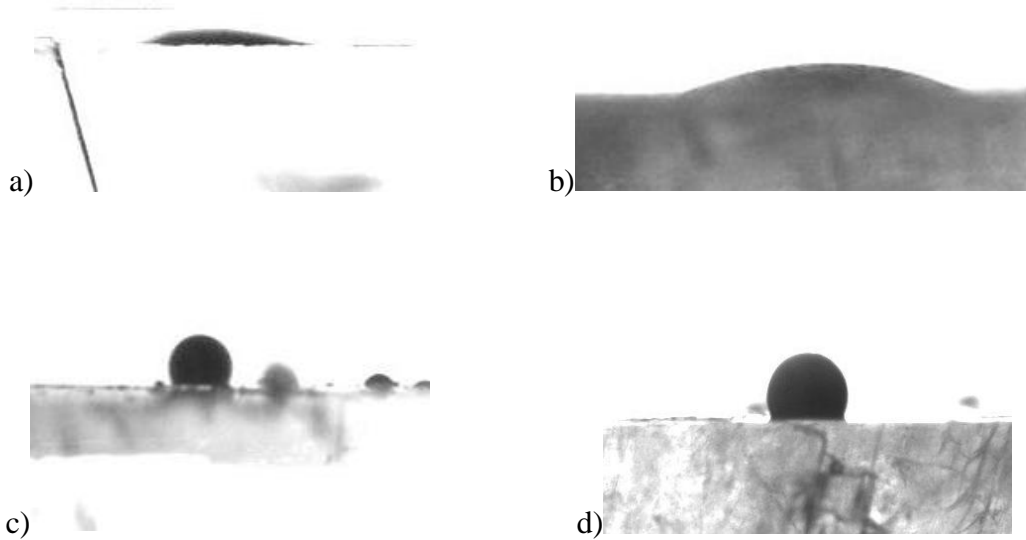


Figure 4.10. Final contact angles for a) brine and b) 4000 ppm LM c) SAE-9 + LM (4000 ppm:4000 ppm) and d) SAE-15 + LM (4000 ppm: 4000 ppm) at 70°C

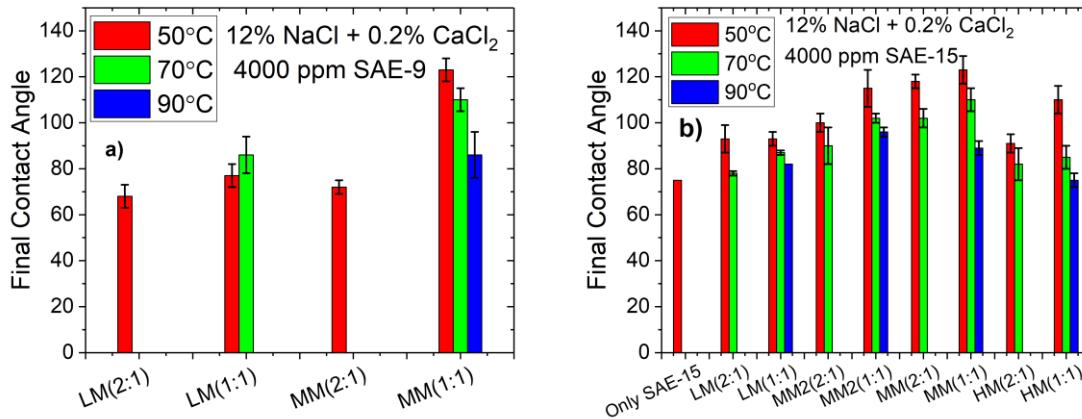


Figure 4.11. Bar plots showing final contact angles in mixed surfactant systems containing a) SAE-9 and b) SAE-15.

The contact angle values lower than 90°, however, still indicate a final water-wet state which is desirable for capillary imbibition processes. Similar behavior is also observed for SAE-9+MM systems. At 50°C, the contact angle was 72° for 2000 ppm (2:1 mixture), which increased to about 120° when the concentration of MM was raised to 4000 ppm (1:1 mixture). These results indicate different degrees of dependence of wettability alteration on the co-surfactant concentration for different co-surfactants.

There is a gradual decrease in the contact angle as the temperature is increased from 50°C to 70°C and then 90°C for the 1:1 SAE-9/MM system. This enhanced wettability alteration at higher temperatures is similar in nature to observations from single surfactant systems.<sup>15</sup> For SAE-9+LM, however, a slight increase in the contact angle from 78° to 84° was observed.

Final contact angle corresponding to just SAE-15 at 50°C was about 74°. The addition of co-surfactant increases the contact angle, irrespective of the co-surfactant. This means that the co-surfactant decreases the extent of wettability alteration in the mixed surfactant system. SAE-15+LM systems exhibit contact angle in the range of 78° to 92° depending on the composition of solution and the temperature. MM and MM2 containing systems exhibit higher contact angles in the range of 90° to 120°. The highest wettability alteration observed for SAE-15+HM systems was at 90°C where a 1:1 surfactant mixture had a contact angle of 75°. Like SAE-9 containing systems, the co-surfactant composition in the mixture affects the wettability alteration to different extents for different co-surfactants. For SAE-15, the increase in contact angle upon addition of co-surfactant is lower for LM than compared to MM and MM2. This behavior is similar to the mixed systems containing SAE-9. For SAE-15+HM, at 50°C a significant increase in contact angle is observed as the percentage of HM is increased in the mixture. However, at 70°C, the change in contact angle is almost independent of the mixture composition. Wettability

alteration for all systems containing SAE-15 is also enhanced as the temperature is increased.

#### 4.4.4. Adsorption Isotherms

Static adsorption experiments were performed for SAE-15 + LM and SAE-15 + HM systems. Two different SAE-15/Co-surfactant compositions – 1/1 and 2/1 by mass were used for these experiments. The temperature was also varied between 70°C and 90°C whenever admissible by the system cloud point. The maximum concentration of primary component was limited to 4000 ppm in all the experiments. Each experiment was repeated at least twice to get an estimate of the associated measurement errors. Figure 4.12 shows the adsorption of primary component SAE-15 and co-surfactant LM in SAE-15 + LM systems at 70°C. The concentration in x-axis is the equilibrium bulk concentration of SAE-15 and LM. The empty and filled red symbols in the figure correspond to 1/1 and 2/1 mass composition of SAE-15 to LM, respectively. Adsorption measurements were done for just SAE-15 previously.<sup>16</sup> These adsorption measurements were done at lower temperatures because of cloud point limitation. However, it can be used to compare the adsorption in single and mixed systems and to understand the role of co-surfactant on the adsorption of primary component. From Fig. 4.12a the maximum adsorptions of SAE-15 at 1/1 and 2/1 compositions are about  $0.4\mu\text{mol}/\text{m}^2$  and  $0.7\mu\text{mol}/\text{m}^2$ , respectively. Both values are lower than the  $1\mu\text{mol}/\text{m}^2$  adsorption observed for just SAE-15 at 50°C (shown in dotted line). This indicates that addition of co-surfactant decreases the adsorption of SAE-15 in the mixed system. It also shows that the adsorption of SAE-15 in SAE-15+LM systems is dependent on the initial surfactant composition - adsorption of SAE-15 increases with an increase in the percentage of SAE-15. Figure 4.12b shows the adsorption of LM for these mixtures. In addition to mixed surfactants, adsorption in single co-surfactant systems were

also evaluated for both LM and HM at the same temperatures. In Fig. 4.12b the adsorption in a solution of just LM is shown in blue circles. For SAE-15+LM systems, the adsorption behavior of LM follows a similar trend to that of SAE-15. At the same bulk concentration, the adsorption of LM increases as the composition of SAE-15 in the mixture increases. A plateau in the adsorption of LM in 1/1 mixture was however not observed for the concentrations evaluated.

Temperature also has a marked effect on the adsorption in this system. Figure 4.13 shows the adsorption behavior of SAE-15 and LM in mixed systems at 90°C. Only the 1/1 blend was stable at this temperature and the maximum adsorption of SAE-15 in the 1/1 blend increases significantly, from 0.4 $\mu\text{mol}/\text{m}^2$  at 70°C to about 1 $\mu\text{mol}/\text{m}^2$  at 90°C. The maximum co-surfactant adsorption also increases from 0.8 $\mu\text{mol}/\text{m}^2$  at 70°C to 1.6 $\mu\text{mol}/\text{m}^2$  at 90°C. Maximum adsorption in LM solutions at 90°C was around 1.1 $\mu\text{mol}/\text{m}^2$ .

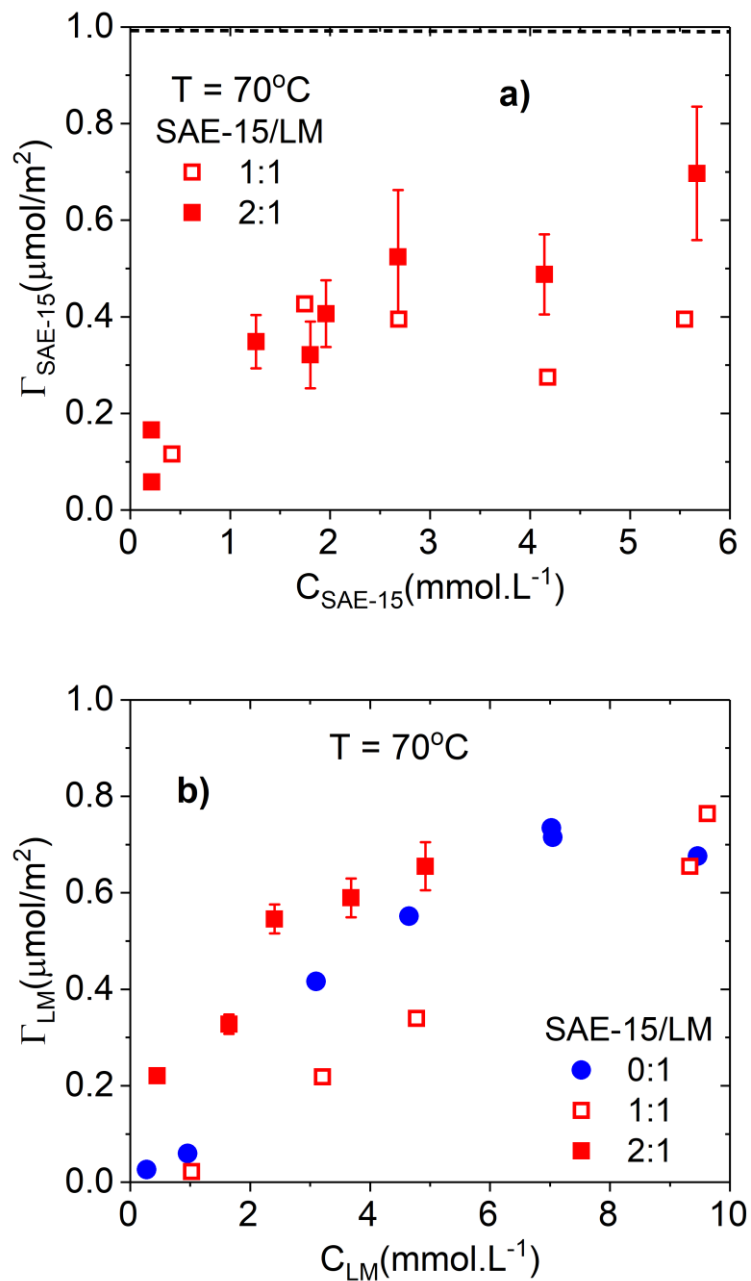


Figure 4.12. Adsorption isotherms of SAE-15+LM mixtures at 70°C. a) Adsorption of SAE-15 versus the bulk SAE-15 concentration. b) Adsorption of LM versus the bulk LM concentration. The dotted lines represent the maximum adsorption of SAE-15 in single surfactant system at 50°C.

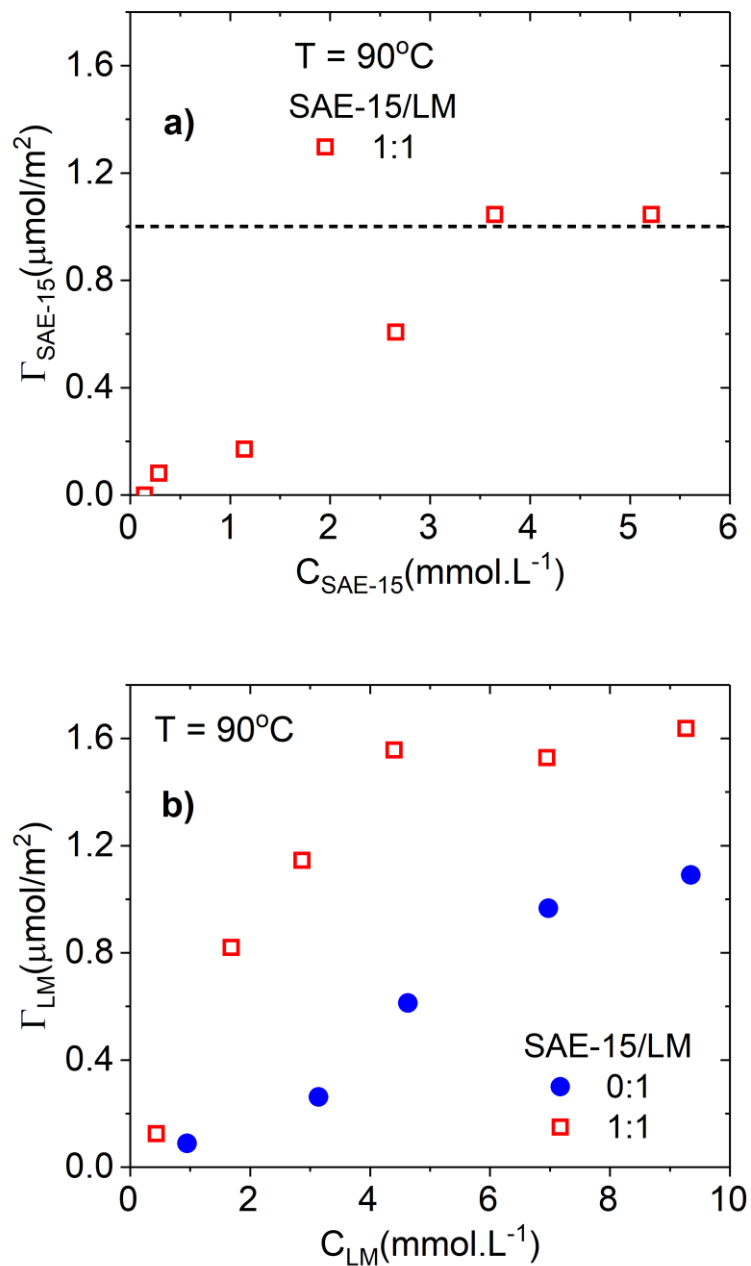


Figure 4.13. Adsorption isotherms of SAE-15+LM at  $90^\circ\text{C}$ . a) Adsorption of SAE-15 versus the bulk SAE-15 concentration. b) Adsorption of LM versus the bulk LM concentration. The dotted lines represent the maximum adsorption of SAE-15 in single surfactant system at  $50^\circ\text{C}$ .

The adsorption isotherms of SAE-15 and HM in SAE-15+HM mixed systems at 70°C are shown in Figs. 4.14a and 4.14b. The green filled and empty symbols represent formulations corresponding to SAE-15/HM mass ratios of 1/1 and 2/1 respectively. At this temperature, the maximum adsorption of SAE-15 was about 0.4 $\mu\text{mol}/\text{m}^2$  for both the different mass compositions. This adsorption is once again lower than the single component adsorption of SAE-15 at a lower temperature (shown in dotted line), indicating that the adsorption of SAE-15 is reduced in the presence of the co-surfactant. Unlike the previous case, the extent of decrease is, however, relatively independent of the composition of the mixture. The adsorption of the co-surfactant HM also exhibits a different behavior than in SAE-15+LM systems. The maximum adsorption of just HM solution at this temperature was around 0.6 $\mu\text{mol}/\text{m}^2$ . This adsorption remained relatively unchanged for a 1/1 SAE-15+HM mixture. However, further increase in the percentage of SAE-15 resulted in a lower adsorption of HM. Figure 4.15 shows the adsorption isotherm of SAE-15 and HM in these systems at 90°C. Once again, only the mixtures corresponding to 1/1 mass compositions could be evaluated at this temperature. The adsorption of SAE-15 in the mixture was around 0.45 $\mu\text{mol}/\text{m}^2$  which is slightly higher than the corresponding adsorption at 70°C. Thus, along with co-surfactant concentration, temperature also did not significantly affect the extent of adsorption of SAE-15 in SAE-15+HM system. Figure 4.15b shows that at 90°C, the addition of SAE-15 reduces the maximum adsorption of HM from 1.1 $\mu\text{mol}/\text{m}^2$  to 0.7 $\mu\text{mol}/\text{m}^2$ .



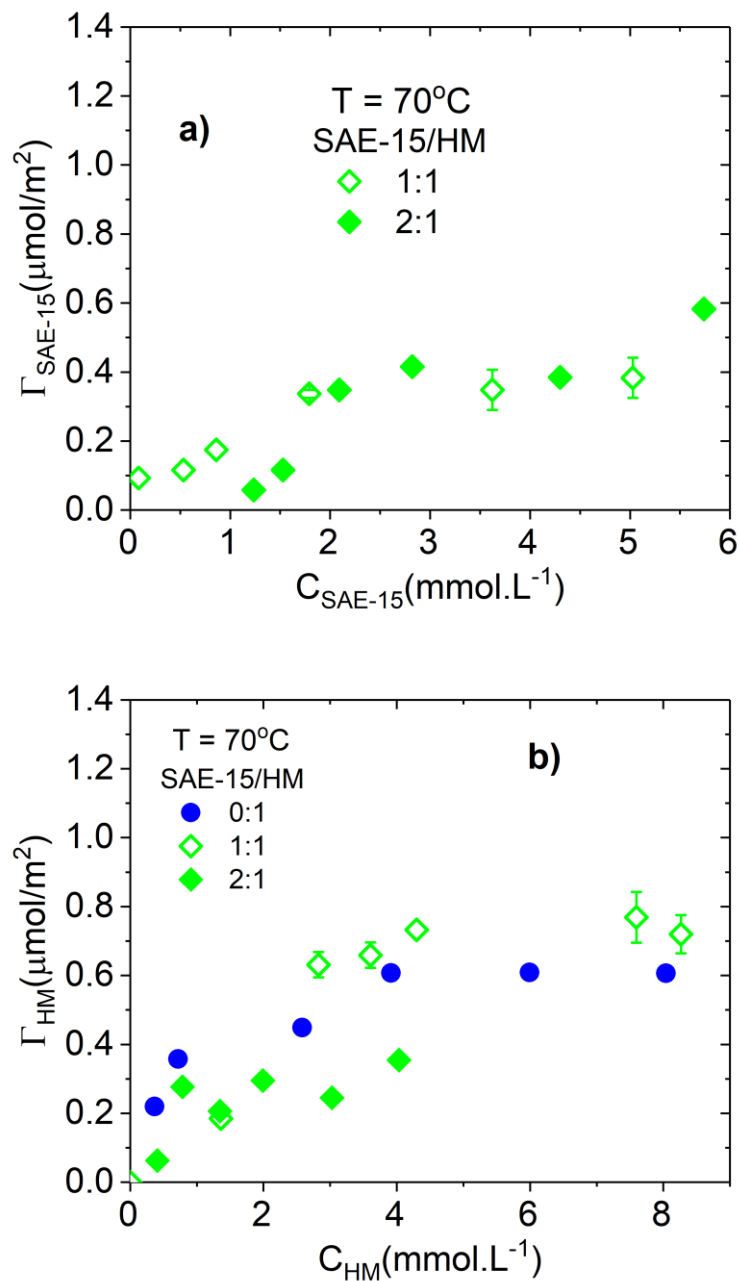


Figure 4.14. Adsorption isotherms of SAE-15+HM at 70°C. a) Adsorption of SAE-15 versus the bulk SAE-15 concentration. b) Adsorption of HM versus the bulk HM concentration. The dotted lines represent the maximum adsorption of SAE-15 in single surfactant system at 50°C.

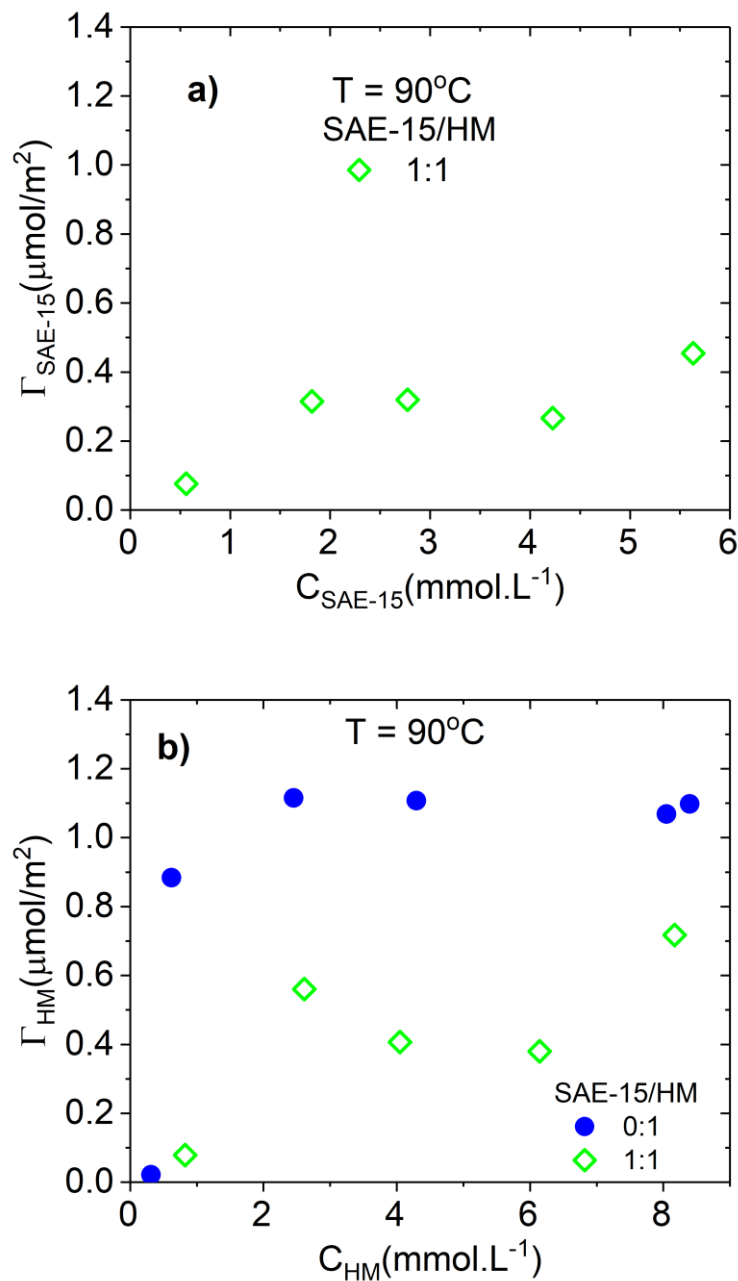


Figure 4.15. Adsorption isotherms of SAE-15+HM mixtures at 90°C. a) Adsorption of SAE-15 versus the bulk SAE-15 concentration. b) Adsorption of HM versus the bulk HM concentration. The dotted lines represent the maximum adsorption of SAE-15 in single surfactant system at 50°C.

## **4.5. DISCUSSIONS**

### **4.5.1. Aqueous Stability**

The presence of charged group delay phase separation and increase the cloud point of non-ionic surfactants. This is seen in the universal increase in cloud point upon the addition of co-surfactant. In both SAE-9 and SAE-15 systems, the cloud point temperatures increase going from LM to MM co-surfactant systems. From MM to HM and VM, however, there is a consistent decrease in the cloud point values. This indicates the importance of the structure of co-surfactant in determining the aqueous stability of mixed surfactant systems. The cloud points rise steadily as the size of the co-surfactant is increased from LM to MM and MM2. The increase is more prominent when the co-surfactant has similar mass fraction as the primary component. MM has a slightly higher increase compared to MM2 and this can be attributed to its higher charge density because of higher degree of sulfonation. A further increase in the size to HM decreases the cloud point. An increase in co-surfactant to VM, again, decreases the cloud point values – an indication of the presence of an optimum co-surfactant structure in MM and MM2. This optimum structure is expected to be different for different families of non-ionic surfactants.

### **4.5.2. O/W IFT Measurements**

In order to understand the effect of co-surfactant addition, the IFTs corresponding to SAE-x + co-surfactants are replotted against the system CPTD and this is shown in Figure 4.16. The IFT values of single component SAE-x are shown in blue circles. Mixture IFTs for 2:1 and 1:1 blends are shown in open and closed symbols respectively. Because of fewer points and the relative closeness of measured IFTs, it is hard to infer any trend from SAE-9 + co-surfactant IFT plot. However for SAE-15, it can be seen that the presence of co-surfactants (dotted lines) reduce the IFT of primary component (solid line) at the

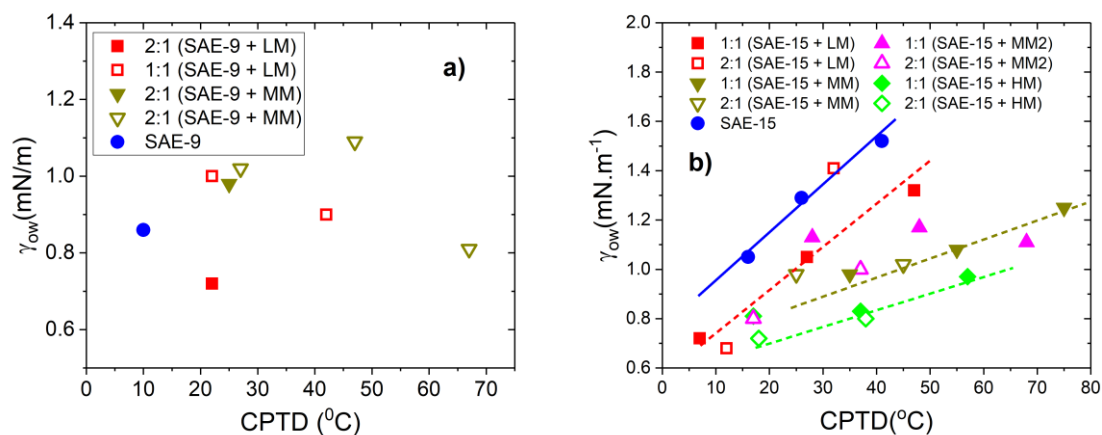


Figure 4.16. Oil/Surfactant IFT for a) SAE-9 and b) SAE-15 + Co-surfactants plotted against CPTD

same CPTD. The plot also shows the effect of co-surfactant structure on IFT reduction – IFT decreases as the size of co-surfactant is progressively increased from LM (red dotted line) to MM and MM2 (dark yellow dotted lines) to HM (green dotted line). Additionally, IFTs of all systems show a universal decreasing trend as the temperature nears cloud point.

#### 4.5.3. Wettability Alteration

A clear effect of the size of co-surfactant can also be observed in the wettability alteration plots. The final contact angle increases as the size of the co-surfactant increases from LM to MM, indicating lower wettability alteration. This observation is seen in both SAE-15 and SAE-9 containing systems. For SAE-15 containing systems, the performance picks up when the co-surfactant size increases to HM. This trend is identical to the one observed in cloud point measurements indicating the correlation between wettability alteration and the cloud point values.

The increase in contact angle associated with systems exhibiting higher cloud points seem to indicate that a better synergy between the nonionic surfactant and the co-surfactant in the bulk lead to poorer wettability alteration.<sup>15</sup> This observation is in accordance to previous findings for single nonionic surfactant systems where a more hydrophilic surfactant, with a higher cloud point, led to a lower wettability alteration. At the same time, the wettability alteration for those single surfactant systems was also enhanced at higher temperatures. To account for both behaviors, the final contact angles are plotted against CPTD as shown in Figure 4.17. To drive the point of universal behavior, contact angles corresponding to SAE-x single surfactant systems (shown in colored circles) are also included in the plot. While there is some scatter in the plot, a general qualitative trend of lower contact angle and hence better wettability alteration can be seen as systems move near their respective cloud points. For wettability alteration induced spontaneous imbibition, optimum contact angles should be at least  $< 90^\circ$ . The dashed line in Figure 4.17 identifies surfactant systems satisfying this criterion and most of these correspond to a CPTD value in the range of 5-40. This plot, hence, can serve as an important tool to select surfactant formulations based on the reservoir temperature and formulation cloud points.

It should, however, be noted that along with contact angle, the oil-water IFT together determines the capillary driving force responsible for spontaneous imbibition. Figure 4.18 plots this driving force as a function of temperature for mixed surfactant systems of SAE-9 and SAE-15, respectively. In all cases, this driving force increases with temperature. However, the trend in driving force with the co-surfactant type is easier to understand when the x-axis is rescaled to CPTD. Figure 4.19 shows the driving forces for different single and mixed-surfactant systems plotted against the CPTD. The colored circles represent the driving force for single surfactant systems. The mixed surfactant systems are shown in non-circular filled (SAE-x/Co-surfactant – 2:1) and open symbols

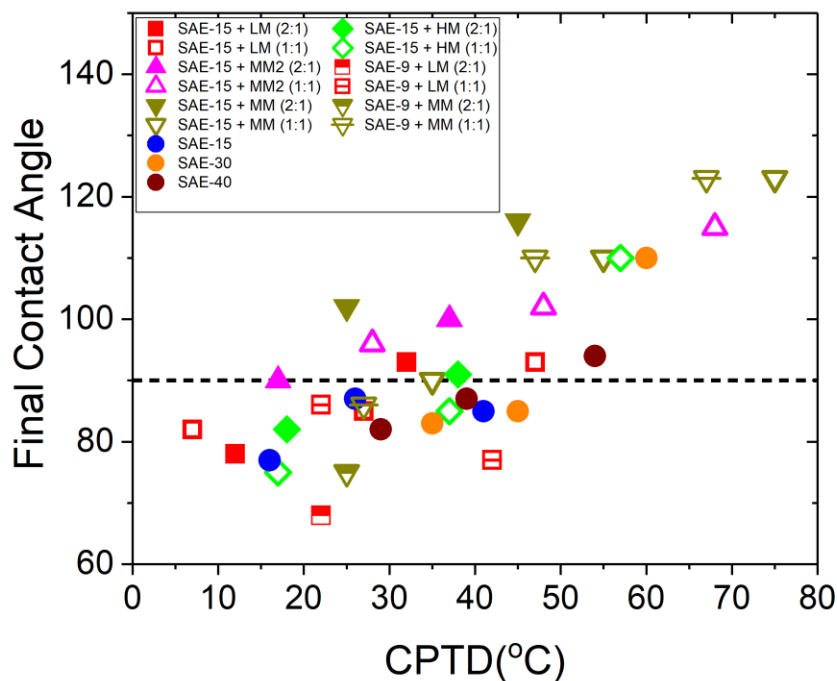


Figure 4.17. Final contact angle as a function of Cloud Point Temperature Difference for single and mixed-surfactant systems.

(SAE-x/Co-surfactant – 1:1). Two features of mixed surfactant systems can be studied from this plot. An offset in driving force can be observed in the mixed surfactant systems by comparing the solid line (single surfactant systems) and the dashed lines. This represents a decrease in driving force which can be attributed to the decrease in O/W IFT and increase in contact angle upon addition of co-surfactants. The effect of co-surfactant structure on the driving force can also be understood from the plot. For LM, the driving force decreases at a moderate rate (red dashed line) with an increase in CPTD. This behavior is the same for both SAE-9 and SAE-15 containing systems. With an increase in the co-surfactant size in MM and MM2, a much faster decrease in driving force is observed as the system moves away from its cloud point (purple and dark yellow dashed lines). Once again this feature is

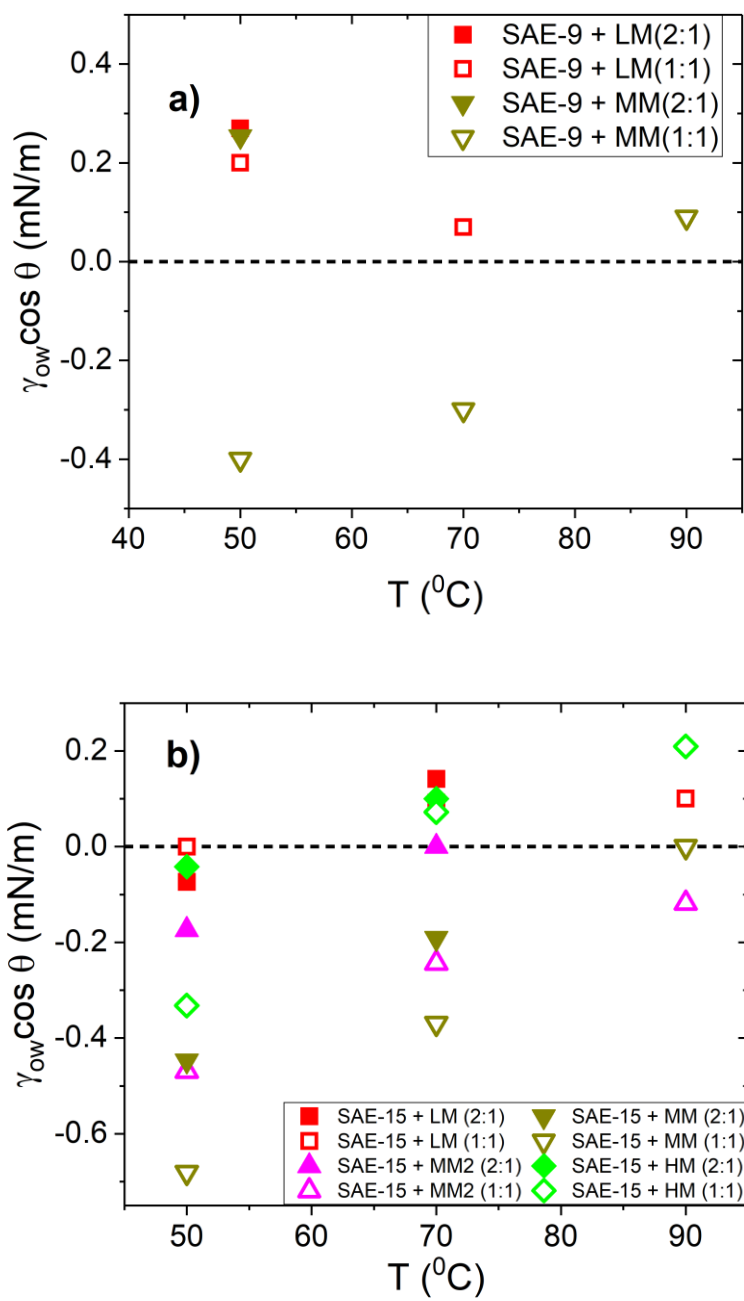


Figure 4.18. Capillary driving force for different mixed surfactant systems as a function of the system temperature for a) SAE-9 and b) SAE-15. The dotted lines represent the zero capillary force corresponding to a switch between oil-wet and water-wet state.

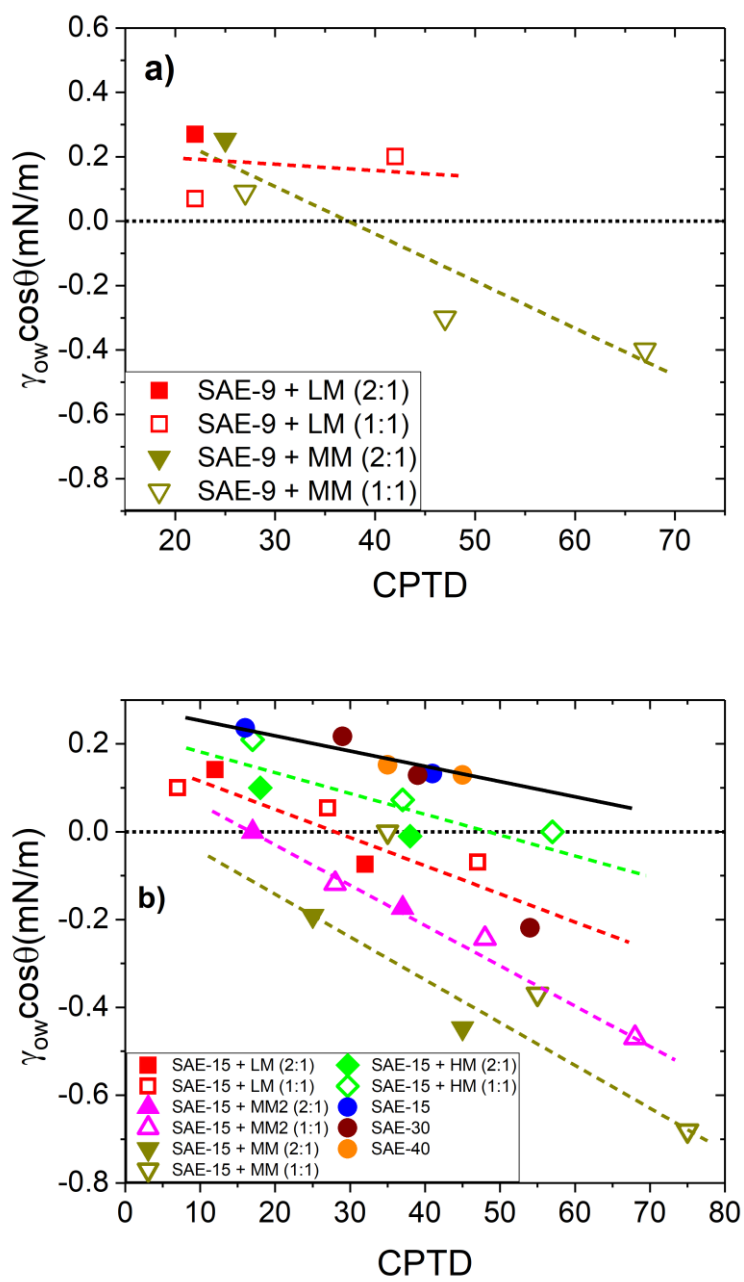


Figure 4.19. Driving force as a function of Cloud Point Temperature Difference for single and mixed-surfactant systems. Lines are meant to be guides to the eye.



observed for both the primary components. A further increase in co-surfactant size is however associated with a reduced rate of decrease in driving force - the driving force change is relatively insignificant for HM containing systems (green dashed line).

#### **4.5.4. Adsorption Isotherms**

Adsorption of non-ionic surfactants has been found to play a critical role in determining the extent of wettability alteration in similar carbonate-based surfaces.<sup>16</sup> In order to get a complete understanding of the different interfacial phenomena taking place here, it is therefore essential to do the same for current systems of mixed surfactants. Owing to the large number of possible combinations, a judicious choice of surfactants is necessary for analyzing adsorption and the representative driving force values are used to make this choice. For a successful spontaneous imbibition, it is essential to have a positive driving force in the system. This comes directly from the fact that the contact angle needs to be less than  $90^\circ$  for a favorable capillary pressure. The dotted line corresponding to zero driving force in Figure 4.19 identifies the promising surfactant formulations based on this criterion. Most of these formulations correspond to LM and HM co-surfactants and these two cases are henceforth selected for adsorption studies. LM and HM also differ significantly in terms of their sizes to allow for an investigation of the co-surfactant structure and its correlation to adsorption and wettability.

Adsorption experiments show that the adsorption of LM in mixed systems is higher than the cases where there is no SAE-15. This enhanced adsorption of co-surfactant, which is observed at both  $70^\circ\text{C}$  and  $90^\circ\text{C}$ , indicates that for this system SAE-15 acts as the more active adsorption species. It should be pointed that LM also has a tendency for adsorption, however, the presence of SAE-15 leads to even higher adsorptions. On the other hand, the fact that SAE-15 shows reduced adsorption in the presence of LM implies that LM hinders

adsorption by stabilizing SAE-15 aggregates in the bulk solution. For this system of mixed surfactants, the extent of stabilization and hence the adsorption depends on the concentration ratio of the two species.

The observations from SAE-15 + HM adsorption experiments, however, indicate a different adsorption mechanism than the SAE-15+LM systems. Since both the primary and the co-surfactant undergo reduced adsorption than the single SAE-15 and HM systems, it is likely that the two components have a better synergistic interaction amongst themselves in the bulk which consequently diminishes their tendency for adsorption. In other words, HM acts as a passivating species for adsorption of SAE-15 and vice-versa.

Thermodynamic correlations exist to determine the micelle composition of mixed surfactant solutions, undergoing mixed micellization, at any given bulk composition, from the knowledge of the CMCs of individual surfactants and that of the mixture. The micelle composition tends to be equal to the bulk composition when the surfactant concentrations are significantly higher than the mixture CMC. Since, the concentrations in discussion are much higher than the measured CMCs, an estimate of micelle composition can provide more insights into the observations. In order to investigate more about the mechanisms of aqueous stabilization and adsorption, the composition of adsorbed aggregates is determined from the adsorption isotherms. Figure 4.20 plots the molar fraction of SAE-15 in adsorbed aggregates against the total molar adsorption for SAE-15+LM and SAE-15+HM systems. The dotted lines represent the initial bulk molar fraction of SAE-15. For SAE-15+LM systems, it can be seen that at all temperatures, the adsorbed composition differs significantly from the bulk composition for a wide range of total adsorption. However, for SAE-15+HM systems, the adsorbed composition is quite identical to the bulk composition. These observations correspond to the two different mechanisms mentioned above. Previously it has been determined that adsorption in nonionic surfactants proceed

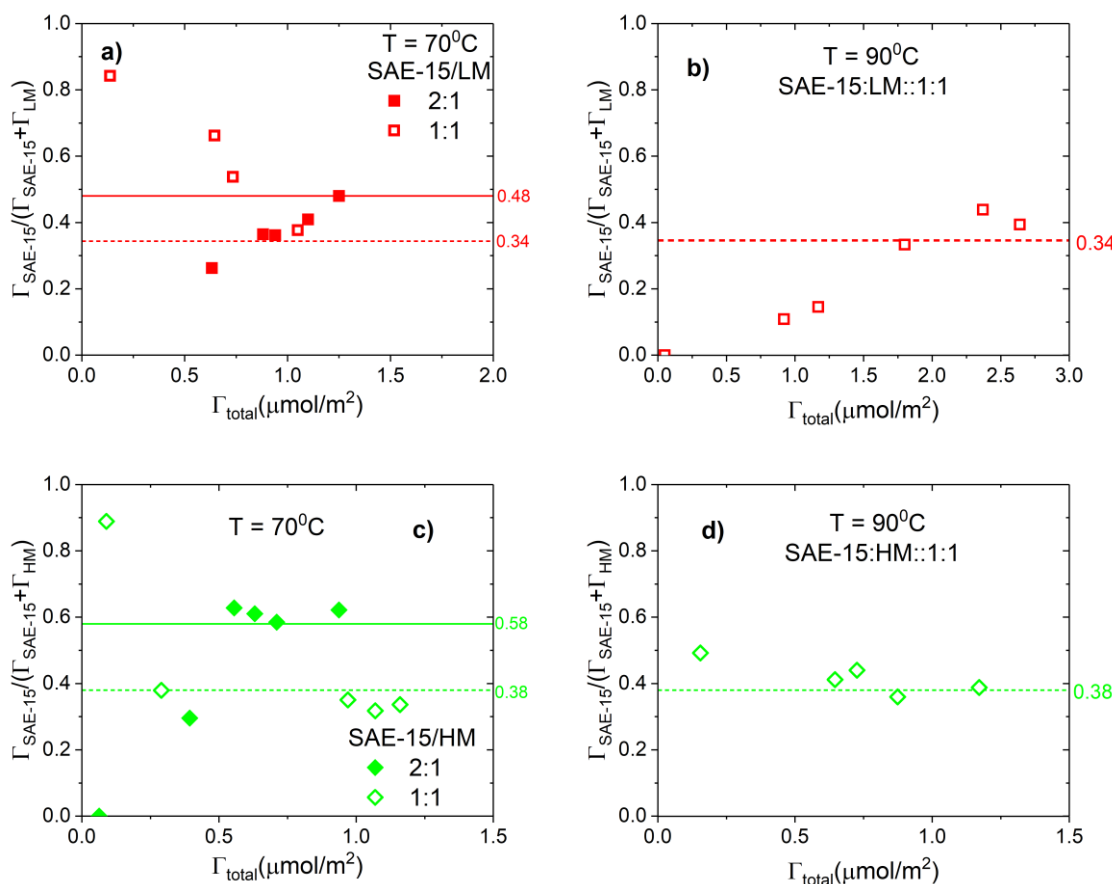


Figure 4.20. Molar fraction of SAE-15 in the adsorbed aggregates versus total molar adsorption for SAE-15+LM mixtures at a)  $70^\circ\text{C}$ , b)  $90^\circ\text{C}$  and for SAE-15+HM mixtures at c)  $70^\circ\text{C}$  and d)  $90^\circ\text{C}$ . The solid lines in a) and c) correspond to bulk molar fraction of SAE-15 in a 2/1 mixture of SAE-15/co-surfactant by mass. The dotted lines in the plots correspond to molar fraction of SAE-15 in a 1/1 mixture of SAE-15/co-surfactant by mass.

via micelle-like aggregates<sup>52</sup>. It is quite likely to be the case for current systems where the concentration ranges are much higher than the mixture CMCs. If that is the case, the adsorbed aggregates are likely to be similar in morphology to the bulk micelles and the composition of these adsorbed aggregates can help understand the different mechanisms in play for LM and HM co-surfactants.<sup>53</sup> Schematically this is shown in Figure 4.21. For SAE-

15+LM systems, the small co-surfactants are unable to penetrate deep into the SAE-15 micelle and hence exist mostly in the periphery as a charged corona which stabilizes the SAE-15 aggregates in solution. The deviation of adsorbed aggregate composition from the bulk composition indicates strong association of LM with SAE-15. As the concentration of SAE-15 increases and more micelles are formed, more LM molecules can be found near them which subsequently lead to higher adsorption of LM. The behavior with temperature is also expected to follow a similar pattern where a higher adsorption of SAE-15 inevitably leads to a higher adsorption of LM. With HM, the bigger co-surfactant molecule is expected to interact much more strongly with SAE-15 micelles and the identical bulk and adsorbed compositions indicate a possible mixed-micelle formation. The mechanism of aqueous stabilization and adsorption are then determined by these mixed-micelles. The correlation between adsorption and wettability alteration has also been developed and studied in the past.<sup>16</sup> The different mechanisms of aggregate formation for different co-surfactants is therefore also likely to be the underlying cause of the trends observed in contact angle and driving force values of these systems. However, a confirmation for this needs a detailed molecular level analysis which is currently being done in a separate work.

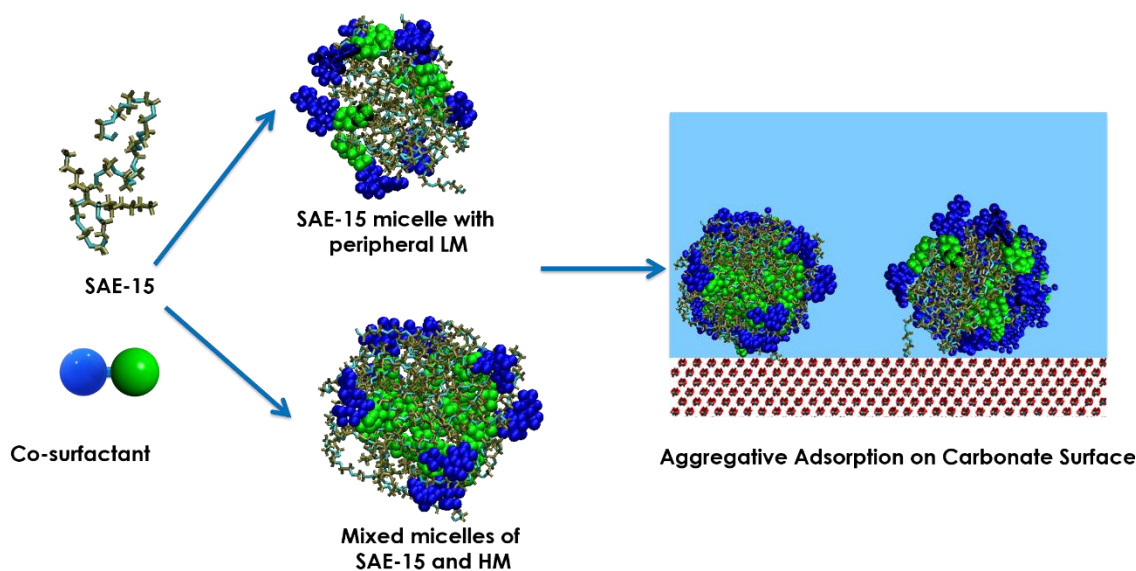


Figure 4.21. Schematic explaining the two different modes of aqueous stabilization for SAE-15+LM and SAE-15+HM systems. LM molecules remain mostly near the periphery of the SAE-15 micelles and stabilize through a solubilization mechanism. HM molecules form mixed micelles and these charged micelles are responsible for aqueous stabilization. In both cases, the mixed aggregates adsorb on the carbonate surface.

#### 4.5.5. Universal Adsorption Behavior

A thermodynamic analysis has been done in the past to correlate the maximum adsorption of a nonionic surfactant to the CPTD.<sup>16</sup> It was found that the maximum adsorption when plotted on a mass basis scales linearly with CPTD and the adsorption increases as the system moves near the cloud point. This was achieved either by decreasing the surfactant hydrophilicity or by increasing the temperature. In order to check whether this behavior holds true for the mixed surfactant systems or not, the maximum adsorptions of SAE-15 have been plotted in Figure 4.22. The adsorptions corresponding to mixed systems are shown in the non-circular symbols. Single-system adsorptions of different SAE surfactants are also shown in the same plot in the filled circles. It can be seen that, the SAE-15 adsorptions in mixed systems still have a good

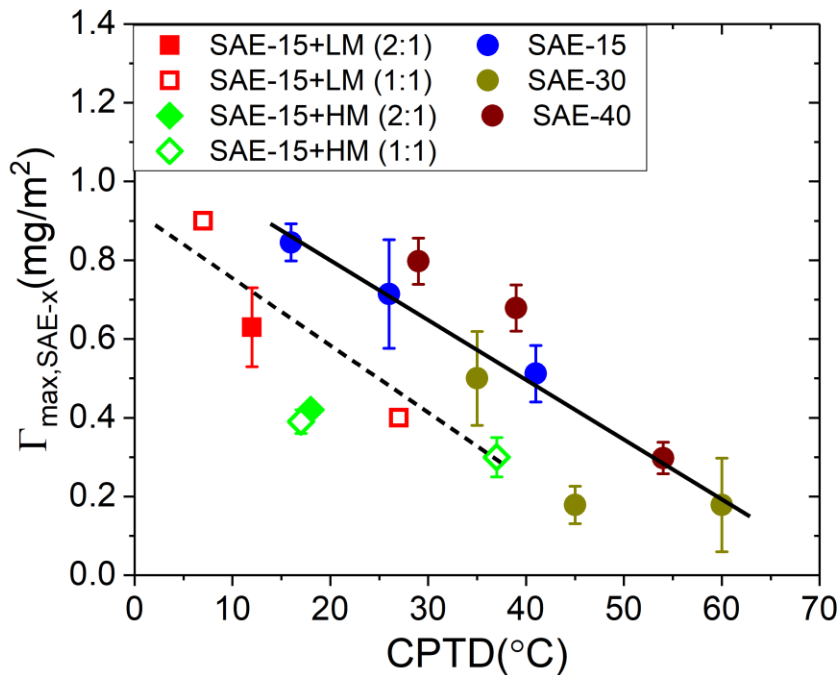


Figure 4.22. Maximum adsorption of SAE-x plotted against the system CPTD. Filled circles correspond to single surfactant systems of SAE-15, SAE-30 and SAE-40. The non-circular symbols are for the mixed systems of SAE-15+LM (red filled and empty squares) and SAE-15+HM (green filled and empty diamonds). The lines are guides for the eyes only. The lines show the offset in adsorption for mixed surfactant systems.

linear dependence on the CPTD. However, this behavior exhibits an offset compared to the single surfactant systems. This offset has a similar trend to the one observed in the driving force vs CPTD plots in Figure 4.19. Thermodynamically, this can be attributed to the difference in adsorption energies associated with aggregate interactions for mixed and single surfactant systems.

#### 4.5.6. Adsorption and Wettability Alteration

The accessibility of bare solid surface around the three-phase contact line has been known to play the dominating role in determining calcite-surfactant interactions which

cause the oil to bead up. The extent of adsorption hence is expected to play a significant role in determining the wettability alteration. This has been found true for the single-surfactant systems. Figure 4.23a plots the final contact angle for the mixed systems against the maximum adsorption of SAE-15(non-circular symbols). The final contact angles corresponding to single surfactant systems of different SAE-x are also shown in the same plot (filled circles). A trend of lower contact angle can be seen as the adsorption increases, which confirms better wettability alteration at high surfactant adsorption. Figure 4.23b shows the plot of capillary driving force versus the maximum adsorption. The offset in driving force is evident in the plot. This further indicates the effect of addition of co-surfactant in the system. The 1/1 SAE-15+HM mixture at 90°C exhibit a driving force value which is quite high for the measured adsorption. The large micelle-size for this particular system, as can be seen in Figure 4.5, is probably responsible for this anomalous behavior. These plots indicate, that while the addition of co-surfactants allow the non-ionic surfactants to be used at a higher temperature, it does so at the cost of lower wettability alteration and driving force even at the same adsorption.

#### **4.6. CONCLUSIONS**

Mixed-surfactant systems consisting of SAE-x and anionic co-surfactants were evaluated in the current study to analyze surfactant formulations with applications in high-temperature, high salinity reservoirs. The addition of co-surfactants increased the aqueous stabilities of nonionic surfactants by raising their cloud points. It is understood that these co-surfactants form mixed aggregates with the nonionic surfactants and the presence of charged groups in the co-surfactants cause a delay in the phase separation happening at the cloud point. The effect of co-surfactant on aqueous stabilization is

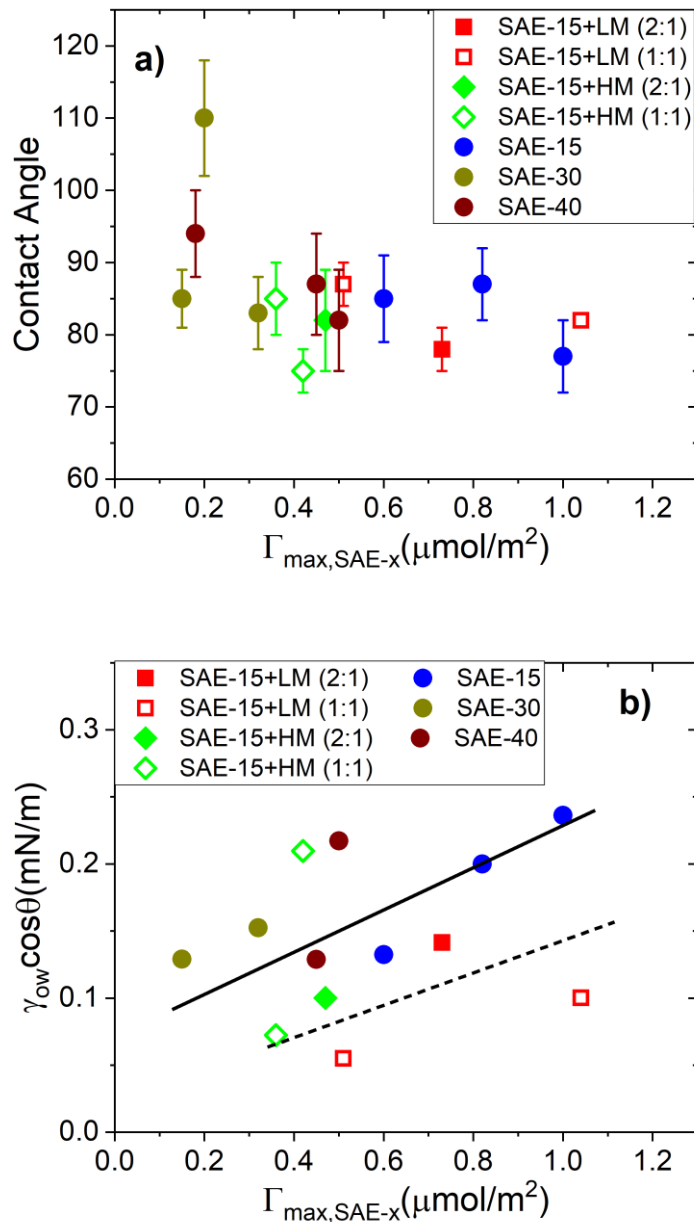


Figure 4.23. a) Final contact angle and b) Capillary driving force versus maximum adsorption of SAE-x in single and mixed systems. Filled circles correspond to single surfactant systems of SAE-15, SAE-30 and SAE-40. The non-circular symbols are for the mixed systems of SAE-15+LM (red filled and empty squares) and SAE-15+HM (green filled and empty diamonds). Lines are guides for the eyes only.



studied by varying the size of the co-surfactants. MM co-surfactants were found to have the maximum increase in cloud point for both the nonionic surfactants.

O/W IFT and contact angle experiments were performed to understand the wettability alteration in these mixed systems. The extent of wettability alteration influenced by co-surfactant structure, concentration and temperature. While the co-surfactants did not alter wettability in their own, their presence caused a decrease in the wettability alteration performance. This is seen as the offset in driving force for mixed surfactant systems compared to the single ones. Stable mixed surfactant systems were identified which modified an initially oil-wet surface to water-wet with final contact angles as low as 70°.

Mixed systems which exhibited a positive driving force were selected for adsorption measurements. Mixed adsorption isotherms showed that the co-surfactants decrease the adsorption of primary component in the system. The adsorption behavior was, however, different for different co-surfactants. In SAE-15+LM systems, SAE-15 acted as the more active adsorption component driving the adsorption of the co-surfactant. Higher adsorptions were observed in systems with higher percentage of the primary surfactant. In SAE-15+HM systems, adsorptions of both the components were hindered indicating a strong inter-component synergy in the bulk. The adsorption of the primary component was also relatively independent of mixture composition and temperature in this case. Based on the calculations of molar compositions two different mechanisms were proposed for aqueous stabilization and surface aggregation – a solubilization mechanism for smaller co-surfactants and a mixed-micellization mechanism for the larger ones.

Adsorptions of nonionic surfactants exhibit a linear relationship with the system CPTD. A similar behavior was also observed for the mixed surfactant systems. However, there was an offset in the adsorption in mixed systems when compared to single surfactant systems. Similar offset was also observed when contact angle and driving force was plotted

against CPTD. In all cases, however, a higher adsorption and a high wettability alteration were associated with systems closer to the cloud point. The correlation between surfactant cloud point, wettability alteration and adsorption done in the current study, is an important step in understanding surfactant formulations for wettability alteration at high temperatures, particularly when nonionic surfactants are not directly applicable and a higher O/W IFT is desired compared to typical anionic surfactants. It is critical to see how the wettability alteration of these single and mixed systems translates to oil recoveries from actual porous media. These need to be investigated through spontaneous imbibition tests in oil-wet cores and this is being done currently. More investigation is also required to develop formulations with higher wettability alteration which is typically associated with higher oil recoveries and this is a part of future work.

## REFERENCES

1. Adibhatla, B., & Mohanty, K. K. Oil recovery from fractured carbonates by surfactant-aided gravity drainage: laboratory experiments and mechanistic simulations. *SPE Reservoir Evaluation & Engineering*, **2008**, 11(01), 119-130.
2. Seethepalli, A., Adibhatla, B., & Mohanty, K. K. Wettability alteration during surfactant flooding of carbonate reservoirs. In *SPE/DOE Symposium on Improved Oil Recovery*. Society of Petroleum Engineers, **2004**.
3. Hirasaki, G., & Zhang, D. L. Surface chemistry of oil recovery from fractured, oil-wet, carbonate formations. *SPE Journal*, **2004**, 9(02), 151-162.
4. Zhang, J., Nguyen, Q. P., Flaaten, A., & Pope, G. A. Mechanisms of enhanced natural imbibition with novel chemicals. *SPE reservoir evaluation & engineering*, **2009**, 12(06), 912-920.
5. Strand, S., Standnes, D. C., & Austad, T. Spontaneous imbibition of aqueous surfactant solutions into neutral to oil-wet carbonate cores: Effects of brine salinity and composition. *Energy & fuels*, **2003**, 17(5), 1133-1144.
6. Standnes, D. C., & Austad, T. Wettability alteration in carbonates: Interaction between cationic surfactant and carboxylates as a key factor in wettability alteration from oil-wet to

water-wet conditions. *Colloids and Surfaces A: Physicochemical and Engineering Aspects*, **2003**, 216(1-3), 243-259.

7. Austad, T., & Standnes, D. C. Spontaneous imbibition of water into oil-wet carbonates. *Journal of Petroleum Science and Engineering*, **2003**, 39(3-4), 363-376.

8. Austad, T. and Milter, J. Spontaneous imbibition of water into low permeable chalk at different wettabilities using surfactants. In *International Symposium on Oilfield Chemistry*, Society of Petroleum Engineers, **1997**.

9. Standnes, D.C., Nogaret, L.A., Chen, H.L. and Austad, T. An evaluation of spontaneous imbibition of water into oil-wet carbonate reservoir cores using a nonionic and a cationic surfactant. *Energy & Fuels*, 16(6), **1997**, pp.1557-1564.

10. Spinler, E.A., Zornes, D.R., Tobola, D.P. and Moradi-Araghi, A. Enhancement of oil recovery using a low concentration of surfactant to improve spontaneous and forced imbibition in chalk. In *SPE/DOE Improved Oil Recovery Symposium*. Society of Petroleum Engineers, **2000**.

11. Chen, Peila, and Kishore K. Mohanty. "Surfactant-enhanced oil recovery from fractured oil-wet carbonates: effects of low ift and wettability alteration." In *SPE International Symposium on Oilfield Chemistry*. Society of Petroleum Engineers, 2015.

12. Ahmadi, M.A., Galedarzadeh, M. and Shadizadeh, S.R., 2015. Wettability alteration in carbonate rocks by implementing new derived natural surfactant: enhanced oil recovery applications. *Transport in porous media*, 106(3), pp.645-667.

13. Kumar, S. and Mandal, A., 2016. Studies on interfacial behavior and wettability change phenomena by ionic and nonionic surfactants in presence of alkalis and salt for enhanced oil recovery. *Applied Surface Science*, 372, pp.42-51.

14. Ershadi, M., Alaei, M., Rashidi, A., Ramazani, A. and Khosravani, S., 2015. Carbonate and sandstone reservoirs wettability improvement without using surfactants for Chemical Enhanced Oil Recovery (C-EOR). *Fuel*, 153, pp.408-415.

15. Das, S., Nguyen, Q., Patil, P.D., Yu, W. and Bonnecaze, R.T., 2018. Wettability alteration of calcite by nonionic surfactants. *Langmuir*, 34(36), pp.10650-10658.

16. Das, S., Katiyar, A., Rohilla, N., Nguyen, Q., Bonnecaze, R.T., Universal Scaling of Adsorption of Nonionic Surfactants on Carbonates using Cloud Point Temperatures. Under Review

17. Na, G.C., Yuan, B.O., Stevens, H.J., Weekley, B.S. and Rajagopalan, N., 1999. Cloud point of nonionic surfactants: modulation with pharmaceutical excipients. *Pharmaceutical research*, 16(4), pp.562-568.

18. Patil, P.D., Rohilla, N., Katiyar, A., Yu, W., Falcone, S., Nelson, C. and Rozowski, P., 2018, March. Surfactant based EOR for tight oil reservoirs through wettability alteration: novel surfactant formulations and their efficacy to induce spontaneous imbibition. In *SPE EOR Conference at Oil and Gas West Asia*. Society of Petroleum Engineers.
19. Sharma, G. and Mohanty, K., 2013. Wettability alteration in high-temperature and high-salinity carbonate reservoirs. *SPE Journal*, 18(04), pp.646-655.
20. Thomas, H.G., Lomakin, A., Blankschtein, D. and Benedek, G.B., 1997. Growth of mixed nonionic micelles. *Langmuir*, 13(2), pp.209-218.
21. Brinck, J. and Tiberg, F., 1996. Adsorption behavior of two binary nonionic surfactant systems at the silica– water interface. *Langmuir*, 12(21), pp.5042-5047.
22. Portet, F., Desbene, P.L. and Treiner, C., 1996. Nonideality of mixtures of pure nonionic surfactants both in solution and at silica/water interfaces. *Journal of colloid and interface science*, 184(1), pp.216-226.
23. Zhang, R. and Somasundaran, P., 2005. Aggregate formation of binary nonionic surfactant mixtures on hydrophilic surfaces. *Langmuir*, 21(11), pp.4868-4873.
24. Xiao, J.X., Zhang, Y., Wang, C., Zhang, J., Wang, C.M., Bao, Y.X. and Zhao, Z.G., 2005. Adsorption of cationic–anionic surfactant mixtures on activated carbon. *Carbon*, 43(5), pp.1032-1038.
25. Lokar, W.J. and Ducker, W.A., 2004. Forces between Glass Surfaces in Mixed Cationic– Zwitterionic Surfactant Systems. *Langmuir*, 20(11), pp.4553-4558.
26. Bergström, M. and Pedersen, J.S., 1999. Formation of tablet-shaped and ribbonlike micelles in mixtures of an anionic and a cationic surfactant. *Langmuir*, 15(7), pp.2250-2253.
27. Wang, L., Liu, R., Hu, Y., Liu, J. and Sun, W., 2016. Adsorption behavior of mixed cationic/anionic surfactants and their depression mechanism on the flotation of quartz. *Powder Technology*, 302, pp.15-20.
28. Misselyn-Bauduin, A.M., Thibaut, A., Grandjean, J., Broze, G. and Jérôme, R., 2000. Mixed micelles of anionic– nonionic and anionic– zwitterionic surfactants analyzed by pulsed field gradient NMR. *Langmuir*, 16(10), pp.4430-4435.
29. Somasundaran, P., Fu, E. and Xu, Q., 1992. Coadsorption of anionic and nonionic surfactant mixtures at the alumina-water interface. *Langmuir*, 8(4), pp.1065-1069.
30. Huang, Z., Yan, Z. and Gu, T., 1989. Mixed adsorption of cationic and anionic surfactants from aqueous solution on silica gel. *Colloids and surfaces*, 36(3), pp.353-358.

31. Thibaut, A., Misselyn-Bauduin, A.M., Grandjean, J., Broze, G. and Jérôme, R., 2000. Adsorption of an aqueous mixture of surfactants on silica. *Langmuir*, 16(24), pp.9192-9198.
32. Wang, L., Hu, Y., Liu, J., Sun, Y. and Sun, W., 2015. Flotation and adsorption of muscovite using mixed cationic–nonionic surfactants as collector. *Powder technology*, 276, pp.26-33.
33. Penfold, J., Tucker, I., Thomas, R.K., Staples, E. and Schuermann, R., 2005. Structure of mixed anionic/nonionic surfactant micelles: experimental observations relating to the role of headgroup electrostatic and steric effects and the effects of added electrolyte. *The Journal of Physical Chemistry B*, 109(21), pp.10760-10770.
34. Liley, J.R., Thomas, R.K., Penfold, J., Tucker, I.M., Petkov, J.T., Stevenson, P. and Webster, J.R., 2017. Surface adsorption in ternary surfactant mixtures above the critical micelle concentration: effects of asymmetry on the composition dependence of the excess free energy. *The Journal of Physical Chemistry B*, 121(13), pp.2825-2838.
35. Sharma, K.S., Rodgers, C., Palepu, R.M. and Rakshit, A.K., 2003. Studies of mixed surfactant solutions of cationic dimeric (gemini) surfactant with nonionic surfactant C12E6 in aqueous medium. *Journal of colloid and interface science*, 268(2), pp.482-488.
36. Sharma, K.S., Hassan, P.A. and Rakshit, A.K., 2006. Self aggregation of binary surfactant mixtures of a cationic dimeric (gemini) surfactant with nonionic surfactants in aqueous medium. *Colloids and Surfaces A: Physicochemical and Engineering Aspects*, 289(1-3), pp.17-24.
37. Azum, N., Rub, M.A. and Asiri, A.M., 2014. Experimental and theoretical approach to mixed surfactant system of cationic gemini surfactant with nonionic surfactant in aqueous medium. *Journal of Molecular Liquids*, 196, pp.14-20.
38. Esumi, K., Miyazaki, M., Arai, T. and Koide, Y., 1998. Mixed micellar properties of a cationic gemini surfactant and a nonionic surfactant. *Colloids and Surfaces A: Physicochemical and Engineering Aspects*, 135(1-3), pp.117-122.
39. Douglas, C.B. and Kaler, E.W., 1994. A scattering study of mixed micelles of hexaethylene glycol mono-n-dodecyl ether and sodium dodecylsulfonate in D<sub>2</sub>O. *Langmuir*, 10(4), pp.1075-1083.
40. Baglioni, P., Dei, L., Rivara-Minten, E. and Kevan, L., 1993. Mixed micelles of SDS/C12E6 and DTAC/C12E6 surfactants. *Journal of the American Chemical Society*, 115(10), pp.4286-4290.

41. Gao, H.C., Zhao, S., Mao, S.Z., Yuan, H.Z., Yu, J.Y., Shen, L.F. and Du, Y.R., 2002. Mixed micelles of polyethylene glycol (23) lauryl ether with ionic surfactants studied by proton 1D and 2D NMR. *Journal of colloid and interface science*, 249(1), pp.200-208.
42. Garamus, V.M., 2003. Formation of mixed micelles in salt-free aqueous solutions of sodium dodecyl sulfate and C12E6. *Langmuir*, 19(18), pp.7214-7218.
43. Israelachvili, J.N., 1976. Mitchell, D.J.; Ninham, B.W.J Chem. Soc. *Faraday Trans. II*, 72, pp.1525-1568.
44. Kumar, V.V., 1991. Complementary molecular shapes and additivity of the packing parameter of lipids. *Proceedings of the National Academy of Sciences*, 88(2), pp.444-448.
45. Holland, P.M. and Rubingh, D.N., 1983. Nonideal multicomponent mixed micelle model. *The Journal of Physical Chemistry*, 87(11), pp.1984-1990.
46. Sarmoria, C., Puvvada, S. and Blankschtein, D., 1992. Prediction of critical micelle concentrations of nonideal binary surfactant mixtures. *Langmuir*, 8(11), pp.2690-2697.
47. Lu, S. and Somasundaran, P., 2008. Tunable synergism/antagonism in a mixed nonionic/anionic surfactant layer at the solid/liquid interface. *Langmuir*, 24(8), pp.3874-3879.
48. Portet-Koltalo, F., Desbene, P.L. and Treiner, C., 2001. Self-desorption of mixtures of anionic and nonionic surfactants from a silica/water interface. *Langmuir*, 17(13), pp.3858-3862.
49. Zhang, R. and Somasundaran, P., 2006. Advances in adsorption of surfactants and their mixtures at solid/solution interfaces. *Advances in colloid and interface science*, 123, pp.213-229.
50. Zhang, L., Zhang, R. and Somasundaran, P., 2006. Adsorption of mixtures of nonionic sugar-based surfactants with other surfactants at solid/liquid interfaces: II. Adsorption of n-dodecyl- $\beta$ -d-maltoside with a cationic surfactant and a nonionic ethoxylated surfactant on solids. *Journal of colloid and interface science*, 302(1), pp.25-31.
51. Alvarez, J.O. and Schechter, D.S., 2017. Wettability alteration and spontaneous imbibition in unconventional liquid reservoirs by surfactant additives. *SPE Reservoir Evaluation & Engineering*, 20(01), pp.107-117.
52. Desbene, P.L., Portet, F. and Treiner, C., 1997. Adsorption of pure nonionic alkylethoxylated surfactants down to low concentrations at a silica/water interface as determined using a HPLC technique. *Journal of Colloid and Interface Science*, 190(2), pp.350-356.

53. Levitz, P. and Van Damme, H., 1986. Fluorescence decay study of the adsorption of nonionic surfactants at the solid-liquid interface. 2. Influence of polar chain length. *The Journal of Physical Chemistry*, 90(7), pp.1302-1310.

## **Chapter 5: Molecular Dynamics Simulations of Aqueous Nonionic Surfactants on a Carbonate Surface**

### **5.1. INTRODUCTION**

Surfactants are amphiphilic molecules used in many industrial applications such as detergency, lubrication, adhesives, and oil recovery because of their surface-active nature. In enhanced oil recovery (EOR) surfactants can be used as wettability altering agents to modify the fluid-solid interfacial energy to change a reservoir rock from oil-wet to water-wet.<sup>1-5</sup> Wettability alteration is essential to promote spontaneous imbibition of the aqueous phase into the porous media to increase oil recovery.<sup>5-9</sup> Spontaneous imbibition requires a moderate to high interfacial tension (IFT) between the oil and water along with a water-wet state. The wettability state is determined by the three-phase (oil-water-rock) contact angle measured through the aqueous phase; a low contact angle is essential for spontaneous imbibition to occur. The interactions between the surfactant and the rock determine the extent of surfactant adsorption and the wettability or contact angle. Understanding the extent and mechanism of adsorption as a function of the structure of the surfactant is necessary to strike the optimum balance between adsorption and wettability alteration. In practice one wants the lowest contact angle for the least amount of adsorbed surfactant. The effectiveness of ionic surfactants is determined to a large extent by their electrostatic interactions with the substrate. Anionic surfactants exhibit prohibitively high adsorption on positively charged carbonate surfaces.<sup>10-11</sup> Cationic surfactants tend to form ion-pair complexes with negatively charged adsorbed oil molecules<sup>12-13</sup> and this often requires high surfactant concentration for maximum effectiveness.<sup>14</sup> The lack of charged moieties in nonionic surfactants provides several benefits. They are insensitive to high concentrations of salts commonly found in oil reservoirs. Nonionic surfactants are also compatible with other surfactants that may be present in the reservoir. However, because they are not



charged, their interactions with the surface and water are determined by weaker van der Waals and hydrogen bonding interactions.<sup>15-17</sup> In a recent study two families of nonionic surfactants were evaluated experimentally to measure the wettability alteration on oil-wet carbonate surfaces at different temperatures.<sup>18</sup> It was shown that surfactants with shorter hydrophilic groups exhibit better wettability alteration with a lower contact angle of the water-wet state. Wettability alteration was also enhanced at higher temperatures. Activation energy calculations and oil-film experiments suggest that the final wettability state is determined by surfactant molecules accessing and adsorbing on the bare carbonate surface near the three-phase contact line. Further, it was found experimentally that an increased adsorption of surfactants with fewer hydrophilic units and higher temperatures leads to an enhanced wettability alteration.<sup>19</sup> It has been proposed that nonionic surfactants adsorb as aggregates or micelles rather than single molecules at concentrations around and above their critical micelle concentration.<sup>16, 20-28</sup> According to this model, nonionic surfactants are hypothesized to form micelle-like aggregates on the carbonate surface.<sup>19</sup> The adsorption is thought to be driven by hydrogen bonding involving the ethoxylate groups on the outside of the aggregate with the surface<sup>15, 17</sup> and van der Waals interactions between the surfactant molecules in the aggregate and the surface.<sup>29</sup> A model for aggregative adsorption has been developed which uses the cloud point temperature as a key thermodynamic parameter to predict adsorption of nonionic surfactants.<sup>19</sup> The cloud point is the temperature above which the nonionic surfactant precipitates from solution. The model predicts a universal curve for adsorption of different nonionic surfactants solely based on the system temperature relative to the cloud point. However, there is no molecular-scale evidence of aggregative adsorption of nonionic surfactants and its connection to the cloud point. Here we aim to use molecular dynamics (MD) simulations to understand the energy landscape associated with adsorption and its relationship to cloud

point temperatures. The adsorption of ionic surfactants on mineral surfaces has been studied using atomistic and coarse-grained molecular dynamics (MD) simulations.<sup>30-34</sup> The competitive adsorption of water and organic surfactants on scheelite (a calcium tungstate mineral with the chemical formula  $\text{CaWO}_4$ ) was studied using atomistic simulations, and it was found that the strongest adsorption happened when the molecules formed multiple interactions with the substrate.<sup>30</sup> The surface-bulk partition of anionic surfactants was predicted using works employing coarse-grained MD simulations.<sup>31</sup> Reasonable predictions of adsorption isotherms and structures were made using the simulation data. The adsorption of ionic surfactants on calcite has been studied using MD.<sup>32</sup> Anionic surfactants were found to have steep adsorption on the positively charged interface. However, cationic surfactants were also observed to exhibit some adsorption, which was attributed to diffuse charge distribution and a combination of hydrophobic interactions and micellar exclusion. Zwitterionic surfactants displayed a composite behavior with charge-driven adsorption and hydrophobic interaction driven aggregation. A similar study was also done to investigate adsorption structures of anionic surfactants on silica.<sup>33</sup> The unfavorable electrostatic interactions led to spherical micellar aggregates in the case of silica whereas a self-assembled film of surfactants was observed on the oppositely charged calcite surface. Anionic and nonionic surfactant aggregates have been observed on silica and MD simulations reveal that surface hydroxylation to be the critical factor determining adsorption mechanism.<sup>34</sup> In the case of cationic surfactants, flat elliptical aggregate structures were observed on silica, and their formation was driven by favorable surfactant-substrate electrostatic interactions. Free energies of surfactant adsorption were also measured using atomistic<sup>35</sup> and coarse-grained MD simulations.<sup>36</sup> To the best of our knowledge, there have been no studies on the adsorption of nonionic surfactants on calcite using molecular dynamics simulations.

In this chapter we use atomistic MD simulations to begin building a picture of the surfactant-substrate interactions driving adsorption for nonionic surfactants onto carbonate surfaces. The simulations in the current work are for surfactants in water without salts to understand the reference adsorption behavior and mechanism. The effect of the surfactant structure is studied by simulating two lengths of ethoxylates on the nonionic surfactant. Simulations at two temperatures are conducting to understand its role in the adsorption of nonionic surfactants.

## **5.2. METHODOLOGY**

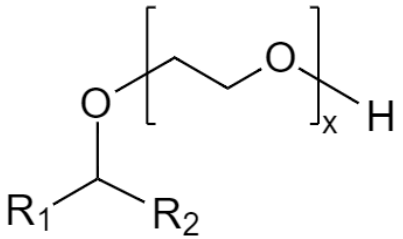
The open-source MD simulation tool LAMMPS<sup>37-38</sup> was used for the simulations. Organic molecules were modeled using the General AMBER force field (GAFF).<sup>39</sup> The antechamber package<sup>40</sup>, which is part of the AmberTools, was used to generate the partial atomic charges based on the AM1-bcc method. The TIP3P<sup>41</sup> model was used to describe the interactions for water molecules that is consistent with GAFF.<sup>42-44</sup> Temperatures and pressures were maintained for isothermal-isobaric (NPT) and canonical (NVT) ensembles using the Nose-Hoover thermostat and barostats, respectively.<sup>45</sup> Non-bonded interactions were cut off at 12 Å, and a long-range tail correction was used for these interactions beyond the cut-off distance. Long-range electrostatics were calculated using the PPPM algorithm.<sup>46</sup>

### **5.2.1. Surfactant-Water Simulations**

The two nonionic surfactants studied are shown in Table 5.1. They are secondary alcohol ethoxylates with 15 and 40 ethoxylate units. The wettability alteration performance and the adsorption of these surfactants have been analyzed experimentally in previous works.<sup>18, 19</sup>

The aggregative behavior of surfactants in water was studied by randomly distributing surfactant molecules in a 400 Å x 400 Å x 400 Å box (Figure 5.1a). The hydrophilic and hydrophobic components are represented in blue and green spheres,

Table 5.1. Nonionic surfactant evaluated in the study. Experimental CMC values are reported at 25°C.<sup>18</sup>

Surfactant	Structure	Specification (x)	CMC (ppm)
SAE-x (Secondary alcohol ethoxylate)		15	162
		40	1314

respectively. The number of surfactant molecules was varied from 10 to 200 to observe the effect of micelle size and shape on aggregation number ( $N_{agg}$ ). 120,000 water molecules were used in each simulation. Initial configurations were obtained by randomly distributing molecules using the packing generator, Packmol.<sup>47</sup> Each simulation was run for 100 ns, which was found to be sufficient for equilibrating the systems. Total energy, as well as surfactant size and shape (discussed in Sec 3.1), were measured over this period to ensure equilibrium.

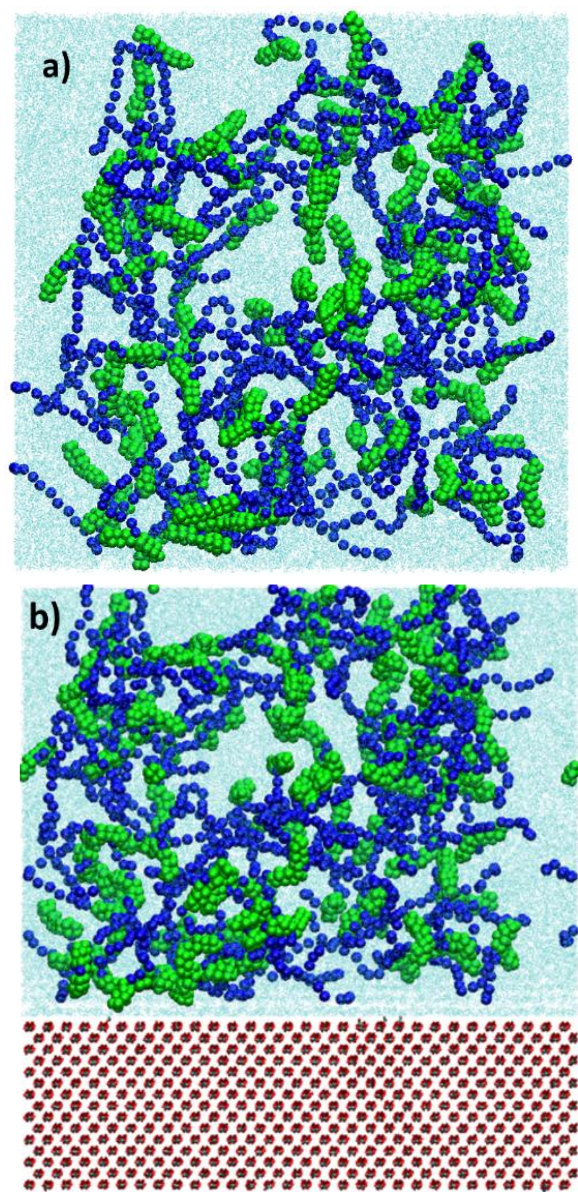


Figure 5.1. a) Randomly distributed 100 SAE-15 and 120,000 water molecules used for surfactant-water simulations. Water molecules are shown in cyan-colored points. b) Randomly distributed 100 SAE-15 molecules to study adsorption on calcite (shown in red). The blue and green spheres represent the surfactant hydrophile and hydrophobe, respectively.

### 5.2.2. Surfactant-Calcite Simulations

To simulate aggregative adsorption, calcite was used as a representative carbonate surface. The crystal structure of calcite was developed using the Xcrysden software.<sup>48</sup> All the interactions were studied on the  $10\bar{1}4$  surface of calcite, which is its most stable surface.<sup>49</sup> The potential model for calcite was taken from the work of Pavese et al.<sup>50</sup> which has been demonstrated to successfully reproduce the properties of calcite and other carbonates. Water-calcite simulations were first performed to calculate the surface energy of the hydrated calcite surface and validate the selection of the potential model. Cross-potential terms involving organic-mineral interactions were computed using the methodology developed by Freeman et al.<sup>51</sup> For these simulations, a cuboidal simulation box of dimensions 121.5 Å x 149.76 Å x 300 Å was used. Randomly distributed surfactant molecules along with 120,000 water molecules were inserted along with a calcite slab of dimensions 121.5 Å x 149.76 Å x 46 Å (Figure 5.1b) and the system was allowed to equilibrate for 70-80 ns. This was followed by 10 ns production runs to generate the energy landscapes associated with aggregative adsorption. The full list of non-bonded interactions is shown in Tables 5.2 and 5.3.

### 5.2.3. Adsorption Energetics

In order to extract the free energy change associated with adsorption of different molecules, the umbrella sampling technique is used.<sup>38</sup> In this technique, the system is traced as a molecule goes from an adsorbed state to a final desorbed state. The reaction coordinate used in the process is the normal distance between the calcite surface and the center of mass of the molecule concerned. A brief thermodynamic justification of the technique is shown below.

Table 5.2: Force-field parameters for Buckingham Potential -  $E = Ae^{-r/\rho} - \frac{C}{r^6}$

Atom type	Atom type	Potential type	A (kcal/mol)	$\rho$ (Å)	C(kcal-Å <sup>6</sup> )
Ca <sub>calcite</sub>	O <sub>calcite</sub>	Buckingham	35697.577	0.297	0
O <sub>calcite</sub>	O <sub>calcite</sub>	Buckingham	377065.402	0.213	0
Ca <sub>calcite</sub>	O <sub>alcohol</sub>	Buckingham	19576.053	0.297	0
Ca <sub>calcite</sub>	O <sub>ether</sub>	Buckingham	15891.180	0.297	0
Ca <sub>calcite</sub>	O <sub>water</sub>	Buckingham	27327.991	0.297	0

Table 5.3: Force-field parameters for Leonard-Jones Potential -  $E = 4\epsilon \left[ \left( \frac{\sigma}{r} \right)^{12} - \left( \frac{\sigma}{r} \right)^6 \right]$

Atom type	Atom type	Potential type	$\epsilon$ (kcal/mol)	$\sigma$ (Å)
O <sub>calcite</sub>	C <sub>surfactant</sub>	LJ	0.036	3.480
O <sub>calcite</sub>	O <sub>ether</sub>	LJ	0.030	3.360
O <sub>calcite</sub>	O <sub>alcohol</sub>	LJ	0.033	3.403
O <sub>calcite</sub>	H <sub>alkyl</sub>	LJ	0.016	3.082
O <sub>calcite</sub>	H <sub>EO</sub>	LJ	0.016	2.993
O <sub>calcite</sub>	H <sub>alcohol</sub>	LJ	0.008	2.050
O <sub>calcite</sub>	O <sub>water</sub>	LJ	0.035	3.376
C <sub>calcite</sub>	C <sub>surfactant</sub>	LJ	0.108	3.398
C <sub>calcite</sub>	O <sub>ether</sub>	LJ	0.089	3.277
C <sub>calcite</sub>	O <sub>alcohol</sub>	LJ	0.100	3.320
C <sub>calcite</sub>	H <sub>alkyl</sub>	LJ	0.047	2.999
C <sub>calcite</sub>	H <sub>EO</sub>	LJ	0.047	2.999
C <sub>calcite</sub>	H <sub>alcohol</sub>	LJ	0.023	1.968
C <sub>calcite</sub>	O <sub>water</sub>	LJ	0.105	3.293

From the canonical ensemble, a system at a temperature  $T$  will sample conformation according to the relation

$$P(q) \propto e^{-\frac{U(q)}{k_B T}}, \quad (1)$$

where  $q$  is a multi-dimensional vector representing the reaction coordinates in the system.

Along a particular reaction coordinate  $z$ , the probability becomes

$$P(z) \propto \int dq e^{-\frac{U(q)}{k_B T}} \delta(z - z(q)). \quad (2)$$

The corresponding free energy change along the reaction coordinate is then given by

$$F(z) = -k_B T \log P(z). \quad (3)$$

In order to sample the entire reaction coordinate selected within a computationally viable time period, an additional bias which is typically in the harmonic form is applied to obtain a biased distribution

$$P'(z) \propto \int dq e^{-\frac{U(q)+V(z(q))}{k_B T}} \delta(z - z(q)) \propto e^{-\frac{V(z(q))}{k_B T}} P(z). \quad (4)$$

Here  $V(z(q))$  is the applied bias along the reaction coordinate of interest.

The biased free energy change is then given by

$$F'(z) = -k_B T \log P'(z) = F(z) + V(z) + C, \quad (5)$$

where  $C$  is an unknown constant. In a general umbrella sampling, a harmonic bias function is used which takes the form

$$V(z) = \frac{k(z - z_o)^2}{2}, \quad (6)$$

where  $z_o$  is the minimum of the bias. To obtain the energy landscape along a particular coordinate, multiple simulations are performed and the bias minimum is varied in each of them to encompass the entire reaction coordinate. The biased probability,  $P'(z)$ , is obtained for each simulation in the process. Since, each biased probability has a different offset in the form of the unknown constant  $C$ , the Weighted Histogram Analysis Method (WHAM)<sup>53</sup> is used to determine the optimal weighting to combine the simulations.



## 5.3. RESULTS

### 5.3.1. Micellization Behavior

Above their critical micelle concentration (CMC) the surfactant molecules form micelles in the bulk aqueous phase. This behavior was studied through simulations where the number of surfactant molecules was varied, and the corresponding aggregation was analyzed. For SAE-15, the number of molecules was varied from 10-200 ( $>$  CMC) and a single micelle was observed in all cases. Figure 5.2a shows one such micelle of SAE-15 formed at 50°C. Studies suggest that surfactant molecules with similar structures typically form spherical aggregates at low concentrations with a gradual transition to rod-shaped structures at higher concentrations.<sup>54</sup> To determine micelle shape, the asphericity  $b$  was calculated according to<sup>55</sup>,

$$b = \left[ \lambda_1 - \frac{1}{2}(\lambda_2 + \lambda_3) \right] R_g^{-2}, \quad (7)$$

where  $\lambda_i$  are the principal components of the radius of gyration squared tensor and  $R_g^2$  is the mean squared, time-averaged radius of gyration, and it is obtained from the trace of the tensor.

Figure 5.2b shows the asphericity of the surfactant micelles as a function of micelle aggregation number,  $N_{agg}$ . The asphericity decreases initially with the  $N_{agg}$  followed by an increase at high aggregation signifying a sphere-rod transition. For SAE-15, this transition happens around  $N_{agg}$  between 150-200. The asphericity is minimum around  $N_{agg}$  of 100 and this size was subsequently used to study the adsorption behavior

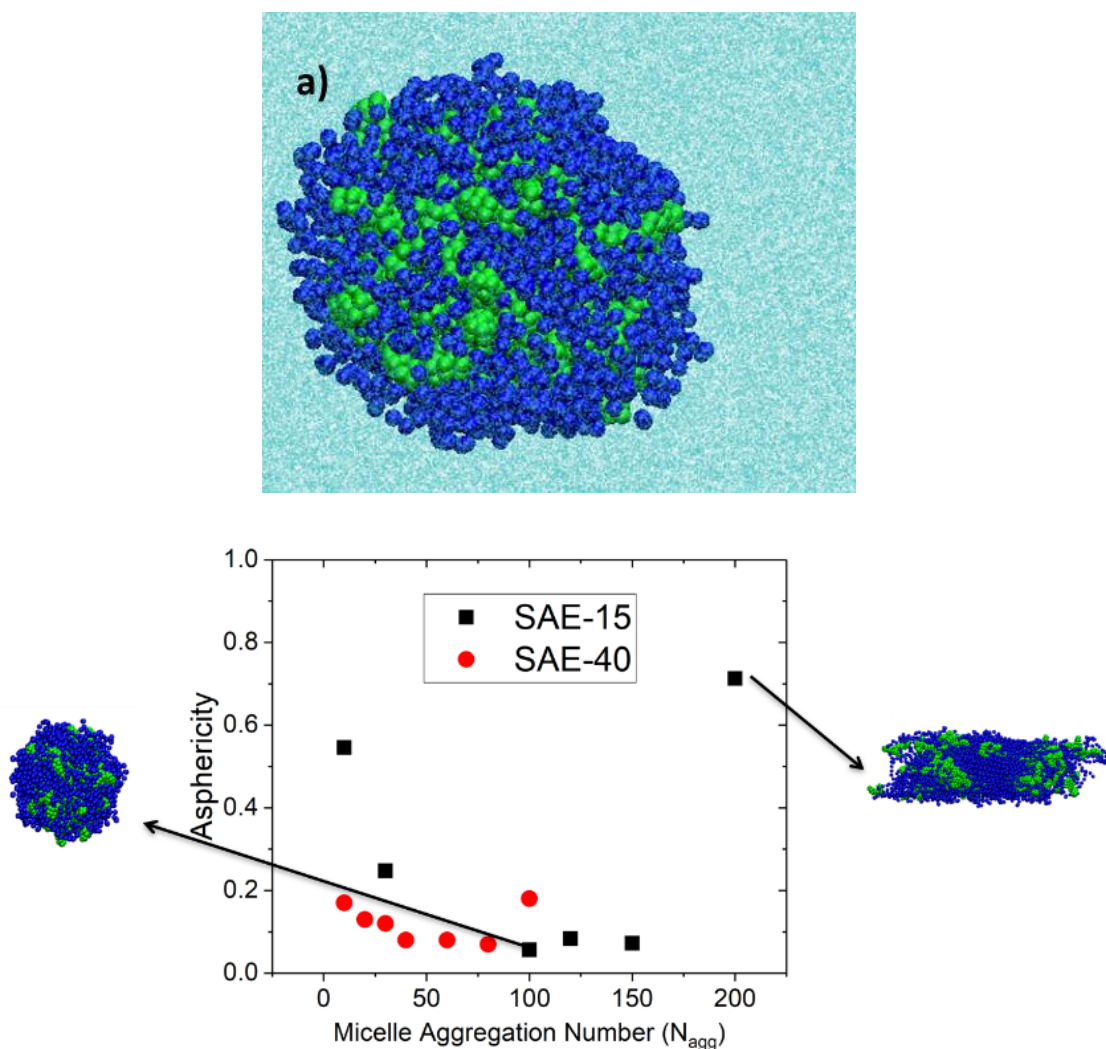


Figure 5.2. a) SAE-15 micelle formation after 100 ns of simulations at 50°C with 100 surfactant molecules. b) Asphericity of SAE-x micelles. Smaller the asphericity, closer the micelle is to a spherical structure.

of SAE-15. For SAE-40 the corresponding  $N_{agg}$  was found to be around 40 for minimum asphericity. The observed trend is in accordance with findings where the aggregation number of micelles is found to decrease with an increase in the hydrophilicity of the surfactant - the increasing unfavorable free energy contribution towards micellization for larger polyoxyethylene headgroups gives rise to smaller aggregates.<sup>56</sup> Experimental

measurements of aggregation numbers for these surfactants in high salinity brines are higher than predicted here.<sup>19</sup> However it is known that aggregation numbers of similar molecules increase in the presence of brine.<sup>57</sup> Compared to similar nonionic surfactants in pure water, the aggregation numbers predicted here are in the same range.<sup>56</sup> Table 5.4 lists the aggregation numbers for these surfactants along with their  $R_g$ . It can be seen that SAE-15 micelles are larger in size compared to SAE-40.

Table 5.4. Micelle aggregation numbers, radius of gyration squared, number of hydrogen-bonded water molecules per surfactant and adsorption well features for SAE-15 and SAE-40.

	$N_{agg}$	Temp.	$R_g(\text{\AA})$	Water/surfactant molecules in micelles	Well position ( $\text{\AA}$ )	Energy well ( $k_bT$ )	Energy Barrier ( $k_bT$ )
SAE-15	100	25°C	25.2	13	10.0	1.2	1.6
		50°C	25.6	8	7.5	1.8	1.2
SAE-40	40	25°C	24.0	38	9.0	1.2	1.8
		50°C	24.2	25	8.0	1.4	1.2

The hydration of the surfactant micelles was determined by measuring the number of water molecules hydrogen-bonded with the surfactant EO units. This is shown in Table 5.4. At 25°C there is about one water molecule per ethoxy group for both surfactants. This number reduces by about a factor of two at 50°C, indicating poorer hydration of the micelle as the temperature is increased. The decreased surfactant hydrations eventually lead to a complete separation of the surfactant and water phases at the cloud point temperature.

### 5.3.2. Micelle Adsorption on Calcite

To study the adsorption, surfactant and water molecules were randomly distributed and introduced over the calcite surface. For SAE-15, 1 and 100 molecules were introduced, and the resulting adsorption behavior was observed. In both cases a strong water-calcite interaction exists that prevents direct adsorption of surfactant molecules on the calcite surface (Figure 5.3). The aggregate formation was observed for 100 molecules with no single molecule adsorption in the limit of “infinite dilution” of one surfactant molecule in the simulation.

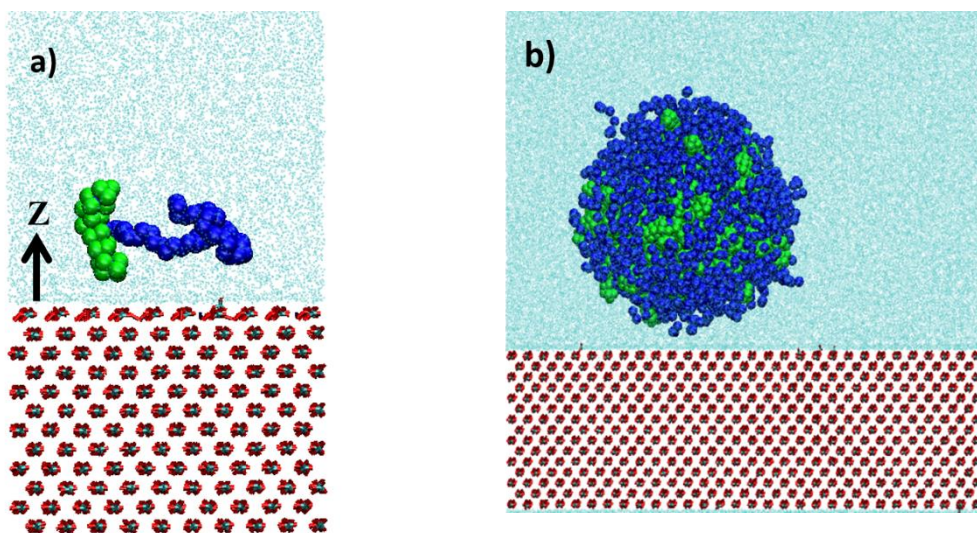


Figure 5.3. Final simulation state for a) Single molecule of SAE-15 + water + calcite and b) 100 molecules of SAE-15+water+calcite at 50°C. Both images correspond to the minimum energy positions discussed in Sec 5.3.2.

Figure 5.3a shows the state of a single surfactant molecule on the calcite surface. There is a thick layer of adsorbed water between the surfactant and the calcite. The hydrophilic EO units have a coiled planar configuration which tries to maximize contacts with both the water and calcite. Figure 5.4a plots the distance between the molecule and

calcite-water interface as the simulation progresses. The fact that the separation continues to increase with time indicates that this adsorption is very weak.

Surfactant aggregates were found to adsorb over the adsorbed water molecules provided they were within a critical distance of about 10 Å. For micelles farther from the surface, no adsorption is observed during the 70 ns MD runs. This can be seen in Figure 5.4b, which

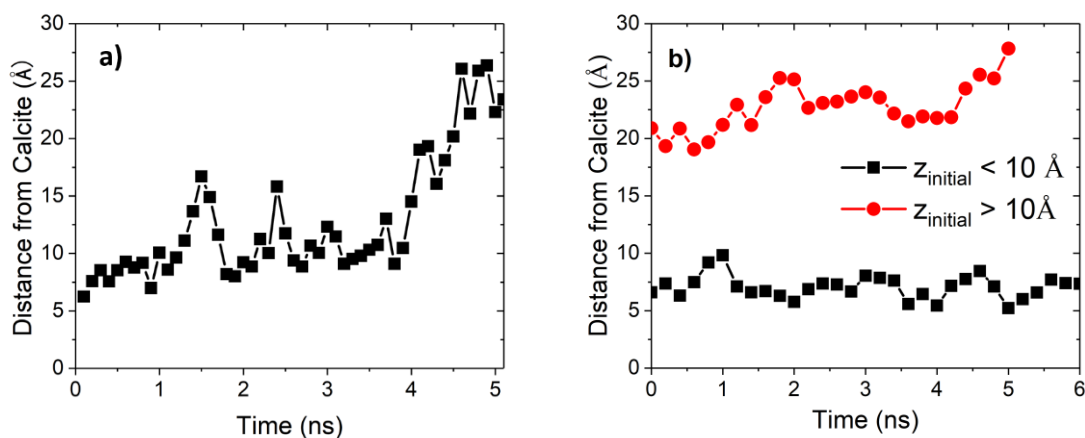


Figure 5.4. a) MD trajectory of single SAE-15 molecule. b) MD trajectories for 100 molecule micelle of SAE-15 for two different initial positions.

shows the distance between the micelle and the calcite surface as a function of time for two unbiased simulations – one in which the micelle was near the calcite surface in the beginning (black squares) and the other where it was farther away (red circles). Unlike, the micelle in bulk, the adsorbed micelle stays near the surface, indicating a stable adsorption.

The free energy landscapes associated with adsorption were investigated for micelles with aggregation numbers listed in Table 5.4. The free energy profile was obtained by performing umbrella sampling where the surfactant molecule(s) were subjected to a harmonic bias given by Eq. (6), where  $z$  refers to the reaction coordinate which in this case was the distance of the surfactant molecule(s) from the calcite perpendicular to the surface

as shown in Figure 5.3.  $K$  is the force constant associated with the bias and  $z_0$  is the set value for a particular sampling window. The values of  $z$  were varied to represent a sampling window extending from the surface to the bulk aqueous phase. For each sampling window, five ns equilibrium simulations were performed followed by five ns production runs to generate the biased probability distributions.

Figures 5.5a-b shows the free energies for a single molecule of SAE-15 and SAE-40 at 50°C plotted as a function of separation from the calcite surface. The difference between the minimum energy value near the surface and energy value at a large separation gives the adsorption free energy of the system. For SAE-15 this is about  $0.45 k_bT$ , whereas for SAE-40 the adsorption free energy is around  $0.65 k_bT$ . The SAE-15 surfactant corresponding to its minimum energy position is shown in Figure 5.3a.

To study micellar adsorption, a 100 molecule SAE-15 micelle and a 40 molecule SAE-40 micelle was used for the umbrella sampling simulations. For these simulations, the reaction coordinate was the perpendicular distance between the calcite surface and the center of the mass of micelle. Figures 5.6a-b show the free energy profile associated with micellar adsorption for the two surfactant molecules at 50°C. The x-axis in the plots shows the separation of closest surfactant molecule from the calcite surface. In both the plots, a local favorable adsorption zone is present near the calcite surface. These energy wells have values of  $1.8 k_bT$  and  $1.4 k_bT$  for SAE-15 and SAE-40, respectively. Another prominent feature of both profiles is the presence of a free-energy barrier to surface adsorption. For both the surfactants, the long-range energy barrier is about  $1.2 k_bT$ . The configuration of SAE-15 micelle corresponding to minimum adsorption energy is shown in Figure 5.3b.

Figures 5.7a-b show the energy profile for adsorption of SAE-15 and 40 at 25°C. The presence of energy barrier and energy well in the plots are qualitatively similar to the

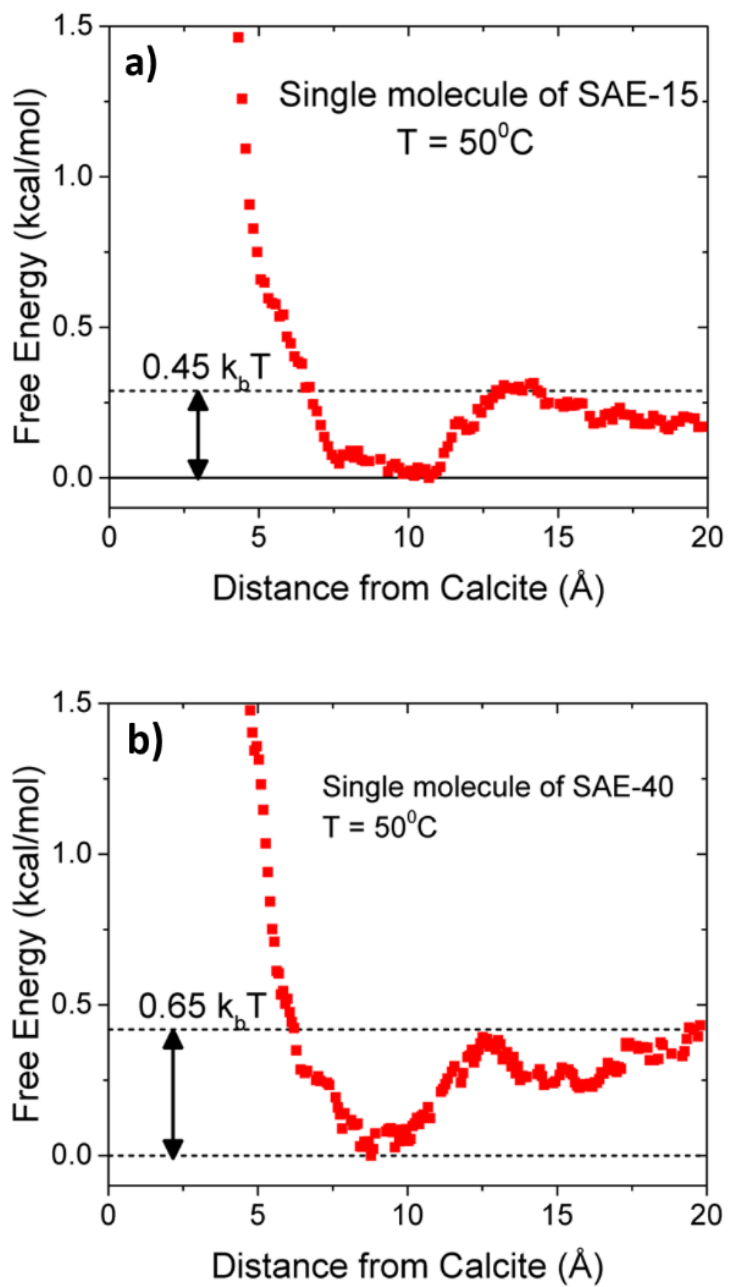


Figure 5.5. Adsorption free energy profiles at infinite dilution for a) SAE-15 and b) SAE-40 at 50°C.

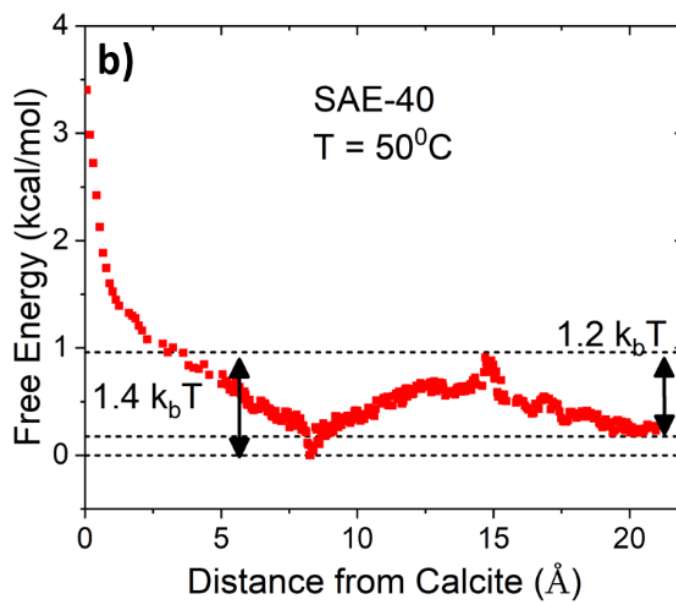
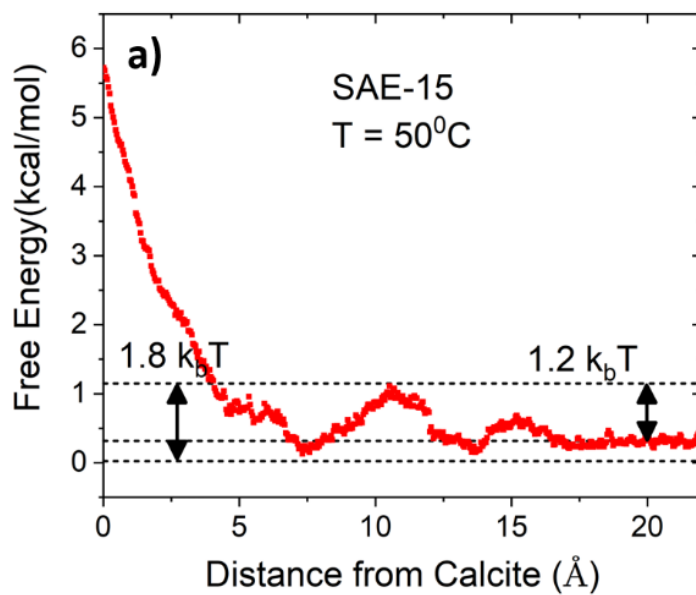


Figure 5.6. Adsorption free energy profiles for a) SAE-15 and b) SAE-40 micelles at 50°C



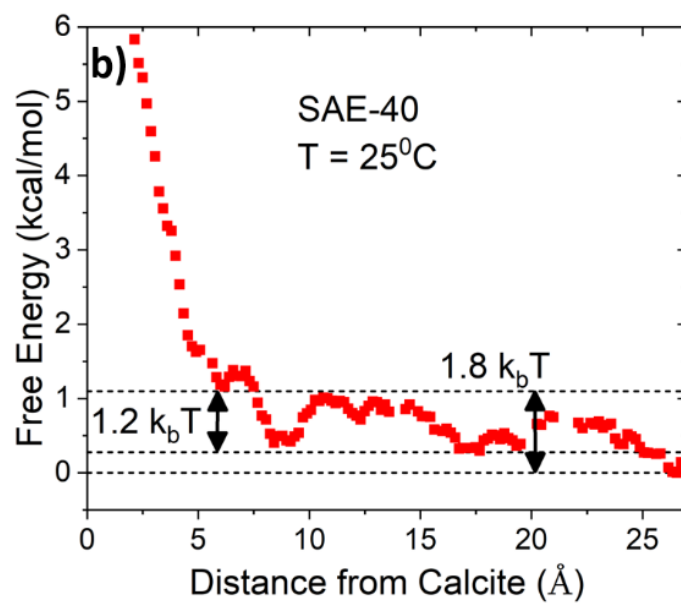
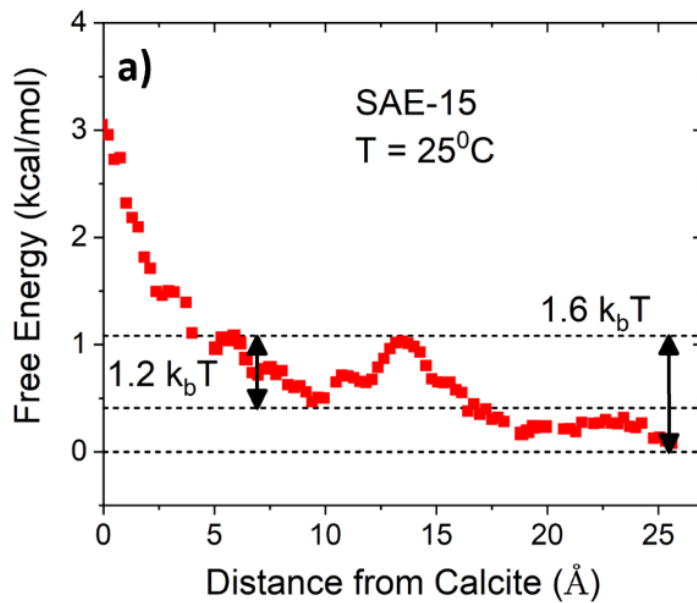


Figure 5.7. Adsorption free energy profiles for a) SAE-15 and b) SAE-40 micelles at 25°C

ones at 50°C. The energy well values decrease at this temperature –  $1.2 k_bT$  for both SAE-15 and SAE-40. The location of the energy well also moves further away from the calcite surface. The energy barriers however increase – about  $1.6 k_bT$  for SAE-15 and  $1.8 k_bT$  for SAE-40. Table 5.4 lists the energy well and barrier values for the surfactants at different temperatures.

#### 5.4. DISCUSSION

The depths of the adsorption energy wells for single molecules of SAE-15 and SAE-40 are shallow. Both are less than  $k_bT$ . Indeed random thermal motion causes a single molecule of SAE-15 to diffuse away from the surface even when it begins near the calcite, as shown in Figure 5.4a. The weak adsorption energy arises from a combination of EO-carbonate interactions and dispersion forces between the surfactant and the surface. Because the water layer is tightly bound to the surface, the surfactant molecule cannot get close enough to the calcite surface to have an adsorption energy higher than  $k_bT$ . The depth of the adsorption well for SAE-40 is larger than SAE-15 because it is a larger molecule with more EO-carbonate and dispersion force interactions.

The depths of the adsorption energy wells for micelles are much larger than that for single molecules, with adsorption energies ranging from  $1.2$ - $1.8 k_bT$ . This indicates a stronger adsorption for the micelles than a single surfactant molecule. The SAE-15 micelle in Figure 5.4b does not diffuse away from an initially close proximity to the calcite surface. The greater strength of adsorption of a micelle compared to a single surfactant molecule is due to the greater integrated energy of EO-carbonate and dispersion interactions with the surface. The micelles have more surfactant molecules and hence an overall greater attraction to the calcite surface.

The presence of aggregative adsorption is in agreement with previous experimental studies which investigated the adsorption of nonionic surfactants on hydrophilic surfaces.<sup>16, 22-24</sup> These aggregates are similar to bulk micelles<sup>27</sup> and are formed by lateral interactions between the surfactant hydrophobes. The structure of the surfactant also determines the depth of the energy well. Previously it was shown that a higher adsorption is correlated to an increase in the size of micelles.<sup>19</sup> The size of the aggregates and aggregation numbers is determined by the surfactant hydrophilicity – aggregation number decreases with increasing hydrophilicity,<sup>56</sup> which is born out in Table 5.4.

The extent of adsorption for a surfactant will be determined by the relative contribution from each of the two energy features. A rough estimate of the partition coefficient can be made from the energy barrier and well values using the relation

$$K = \frac{K_{surface}}{K_{bulk}} = \exp\left(\frac{\Delta G_{well} - \Delta G_{barrier}}{k_b T}\right), \quad (8)$$

where  $\Delta G_{well}$  and  $\Delta G_{barrier}$  denote the energy change associated with the energy well and energy barrier from the free energy plots,  $k_b$  is the Boltzmann's constant and  $T$  is the temperature.

Table 5.5 lists the values of partition coefficient and experimentally obtained maximum adsorption for SAE-15 and 40 at 25°C and 50°C. The partition coefficients predict higher adsorption for the more hydrophobic surfactant, SAE-15, at all temperatures. The coefficients also predict an increase in adsorption as the temperature is increased to 50°C. This is true for both SAE-15 and SAE-40. Both these predictions are in good qualitative agreement with the experimental observations as seen in the table.<sup>19</sup> The listed experimental values refer to maximum adsorptions observed for these surfactants under similar temperatures but in the presence of a brine salinity of 12% NaCl and 0.2% CaCl<sub>2</sub>. The increased adsorption with increasing temperature appears to be caused by closer

proximity of the micelle to the calcite surface. The micelles are 1-2.5 Å closer to the surface at 50°C compared to 25°C.

Table 5.5. Estimation of the partition coefficient and comparison with experimentally measured adsorptions for SAE-15 and SAE from ref. 19.

	Temperature	$K_{\text{surface:bulk}}$	Adsorption from Experiments ( $\mu\text{mol.m}^{-2}$ )
SAE-15	25°C	0.64	0.6
	50°C	1.65	1.0
SAE-40	25°C	0.55	0.2
	50°C	1.35	0.4

Because the EO-carbonate and dispersion force interactions are greater the closer to the calcite, there is a deepening of the adsorption energy well, leading to greater adsorption. The micelle is able to get closer to the surface because the structuring of the water near the calcite decreases with increasing temperature. Figure 5.8 illustrates the density profiles of water and surfactant micelle as a function of distance from the calcite surface. We see structural ordering of water by the surface of the calcite. As the temperature increases, the structure is weakened due to thermal motion of the water.

At 25°C, the depth of adsorption wells is lower than that at 50°C for both the surfactants. The stronger interactions of water with calcite, also makes it difficult for the surfactant micelle to go near the surface and access the adsorption sites. This behavior is confirmed in Figure 5.8, where the density of adsorbed water molecules increases at lower temperatures. The energy wells are also pushed further from the water-calcite interface confirming weaker calcite-surfactant interactions. The hindering action of the strongly wetting water-film means the energy wells are comparable for both the surfactants even

though SAE-15 aggregates are slightly bigger than the SAE-40 aggregate. The energy barrier values are higher at lower temperatures. This also arises because of the increased water density near the calcite surface. As shown in Table 5.4, the surfactant micelles also have a higher affinity to the bulk phase at a lower temperature, where hydrogen bonding and consequently, the aqueous hydration of surfactant molecules is stronger compared to the hydration at 50°C.

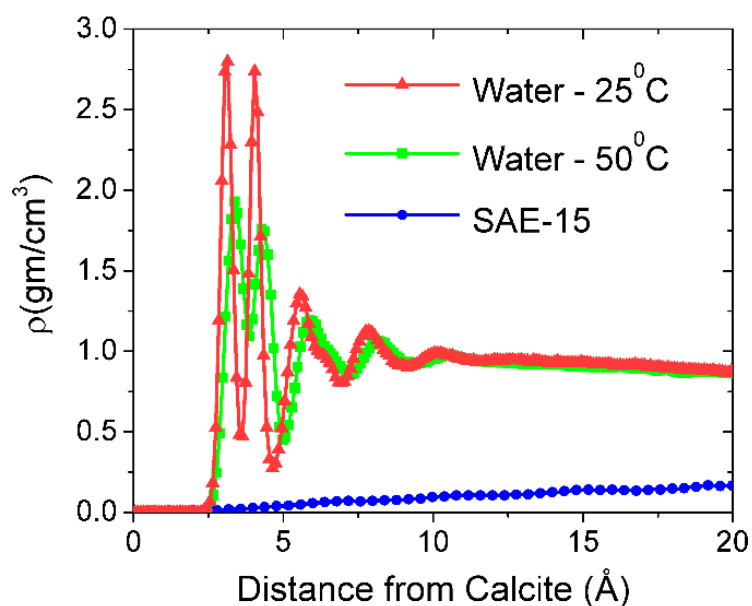


Figure 5.8. Density profiles of water and surfactant micelle as a function of separation from the calcite surface.

The predicted correlation<sup>19</sup> between surfactant cloud point and adsorption can also be qualitatively explained from the current findings. The model uses the parameter, cloud point temperature difference,  $CPTD = CP - T$ , to predict the micellar adsorption of nonionic surfactants. Here  $CP$  is the cloud point of the surfactant solution, and  $T$  is the temperature of the system. It is found that surfactant adsorption increases as the temperature approaches the cloud point or  $CPTD$  approaches zero. At the cloud point, the

surfactant solution starts separating into water and surfactant phases and is an indicator of surfactant hydrophilicity. The rescaled parameter *CPTD* combines the effect of both surfactant hydrophilicity and temperature on the underlying surfactant-water and surfactant-solid interactions, which in turn determine the extent of adsorption. As temperature increases, micelles adsorb more strongly because of closer proximity to the surface. From Table 5.4, it can also be seen that ethoxy groups have poorer hydration at higher temperatures. At higher temperatures, closer to the cloud point, these behaviors increase surfactant adsorption. The trend with respect to surfactant hydrophilicity can also be understood by considering the energy well depths and their relation to the micelle sizes. Micelle sizes and aggregation numbers are determined by surfactant hydrophilicity<sup>19, 56</sup> and it is found that a larger micelle size is associated with a higher tendency of adsorption. Typically, micelle sizes of these surfactants increase moving closer to their cloud points.<sup>19, 57</sup> This qualitatively follows the predicted behavior of higher adsorption near the cloud point.

#### **5.4. CONCLUSIONS**

Nonionic surfactants like secondary alcohol ethoxylate have been found to be effective in altering the wettability of an oil-wet carbonate surface to water-wet. The mechanism and estimation of the extent of adsorption for such molecules were analyzed, for the first time, using molecular dynamics simulations. The extent of adsorption was found to depend both on surfactant structure and temperature – increased adsorption at high temperatures and for more hydrophobic surfactants. Based on the empirically calculated values of packing parameters obtained from the experiments, a micellar aggregative mechanism was proposed. MD simulations confirmed the tendency of aggregative adsorption as monomer adsorption was found to be energetically unfavorable. Free energy

profiles of micellar adsorption exhibit a locally favorable energy well and a surfactant and temperature-dependent long-range energy barrier to adsorption. The depth of the energy well increases with temperature. This along with a decrease in the energy-barrier implies higher adsorption at high temperatures. The sparse nature of adsorbed aggregates is attributed to the typical low energy interactions of  $1.1 k_bT$  to  $1.8 k_bT$ . A rough estimation of the surface to bulk partition coefficients for micellar aggregates agrees very well qualitatively with experimental findings. The experimentally observed trend of increased adsorption near the surfactant cloud point is also explained by considering the surfactant-water and surfactant-solid interactions. The effect of surfactant aggregation number and shape, particularly, near the surfactant cloud point, on adsorption warrants further investigation to obtain a complete picture of micellar adsorption and its universal correlation to cloud points.

## REFERENCES

1. Adibhatla, B., & Mohanty, K. K. Oil recovery from fractured carbonates by surfactant-aided gravity drainage: laboratory experiments and mechanistic simulations. *SPE Reservoir Evaluation & Engineering*, **2008**, 11(01), 119-130.
2. Seethepalli, A., Adibhatla, B., & Mohanty, K. K. Wettability alteration during surfactant flooding of carbonate reservoirs. In *SPE/DOE Symposium on Improved Oil Recovery*. Society of Petroleum Engineers, **2004**.
3. Hirasaki, G., & Zhang, D. L. Surface chemistry of oil recovery from fractured, oil-wet, carbonate formations. *SPE Journal*, **2004**, 9(02), 151-162.
4. Zhang, J., Nguyen, Q. P., Flaaten, A., & Pope, G. A. Mechanisms of enhanced natural imbibition with novel chemicals. *SPE reservoir evaluation & engineering*, **2009**, 12(06), 912-920.
5. Strand, S., Standnes, D. C., & Austad, T. Spontaneous imbibition of aqueous surfactant solutions into neutral to oil-wet carbonate cores: Effects of brine salinity and composition. *Energy & fuels*, **2003**, 17(5), 1133-1144.
6. Austad, T., & Standnes, D. C. Spontaneous imbibition of water into oil-wet carbonates. *Journal of Petroleum Science and Engineering*, **2003**, 39(3-4), 363-376.
7. Austad, T. and Milter, J. Spontaneous imbibition of water into low permeable chalk at different wettabilities using surfactants. In *International Symposium on Oilfield Chemistry*, Society of Petroleum Engineers, **1997**.
8. Standnes, D.C., Nogaret, L.A., Chen, H.L. and Austad, T. An evaluation of spontaneous imbibition of water into oil-wet carbonate reservoir cores using a nonionic and a cationic surfactant. *Energy & Fuels*, **16**(6), **1997**, 1557-1564.
9. Spinler, E.A., Zornes, D.R., Tobola, D.P. and Moradi-Araghi, A. Enhancement of oil recovery using a low concentration of surfactant to improve spontaneous and forced imbibition in chalk. In *SPE/DOE Improved Oil Recovery Symposium*. Society of Petroleum Engineers, **2000**.
10. Ma, K., Cui, L., Dong, Y., Wang, T., Da, C., Hirasaki, G. J., & Biswal, S. L. Adsorption of cationic and anionic surfactants on natural and synthetic carbonate materials. *Journal of colloid and interface science*, **2013**, 408, 164-172.
11. Fletcher, P. D., Savory, L. D., Clarke, A., & Howe, A. M. Model Study of Enhanced Oil Recovery by Flooding with Aqueous Solutions of Different Surfactants: How the



Surface Chemical Properties of the Surfactants Relate to the Amount of Oil Recovered. *Energy & Fuels*, **2016**, 30(6), 4767-4780.

12. Standnes, D. C., & Austad, T. Wettability alteration in carbonates: Interaction between cationic surfactant and carboxylates as a key factor in wettability alteration from oil-wet to water-wet conditions. *Colloids and Surfaces A: Physicochemical and Engineering Aspects*, **2003**, 216(1-3), 243-259.

13. Jarrahan, K., Seiedi, O., Sheykhan, M., Sefti, M. V., & Ayatollahi, S. Wettability alteration of carbonate rocks by surfactants: a mechanistic study. *Colloids and Surfaces A: Physicochemical and Engineering Aspects*, **2012**, 410, 1-10.

14. Wu, Y., Shuler, P. J., Blanco, M., Tang, Y., & Goddard, W. A. A study of wetting behavior and surfactant EOR in carbonates with model compounds. In *SPE/DOE Symposium on Improved Oil Recovery*. Society of Petroleum Engineers, **2006**.

15. Somasundaran, P. and Krishnakumar, S., **1997**. Adsorption of surfactants and polymers at the solid-liquid interface. *Colloids and Surfaces A: physicochemical and engineering aspects*, 123(124), pp.491-513.

16. Desbene, P.L., Portet, F. and Treiner, C., **1997**. Adsorption of pure nonionic alkylethoxylated surfactants down to low concentrations at a silica/water interface as determined using a HPLC technique. *Journal of Colloid and Interface Science*, 190(2), pp.350-356.

17. Jian, G., Puerto, M.C., Wehowsky, A., Dong, P., Johnston, K.P., Hirasaki, G.J. and Biswal, S.L., **2016**. Static adsorption of an ethoxylated nonionic surfactant on carbonate minerals. *Langmuir*, 32(40), pp.10244-10252.

18. Das, S., Nguyen, Q., Patil, P.D., Yu, W. and Bonnecaze, R.T., **2018**. Wettability alteration of calcite by nonionic surfactants. *Langmuir*, 34(36), pp.10650-10658.

19. Das, S., Katiyar, A., Rohilla, N., Nguyen, Q., and Bonnecaze, R.T., **2020**. Universal Scaling of Adsorption of Non-Ionic Surfactants on Carbonates using Cloud Point Temperatures. Under Review

20. Curbelo, F.D., Santanna, V.C., Neto, E.L.B., Dutra Jr, T.V., Dantas, T.N.C., Neto, A.A.D. and Garnica, A.I., **2007**. Adsorption of nonionic surfactants in sandstones. *Colloids and Surfaces A: Physicochemical and Engineering Aspects*, 293(1-3), pp.1-4.

21. Caruso, F., Serizawa, T., Furlong, D.N. and Okahata, Y., **1995**. Quartz crystal microbalance and surface plasmon resonance study of surfactant adsorption onto gold and chromium oxide surfaces. *Langmuir*, 11(5), pp.1546-1552.

22. Levitz, P.E., **2002**. Adsorption of non ionic surfactants at the solid/water interface. *Colloids and Surfaces A: Physicochemical and Engineering Aspects*, 205(1-2), pp.31-38.
23. Levitz, P., **1991**. Aggregative adsorption of nonionic surfactants onto hydrophilic solid/water interface. Relation with bulk micellization. *Langmuir*, 7(8), pp.1595-1608.
24. Tiberg, F., **1996**. Physical characterization of non-ionic surfactant layers adsorbed at hydrophilic and hydrophobic solid surfaces by time-resolved ellipsometry. *Journal of the Chemical Society, Faraday Transactions*, 92(4), pp.531-538.
25. Tiberg, F., Joensson, B., Tang, J.A. and Lindman, B., **1994**. Ellipsometry studies of the self-assembly of nonionic surfactants at the silica-water interface: equilibrium aspects. *Langmuir*, 10(7), pp.2294-2300.
26. Levitz, P., Van Damme, H. and Keravis, D., **1984**. Fluorescence decay study of the adsorption of nonionic surfactants at the solid-liquid interface. 1. Structure of the adsorption layer on a hydrophilic solid. *The Journal of Physical Chemistry*, 88(11), pp.2228-2235.
27. Levitz, P. and Van Damme, H., **1986**. Fluorescence decay study of the adsorption of nonionic surfactants at the solid-liquid interface. 2. Influence of polar chain length. *The Journal of Physical Chemistry*, 90(7), pp.1302-1310.
28. Portet, F., Desbene, P.L. and Treiner, C., **1997**. Adsorption isotherms at a silica/water interface of the oligomers of polydispersed nonionic surfactants of the alkylpolyoxyethylated series. *Journal of colloid and interface science*, 194(2), pp.379-391.
29. Rigo, V.A., Metin, C.O., Nguyen, Q.P. and Miranda, C.R., **2012**. Hydrocarbon adsorption on carbonate mineral surfaces: a first-principles study with van der Waals interactions. *The Journal of Physical Chemistry C*, 116(46), pp.24538-24548.
30. Cooper, T.G. and de Leeuw, N.H., **2004**. A computer modeling study of the competitive adsorption of water and organic surfactants at surfaces of the mineral scheelite. *Langmuir*, 20(10), pp.3984-3994.
31. Yang, C. and Sun, H., **2014**. Surface–bulk partition of surfactants predicted by molecular dynamics simulations. *The Journal of Physical Chemistry B*, 118(36), pp.10695-10703.
32. Durán-Álvarez, A., Maldonado-Domínguez, M., González-Antonio, O., Durán-Valencia, C., Romero-Ávila, M., Barragán-Aroche, F. and López-Ramírez, S., **2016**. Experimental–Theoretical Approach to the Adsorption Mechanisms for Anionic, Cationic,

and Zwitterionic Surfactants at the Calcite–Water Interface. *Langmuir*, 32(11), pp.2608-2616.

33. Wang, X., Wu, G., Yuan, C., Zhu, Q., Li, C., Sun, S. and Hu, S., **2018**. Molecular dynamics simulations of aggregation behavior of sodium dodecyl sulfate on SiO<sub>2</sub> and CaCO<sub>3</sub> surfaces. *Surface and Interface Analysis*, 50(3), pp.284-289.

34. Tummala, N.R., Shi, L. and Striolo, A., **2011**. Molecular dynamics simulations of surfactants at the silica–water interface: Anionic vs nonionic headgroups. *Journal of colloid and interface science*, 362(1), pp.135-143.

35. Xu, Z., Yang, X. and Yang, Z., **2008**. On the mechanism of surfactant adsorption on solid surfaces: Free-energy investigations. *The Journal of Physical Chemistry B*, 112(44), pp.13802-13811.

36. Kurapati, Y. and Sharma, S., **2018**. Adsorption Free Energies of Imidazolium-Type Surfactants in Infinite Dilution and in Micellar State on Gold Surface. *The Journal of Physical Chemistry B*, 122(22), pp.5933-5939.

37. Plimpton, S., **1995**. Fast parallel algorithms for short-range molecular dynamics. *Journal of computational physics*, 117(1), pp.1-19.

38. Plimpton, S., Thompson, A., Crozier, P. and Kohlmeyer, A., **2011**. LAMMPS molecular dynamics simulator. 2015-5-15]. <http://lammps.sandia.gov>.

39. Wang, J., Wolf, R.M., Caldwell, J.W., Kollman, P.A. and Case, D.A., **2004**. Development and testing of a general amber force field. *Journal of computational chemistry*, 25(9), pp.1157-1174.

40. Case, D.A., Cheatham III, T.E., Darden, T., Gohlke, H., Luo, R., Merz Jr, K.M., Onufriev, A., Simmerling, C., Wang, B. and Woods, R.J., **2005**. The Amber biomolecular simulation programs. *Journal of computational chemistry*, 26(16), pp.1668-1688.

41. Price, D.J. and Brooks III, C.L., **2004**. A modified TIP3P water potential for simulation with Ewald summation. *The Journal of chemical physics*, 121(20), pp.10096-10103.

42. Mani, S., Khabaz, F., Godbole, R.V., Hedden, R.C. and Khare, R., **2015**. Structure and hydrogen bonding of water in polyacrylate gels: effects of polymer hydrophilicity and water concentration. *The Journal of Physical Chemistry B*, 119(49), pp.15381-15393.

43. Khabaz, F., Mani, S. and Khare, R., **2016**. Molecular origins of dynamic coupling between water and hydrated polyacrylate gels. *Macromolecules*, 49(19), pp.7551-7562.

44. Godbole, R.V., Khabaz, F., Khare, R. and Hedden, R.C., **2017**. Swelling of Random Copolymer Networks in Pure and Mixed Solvents: Multi-Component Flory–Rehner Theory. *The Journal of Physical Chemistry B*, 121(33), pp.7963-7977.
45. Evans, D.J. and Holian, B.L., **1985**. The nose–hoover thermostat. *The Journal of chemical physics*, 83(8), pp.4069-4074.
46. Hockney, R.W. and Eastwood, J.W., **1988**. Computer simulation using particles. crc Press.
47. Martínez, L., Andrade, R., Birgin, E.G. and Martínez, J.M., **2009**. PACKMOL: a package for building initial configurations for molecular dynamics simulations. *Journal of computational chemistry*, 30(13), pp.2157-2164.
48. Kokalj, A., **1999**. XCrySDen—a new program for displaying crystalline structures and electron densities. *Journal of Molecular Graphics and Modelling*, 17(3-4), pp.176-179.
49. Kerisit, S., Marmier, A. and Parker, S.C., **2005**. Ab initio surface phase diagram of the {1014} calcite surface. *The Journal of Physical Chemistry B*, 109(39), pp.18211-18213.
50. Pavese, A., Catti, M., Parker, S.C. and Wall, A., **1996**. Modelling of the thermal dependence of structural and elastic properties of calcite, CaCO<sub>3</sub>. *Physics and chemistry of minerals*, 23(2), pp.89-93.
51. Freeman, C.L., Harding, J.H., Cooke, D.J., Elliott, J.A., Lardge, J.S. and Duffy, D.M., **2007**. New forcefields for modeling biomineralization processes. *The Journal of Physical Chemistry C*, 111(32), pp.11943-11951.
52. Torrie, G.M. and Valleau, J.P., **1977**. Nonphysical sampling distributions in Monte Carlo free-energy estimation: Umbrella sampling. *Journal of Computational Physics*, 23(2), pp.187-199.
53. Kumar, S., Rosenberg, J.M., Bouzida, D., Swendsen, R.H. and Kollman, P.A., **1992**. The weighted histogram analysis method for free-energy calculations on biomolecules. I. The method. *Journal of computational chemistry*, 13(8), pp.1011-1021.
54. Velinova, M., Sengupta, D., Tadjer, A.V. and Marrink, S.J., **2011**. Sphere-to-rod transitions of nonionic surfactant micelles in aqueous solution modeled by molecular dynamics simulations. *Langmuir*, 27(23), pp.14071-14077.
55. Khabaz, F. and Khare, R., **2014**. Effect of chain architecture on the size, shape, and intrinsic viscosity of chains in polymer solutions: A molecular simulation study. *The Journal of chemical physics*, 141(21), p.214904.

56. El Eini, D.I.D., Barry, B.W. and Rhodes, C.T., **1976**. Micellar size, shape, and hydration of long-chain polyoxyethylene nonionic surfactants. *Journal of Colloid and Interface Science*, 54(3), pp.348-351.

57. Bahadur, P., Pandya, K., Almgren, M., Li, P. and Stilbs, P., **1993**. Effect of inorganic salts on the micellar behaviour of ethylene oxide-propylene oxide block copolymers in aqueous solution. *Colloid and Polymer Science*, 271(7), pp.657-667.

## **Chapter 6: Wettability Alteration and Spontaneous Imbibition by Single and Mixed Surfactants in Carbonates**

### **6.1. INTRODUCTION**

Carbonate-based reservoirs contain more than half of world's oil reserves.<sup>1</sup> Two key features of these reservoirs – high natural fracturing and initial oil-wet state determine oil recovery rates. The oil-wetness arises from the adsorption of acidic components from the oil onto the carbonate surfaces.<sup>2-3</sup> This inhibits the major mechanism of imbibition of injection fluid in conventional waterflooding of fractured carbonates and results in low oil production. Typically only about 20-30% of original oil in place (OOIP) is obtained through primary and secondary recovery methods.

Surfactants have been an integral component of chemical enhanced oil recovery (EOR) techniques to boost oil production. Surfactants can improve oil recoveries by either lowering the oil-water (O/W) interfacial tensions (IFT) or by changing the wettability of the solid surfaces. EOR technologies like surfactant-polymer flooding<sup>4-5</sup> and alkaline surfactant polymer flooding<sup>6-8</sup> involve lowering O/W IFTs to ultra-low values to improve oil mobilization inside the pores.<sup>4-11</sup> Surfactants have also been used to improve oil recovery by altering the wettability of carbonate surfaces from oil-wet to water-wet.<sup>12-18</sup> Altering the wettability to water-wet ensures a positive capillary force and allows spontaneous imbibition of the aqueous phase into the formation to drive out oil into the production wells. Cationic surfactants are believed to form ion pairs with adsorbed oil molecules, which in turn leads to restoration of the water-wet state of the underlying surface.<sup>12-14</sup> Anionic surfactants have been widely investigated and the primary mechanism in this case is the lowering of O/W IFT, leading to emulsification.<sup>19-20</sup> Distinction between the capillary and emulsification driven imbibition mechanisms were provided by Zhang and co-workers.<sup>20</sup> Recently, it has been observed that stable surfactant formulations

containing both wettability altering and IFT reducing agents have a synergistic effect leading to higher oil recovery than through wettability alteration alone.<sup>21</sup> Limited literature is available on the wettability alteration effect of nonionic surfactants on carbonate surfaces.<sup>18, 22-25</sup> A surface hydrophilization mechanism arising from surfactant coating is believed to be the driving force of surfactant action in this case.<sup>18, 26</sup> Along with surfactants, brine salinity has also been found to determine the wettability alteration potential of carbonates.<sup>27-31</sup> The effect of potential-determining ions like  $\text{Ca}^{2+}$ ,  $\text{Mg}^{2+}$  and  $\text{SO}_4^{2-}$  has been investigated in multiple works.<sup>32-33</sup> Using  $\text{SO}_4^{2-}$  and  $\text{Ca}^{2+}$ , oil-wet surfaces like chalk have been altered to a water-wet one. These divalents have been known to influence charge distribution on mineral surfaces. Addition of  $\text{SO}_4^{2-}$  can reduce the positive charge density of carbonate surfaces which can lead to increased surface accumulation of other cations like  $\text{Ca}^{2+}$ , and  $\text{Mg}^{2+}$ . These cations can form ion-pairs with adsorbed carboxylates, which then move to the bulk aqueous phase, thus altering the wettability. Sulphates can also promote desorption of carboxylates through a displacement mechanism on the positively charged carbonate surface.

Spontaneous imbibition measurements combined with contact angle measurements have been used in the past to highlight the effect of wettability alteration for such systems.<sup>14, 16, 20, 21, 24-25, 29</sup> Final contact angles have been reported for different anionic and nonionic surfactants on calcite as a representative carbonate surface.<sup>17-18, 23-25</sup> Contact angle values combined with O/W IFT give an estimate of the capillary driving force,  $\gamma_{ow} \cos \theta$ , which is responsible for spontaneous imbibition. Along with a low contact angle, a moderate O/W IFT is hence desirable for spontaneous imbibition-driven oil recovery. For such initially oil-wet surfaces and moderate O/W IFT systems, buoyancy driven co-current imbibition leads to oil production mainly from the top face.

Oil recoveries to the extent of 40-70% have been reported for cationic surfactants in multiple works.<sup>12-14</sup> The same authors have also highlighted the importance of the core ageing process on the oil recoveries.<sup>34</sup> Using sulfated and sulfonated anionic surfactants and ethoxylated nonionic surfactants, oil recoveries in the range of 20-40% have been observed.<sup>24-25</sup> Significant increase in oil recoveries (up to 70%) and recovery rates have been reported for both anionic and nonionic surfactants with an increase in temperature.<sup>24</sup> The efficiency and success of spontaneous imbibition is also dependent on other factors like pore structure, rock permeability, and fluid saturation.<sup>35-36</sup> Spontaneous imbibition experiments performed for nonionic and cationic surfactants have not revealed a universal correlation with permeability. However, a maximum in oil production was observed in many cases at an optimum permeability value which varied for different systems.<sup>37</sup> Similar behavior was also observed for oil recoveries, through spontaneous imbibition of brine, as a function of initial water saturation.<sup>38-39</sup> The type of surfactants and reservoir conditions also determine the rate of oil production through spontaneous imbibition. Typically higher recovery rates are observed for high permeable systems.<sup>37</sup> The parameter  $\sqrt{k/\phi}$ , where  $k$  and  $\phi$  are the permeability and porosity respectively, is representative of the microscopic pore dimensions and has been found to capture the effect of imbibition rates for different porous systems. For a capillary driven process, a decrease in O/W IFT because of surfactant addition is associated with a reduction in oil recovery rate. The dependence of recovery rates is less for gravity or buoyancy-driven imbibitions. Universal scalings of oil recovery with time incorporating system parameters like permeability, porosity, O/W IFT, phase viscosities, and characteristic length have been developed by multiple works in the past.<sup>40-</sup>

42

The adsorption of surfactants also plays an important role in determining the efficiency of a wettability alteration process.<sup>43</sup> The adsorption of surfactants is essential for



successful wettability alteration. However, very high adsorption implies surfactant loss resulting in high surfactant requirements and inefficient process economics. A direct correlation has been observed between surfactant adsorption and contact angle measurements in the past and it is essential to understand if the correlation extends to ultimate oil recoveries.

For wettability alteration, nonionic surfactants offer significant advantages compared to other surfactant types through lower adsorption, low surfactant requirements and by maintaining moderate O/W IFT values. In the current study, two nonionic surfactants of the family of secondary alcohol ethoxylates are evaluated for wettability alteration-based oil recovery through contact angle, adsorption, and spontaneous imbibition experiments. Both contact angle and adsorption have been correlated in the past to the thermodynamic parameter of cloud point temperature difference,

$$CPTD = T_c - T, \quad (1)$$

where  $T_c$  and  $T$  are the system cloud point and temperature respectively. The current study is an extension of the past works to investigate the dependence of ultimate oil recoveries on capillary driving force, surfactant adsorption, initial water saturation, and *CPTD*. Nonionic surfactants exhibit phase separation at high temperatures which prevent successful application for reservoirs with high salinity and temperature. The aqueous stability of these surfactants can be increased by adding anionic hydrotropes to form mixed surfactant solutions. While the concept of improving aqueous stability of nonionic surfactants is not new, there have been very few systematic studies on wettability alteration of such mixed surfactant systems in the past.<sup>25,44</sup> In order to address this, mixed surfactant systems of secondary alcohol ethoxylates and anionic cosurfactants were also evaluated and the effect of the introduction of secondary component was analyzed in detail. The effect of brine salinity, particularly of the concentration of  $\text{SO}_4^{2-}$ , was also studied both for

single and mixed-surfactant systems. The concept of *CPTD* is extended to these mixed systems and an attempt was made at universal oil recovery predictions.

## 6.2. MATERIALS

Tables 6.1 and 6.2 list the surfactants used in the current study with their molecular structures. All surfactants were provided by The Dow Chemical Company.

Table 6.1: List of nonionic surfactants evaluated in the study.

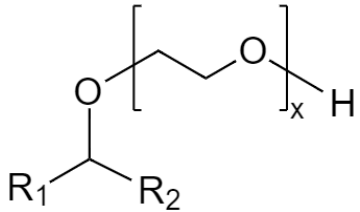
Structure	Surfactant name	Specification (x)
	SAE-x (Secondary alcohol ethoxylate)	9
		15

Table 6.2: List of anionic cosurfactants evaluated in the study.

Surfactant name	Specification
LM	Low molecular weight
MM	Medium molecular weight
HM	High molecular weight

The family of nonionic surfactants studied were secondary alcohol ethoxylates represented by SAE-x. The hydrophilic and hydrophobic components in this family are repeating units of ethylene oxide (EO) and secondary alcohol respectively. The co-surfactants are anionic surfactants, differentiated by their size. Calcite plates (Iceland Spar) were used as a representative carbonate surface and they were obtained from Wards Natural Sciences. Crude oil used in the experiments was obtained from a carbonate oil formation. Sodium chloride and calcium chloride (Fisher) were used as received. Indiana limestone was used

as the representative carbonate surface for adsorption and spontaneous imbibition experiments. Indiana limestone for imbibition and adsorption experiments was obtained from Kocurek Industries (TX, USA). Prior to adsorption experiments Indiana limestone particles were sieved with 200-400 mesh, washed and dried. HPLC grade water (Fisher Scientific) was used to make all the solutions.

### **6.3. METHODOLOGY**

#### **6.3.1. Cloud Point Measurements**

Aqueous stability tests were performed by measuring the cloud point of surfactant solutions (single and mixed). To do so, surfactant solutions were first prepared in glass vials and then heated inside an oven for 20 minutes at a particular temperature. This was followed by mild shaking to observe for the formation of white opaque phase. The temperature was then increased by 1° and the above step was repeated. The onset of opacity was reported as the cloud point temperature.

#### **6.3.2. Capillary Driving Force Measurements**

The O/W IFT and contact angle measurements were performed separately to obtain the capillary driving force. The inverted pendant drop method was used to measure the IFT values. Oil drops were introduced in a surfactant solution, heated to the required temperature, using a syringe with inverted needle. The shape of the oil drop was monitored using a high magnification camera and the IFT values were extracted from the images using the Pendant drop plug-in in ImageJ.

Calcite blocks were used as representative carbonate surface for the contact angle measurements. Calcite plates (3cm x 3cm x 1cm) were first cut from calcite blocks by breaking across the cleavage planes. They were cleaned using ethanol and dried at 120°C

for 2 days. A small drop of oil (~ 1mm size) was placed on the calcite and allowed to age at 70°C for 3 days. Following the ageing process, a uniform oil-patch was formed. The calcite plate was then placed inside a quartz cell containing the heated surfactant solutions. The temperature was regulated by an environmental chamber. The shape of the drops was monitored using a high magnification camera and the contact angles were measured using the ImageJ software. Contact angle measurements for a given system were repeated at least three times and the average value was used.

### **6.3.3. Adsorption Measurements**

Static adsorption experiments were carried out for the single and mixed surfactants to obtain adsorption isotherms. The choice of temperature was determined by the cloud point of the surfactants. A constant brine salinity of 12% NaCl and 0.2% CaCl<sub>2</sub> was used for all the experiments. Surfactant stock solutions were first prepared at different concentrations and equilibrated with limestone particles. This pre-equilibration step takes care of the effect of limestone dissolution on brine composition. 10 mL of surfactant solutions were added to 2.75 g of prepared limestone particles in centrifuge tubes and placed in an oven at the experimental temperature. The mixture was shaken periodically for 24 hours and then allowed to settle for another 24 hours. The supernatant solution was then separated to analyze the equilibrium bulk surfactant concentration.

The concentration of SAE-x in a single component system was measured using High Performance Liquid Chromatography (HPLC) with an Evaporative Light Scattering Detector (ELSD). Surfactant concentrations in mixed systems were analyzed using the NMR technique. Detailed methodologies are available from previous works involving the same family of surfactants.<sup>43, 46</sup> Separate calibration curves were prepared for each

experiment prior to determining the unknown concentrations. The adsorption is obtained from a simple mass balance

$$\Gamma = m_{sol} (C_0 - C) / Sm_c . \quad (2)$$

#### **6.3.4. Spontaneous Imbibition Experiments**

Outcrop Indiana limestone cores were prepared for the spontaneous imbibition tests. Small cylindrical plugs of 1” height and 1” diameter were first drilled from these cores. These core plugs were dried by heating them at 80°C for a week. Different procedure was followed to prepare cores with different initial brine saturations.

##### ***6.3.4.1. Zero Initial Water Saturation***

Dried cores were weighed and placed inside a vacuum flask with a three-way valve connection. The vacuum connection was opened, and the cores were vacuumed for a day. The valve was switched to an oil reservoir following the vacuum operation and closed once all the cores were submerged in oil. The cores were weighed again to obtain the pore volume and porosity ( $\phi$ ) values. Following the oil saturation step, the cores were aged by keeping them inside oil at 70°C for 2 weeks.

##### ***6.3.4.2. Low Initial Water Saturation (10% – 20%)***

Dried cores were weighed and vacuumed as mentioned in the previous section. Following the vacuum operation, the cores were saturated with brine by switching the valve to a brine reservoir. The cores were taken out and weighed to obtain the pore volume and porosity. These cores were then centrifuged in a Beckman ultracentrifuge (Model L8-80M) by first placing them in appropriate core holders. The core holders allow displacement of the water phase by air or oil. In this mode of preparation, brine was allowed to drain by centrifuging at 7000 rpm for 1 day. After 1 day, the cores were reversed and centrifuged

again to ensure uniform fluid distribution. The cores were weighed after the centrifuge step to measure the residual water saturation. These cores were then placed in the vacuum flasks again and oil saturation was performed following the steps mentioned in the previous section. The procedure generated cores with initial water saturation in the range of 13% - 20%. Cores were aged by keeping them immersed in oil at 70°C for 2 weeks.

#### **6.3.4.3. Moderate to High Initial Water Saturation (30% - 50%)**

Cores were first saturated with brine as mentioned in the previous section. The cores were then placed in the centrifuge and the brine was displaced with oil by centrifuging at 7000 rpm for 1 day. The process was repeated with the core direction switched to ensure uniform distribution of fluids. Higher initial water saturations of 30%-45% were generated using this process. The cores were aged in a similar manner as before.

Following the ageing process, the cores were placed inside custom-made imbibition cells and filled with surfactant solutions. Imbibition tests were performed, and oil recoveries were reported at different temperatures for different surfactant systems.

## **6.4. RESULTS AND DISCUSSIONS**

### **6.4.1. Aqueous Stability and Cloud Point Measurements**

Cloud point measurements for SAE-9 and SAE-15 surfactants with different co-surfactants are shown in Figs. 6.1a and 6.1b. The brine salinity used for these measurements were 12% NaCl and 0.2% CaCl<sub>2</sub>. The concentration of the primary surfactants – SAE-9 and SAE-15 were kept constant at 4000 ppm. Co-surfactant concentrations of 2000 ppm and 4000 ppm were used to observe the effect on cloud point. The co-surfactants raise the cloud point of the primary surfactants and the increase is higher at a higher co-surfactant concentration. The increase in cloud point is attributed to a delay

in phase separation of surfactant aggregates because of the presence of charged groups. Both surfactant and co-surfactant structure also influence the extent of increase in cloud point. Medium molecular weight, MM, gives the maximum increase for both SAE-9 and SAE-15. While high molecular weight co-surfactant, HM, increases the cloud point of SAE-15 significantly, it performs poorly for SAE-9. Based on the cloud point values, selected surfactant systems were subsequently evaluated in wettability alteration, adsorption and spontaneous imbibition experiments.

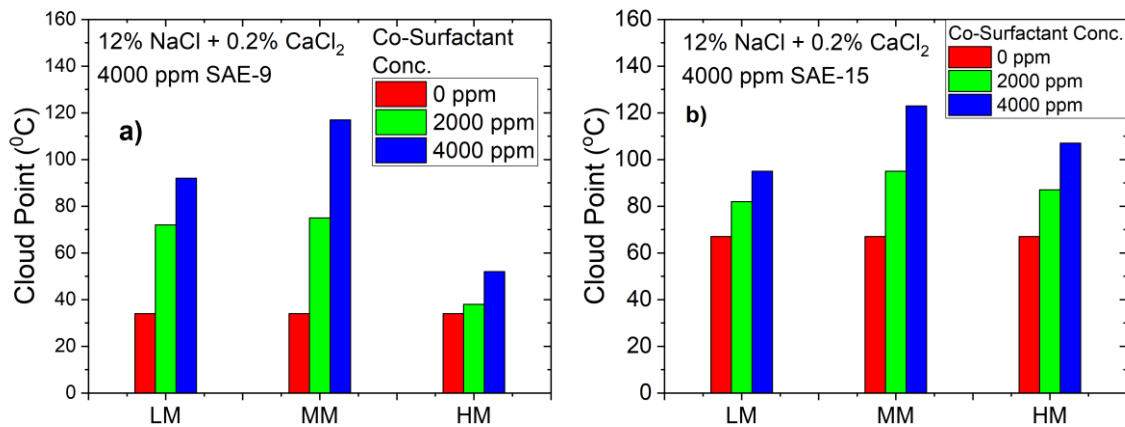


Figure 6.1. Cloud point values for a) SAE-9 and b) SAE-15 with co-surfactants

#### 6.4.2. O/W IFT Measurements

O/W IFT values for the surfactants, measured using the pendent drop technique, are shown in Figs. 6.2a and 6.2b. Brine salinity and surfactant concentrations as mentioned in the previous section were used for these measurements. The temperatures were varied between 50°C and 90°C whenever allowed by the system cloud points. IFT values for single and mixed SAE-9 systems varied between 0.7 – 1 mN/m. For SAE-15 systems IFTs were between 0.7 – 1.4 mN/m. The high IFT values compared to the ultralow IFT regime

(IFT <math>10^{-3}</math> mN/m) eliminates the possibility of wettability alteration through a spontaneous emulsification mechanism. No universal correlation between concentration of co-surfactants and IFT values can be observed from the plot. However, a higher temperature is typically associated with lower IFT values, particularly for SAE-15 systems.

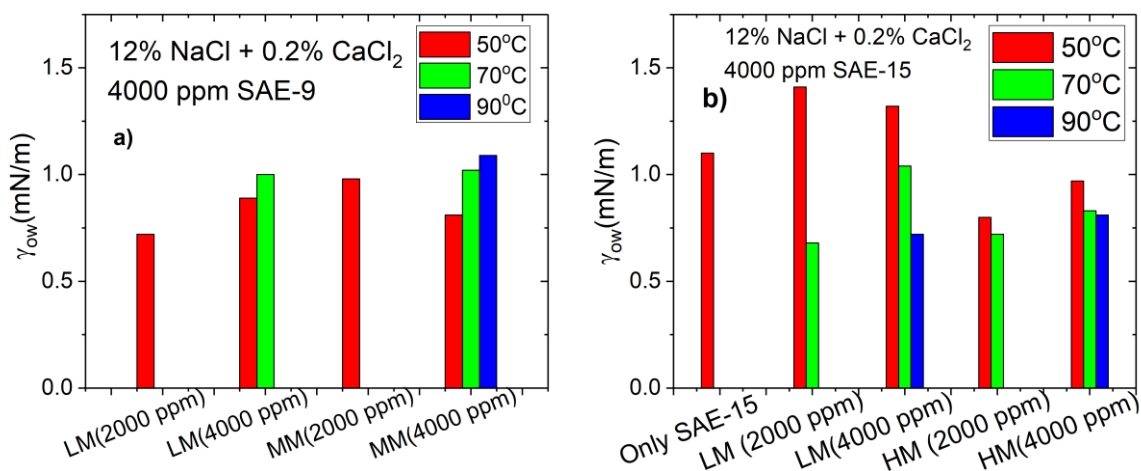


Figure 6.2. Oil/Surfactant IFT values for a) SAE-9 and b) SAE-15 + Co-surfactants

### 6.4.3. Contact Angle Measurements

Contact angle measurements were performed on calcite surfaces to evaluate wettability alteration using surfactant systems. The surfactant concentrations and temperatures used were same as those used for IFT measurements. Figure 6.3a shows the final contact angle of aged oil drop on calcite when the system was placed in just brine of 12% NaCl and 0.2% CaCl<sub>2</sub>. In this case the contact angle is around 160° implying no wettability alteration. Similar behavior is also observed for solutions containing just the co-surfactants as shown in Fig. 3b. Contact angles corresponding to SAE-9 + LM (4000 ppm: 4000 ppm) and SAE-15 + LM (4000 ppm: 4000 ppm) are shown in Figs. 6.3c and



6.3d. The addition of primary surfactant causes the oil drop to bead up, which indicates wettability alteration driven by the primary surfactant.

The final contact angles measured through the aqueous phase are plotted for the different surfactant mixtures in Figs. 6.4a and 6.4b. The effect of co-surfactant addition can be clearly seen in the plots. At 50°C, the contact angle for the pure component primary surfactant is the lowest and the addition of co-surfactants increases the contact angle indicating a shift towards lower wettability alteration. This implies that while the co-surfactant doesn't itself affect wettability alteration, it does hinder the performance of the primary surfactant. The effect of surfactant structure can also be studied from the plots – surfactant systems with MM as the co-surfactant exhibit the poorest wettability alteration. Better performances are observed with the smaller sized LM and the larger HM as co-surfactants. Another common trend that is observed from the plots is that the final contact angles always decreased with an increase in temperature. This indicates enhanced wettability alteration at higher temperatures, and this is true for both single and mixed-surfactant systems.<sup>18</sup> The effect of addition of  $\text{SO}_4^{2-}$  is shown for two cases – SAE-15 at 50°C and SAE-15+HM mixture at 90°C. In both these systems the final contact angle is

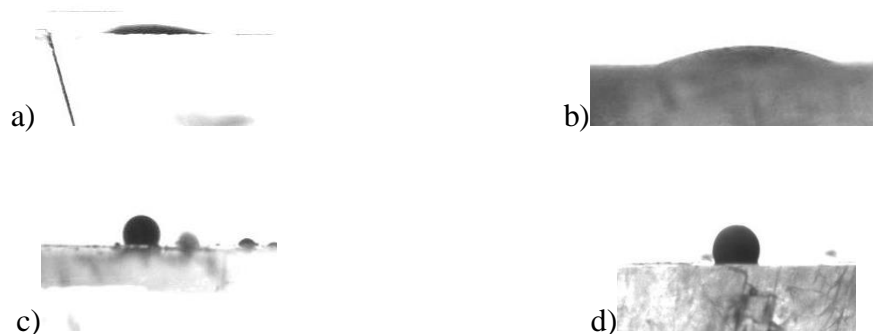


Figure 6.3. Final contact angles for a) Brine and b) 4000 ppm LM c) SAE-9 + LM (4000 ppm:4000 ppm) and d) SAE-15 +LM (4000 ppm: 4000 ppm) at 70°C

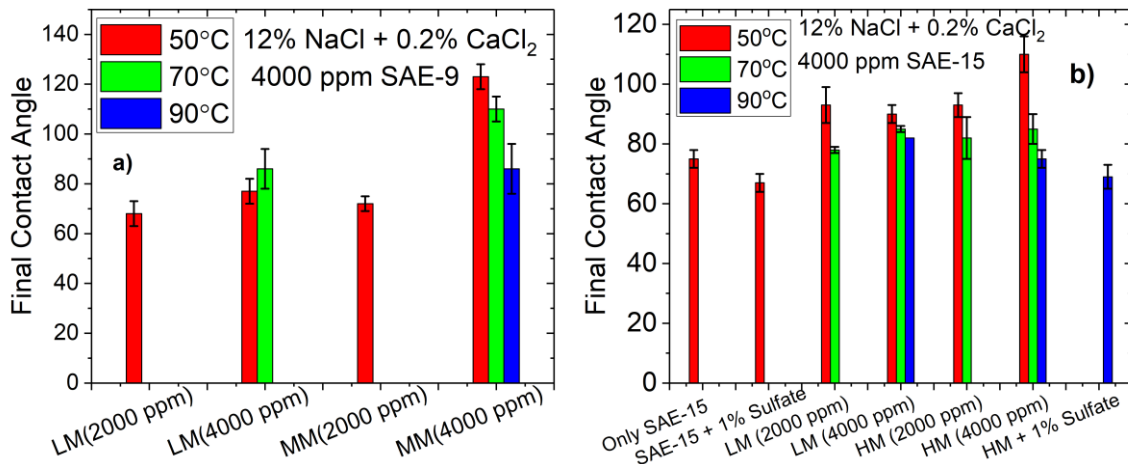


Figure 6.4. Bar plots showing final contact angles in mixed surfactant systems containing a) SAE-9 and b) SAE-15. Initial contact angles are typically between 160°-170°.

less than the one in which there is no  $\text{SO}_4^{2-}$ , highlighting the enhanced wettability alteration effect of  $\text{SO}_4^{2-}$ .

#### 6.4.4. Capillary Driving Force

The O/W IFT and the contact angle values together can be used to generate the capillary force that is necessary to drive spontaneous imbibition of the aqueous phase. Figures 6.5a and 6.5b show this driving force for SAE-9 and SAE-15 systems as a function of their CPTDs. The reason for doing so is to normalize the difference in cloud points of different surfactant solutions and get a more meaningful comparison between the single and mixed-surfactant systems. Besides, CPTD has been found to be a thermodynamic parameter that is closely associated with wettability alteration and surfactant adsorption in the past.<sup>43</sup> The colored circles in Figures 6.5b represent the single component systems. The open symbols are for mixed systems with equal mass composition of surfactant and co-surfactant whereas the closed non-circular symbols are for systems with 2:1 composition

of surfactant to co-surfactant by mass. The concentration of primary surfactant was fixed at 4000 ppm. It can be seen from the plots that single component systems exhibit a positive driving force between 0.1 to 0.3 mN/m. The driving force reduces upon addition of co-surfactant and this decrease is because of both the decrease in O/W IFT and increase in contact angle for the mixed systems. Once again, the effect of co-surfactant structure can be seen from the plots. For both SAE-9+LM and SAE-15+LM systems, the driving force reduces at a low rate with respect to CPTD. However, a steeper decrease in driving force is observed for the MM systems. The rate then decreases once again for the SAE-15+HM systems. A successful spontaneous imbibition necessitates the presence of a positive driving force as shown by the dotted line in Figures 6.5a and 6.5b. This is exhibited mainly for the SAE-9+LM, SAE-15, SAE-15+LM and SAE-15+HM systems and these systems were picked for spontaneous imbibition experiments.

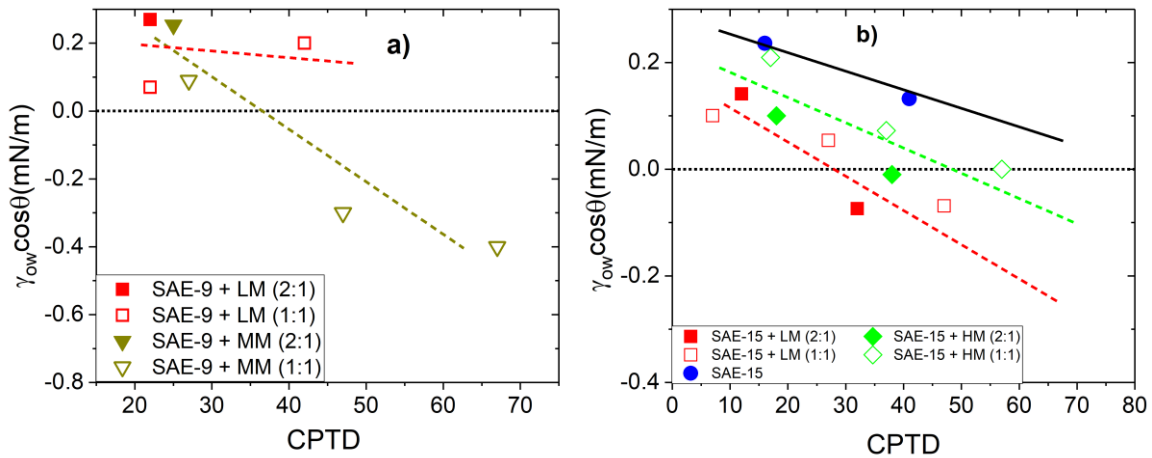


Figure 6.5. Capillary driving force for a) SAE-9 and b) SAE-15 containing systems

### 6.4.5. Adsorption Experiments

The systems of SAE-15, SAE-15+LM, and SAE-15+HM have been analyzed for adsorption in the past. Figures 6.6a-c show adsorption isotherms for SAE-15, SAE-15+LM and SAE-15+HM at different temperatures. A maximum adsorption of around 0.7 mg/gm

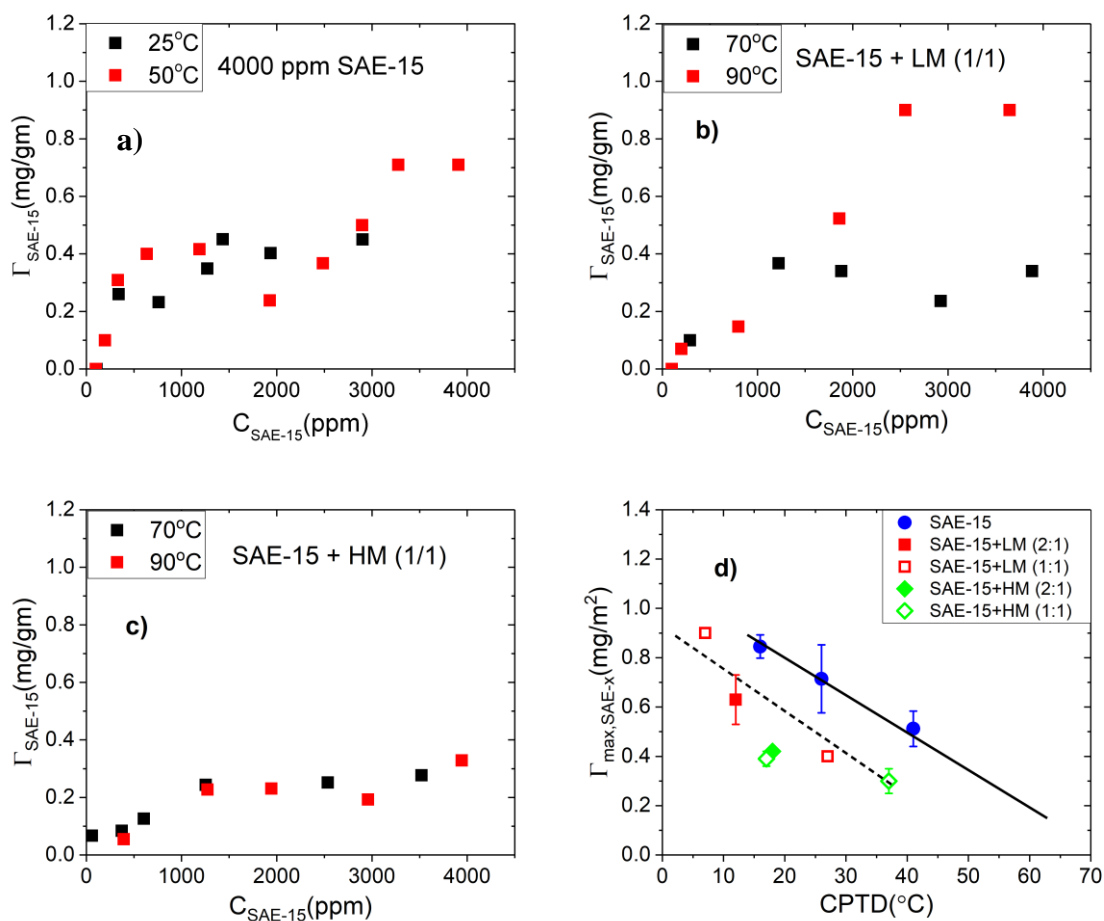


Figure 6.6. Adsorption of SAE-15 at different temperatures for a) single surfactant and mixed-systems with b) 1/1 mixture (by mass) with LM and c) 1/1 mixture (by mass) with HM. d) Maximum adsorption of SAE-15 as a function of system CPTD

was observed for SAE-15 at 50°C. Mixed surfactant adsorptions were carried out at both 70°C and 90°C. Both systems exhibited an increase in adsorption with temperature; however, the increase was more prominent for SAE-15+LM systems. The maximum

adsorptions of the primary component SAE-15 in SAE-15+LM were 0.3 mg/gm and 0.9 mg/gm at 70°C and 90°C, respectively. For the SAE-15+HM system these values were 0.3 mg/gm and 0.35 mg/gm, respectively. The maximum adsorption,  $\Gamma_{\max, \text{SAE-x}}$ , of SAE-15 in both single and mixed systems can be plotted against the CPTD to understand the effect of co-surfactant addition. This plot is shown in Fig. 6.6d and mixed systems exhibit reduced adsorption at the same CPTD values. The behavior is identical to capillary driving force trends for single and mixed systems.

#### 6.4.6. Spontaneous Imbibition Experiments

Indiana limestone cores saturated with different initial oil saturations were used for spontaneous imbibition experiments. The importance of the ageing process for carbonate cores have been discussed in previous works where it was found that strongly adsorbing surface-active molecules tend to coat the outer core surface, giving rise to inaccurate oil-wetness and preventing imbibition of nonionic surfactant solutions.<sup>34</sup> To check if this was the case for the current work or not, one drop each of brine and SAE-15 solution was placed on the outer surface of an aged limestone core and the state of the drops was observed over time. Figures 6.7a and 6.7b show the initial and final drop states for the case of brine. Figures 6.7c and 6.7d are for the SAE-15 drop. For brine, an initial contact angle of around 90° was observed which remained constant over time with no change in the drop size or state. For SAE-15, an initial contact angle of 160° was observed and within four minutes, the drop completely seeped inside the core. These observations together indicate that while the outer core surface is oil-wet, it still allows imbibition of the surfactant solutions.

Table 6.3 lists the core properties, experimental conditions, and the results of different spontaneous imbibition experiments. Brine solutions were first used at three different water saturations and only about 2 – 4% of OOIP was recovered as shown in Fig.

6.8a. The typical observation during the surfactant-enhanced oil recovery process is shown in Fig. 6.8b. Clear separation was observed between the aqueous and oleic phases indicating the absence of any emulsification. Oil drops were mostly generated from the top

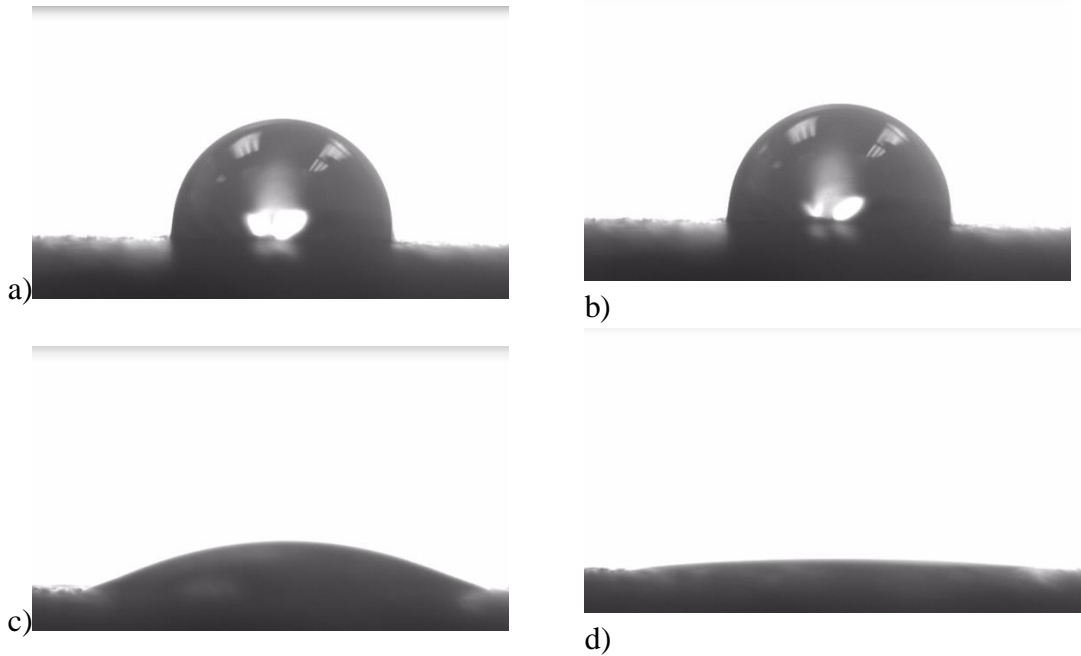


Figure 6.7. a) Initial and b) final contact angles of brine on outer surface of oil-aged Indiana limestone. c) Initial and d) final contact angles corresponding to 4000 ppm SAE-15

of the core and collected at the top of the cell. This indicates that oil recovery in these cases was dominated by buoyancy-driven imbibition mechanism. Figure 6.9a shows the oil recovery profiles for SAE-15 at 50°C. These imbibition experiments were performed at three different initial water saturations ( $S_{wi}$ ). For 100% oil saturated core, about 36% of OOIP was recovered. The oil recovery increased to 47% when  $S_{wi}$  was increased to 10%. In both these cases most of the oil recovery was obtained within 20 days of the start of experiment. At a high  $S_{wi}$  of 42% only 12% recovery was observed. It took about 10 days to reach the final oil recovery. These findings indicate the importance of initial water

saturation on ultimate oil recoveries. The oil recoveries first increase going from  $S_{wi} = 0$  to  $S_{wi} = 10\%$ . This is because the presence of water-only zones inside the pores, where the surface is still hydrophilic, promotes enhanced imbibition of the aqueous phase compared

Table 6.3. Core properties, experimental conditions, and results for spontaneous imbibition experiments

	$\phi$ (%)	$S_{wi}$ (%)	T(°C)	Surfactants	CP (°C)	IFT (mN/m)	Driving Force (mN/m)	Oil Recovery (% OOIP)
Brine	13.6	0	60	-	-	15.7	-	1.1
	13.8	15	60	-	-	15.7	-	2.2
	14.2	33	80	-	-	17.0	-	4.1
SAE-15	13.8	0	50	SAE-15	67	1.1	0.27	36.4
	14.4	10	50	SAE-15	67	1.1	0.27	47.5
	13.5	42	50	SAE-15	67	1.1	0.27	12.3
	13.4	0	90	SAE-15+LM	95	0.8	0.14	14.0
	14.0	10	90	SAE-15+HM	108	0.7	0.21	26.0
	14.2	20	90	SAE-15+LM	95	0.8	0.14	25.1
	14.0	17	50	SAE-15+1%SO <sub>4</sub> <sup>2-</sup>	62	17.0	0.30	57.1
	13.9	17	90	SAE-15+HM +1%SO <sub>4</sub> <sup>2-</sup>	100	0.7	0.24	29.0
SAE-9	13.6	37	50	SAE-9+LM	90	0.8	0.20	10.0
	14.8	20	50	SAE-9+LM	90	0.8	0.20	21.5
	14.1	18	90	SAE-9+MM	120	1.1	0.09	18.3

to cores where water is initially absent. The low oil recoveries at high water saturations, on the other hand, correspond to poor mobility of the oil phase because of disconnected oil zones and subsequent oil trapping.

In order to perform these experiments at an elevated temperature of 90°C, co-surfactants LM and HM were added to SAE-15. All formulations consisted of 4000 ppm SAE-15 and 4000 ppm co-surfactant. Oil recovery curves corresponding to three different systems – SAE-15+LM at  $S_{wi} = 0$ ,  $S_{wi} = 20\%$  and SAE-15+HM at  $S_{wi} = 10\%$ , are shown in

Fig. 6.9b. The maximum oil recovery at zero initial water saturation was 15% and at low initial water saturation they were about 25% and 26% for the SAE-15+LM and SAE-15+HM system, respectively. These oil recoveries are lower than those observed for single-component surfactant SAE-15 at 50°C and the decrease can be attributed to the lowering

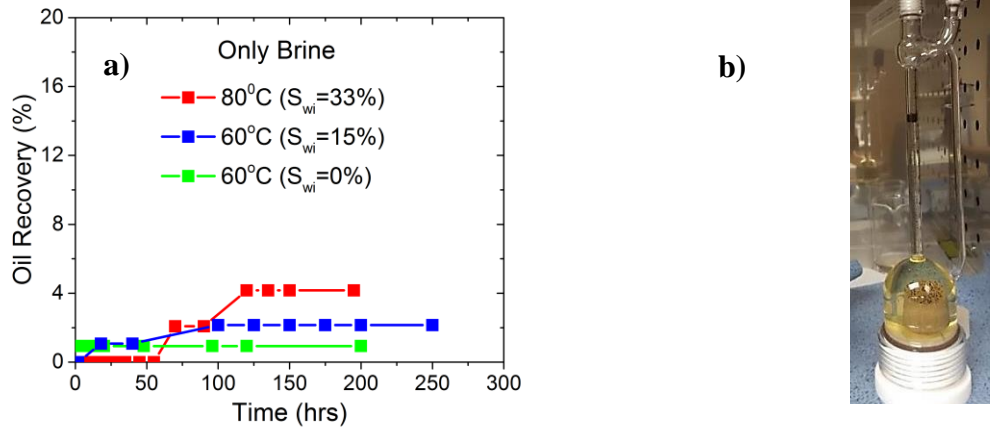


Figure 6.8. a) Oil recovery plots for brine solutions. b) Typical oil recoveries in the presence of surfactants. Oil is generated mostly from the top surface of the core.

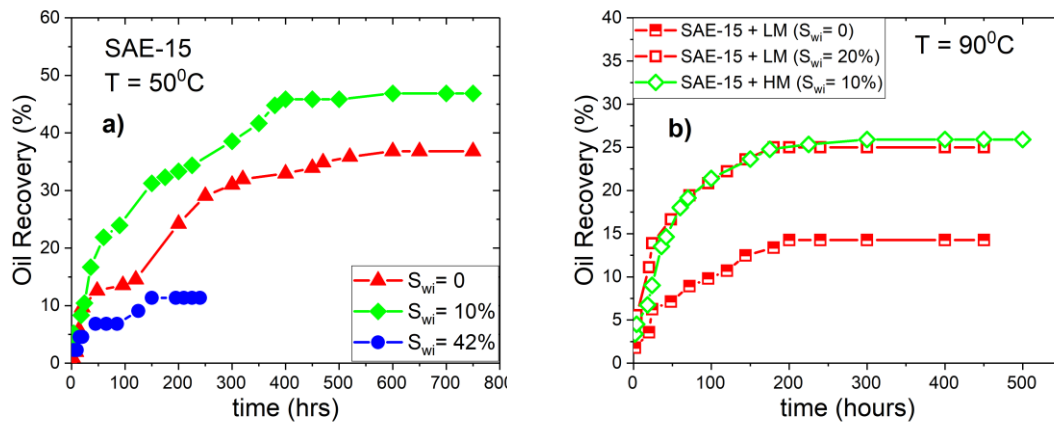


Figure 6.9. Oil recovery plots for a) single SAE-15 at 50°C and b) mixed systems containing SAE-15 and co-surfactants at 90°C



of capillary driving force in mixed systems as discussed previously. The effect of capillary driving force on ultimate oil recoveries is discussed later.

Imbibition experiments were also performed for SAE-9 with co-surfactants LM and HM. Like in the previous case, all surfactant concentrations were fixed at 4000 ppm. The oil recovery plots are shown in Fig. 6.10. At 50°C, the maximum oil recoveries were 22% and 10% for low and high initial water saturations, respectively. These oil recoveries took place within a week. The SAE-9+MM mixture was used at 90°C with a core with  $S_{wi}=18\%$  and an oil recovery of 17% was observed in this case.

The effect of brine salinity on oil recoveries from spontaneous imbibition was also studied. Figure 6.11 shows the oil recoveries for surfactant solutions in a brine of 12% NaCl, 0.2% CaCl<sub>2</sub> and 1% SO<sub>4</sub><sup>2-</sup>. The two surfactant systems are SAE-15 at 50°C and SAE-15+HM at 90°C. The initial water saturation in both the cases was 17%. The ultimate oil recovery for SAE-15 with 1% SO<sub>4</sub><sup>2-</sup> at 50°C was about 57% which was 10% more than the oil recovery for SAE-15 alone. Similarly, addition of 1% SO<sub>4</sub><sup>2-</sup> in SAE-15+HM at 90°C gave an additional oil recovery of 3%. This indicates the positive effect of divalent ions like SO<sub>4</sub><sup>2-</sup> on wettability alteration and imbibition-driven oil recovery.

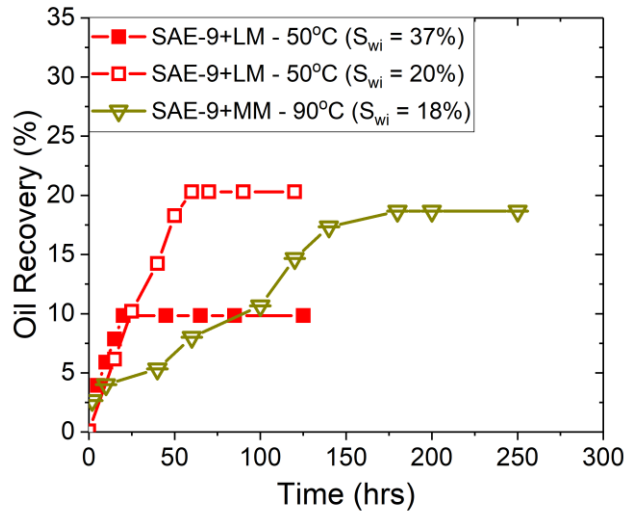


Figure 6.10. Oil recovery plots for system containing SAE-9 and co-surfactants at 50°C and 90°C.

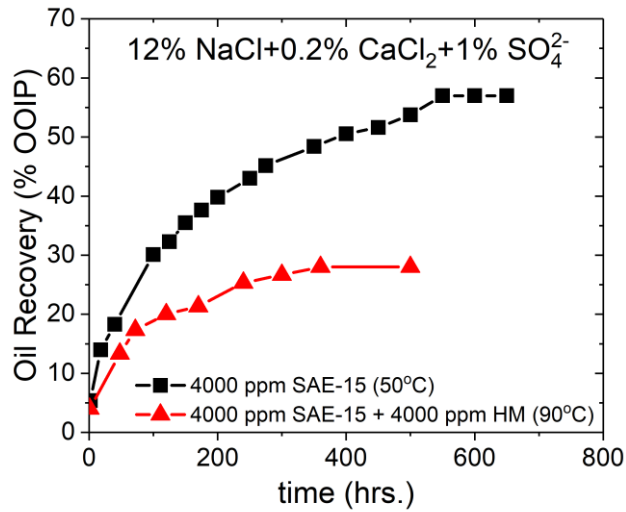


Figure 6.11. Oil recovery plots for systems containing 1%  $\text{SO}_4^{2-}$ .

Multiple scaling laws have been proposed in the past to scale imbibition rate from laboratory to reservoir scale.<sup>40-42</sup> These are dependent based on whether the imbibition is

driven by gravity or capillary forces. The dominant mechanism for imbibition can be obtained by measuring the inverse of Bond number,  $N_B^{-1}$ :

$$N_B^{-1} = C \frac{\sqrt{\frac{\phi}{k}} \gamma_{ow}}{\Delta \rho g L}, \quad (3)$$

where  $\Delta \rho$  is the density difference between the two phases,  $k$  is the permeability,  $g$  is the acceleration due to gravity and  $L$  is a characteristic length.  $C$  is a dimensionless constant which has a value of 0.4 for capillary tube model.  $N_B^{-1}$  gives the ratio of gravity and capillary forces in the system.  $N_B^{-1} > 5$  imply capillary force-dominated recovery whereas values  $< 0.1$  imply a gravity dominated process. Intermediate values suggest that both forces govern the imbibition.<sup>45</sup>  $N_B^{-1}$  for the current system of surfactants and cores were between 0.7 - 2 implying that imbibition process consists of both mechanisms but mostly dominated by gravity forces. This was confirmed from the fact that most of the oil was produced from the top surface of the core. Based on the values of  $N_B^{-1}$ , two different time-scalings are attempted – one for systems where capillary forces are reasonably high to use the time-scaling developed for moderate to high IFT systems,<sup>42</sup>

$$t_{d,cap} = t \frac{\gamma_{ow}}{\sqrt{\mu_o \mu_w} L_c^2} \sqrt{\frac{k}{\phi}}, \quad (4)$$

and the other which is developed for systems dominated by gravity,<sup>41</sup>

$$t_{d,gravity} = t \frac{k \Delta \rho g}{L_c \mu_o}, \quad (5)$$

where  $t_d$  is the dimensionless time,  $t$  is time,  $\mu_o$  and  $\mu_w$  are oil and water viscosities and  $L_c$  is a characteristic length for imbibition process. (4) has been modified accordingly with the contact angle to consider the effect of wettability alteration in the current study. (4) is thus rewritten as

$$t_{d,cap} = t \frac{\gamma_{ow} \cos \theta}{\sqrt{\mu_o \mu_w} L_c^2} \sqrt{\frac{k}{\phi}}, \quad (6)$$

where  $\cos \theta$  is the final contact angle in a particular system. For the current study, the only variables are driving force and viscosities. The dimensionless oil recovery plots are shown in Figs. 6.12a and 6.12b. It can be seen that a better collapse of the dimensionless recoveries is obtained when the time-scaling based on gravity as the dominant mechanism, is used. This is not surprising considering the values of  $N_B^{-1}$ .

Figure 6.13 shows the ultimate oil recoveries as a function of initial water saturations for the different systems studied. As discussed before, a trend of maximum oil recovery at an optimum low initial water saturation is observed in the spontaneous imbibition experiments. It can also be seen that mixed surfactant systems have lower oil recoveries than the single surfactant ones. The fact that these mixed systems have a lower driving force indicates there is a correlation between the capillary force and the oil recoveries. Any attempt at a universal prediction of oil recoveries, hence, must take this

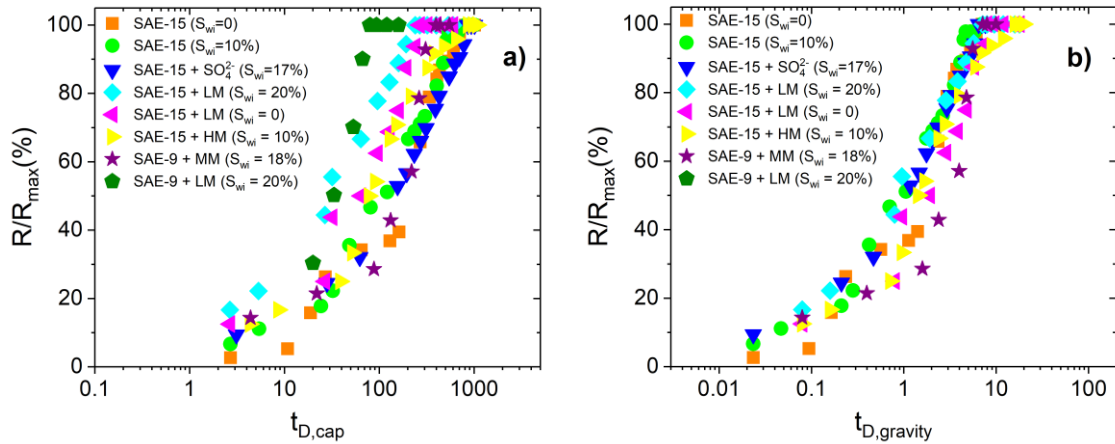


Figure 6.12. Plot of fractional oil recovery vs dimensionless time for different spontaneous imbibition experiments

capillary force into account. Also, as mentioned previously, wettability alteration and capillary driving force can be correlated to CPTD.<sup>43, 46</sup> Figure 6.14a plots the maximum oil

recovery at similar initial water saturations versus the system CPTD. Qualitatively, oil recoveries increase as the system moves near the cloud point. The offset observed before in Fig. 6.7 also appears in this plot in the form of lower oil recoveries for the mixed systems.

A common linear behavior however appears when the rescaled oil recovery,  $R_m = \frac{R\gamma_o}{\gamma_{ow} \cos \theta}$  is plotted against CPTD at similar initial water saturations. Here  $\gamma_o$  is the oil-brine IFT at a given temperature. This plot is shown in Fig. 6.14b and it highlights the universality of the parameter CPTD in determining wettability alteration for different surfactant systems. Figures 6.7 and 6.14 together can serve as a critical tool to predict oil recoveries by surfactant-based wettability alteration.

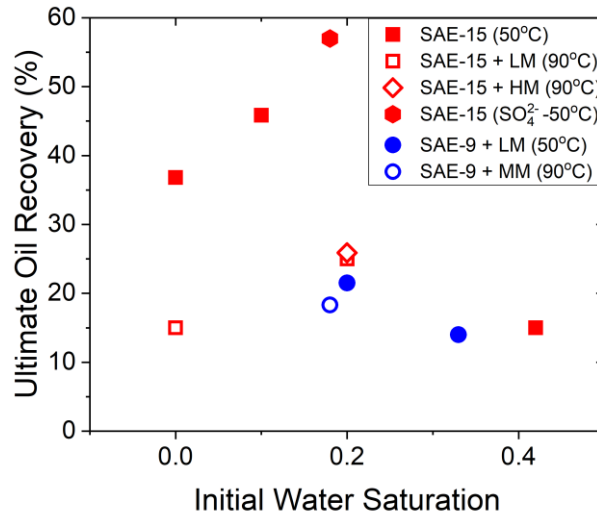


Figure 6.13. Ultimate oil recoveries as a function of initial water saturations

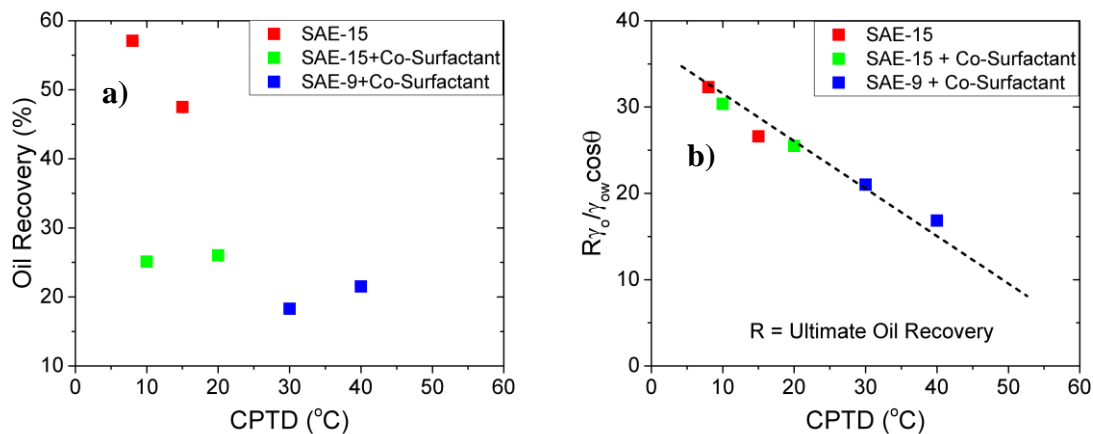


Figure 6.14. a) Maximum oil recoveries plotted against system CPTD for different single and mixed-surfactant systems. b) Ultimate oil recoveries rescaled by capillary driving force plotted against CPTD. The dotted line is a guide for the eye only.

## 6.5. CONCLUSIONS

Surfactant formulations from the family of nonionic secondary alcohol ethoxylates were evaluated for wettability alteration and oil recovery from oil-wet carbonate surfaces. Contact angle and O/W IFT measurements were performed to derive the capillary driving forces responsible for imbibition-driven recovery processes. Anionic co-surfactants were added to form mixed surfactants with enhanced aqueous stabilities to raise the operating temperatures beyond the cloud point of the nonionic surfactants. The effect of the addition of co-surfactant was also analyzed in terms of wettability alteration and it was found that these mixed systems exhibit a decreased driving force compared to the single surfactant ones. When plotted against the thermodynamic parameter CPTD, a decreased driving force was observed for the mixed systems. Similar behavior was also observed when adsorption of SAE-15 was measured in these systems. Both driving force and adsorption were correlated to CPTD – better wettability alteration and higher adsorption as a system moves

towards the cloud point. Spontaneous imbibition measurements were performed to observe the effect of wettability alteration in oil-wet Indiana limestone cores.

Surfactant mediated imbibition resulted in additional oil recoveries over brine and the extent of oil recovery was determined by the surfactant type, initial water saturation, and brine salinity. A maximum oil recovery of 47% was observed for SAE-15 while with co-surfactant a maximum oil recovery of 27% was observed. The maximum recoveries were typically observed at a low initial water saturation of 10-20%. There was a steady drop in oil recovery as the initial water saturation was increased indicating an optimum range of saturations which correspond to high oil recovery. Addition of  $\text{SO}_4^{2-}$  in the brine had a positive effect on the oil recovery – approximately 10% and 3% incremental oil recovery was observed at 1%  $\text{SO}_4^{2-}$  concentrations for single and mixed systems, respectively.

Oil recovery rates scaled by a modified dimensionless time exhibit reasonable collapse in a universal rate curve and this can be used for reservoir scale estimations. The ultimate oil recoveries when scaled by the system driving force generate a universal oil recovery curve versus the initial water saturation and CPTD. With the information on driving force these curves can be used to predict oil recoveries for similar systems.

## REFERENCES

1. Schlumberger Market Analysis, **2007**.
2. Buckley, J. S., Liu, Y., & Monsterleet, S. Mechanisms of wetting alteration by crude oils. *SPE journal*, 1998, 3(01), 54-61.
3. Al-Maamari, R. S., & Buckley, J. S. Asphaltene precipitation and alteration of wetting: the potential for wettability changes during oil production. *SPE Reservoir Evaluation & Engineering*, 2003, 6(04), 210-214.
4. Maerker, J.M. and Gale, W.W., 1992. Surfactant flood process design for Loudon. *SPE reservoir engineering*, 7(01), pp.36-44.
5. Bragg, J.R., Gale, W.W., McElhannon Jr, W.A., Davenport, O.W., Petrichuk, M.D. and Ashcraft, T.L., 1982, January. Loudon surfactant flood pilot test. In SPE Enhanced Oil Recovery Symposium. Society of Petroleum Engineers.
6. Liu, S., Zhang, D., Yan, W., Puerto, M., Hirasaki, G.J. and Miller, C.A., 2008. Favorable attributes of alkaline-surfactant-polymer flooding. *SPE Journal*, 13(01), pp.5-16.
7. Zerpa, L.E., Queipo, N.V., Pintos, S. and Salager, J.L., 2005. An optimization methodology of alkaline-surfactant-polymer flooding processes using field scale numerical simulation and multiple surrogates. *Journal of Petroleum Science and Engineering*, 47(3-4), pp.197-208.
8. Vargo, J., Turner, J., Vergnani, B., Pitts, M.J., Wyatt, K., Surkalo, H. and Patterson, D., 1999, January. Alkaline-surfactant-polymer flooding of the Cambridge Minnelusa field. In *SPE Rocky Mountain Regional Meeting*. Society of Petroleum Engineers.
9. Delshad, M., Bhuyan, D., Pope, G.A. and Lake, L.W., 1986, January. Effect of capillary number on the residual saturation of a three-phase micellar solution. In *SPE enhanced oil recovery symposium*. Society of Petroleum Engineers.
10. Lake, L.W., 1989. Enhanced oil recovery.
11. Hirasaki, G.J., Miller, C.A. and Puerto, M., 2008, January. Recent advances in surfactant EOR. In *SPE Annual Technical Conference and Exhibition*. Society of Petroleum Engineers.
12. Strand, S., Standnes, D. C., & Austad, T. Spontaneous imbibition of aqueous surfactant solutions into neutral to oil-wet carbonate cores: Effects of brine salinity and composition. *Energy & fuels*, 2003, 17(5), 1133-1144.



13. Standnes, D. C., & Austad, T. Wettability alteration in carbonates: Interaction between cationic surfactant and carboxylates as a key factor in wettability alteration from oil-wet to water-wet conditions. *Colloids and Surfaces A: Physicochemical and Engineering Aspects*, 2003, 216(1-3), 243-259.
14. Austad, T., & Standnes, D. C. Spontaneous imbibition of water into oil-wet carbonates. *Journal of Petroleum Science and Engineering*, 2003, 39(3-4), 363-376.
15. Somasundaran, P. and Zhang, L., 2006. Adsorption of surfactants on minerals for wettability control in improved oil recovery processes. *Journal of Petroleum Science and Engineering*, 52(1-4), pp.198-212.
16. Seethepalli, A., Adibhatla, B., & Mohanty, K. K. Wettability alteration during surfactant flooding of carbonate reservoirs. In *SPE/DOE Symposium on Improved Oil Recovery*. Society of Petroleum Engineers, **2004**.
17. Salehi, M., Johnson, S.J. and Liang, J.T., 2008. Mechanistic study of wettability alteration using surfactants with applications in naturally fractured reservoirs. *Langmuir*, 24(24), pp.14099-14107.
18. Das, S., Nguyen, Q., Patil, P.D., Yu, W. and Bonnecaze, R.T., 2018. Wettability alteration of calcite by nonionic surfactants. *Langmuir*, 34(36), pp.10650-10658.
19. Hirasaki, G. and Zhang, D.L., 2004. Surface chemistry of oil recovery from fractured, oil-wet, carbonate formations. *Spe Journal*, 9(02), pp.151-162.
20. Zhang, J., Nguyen, Q. P., Flaaten, A., & Pope, G. A. Mechanisms of enhanced natural imbibition with novel chemicals. *SPE reservoir evaluation & engineering*, **2009**, 12(06), 912-920.
21. Chen, P. and Mohanty, K.K., 2015, April. Surfactant-enhanced oil recovery from fractured oil-wet carbonates: effects of low ift and wettability alteration. In *SPE International Symposium on Oilfield Chemistry*. Society of Petroleum Engineers.
22. Alvarez, J.O., Neog, A., Jais, A. and Schechter, D.S., 2014, April. Impact of surfactants for wettability alteration in stimulation fluids and the potential for surfactant EOR in unconventional liquid reservoirs. In *SPE Unconventional Resources Conference*. Society of Petroleum Engineers.
23. Jarrahan, K., Seiedi, O., Sheykhani, M., Sefti, M. V., & Ayatollahi, S. Wettability alteration of carbonate rocks by surfactants: a mechanistic study. *Colloids and Surfaces A: Physicochemical and Engineering Aspects*, **2012**, 410, 1-10.
24. Gupta, R., & Mohanty, K. Temperature effects on surfactant-aided imbibition into fractured carbonates. *SPE Journal*, 2010, 15(03), 588-597.

25. Sharma, G., & Mohanty, K. Wettability alteration in high-temperature and high-salinity carbonate reservoirs. *SPE Journal*, 2013, 18(04), 646-655.
26. Standnes, D.C. and Austad, T., 2000. Wettability alteration in chalk: 2. Mechanism for wettability alteration from oil-wet to water-wet using surfactants. *Journal of Petroleum Science and Engineering*, 28(3), pp.123-143.
27. Austad, T., Shariatpanahi, S.F., Strand, S., Black, C.J.J. and Webb, K.J., 2011. Conditions for a low-salinity enhanced oil recovery (EOR) effect in carbonate oil reservoirs. *Energy & fuels*, 26(1), pp.569-575.
28. Yousef, A.A., Al-Saleh, S.H., Al-Kaabi, A. and Al-Jawfi, M.S., 2011. Laboratory investigation of the impact of injection-water salinity and ionic content on oil recovery from carbonate reservoirs. *SPE Reservoir Evaluation & Engineering*, 14(05), pp.578-593.
29. Strand, S., Standnes, D.C. and Austad, T., 2003. Spontaneous imbibition of aqueous surfactant solutions into neutral to oil-wet carbonate cores: Effects of brine salinity and composition. *Energy & fuels*, 17(5), pp.1133-1144.
30. Hognesen, E.J., Strand, S. and Austad, T., 2005, January. Waterflooding of preferential oil-wet carbonates: Oil recovery related to reservoir temperature and brine composition. In *SPE Europec/EAGE Annual Conference*. Society of Petroleum Engineers.
31. Yousef, A.A., Al-Saleh, S. and Al-Jawfi, M.S., 2012, January. Improved/enhanced oil recovery from carbonate reservoirs by tuning injection water salinity and ionic content. In *SPE Improved Oil Recovery Symposium*. Society of Petroleum Engineers.
32. Zhang, P., Tweheyo, M.T. and Austad, T., 2006. Wettability alteration and improved oil recovery in chalk: The effect of calcium in the presence of sulfate. *Energy & fuels*, 20(5), pp.2056-2062.
33. Zhang, P. and Austad, T., 2006. Wettability and oil recovery from carbonates: Effects of temperature and potential determining ions. *Colloids and Surfaces A: Physicochemical and Engineering Aspects*, 279(1-3), pp.179-187.
34. Standnes, D.C. and Austad, T., 2000. Wettability alteration in chalk: 1. Preparation of core material and oil properties. *Journal of Petroleum Science and Engineering*, 28(3), pp.111-121.
35. Zhou, X., Morrow, N.R. and Ma, S., 2000. Interrelationship of wettability, initial water saturation, aging time, and oil recovery by spontaneous imbibition and waterflooding. *SPE Journal*, 5(02), pp.199-207.
36. Hamouda, A. and Karoussi, O., 2008. Effect of temperature, wettability and relative permeability on oil recovery from oil-wet chalk. *Energies*, 1(1), pp.19-34.

37. Standnes, D.C., Nogaret, L.A., Chen, H.L. and Austad, T., 2002. An evaluation of spontaneous imbibition of water into oil-wet carbonate reservoir cores using a nonionic and a cationic surfactant. *Energy & Fuels*, 16(6), pp.1557-1564.
38. Viksund, B.G., Morrow, N.R., Ma, S., Wang, W. and Graue, A., 1998, September. Initial water saturation and oil recovery from chalk and sandstone by spontaneous imbibition. In *Proceedings, 1998 International Symposium of Society of Core Analysts, The Hague*.
39. Zaeri, M.R., Hashemi, R., Shahverdi, H. and Sadeghi, M., 2018. Enhanced oil recovery from carbonate reservoirs by spontaneous imbibition of low salinity water. *Petroleum Science*, 15(3), pp.564-576.
40. Mattax, C.C. and Kyte, J.R., 1962. Imbibition oil recovery from fractured, water-drive reservoir. *Society of Petroleum Engineers Journal*, 2(02), pp.177-184.
41. Cuiec, L., Bourbiaux, B. and Kalaydjian, F., 1994. Oil recovery by imbibition in low-permeability chalk. *SPE Formation Evaluation (Society of Petroleum Engineers);(United States)*, 9(3).
42. Zhang, X., Morrow, N.R. and Ma, S., 1996. Experimental verification of a modified scaling group for spontaneous imbibition. *SPE Reservoir Engineering*, 11(04), pp.280-285.
43. Das, S., Katiyar, A., Rohilla, N., Nguyen, Q., Bonnecaze, R.T., Universal Scaling of Adsorption of Nonionic Surfactants on Carbonates using Cloud Point Temperatures. Under Review
44. Mandal, A., Kar, S. and Kumar, S., 2016. The synergistic effect of a mixed surfactant (Tween 80 and SDBS) on wettability alteration of the oil wet quartz surface. *Journal of Dispersion Science and Technology*, 37(9), pp.1268-1276.
45. Schechter, D.S., Zhou, D. and Orr Jr, F.M., 1994. Low IFT drainage and imbibition. *Journal of Petroleum Science and Engineering*, 11(4), pp.283-300.
46. Das, S., Katiyar, A., Nguyen, Q., Bonnecaze, R.T., Wettability Alteration and Adsorption of Mixed Nonionic and Anionic Surfactants on Carbonates. Under Review

## Chapter 7: Concluding Remarks

### 7.1. CONCLUSIONS

This dissertation focused on the study of surfactants which are amphiphilic molecules with surface-active properties. Their ability to modify interfacial properties makes them a critical component in different industrial applications. One such application is in enhanced oil recovery from oil reservoirs where surfactants can alter rock properties from an initial oil-wet to a water-wet state. This change in wettability leads to spontaneous imbibition of aqueous phase and displaces the oil which is eventually recovered. Different aspects of wettability alteration using surfactants were investigated using pore-scale experiments and molecular-level simulations. A high-level summary and discussion on the important findings from the study and their impact are highlighted in the following sections.

#### 7.1.1. Summary

- A simple and effective methodology was developed to evaluate nonionic surfactants for wettability alteration
- The effect of surfactant molecular structure was investigated and several key structure-property relationships were identified
  - At fixed temperatures, surfactants with shorter hydrophilic groups of oxyethylene chains exhibited better wettability alteration
  - The closer the surfactant is to its cloud point, lower is the contact angle implying better wettability alteration
  - Greater adsorption corresponds to a higher wettability alteration
- Surfactants are adsorbed as micellar aggregates onto the surface instead of individual molecules

- Adsorption increases for surfactants with shorter hydrophilic groups
- Anionic hydrotropes raise the cloud point of nonionic surfactants, but lower the wettability alteration and reduce the imbibition driving force.
- Oil recovery obtained from spontaneous imbibition experiments correlates with the imbibition driving force.

### **7.1.2. Wettability alteration by nonionic surfactants on carbonates**

Nonionic surfactants of two distinct groups were evaluated to measure their wettability alteration properties on oil-aged calcite surface. The effect of surfactant hydrophilicity was studied by varying the number of hydrophilic units. It was found that wettability alteration was better for more hydrophobic surfactants and when the temperature was increased. Kinetic analysis of contact angle measurements revealed enhanced wettability alteration rates at higher temperatures. The activation energies or the energy barriers associated with the wettability alteration process were determined and together with a series of qualitative oil-film experiments, a simple conceptual model explaining the mechanism of surfactant action was proposed.

### **7.1.3. Adsorption of nonionic surfactants on carbonates**

Nonionic surfactants alter the wettability of oil-wet carbonate surfaces to a water-wet state. The degree of surfactant adsorption is expected to determine the extent of the wettability alteration. Furthermore, the structure of the hydrophobic and hydrophilic units of the surfactant should affect the degree of adsorption and correlate with the wettability alteration. The adsorption on Indiana limestone was measured for nonionic surfactants with two different types of hydrophobic units and hydrophilic polyethoxylate units ranging from

15 to 40 mers. Measurements were conducted for several surfactant concentrations and temperatures. Adsorption increased with temperature and for surfactants with fewer hydrophilic groups. The adsorption occurs as micelles rather than individual surfactant molecules. An increase in adsorption is observed for the more hydrophobic surfactants at higher temperature and is attributed to the increase in micelle sizes. Adsorption collapses onto a universal curve as a function of the difference between cloud point of the surfactant and system temperature. At the same time wettability alteration was found to have a direct correlation with surfactant adsorption. These findings are critical for judicious selection of nonionic surfactants for analysis and design of wettability alteration for oil reservoirs.

#### **7.1.4. Mixed-surfactant Formulations for Wettability Alteration**

In this chapter mixed-surfactant systems consisting of secondary alcohol ethoxylates (SAE) and anionic cosurfactants are evaluated as wettability alteration agents for enhanced oil recovery. The cloud points of the non-ionic surfactants are raised by the addition of cosurfactants. The oil/water interfacial tension and contact angles of oil on initially oil wet calcite are reported at different temperatures and surfactant compositions. Adsorption experiments are performed for select mixed systems at high temperatures. The extent of the increase in cloud point, changes in the contact angle and adsorption are influenced by co-surfactant structure, concentration and temperature. Mixed surfactant systems were identified which modified the oil-wet surface to water-wet with final contact angles as low as 70°. The adsorption isotherms reveal that these co-surfactants decrease adsorption of primary component (SAE) in mixed systems compared to single surfactant systems. Based on the calculations of molar compositions two different mechanisms of aggregate formation and adsorption are proposed. Like single surfactants, mixed surfactants also exhibited a linear trend in adsorption and wettability alteration with the

thermodynamic descriptor of cloud point temperature difference. These findings are critical to design stable surfactant formulations for wettability alteration in high temperature, high salinity reservoirs.

#### **7.1.5. Molecular dynamics simulations for adsorption of nonionic surfactants on carbonates**

In this chapter the interactions and structure of secondary alcohol ethoxylates with 15 and 40 ethoxylate units in water near a calcite surface are studied. It is found that water binds preferentially to the calcite surface. Prediction of the free energy landscape for surfactant molecules shows that single surfactant molecules do not adsorb because they cannot get close enough to the surface because of the water layer for attractive ethoxylate-calcite or dispersion interactions to be significant. Micelles can adsorb onto the surface even with the intervening water layer because of the integrative effect of the attractive interactions of all the surfactant molecules. Adsorption is found to increase due to the closer proximity of the micelles to the surface due to a weakened water layer at higher temperatures. The free energy well and barrier values are used to estimate surface to bulk partition coefficients for different surfactants and temperatures, and qualitative agreement is found with experimental observations. The combined effect of surfactant-water and surfactant-solid interactions are found to be responsible for an increased adsorption for nonionic surfactants as the system approaches the cloud point.

#### **7.1.6. Spontaneous Imbibition Tests for Wettability Alteration**

Oil recovery tests were performed to evaluate the performance of different single and mixed-surfactant systems. Contact angle and O/W IFT measurements were first used to derive the capillary driving forces necessary for spontaneous imbibition. Oil-wet Indiana limestone cores served as representative porous medium for the spontaneous imbibition

measurements. Surfactant mediated imbibition resulted in additional oil recoveries over brine and the extent of oil recovery was determined by the surfactant type, initial water saturation, and brine salinity. A maximum oil recovery of 47% was observed with SAE-15 while a maximum oil recovery of 27% was observed for mixed surfactant systems. The effect of initial water saturation was also studied, and it was found that there is an optimum water saturation which corresponds to high oil recoveries. The positive effect of  $\text{SO}_4^{2-}$  ions on wettability alteration was also highlighted - approximately 10% incremental oil recovery was observed at 1% sulfate concentration. Different scaling laws were used to obtain universal recovery curves. The time-scaling corresponding to gravity-driven imbibition process gave the best universal behavior. To obtain predictive tools for oil recovery, the ultimate oil recoveries were scaled by system driving force to generate a universal oil recovery curve versus the initial water saturation and CPTD.

## **7.2. SUGGESTED FUTURE WORK**

### **7.2.1. Effect of oil composition on wettability alteration and oil recoveries**

The composition of oil particularly the wettability-altering ingredients like asphaltenes and fatty acids play a key role in determining the initial oil-wetness of a surface.<sup>1-3</sup> This is more important for carbonates where the positively charged carbonate surfaces tend to have a strong affinity towards these polar components. Using model oils with known compositions of polar molecules, a systematic study can be done to determine their effect on final contact angle values and oil recoveries.

### **7.2.2. Effect of brine salinity and composition on wettability alteration**

The importance of brine salinity has already been described in the text by studying the effect of  $\text{SO}_4^{2-}$  ions. Along with  $\text{SO}_4^{2-}$ , other potential-determining ions like  $\text{Ca}^{2+}$ ,  $\text{Mg}^{2+}$



and  $\text{CO}_3^{2-}$  also effect the wettability alteration and this can be investigated.<sup>4-6</sup> While the brine salinity didn't seem to have any significant effect in the current study, recent studies have found that lower brine salinities<sup>7-9</sup> combined with the presence of potential-determining ions can improve wettability alteration.<sup>8</sup> Few studies have reported higher oil recoveries from carbonates with low-salinity injections. Different explanations like change in surface charge<sup>9</sup> and surface dissolution<sup>6</sup> have been provided by different works in the past. The effect of surfactants in such low salinity brine can be investigated by a combination of wettability alteration and adsorption experiments.

### **7.2.3. Effect of different combinations of surfactant chemistries**

The current study investigates two different families of nonionic surfactants on their performance in wettability alteration. In both the cases the hydrophilic groups are repeating ethylene oxide units. Surfactant structure plays a critical role in determining the efficiency as well as the mechanism of wettability alteration. The relative ease in manufacturing and abundance of these surfactants make them quite attractive for large-scale applications. These surfactants also exhibit desirable features like better compatibility with all other surfactants and insensitiveness to electrolytes. As such, it is imperative to investigate other families of nonionic surfactants like amine ethoxylates, acid ethoxylates, alkyl polyglucosides and propoxylated surfactants. Limited studies have been done on some of these families with promising results.<sup>10-13</sup> These surfactants can also be considered as a secondary component in surfactant mixtures to improve the performance of the primary component. Unlike ethoxylated surfactants, sugar-based nonionic surfactants like alkyl polyglucosides exhibit increased solubility with temperature and can be used to promote aqueous stability in a surfactant mixture. Similarly special nonionic surfactants like methyl

ester ethoxylates display a high solubility along with a high interfacial activity – both desirable features when considering a reservoir-based application.

Ionic co-surfactants can also play an important role in imparting synergistic behavior and increasing the efficiency and effectiveness of nonionic surfactants. This is seen in Chapter 4 where the presence of anionic co-surfactants improved the aqueous stability of primary nonionic surfactants. The vast body of available ionic surfactants provides several different possible combinations of surfactant chemistries and this should also be investigated keeping in mind the potential improvements in wettability alteration and oil recovery performances, particularly at high temperatures and salinities. Studies should be done where the co-surfactants actively effect wettability alteration and contribute to the oil recovery. In fact studies done on surfactant mixtures containing both wettability-altering and emulsion forming components have reported a better performance compared to either one of them.<sup>14</sup> The presence of small amount of cationic surfactants can also potentially improve the performance of nonionic surfactants by contributing to desorption of oil by forming ion-pairs. Along with wettability alteration, the adsorption of surfactants should also be investigated to determine their efficiencies. So far, the wettability alteration is found to be directly proportional to amount of surfactant adsorption. In order to optimize surfactant formulations, it is necessary to achieve the desired wettability alteration at lower surfactant adsorptions and different surfactant chemistries need to be evaluated to this end. The shape of adsorbed surfactant aggregates plays a critical role in determining the efficiency – a flattened structure with increased proximity to the substrate is expected to exhibit better performance than a spherical one. Addition of secondary components is known to initiate a transition in the shape of surfactant aggregates and this should be investigated in detail.

#### **7.2.4. Molecular dynamics simulations to study the mechanism of wettability alteration for different oil type and surfactant chemistries**

MD simulations can be used to investigate the atomistic interactions between organic components typically found in crude oil and mineral surfaces. In doing so, a complete picture of the effect of different functional groups in altering the wettability of initially water-wet mineral surfaces can be developed. Some of the works that have been done in this direction have looked into calcite-carboxylate interactions.<sup>15-16</sup> MD simulations can also look into the effect of surfactant on oil-wet mineral surfaces and help understand the mechanism of wettability alteration. Most works on surfactant-solid-oil interactions have focused on ionic surfactants and similar studies can be done for nonionic surfactants also.<sup>17-20</sup>

#### **7.2.5. Implementation of surfactant-based EOR pilots**

The extent of oil recoveries observed in Chapter 6 from spontaneous imbibition tests call for upscaling experiments to the reservoir scale. This can be done both computationally and by establishing pilot plants for surfactant-based EOR. The existing experimental data can be used in simulators like the University of Texas Chemical Simulator (UTCHEM). UTCHEM is a 3D reservoir simulator that can model wettability alteration and spontaneous imbibition during surfactant flooding.<sup>14, 21</sup> Imbibition experiments can be history-matched with simulations to generate unknown parameters essential for reservoir-scale modeling.

In recent years, there have been few studies which have utilized the laboratory-scale knowledge to implement field trials based on wettability alteration.<sup>22-26</sup> Using appropriate surfactant formulations in sandstone and ULR formations, additional oil recoveries have been obtained in the order of 20% - 30%. Because of limited number of

field-trials available for fractured carbonate reservoirs,<sup>28-29</sup> similar pilot tests need to be implemented for carbonate formations also.

## REFERENCES

1. Buckley, J.S., Liu, Y. and Monsterleet, S., 1998. Mechanisms of wetting alteration by crude oils. *SPE journal*, 3(01), pp.54-61.
2. Buckley, J.S., Liu, Y., Xie, X. and Morrow, N.R., 1997. Asphaltenes and crude oil wetting-the effect of oil composition. *SPE journal*, 2(02), pp.107-119.
3. Gomari, K.R. and Hamouda, A.A., 2006. Effect of fatty acids, water composition and pH on the wettability alteration of calcite surface. *Journal of petroleum science and engineering*, 50(2), pp.140-150.
4. Strand, S., Høgnesen, E.J. and Austad, T., 2006. Wettability alteration of carbonates—Effects of potential determining ions ( $\text{Ca}^{2+}$  and  $\text{SO}_4^{2-}$ ) and temperature. *Colloids and Surfaces A: Physicochemical and Engineering Aspects*, 275(1-3), pp.1-10.
5. Zhang, P., Tweheyo, M.T. and Austad, T., 2007. Wettability alteration and improved oil recovery by spontaneous imbibition of seawater into chalk: Impact of the potential determining ions  $\text{Ca}^{2+}$ ,  $\text{Mg}^{2+}$ , and  $\text{SO}_4^{2-}$ . *Colloids and Surfaces A: Physicochemical and Engineering Aspects*, 301(1-3), pp.199-208.
6. Song, J., Zeng, Y., Wang, L., Duan, X., Puerto, M., Chapman, W.G., Biswal, S.L. and Hirasaki, G.J., 2017. Surface complexation modeling of calcite zeta potential measurements in brines with mixed potential determining ions ( $\text{Ca}^{2+}$ ,  $\text{CO}_3^{2-}$ ,  $\text{Mg}^{2+}$ ,  $\text{SO}_4^{2-}$ ) for characterizing carbonate wettability. *Journal of colloid and interface science*, 506, pp.169-179.
7. Romanuka, J., Hofman, J., Ligthelm, D.J., Suijkerbuijk, B., Marcelis, F., Oedai, S., Brussee, N., van der Linde, H., Aksulu, H. and Austad, T., 2012, January. Low salinity EOR in carbonates. In *SPE Improved Oil Recovery Symposium*. Society of Petroleum Engineers.
8. Austad, T., Shariatpanahi, S.F., Strand, S., Black, C.J.J. and Webb, K.J., 2011. Conditions for a low-salinity enhanced oil recovery (EOR) effect in carbonate oil reservoirs. *Energy & fuels*, 26(1), pp.569-575.
9. Mahani, H., Keya, A.L., Berg, S., Bartels, W.B., Nasralla, R. and Rossen, W.R., 2015. Insights into the mechanism of wettability alteration by low-salinity flooding (LSF) in carbonates. *Energy & Fuels*, 29(3), pp.1352-1367.
10. Chen, P. and Mohanty, K.K., 2014, April. Wettability alteration in high temperature carbonate reservoirs. In *SPE Improved Oil Recovery Symposium*. Society of Petroleum Engineers.

11. Standnes, D.C. and Austad, T., 2003. Nontoxic low-cost amines as wettability alteration chemicals in carbonates. *Journal of Petroleum Science and Engineering*, 39(3-4), pp.431-446.
12. Totland, C. and Lewis, R.T., 2016. Mechanism of calcite wettability alteration by alkyl polyglucoside. *Colloids and Surfaces A: Physicochemical and Engineering Aspects*, 488, pp.129-137.
13. Yin, D.Y. and Zhang, X.R., 2013. Evaluation and research on performance of a blend surfactant system of alkyl polyglycoside in carbonate reservoir. *Journal of Petroleum Science and Engineering*, 111, pp.153-158.
14. Chen, P. and Mohanty, K.K., 2015, April. Surfactant-enhanced oil recovery from fractured oil-wet carbonates: effects of low ift and wettability alteration. In *SPE International Symposium on Oilfield Chemistry*. Society of Petroleum Engineers.
15. Ghatee, Mohammad Hadi, Mohammad Mehdi Koleini, and Shahab Ayatollahi. "Molecular dynamics simulation investigation of hexanoic acid adsorption onto calcite () surface." *Fluid Phase Equilibria* 387 (2015): 24-31.
16. Chun, Byeong Jae, et al. "Adsorption of carboxylate on calcium carbonate () surface: Molecular simulation approach." *Colloids and Surfaces A: Physicochemical and Engineering Aspects* 474 (2015): 9-17.
17. Yan, Hui, and Shiling Yuan. "Molecular Dynamics Simulation of the Oil Detachment Process within Silica Nanopores." *The Journal of Physical Chemistry C* 120.5 (2016): 2667-2674.
18. Liu, Qian, et al. "Mechanism of oil detachment from a silica surface in aqueous surfactant solutions: molecular dynamics simulations." *The Journal of Physical Chemistry B* 116.9 (2012): 2867-2875.
19. Li, Xiaofang, et al. "Oil detachment from silica surface modified by carboxy groups in aqueous cetyltriethylammonium bromide solution." *Applied Surface Science* 353 (2015): 1103-1111.
20. Lu, Guiwu, et al. "Molecular dynamics simulation of adsorption of an oil-water-surfactant mixture on calcite surface." *Petroleum Science* 6.1 (2009): 76-81.
21. Delshad, M., Najafabadi, N.F., Anderson, G., Pope, G.A. and Sepehrnoori, K., 2009. Modeling wettability alteration by surfactants in naturally fractured reservoirs. *SPE Reservoir Evaluation & Engineering*, 12(03), pp.361-370.
22. Phan, T., Kazempour, M., Nguyen, D. and Champion, N., 2018, February. Treating Liquid Banking Problem to Increase Shale Gas Wells Productivity. In *SPE*

*International Conference and Exhibition on Formation Damage Control*. Society of Petroleum Engineers.

23. Bidhendi\*, M.M., Kazempour, M., Ibanga, U., Nguyen, D., Arruda, J., Lantz, M. and Mazon, C., 2019, October. A Set of Successful Chemical EOR Trials in Permian Basin: Promising Field and Laboratory Results. In *Unconventional Resources Technology Conference, Denver, Colorado, 22-24 July 2019* (pp. 3498-3520). Unconventional Resources Technology Conference (URTeC); Society of Exploration Geophysicists.
24. Kazempour, M., Kiani, M., Nguyen, D., Salehi, M., Bidhendi, M.M. and Lantz, M., 2018, April. Boosting Oil Recovery in Unconventional Resources Utilizing Wettability Altering Agents: Successful Translation from Laboratory to Field. In *SPE Improved Oil Recovery Conference*. Society of Petroleum Engineers.
25. Kiani\*, M., Hsu, T.P., Roostapour, A., Kazempour, M. and Tudor, E., 2019, October. A Novel Enhanced Oil Recovery Approach to Water Flooding in Saskatchewan's Tight Oil Plays. In *Unconventional Resources Technology Conference, Denver, Colorado, 22-24 July 2019* (pp. 256-270). Unconventional Resources Technology Conference (URTeC); Society of Exploration Geophysicists.
26. Hongyan, C., Wenli, L., Desheng, M., Xinyu, Z., Jian, F., Jianguo, L., Jianfeng, S. and Yi, Z., 2017, March. Experimental Study and Pilot Test of Combined Gel Treatment and Surfactant Imbibition Technology in High Temperature, High Salinity Reservoir. In *SPE Oklahoma City Oil and Gas Symposium*. Society of Petroleum Engineers.
27. Saputra, I.W.R., Park, K.H., Zhang, F., Adel, I.A. and Schechter, D.S., 2019. Surfactant-Assisted Spontaneous Imbibition to Improve Oil Recovery on the Eagle Ford and Wolfcamp Shale Oil Reservoir: Laboratory to Field Analysis. *Energy & Fuels*, 33(8), pp.6904-6920.
28. Cheng, A. and Kwan, J.T., 2012, January. Optimal Injection Design Utilizing Tracer and Simulation in a Surfactant Pilot for a Fractured Carbonate Yates Field. In *SPE Improved Oil Recovery Symposium*. Society of Petroleum Engineers.
29. Pal, M., Tarsauliya, G., Patil, P., Rohilla, N., Mounzer, H., Bacaud, B., Gilani, S.F., Katiyar, A. and Rozwski, P., 2019, April. Dreaming Big “Surfactant Injection in a Giant Offshore Carbonate Field”, From Successful Injection Trials to Pilot Design and Implementation. In *IOR 2019–20th European Symposium on Improved Oil Recovery* (Vol. 2019, No. 1, pp. 1-22). European Association of Geoscientists & Engineers.

## Appendices

### APPENDIX A: PHASE BEHAVIOR

Phase behavior and wettability alteration properties of two additional nonionic surfactants, belonging to different families, were evaluated in this study. The structures of the surfactants are shown in Table A1. Phase behavior of these surfactants at two different brine salinities at 50°C are shown in Fig. A1. The clear solutions indicate the absence of any emulsion formation under these conditions as also shown in the phase behavior table A2. Fig. A2 shows the initial and final contact angles corresponding to these two surfactants at 50°C and brine salinity of 12% NaCl + 0.2% CaCl<sub>2</sub>. The final contact angles are in the range of 130° - 150° indicating very little wettability alteration. Because of this low wettability alteration, they were not considered for further evaluation.

Table A1. Structure and specification of additional nonionic surfactants

Surfactant Name	Specification
BG-10	Alkyl polyglucoside
RW-150	Amine ethoxylate



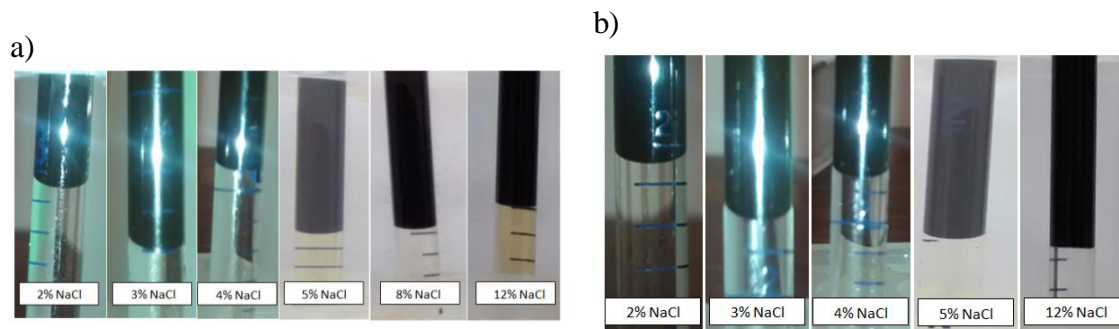


Figure A1. Phase behaviors of a) BG-10 and b) RW-150 at 50°C

Table A2. Phase behavior results - ■ - No microemulsion phase, ■ - Separate microemulsion, ■ - Slight three-phase separation ■ - Wax like deposition

Surfactant	2%	3%	4%	5%	6%		12%	
BG-10	50°C	50°C	50°C	50°C	50°C	80°C	50°C	80°C
RW-150	50°C	50°C	50°C	50°C	50°C	80°C	50°C	80°C

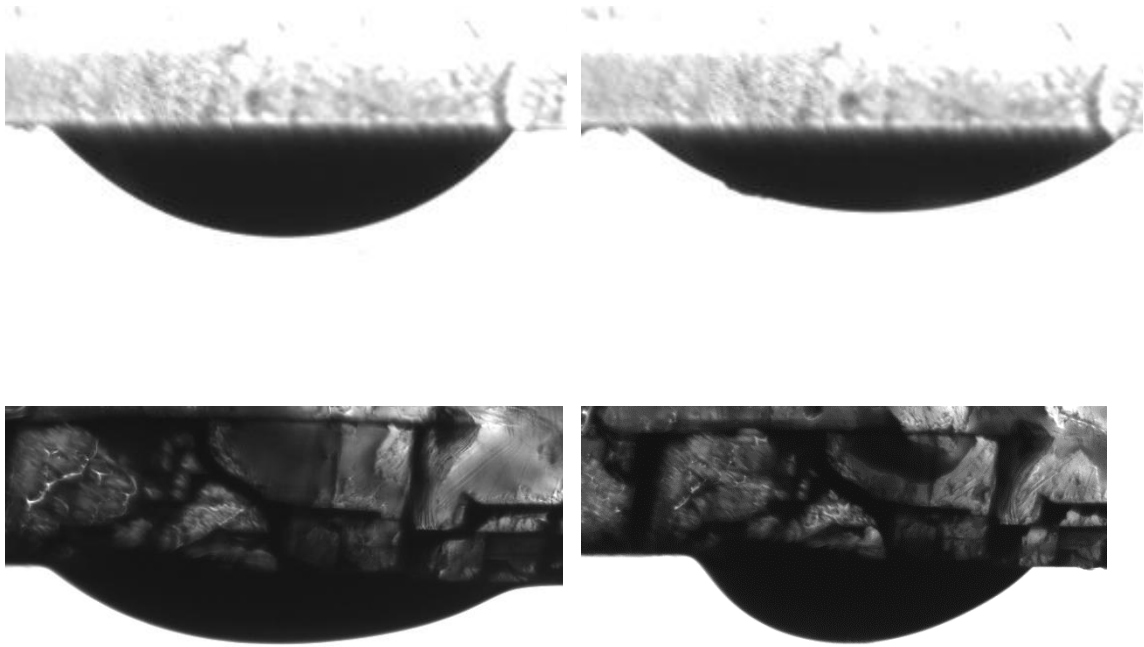


Figure A2. Initial and final contact angles at 25°C for a) BG-10 and b) RW-150

**APPENDIX B: ESTIMATION OF INCREMENTAL OIL RECOVERY AND SURFACTANT REQUIREMENTS IN A RESERVOIR**

Reservoir dimensions – 500m x 500m x 60m (250ft x 250ft x 500ft)

Porosity – 0.14

PV –  $2.1 \times 10^6 \text{ m}^3$

Oil saturation – 80%

Estimated adsorption – Radius of pores  $\sim \sqrt{\frac{k}{\phi}} \sim 10^{-8} \text{ m}$

$$\text{Surface area} \sim \frac{2.1 \times 10^6}{10^{-8}} \text{ m}^2 \sim 2.1 \times 10^{14} \text{ m}^2$$

With average adsorption of  $1 \text{ mg/m}^2$ , net adsorption comes around  $10^8 \text{ kg}$

Incremental Oil recovery –  $\sim 30\% = 5 \times 10^5 \text{ m}^3$  ( $3 \times 10^6 \text{ bbls}$ )

Incremental oil/Adsorbed surfactant –  $3 \times 10^{-2} \text{ bbl/kg}$

## Bibliography

1. Adibhatla, B. and Mohanty, K.K., **2006**, January. Oil recovery from fractured carbonates by surfactant-aided gravity drainage: laboratory experiments and mechanistic simulations. In *SPE/DOE Symposium on Improved Oil Recovery*. Society of Petroleum Engineers.
2. Adibhatla, B., & Mohanty, K. K. Oil recovery from fractured carbonates by surfactant-aided gravity drainage: laboratory experiments and mechanistic simulations. *SPE Reservoir Evaluation & Engineering*, **2008**, 11(01), 119-130.
3. Ahmadall, T., Gonzalez, M.V., Harwell, J.H. and Scamehorn, J.F., **1993**. Reducing surfactant adsorption in carbonate reservoirs. *SPE reservoir engineering*, 8(02), pp.117-122.
4. Ahmadi, M.A., Galedarzadeh, M. and Shadizadeh, S.R., **2015**. Wettability alteration in carbonate rocks by implementing new derived natural surfactant: enhanced oil recovery applications. *Transport in porous media*, 106(3), pp.645-667.
5. Akers, R.J. and Riley, P.M., **1974**. Adsorption of polyoxyethylene alkyl-phenols onto calcium carbonate from aqueous solution. *J. Colloid Interface Sci.*(United States), 48(1).
6. Al-Maamari, R. S., & Buckley, J. S. Asphaltene precipitation and alteration of wetting: the potential for wettability changes during oil production. *SPE Reservoir Evaluation & Engineering*, **2003**, 6(04), 210-214.
7. Alvarez, J.O. and Schechter, D.S., **2017**. Wettability alteration and spontaneous imbibition in unconventional liquid reservoirs by surfactant additives. *SPE Reservoir Evaluation & Engineering*, 20(01), pp.107-117.
8. Alvarez, J.O., Neog, A., Jais, A. and Schechter, D.S., **2014**, April. Impact of surfactants for wettability alteration in stimulation fluids and the potential for surfactant EOR in unconventional liquid reservoirs. In *SPE Unconventional Resources Conference*. Society of Petroleum Engineers.
9. Amott, E., **1959**. Observations relating to the wettability of porous rock.
10. Ananthapadmanabhan, K.P. and Somasundaran, P., **1983**. Mechanism for adsorption maximum and hysteresis in a sodium dodecylbenzenesulfonate/kaolinite system. *Colloids and Surfaces*, 7(2), pp.105-114.
11. Anderson, G.A., **2006**. *Simulation of chemical flood enhanced oil recovery processes including the effects of reservoir wettability* (Doctoral dissertation, University of Texas at Austin).
12. Austad, T., & Standnes, D. C. Spontaneous imbibition of water into oil-wet carbonates. *Journal of Petroleum Science and Engineering*, **2003**, 39(3-4), 363-376.

14. Austad, T. and Milner, J. Spontaneous imbibition of water into low permeable chalk at different wettabilities using surfactants. In *International Symposium on Oilfield Chemistry*, Society of Petroleum Engineers, **1997**.
15. Austad, T., Shariatpanahi, S.F., Strand, S., Black, C.J.J. and Webb, K.J., **2011**. Conditions for a low-salinity enhanced oil recovery (EOR) effect in carbonate oil reservoirs. *Energy & fuels*, 26(1), pp.569-575.
16. Azum, N., Rub, M.A. and Asiri, A.M., **2014**. Experimental and theoretical approach to mixed surfactant system of cationic gemini surfactant with nonionic surfactant in aqueous medium. *Journal of Molecular Liquids*, 196, pp.14-20.
17. Baglioni, P., Dei, L., Rivara-Minten, E. and Kevan, L., **1993**. Mixed micelles of SDS/C12E6 and DTAC/C12E6 surfactants. *Journal of the American Chemical Society*, 115(10), pp.4286-4290.
18. Bahadur, P., Pandya, K., Almgren, M., Li, P. and Stilbs, P., **1993**. Effect of inorganic salts on the micellar behaviour of ethylene oxide-propylene oxide block copolymers in aqueous solution. *Colloid and Polymer Science*, 271(7), pp.657-667.
19. Barati, A., Najafi, A., Daryasafar, A., Nadali, P. and Moslehi, H., **2016**. Adsorption of a new nonionic surfactant on carbonate minerals in enhanced oil recovery: experimental and modeling study. *Chemical Engineering Research and Design*, 105, pp.55-63.
20. Bastrzyk, A.P.I.S.E., Polowczyk, I., Szelag, E. and Sadowski, Z., **2012**. Adsorption and co-adsorption of PEO-PPO-PEO block copolymers and surfactants and their influence on zeta potential of magnesite and dolomite. *Physicochemical Problems of Mineral Processing*, 48(1), p.2012.
21. Bera, A., Ojha, K., Kumar, T., & Mandal, A. Mechanistic study of wettability alteration of quartz surface induced by nonionic surfactants and interaction between crude oil and quartz in the presence of sodium chloride salt. *Energy & Fuels*, **2012**, 26(6), 3634-3643.
22. Bera, A., Kumar, T., Ojha, K. and Mandal, A., **2013**. Adsorption of surfactants on sand surface in enhanced oil recovery: Isotherms, kinetics and thermodynamic studies. *Applied Surface Science*, 284, pp.87-99.
23. Bergström, M. and Pedersen, J.S., **1999**. Formation of tablet-shaped and ribbonlike micelles in mixtures of an anionic and a cationic surfactant. *Langmuir*, 15(7), pp.2250-2253.
24. Bidhendi\*, M.M., Kazempour, M., Ibanga, U., Nguyen, D., Arruda, J., Lantz, M. and Mazon, C., **2019**, October. A Set of Successful Chemical EOR Trials in Permian Basin: Promising Field and Laboratory Results. In *Unconventional Resources Technology Conference, Denver, Colorado, 22-24 July 2019* (pp. 3498-3520). Unconventional Resources Technology Conference (URTeC); Society of Exploration Geophysicists.

25. Blankschtein, D., Thurston, G.M. and Benedek, G.B., **1986**. Phenomenological theory of equilibrium thermodynamic properties and phase separation of micellar solutions. *The Journal of chemical physics*, 85(12), pp.7268-7288.
26. Blokhus, A.M., HØiland, H., Gjerde, M.I. and Ersland, E.K., **1996**. Adsorption of sodium dodecyl sulfate on kaolin from different alcohol–water mixtures. *Journal of colloid and interface science*, 179(2), pp.625-627.
27. Bragg, J.R., Gale, W.W., McElhannon Jr, W.A., Davenport, O.W., Petrichuk, M.D. and Ashcraft, T.L., **1982**, January. Loudon surfactant flood pilot test. In SPE Enhanced Oil Recovery Symposium. Society of Petroleum Engineers.
28. Brinck, J., Jönsson, B. and Tiberg, F., **1998**. Kinetics of nonionic surfactant adsorption and desorption at the silica– water interface: One component. *Langmuir*, 14(5), pp.1058-1071.
29. Brinck, J. and Tiberg, F., **1996**. Adsorption behavior of two binary nonionic surfactant systems at the silica– water interface. *Langmuir*, 12(21), pp.5042-5047.
30. Brown, W., Johnsen, R., Stilbs, P. and Lindman, B., **1983**. Size and shape of nonionic amphiphile (C12E6) micelles in dilute aqueous solutions as derived from quasielastic and intensity light scattering, sedimentation, and pulsed-field-gradient nuclear magnetic resonance self-diffusion data. *The Journal of Physical Chemistry*, 87(22), pp.4548-4553.
31. Buckley, J. S., Liu, Y., & Monsterleet, S. Mechanisms of wetting alteration by crude oils. *SPE journal*, **1998**, 3(01), 54-61.
32. Buckley, J.S., Liu, Y., Xie, X. and Morrow, N.R., **1997**. Asphaltenes and crude oil wetting-the effect of oil composition. *SPE journal*, 2(02), pp.107-119.
33. Caruso, F., Serizawa, T., Furlong, D.N. and Okahata, Y., **1995**. Quartz crystal microbalance and surface plasmon resonance study of surfactant adsorption onto gold and chromium oxide surfaces. *Langmuir*, 11(5), pp.1546-1552.
34. Case, D.A., Cheatham III, T.E., Darden, T., Gohlke, H., Luo, R., Merz Jr, K.M., Onufriev, A., Simmerling, C., Wang, B. and Woods, R.J., **2005**. The Amber biomolecular simulation programs. *Journal of computational chemistry*, 26(16), pp.1668-1688.
35. Chandar, P., Somasundaran, P. and Turro, N.J., **1987**. Fluorescence probe studies on the structure of the adsorbed layer of dodecyl sulfate at the alumina—water interface. *Journal of colloid and interface science*, 117(1), pp.31-46.
36. Chen, P. and Mohanty, K.K., **2015**, April. Surfactant-enhanced oil recovery from fractured oil-wet carbonates: effects of low ift and wettability alteration. In *SPE International Symposium on Oilfield Chemistry*. Society of Petroleum Engineers.

37. Chen, P. and Mohanty, K.K., **2014**, April. Wettability alteration in high temperature carbonate reservoirs. In *SPE Improved Oil Recovery Symposium*. Society of Petroleum Engineers.
38. Cheng, A. and Kwan, J.T., **2012**, January. Optimal Injection Design Utilizing Tracer and Simulation in a Surfactant Pilot for a Fractured Carbonate Yates Field. In *SPE Improved Oil Recovery Symposium*. Society of Petroleum Engineers.
39. Chun, Byeong Jae, et al. "Adsorption of carboxylate on calcium carbonate () surface: Molecular simulation approach." *Colloids and Surfaces A: Physicochemical and Engineering Aspects* 474 (**2015**): 9-17.
40. Cooper, T.G. and de Leeuw, N.H., **2004**. A computer modeling study of the competitive adsorption of water and organic surfactants at surfaces of the mineral scheelite. *Langmuir*, 20(10), pp.3984-3994.
41. Corkill, J.M., Goodman, J.F. and Tate, J.R., **1966**. Adsorption of nonionic surface-active agents at the graphon/solution interface. *Transactions of the Faraday Society*, 62, pp.979-986.
42. Cuiec, L., Bourbiaux, B. and Kalaydjian, F., **1994**. Oil recovery by imbibition in low-permeability chalk. *SPE Formation Evaluation (Society of Petroleum Engineers)*; (United States), 9(3).
43. Curbelo, F.D., Santanna, V.C., Neto, E.L.B., Dutra Jr, T.V., Dantas, T.N.C., Neto, A.A.D. and Garnica, A.I., 2007. Adsorption of nonionic surfactants in sandstones. *Colloids and Surfaces A: Physicochemical and Engineering Aspects*, 293(1-3), pp.1-4.
44. Das, S., Katiyar, A., Rohilla, N., Nguyen, Q., Bonnecaze, R.T., Universal Scaling of Adsorption of Nonionic Surfactants on Carbonates using Cloud Point Temperatures. Under Review
45. Das, S., Nguyen, Q., Patil, P.D., Yu, W. and Bonnecaze, R.T., **2018**. Wettability alteration of calcite by nonionic surfactants. *Langmuir*, 34(36), pp.10650-10658.
46. Das, S., Katiyar, A., Nguyen, Q., Bonnecaze, R.T., Wettability Alteration and Adsorption of Mixed Nonionic and Anionic Surfactants on Carbonates. Under Review
47. Delshad, M., Najafabadi, N.F., Anderson, G.A., Pope, G.A. and Sepehrnoori, K., **2006**, January. Modeling wettability alteration in naturally fractured reservoirs. In *SPE/DOE Symposium on Improved Oil Recovery*. Society of Petroleum Engineers.
48. Delshad, M., Najafabadi, N.F. and Sepehrnoori, K., **2009**, January. Scale Up Methodology for Wettability Modification in Fractured Carbonates. In *SPE Reservoir Simulation Symposium*. Society of Petroleum Engineers.
49. Delshad, M., Bhuyan, D., Pope, G.A. and Lake, L.W., **1986**, January. Effect of capillary number on the residual saturation of a three-phase micellar solution. In *SPE enhanced oil recovery symposium*. Society of Petroleum Engineers.

50. Desbene, P.L., Portet, F. and Treiner, C., **1997**. Adsorption of pure nonionic alkylethoxylated surfactants down to low concentrations at a silica/water interface as determined using a HPLC technique. *Journal of Colloid and Interface Science*, 190(2), pp.350-356.
51. DiCarlo, D.A., **2006**. Quantitative network model predictions of saturation behind infiltration fronts and comparison with experiments. *Water resources research*, 42(7).
52. Douglas, C.B. and Kaler, E.W., **1994**. A scattering study of mixed micelles of hexaethylene glycol mono-n-dodecyl ether and sodium dodecylsulfonate in D2O. *Langmuir*, 10(4), pp.1075-1083.
53. Durán-Álvarez, A., Maldonado-Domínguez, M., González-Antonio, O., Durán-Valencia, C., Romero-Ávila, M., Barragán-Aroche, F. and López-Ramírez, S., **2016**. Experimental–Theoretical Approach to the Adsorption Mechanisms for Anionic, Cationic, and Zwitterionic Surfactants at the Calcite–Water Interface. *Langmuir*, 32(11), pp.2608-2616.
54. El Eini, D.I.D., Barry, B.W. and Rhodes, C.T., **1976**. Micellar size, shape, and hydration of long-chain polyoxyethylene nonionic surfactants. *Journal of Colloid and Interface Science*, 54(3), pp.348-351.
55. Ershadi, M., Alaei, M., Rashidi, A., Ramazani, A. and Khosravani, S., **2015**. Carbonate and sandstone reservoirs wettability improvement without using surfactants for Chemical Enhanced Oil Recovery (C-EOR). *Fuel*, 153, pp.408-415.
56. Esumi, K., Miyazaki, M., Arai, T. and Koide, Y., **1998**. Mixed micellar properties of a cationic gemini surfactant and a nonionic surfactant. *Colloids and Surfaces A: Physicochemical and Engineering Aspects*, 135(1-3), pp.117-122.
57. Evans, D.J. and Holian, B.L., **1985**. The nose–hoover thermostat. *The Journal of chemical physics*, 83(8), pp.4069-4074.
58. Fletcher, P. D., Savory, L. D., Clarke, A., & Howe, A. M. Model Study of Enhanced Oil Recovery by Flooding with Aqueous Solutions of Different Surfactants: How the Surface Chemical Properties of the Surfactants Relate to the Amount of Oil Recovered. *Energy & Fuels*, **2016**, 30(6), 4767-4780.
59. Fletcher, P. D., Savory, L. D., Woods, F., Clarke, A., & Howe, A. M. Model study of enhanced oil recovery by flooding with aqueous surfactant solution and comparison with theory. *Langmuir*, **2015**, 31(10), 3076-3085.
60. Freeman, C.L., Harding, J.H., Cooke, D.J., Elliott, J.A., Lardge, J.S. and Duffy, D.M., **2007**. New forcefields for modeling biomineralization processes. *The Journal of Physical Chemistry C*, 111(32), pp.11943-11951.
61. Gao, H.C., Zhao, S., Mao, S.Z., Yuan, H.Z., Yu, J.Y., Shen, L.F. and Du, Y.R., **2002**. Mixed micelles of polyethylene glycol (23) lauryl ether with ionic surfactants studied



- by proton 1D and 2D NMR. *Journal of colloid and interface science*, 249(1), pp.200-208.
62. Garamus, V.M., **2003**. Formation of mixed micelles in salt-free aqueous solutions of sodium dodecyl sulfate and C12E6. *Langmuir*, 19(18), pp.7214-7218.
  63. Gellan, A. and Rochester, C.H., **1985**. Adsorption of n-alkylpolyethylene glycol nonionic surfactants from aqueous solution on to silica. *Journal of the Chemical Society, Faraday Transactions 1: Physical Chemistry in Condensed Phases*, 81(9), pp.2235-2245.
  64. Ghatee, Mohammad Hadi, Mohammad Mehdi Koleini, and Shahab Ayatollahi. "Molecular dynamics simulation investigation of hexanoic acid adsorption onto calcite () surface." *Fluid Phase Equilibria* 387 (**2015**): 24-31.
  65. Godbole, R.V., Khabaz, F., Khare, R. and Hedden, R.C., **2017**. Swelling of Random Copolymer Networks in Pure and Mixed Solvents: Multi-Component Flory–Rehner Theory. *The Journal of Physical Chemistry B*, 121(33), pp.7963-7977.
  66. Gomari, K.R. and Hamouda, A.A., **2006**. Effect of fatty acids, water composition and pH on the wettability alteration of calcite surface. *Journal of petroleum science and engineering*, 50(2), pp.140-150.
  67. Gupta, R. and Mohanty, K.K., **2007**, January. Temperature effects on surfactant-aided imbibition into fractured carbonates. In *SPE Annual Technical Conference and Exhibition*. Society of Petroleum Engineers.
  68. Gupta, R., & Mohanty, K. Temperature effects on surfactant-aided imbibition into fractured carbonates. *SPE Journal*, **2010**, 15(03), 588-597.
  69. Gutig, C., Grady, B.P. and Striolo, A., **2008**. Experimental Studies on the Adsorption of Two Surfactants on Solid– Aqueous Interfaces: Adsorption Isotherms and Kinetics. *Langmuir*, 24(9), pp.4806-4816.
  70. Hammond, P.S. and Unsal, E., **2012**. A dynamic pore network model for oil displacement by wettability-altering surfactant solution. *Transport in porous media*, 92(3), pp.789-817.
  71. Hammond, P.S. and Unsal, E., **2009**. Spontaneous and forced imbibition of aqueous wettability altering surfactant solution into an initially oil-wet capillary. *Langmuir*, 25(21), pp.12591-12603.
  72. Hammond, P.S. and Unsal, E., **2010**. Forced and spontaneous imbibition of surfactant solution into an oil-wet capillary: the effects of surfactant diffusion ahead of the advancing meniscus. *Langmuir*, 26(9), pp.6206-6221.
  73. Hammond, P.S. and Unsal, E., **2011**. Spontaneous imbibition of surfactant solution into an oil-wet capillary: wettability restoration by surfactant– contaminant complexation. *Langmuir*, 27(8), pp.4412-4429.

74. Hamouda, A. and Karoussi, O., **2008**. Effect of temperature, wettability and relative permeability on oil recovery from oil-wet chalk. *Energies*, 1(1), pp.19-34.
75. Hirasaki, G. and Zhang, D.L., **2004**. Surface chemistry of oil recovery from fractured, oil-wet, carbonate formations. *Spe Journal*, 9(02), pp.151-162.
76. Hirasaki, G.J., Miller, C.A. and Puerto, M., **2008**, January. Recent advances in surfactant EOR. In *SPE Annual Technical Conference and Exhibition*. Society of Petroleum Engineers.
77. Hockney, R.W. and Eastwood, J.W., **1988**. Computer simulation using particles. crc Press.
78. Hognesen, E.J., Strand, S. and Austad, T., **2005**, January. Waterflooding of preferential oil-wet carbonates: Oil recovery related to reservoir temperature and brine composition. In *SPE Europec/EAGE Annual Conference*. Society of Petroleum Engineers.
79. Holland, P.M. and Rubingh, D.N., **1983**. Nonideal multicomponent mixed micelle model. *The Journal of Physical Chemistry*, 87(11), pp.1984-1990.
80. Holmberg, K., JoËnsson, B., Kronberg, B. and Lindman, B., **2002**. SURFACTANTS AND POLYMERS IN AQUEOUS SOLUTION.
81. Hongyan, C., Wenli, L., Desheng, M., Xinyu, Z., Jian, F., Jianguo, L., Jianfeng, S. and Yi, Z., **2017**, March. Experimental Study and Pilot Test of Combined Gel Treatment and Surfactant Imbibition Technology in High Temperature, High Salinity Reservoir. In *SPE Oklahoma City Oil and Gas Symposium*. Society of Petroleum Engineers.
82. Howe, A. M., Clarke, A., Mitchell, J., Staniland, J., Hawkes, L., & Whalan, C. Visualising surfactant enhanced oil recovery. *Colloids and Surfaces A: Physicochemical and Engineering Aspects*, **2015**, 480, 449-461.
83. Huang, Z., Yan, Z. and Gu, T., **1989**. Mixed adsorption of cationic and anionic surfactants from aqueous solution on silica gel. *Colloids and surfaces*, 36(3), pp.353-358.
84. Israelachvili, J.N., **1976**. Mitchell, DJ.; Ninham, BWJ Chem. Soc. *Faraday Trans. II*, 72, pp.1525-1568.
85. Ivanova, N.I., Volchkova, I.L. and Shchukin, E.D., **1995**. Adsorption of nonionic and cationic surfactants from aqueous binary mixtures onto the solid/liquid interface. *Colloids and Surfaces A: Physicochemical and Engineering Aspects*, 101(2-3), pp.239-243.
86. Jadhunandan, P.P. and Morrow, N.R., **1995**. Effect of wettability on waterflood recovery for crude-oil/brine/rock systems. *SPE reservoir engineering*, 10(01), pp.40-46.

87. Jarrahan, K., Seiedi, O., Sheykhan, M., Sefti, M. V., & Ayatollahi, S. Wettability alteration of carbonate rocks by surfactants: a mechanistic study. *Colloids and Surfaces A: Physicochemical and Engineering Aspects*, **2012**, 410, 1-10.
88. Jian, G., Puerto, M.C., Wehowsky, A., Dong, P., Johnston, K.P., Hirasaki, G.J. and Biswal, S.L., **2016**. Static adsorption of an ethoxylated nonionic surfactant on carbonate minerals. *Langmuir*, 32(40), pp.10244-10252.
89. Joseph, J., Gunda, N. S. K., & Mitra, S. K. On-chip porous media: Porosity and permeability measurements. *Chemical Engineering Science*, **2013**, 99, 274-283.
90. Kalaei, M.H., Green, D. and Willhite, G.P., **2013**. A new dynamic wettability-alteration model for oil-wet cores during surfactant-solution imbibition. *SPE Journal*, 18(05), pp.818-828.
91. Kato, T., Terao, T., & Seimiya, T. Intermicellar migration of surfactant molecules in entangled micellar solutions. *Langmuir*, **1994**, 10(12), 4468-4474.
92. Kazempour, M., Kiani, M., Nguyen, D., Salehi, M., Bidhendi, M.M. and Lantz, M., **2018**, April. Boosting Oil Recovery in Unconventional Resources Utilizing Wettability Altering Agents: Successful Translation from Laboratory to Field. In *SPE Improved Oil Recovery Conference*. Society of Petroleum Engineers.
93. Kerisit, S., Marmier, A. and Parker, S.C., **2005**. Ab initio surface phase diagram of the {1014} calcite surface. *The Journal of Physical Chemistry B*, 109(39), pp.18211-18213.
94. Khabaz, F., Mani, S. and Khare, R., **2016**. Molecular origins of dynamic coupling between water and hydrated polyacrylate gels. *Macromolecules*, 49(19), pp.7551-7562.
95. Khabaz, F. and Khare, R., **2014**. Effect of chain architecture on the size, shape, and intrinsic viscosity of chains in polymer solutions: A molecular simulation study. *The Journal of chemical physics*, 141(21), p.214904.
96. Kiani\*, M., Hsu, T.P., Roostapour, A., Kazempour, M. and Tudor, E., **2019**, October. A Novel Enhanced Oil Recovery Approach to Water Flooding in Saskatchewan's Tight Oil Plays. In *Unconventional Resources Technology Conference, Denver, Colorado, 22-24 July 2019* (pp. 256-270). Unconventional Resources Technology Conference (URTeC); Society of Exploration Geophysicists.
97. Kokalj, A., **1999**. XCrySDen—a new program for displaying crystalline structures and electron densities. *Journal of Molecular Graphics and Modelling*, 17(3-4), pp.176-179.
98. Koopal, L.K., Lee, E.M. and Böhmer, M.R., **1995**. Adsorption of cationic and anionic surfactants on charged metal oxide surfaces. *Journal of colloid and interface science*, 170(1), pp.85-97.

99. Kumar, S. and Mandal, A., **2016**. Studies on interfacial behavior and wettability change phenomena by ionic and nonionic surfactants in presence of alkalis and salt for enhanced oil recovery. *Applied Surface Science*, 372, pp.42-51.
100. Kumar, S., Rosenberg, J.M., Bouzida, D., Swendsen, R.H. and Kollman, P.A., **1992**. The weighted histogram analysis method for free-energy calculations on biomolecules. I. The method. *Journal of computational chemistry*, 13(8), pp.1011-1021.
101. Kumar, V.V., **1991**. Complementary molecular shapes and additivity of the packing parameter of lipids. *Proceedings of the National Academy of Sciences*, 88(2), pp.444-448.
102. Kuno, H. and Abe, R., **1961**. The adsorption of polyoxyethylated nonylphenol on calcium carbonate in aqueous solution. *Kolloid-Zeitschrift*, 177(1), pp.40-44.
103. Kurapati, Y. and Sharma, S., **2018**. Adsorption Free Energies of Imidazolinium-Type Surfactants in Infinite Dilution and in Micellar State on Gold Surface. *The Journal of Physical Chemistry B*, 122(22), pp.5933-5939.
104. Lake, L.W., 1989. Enhanced oil recovery.
105. Lee, E.M., Thomas, R.K., Cummins, P.G., Staples, E.J., Penfold, J. and Rennie, A.R., **1989**. Determination of the structure of a surfactant layer adsorbed at the silica/water interface by neutron reflection. *Chemical physics letters*, 162(3), pp.196-202.
106. Lenormand, R., Touboul, E. and Zarcone, C., **1988**. Numerical models and experiments on immiscible displacements in porous media. *Journal of fluid mechanics*, 189, pp.165-187.
107. Levitz, P.E., **2002**. Adsorption of non ionic surfactants at the solid/water interface. *Colloids and Surfaces A: Physicochemical and Engineering Aspects*, 205(1-2), pp.31-38.
108. Levitz, P., Van Damme, H. and Keravis, D., **1984**. Fluorescence decay study of the adsorption of nonionic surfactants at the solid-liquid interface. 1. Structure of the adsorption layer on a hydrophilic solid. *The Journal of Physical Chemistry*, 88(11), pp.2228-2235.
109. Levitz, P. and Van Damme, H., **1986**. Fluorescence decay study of the adsorption of nonionic surfactants at the solid-liquid interface. 2. Influence of polar chain length. *The Journal of Physical Chemistry*, 90(7), pp.1302-1310.
110. Levitz, P., **1991**. Aggregative adsorption of nonionic surfactants onto hydrophilic solid/water interface. Relation with bulk micellization. *Langmuir*, 7(8), pp.1595-1608.
111. Li, N., Zhang, G., Ge, J., Luchao, J., Jianqiang, Z., Baodong, D. and Pei, H., 2011. Adsorption behavior of betaine-type surfactant on quartz sand. *Energy & Fuels*, 25(10), pp.4430-4437.

112. Li, X., Xue, Q., Wu, T., Jin, Y., Ling, C. and Lu, S., **2015**. Oil detachment from silica surface modified by carboxy groups in aqueous cetyltriethylammonium bromide solution. *Applied Surface Science*, 353, pp.1103-1111.
113. Li, X., Xue, Q., Zhu, L., Jin, Y., Wu, T., Guo, Q., Zheng, H. and Lu, S., **2016**. How to select an optimal surfactant molecule to speed up the oil-detachment from solid surface: a computational simulation. *Chemical Engineering Science*, 147, pp.47-53.
114. Li, Xiaofang, et al. "Oil detachment from silica surface modified by carboxy groups in aqueous cetyltriethylammonium bromide solution." *Applied Surface Science* 353 (2015): 1103-1111.
115. Liley, J.R., Thomas, R.K., Penfold, J., Tucker, I.M., Petkov, J.T., Stevenson, P. and Webster, J.R., **2017**. Surface adsorption in ternary surfactant mixtures above the critical micelle concentration: effects of asymmetry on the composition dependence of the excess free energy. *The Journal of Physical Chemistry B*, 121(13), pp.2825-2838.
116. Liu, Q., Yuan, S., Yan, H. and Zhao, X., **2012**. Mechanism of oil detachment from a silica surface in aqueous surfactant solutions: molecular dynamics simulations. *The Journal of Physical Chemistry B*, 116(9), pp.2867-2875.
117. Liu, S., Zhang, D., Yan, W., Puerto, M., Hirasaki, G.J. and Miller, C.A., **2008**. Favorable attributes of alkaline-surfactant-polymer flooding. *SPE Journal*, 13(01), pp.5-16.
118. Lokar, W.J. and Ducker, W.A., **2004**. Forces between Glass Surfaces in Mixed Cationic– Zwitterionic Surfactant Systems. *Langmuir*, 20(11), pp.4553-4558.
119. Lu, G., Zhang, X., Shao, C. and Yang, H., **2009**. Molecular dynamics simulation of adsorption of an oil-water-surfactant mixture on calcite surface. *Petroleum Science*, 6(1), pp.76-81.
120. Lu, S. and Somasundaran, P., **2008**. Tunable synergism/antagonism in a mixed nonionic/anionic surfactant layer at the solid/liquid interface. *Langmuir*, 24(8), pp.3874-3879.
121. Ma, K., Cui, L., Dong, Y., Wang, T., Da, C., Hirasaki, G. J., & Biswal, S. L. Adsorption of cationic and anionic surfactants on natural and synthetic carbonate materials. *Journal of colloid and interface science*, **2013**, 408, 164-172.
122. Maerker, J.M. and Gale, W.W., **1992**. Surfactant flood process design for Loudon. *SPE reservoir engineering*, 7(01), pp.36-44.
123. Mahani, H., Keya, A.L., Berg, S., Bartels, W.B., Nasralla, R. and Rossen, W.R., **2015**. Insights into the mechanism of wettability alteration by low-salinity flooding (LSF) in carbonates. *Energy & Fuels*, 29(3), pp.1352-1367.

124. Mandal, A., Kar, S. and Kumar, S., **2016**. The synergistic effect of a mixed surfactant (Tween 80 and SDBS) on wettability alteration of the oil wet quartz surface. *Journal of Dispersion Science and Technology*, 37(9), pp.1268-1276.
125. Mani, S., Khabaz, F., Godbole, R.V., Hedden, R.C. and Khare, R., **2015**. Structure and hydrogen bonding of water in polyacrylate gels: effects of polymer hydrophilicity and water concentration. *The Journal of Physical Chemistry B*, 119(49), pp.15381-15393.
126. Martínez, L., Andrade, R., Birgin, E.G. and Martínez, J.M., **2009**. PACKMOL: a package for building initial configurations for molecular dynamics simulations. *Journal of computational chemistry*, 30(13), pp.2157-2164.
127. Mattax, C.C. and Kyte, J.R., **1962**. Imbibition oil recovery from fractured, water-drive reservoir. *Society of Petroleum Engineers Journal*, 2(02), pp.177-184.
128. Misselyn-Bauduin, A.M., Thibaut, A., Grandjean, J., Broze, G. and Jérôme, R., **2000**. Mixed micelles of anionic– nonionic and anionic– zwitterionic surfactants analyzed by pulsed field gradient NMR. *Langmuir*, 16(10), pp.4430-4435.
129. Muherei, M.A., Junin, R. and Merdhah, A.B.B. Adsorption of sodium dodecyl sulfate, Triton X100 and their mixtures to shale and sandstone: a comparative study. *Journal of Petroleum Science and Engineering*, **2009**, 67(3-4), pp.149-154.
130. Na, G.C., Yuan, B.O., Stevens, H.J., Weekley, B.S. and Rajagopalan, N., **1999**. Cloud point of nonionic surfactants: modulation with pharmaceutical excipients. *Pharmaceutical research*, 16(4), pp.562-568.
131. Pal, M., Tarsauliya, G., Patil, P., Rohilla, N., Mounzer, H., Bacaud, B., Gilani, S.F., Katiyar, A. and Rozowski, P., **2019**, April. Dreaming Big “Surfactant Injection in a Giant Offshore Carbonate Field”, From Successful Injection Trials to Pilot Design and Implementation. In *IOR 2019–20th European Symposium on Improved Oil Recovery* (Vol. 2019, No. 1, pp. 1-22). European Association of Geoscientists & Engineers.
132. Paria, S. and Khilar, K.C., **2004**. A review on experimental studies of surfactant adsorption at the hydrophilic solid–water interface. *Advances in colloid and interface science*, 110(3), pp.75-95.
133. Partyka, S., Zaini, S., Lindheimer, M. and Brun, B., **1984**. The adsorption of nonionic surfactants on a silica gel. *Colloids and surfaces*, 12, pp.255-270.
134. Patil, P.D., Rohilla, N., Katiyar, A., Yu, W., Falcone, S., Nelson, C. and Rozowski, P., **2018**, March. Surfactant based EOR for tight oil reservoirs through wettability alteration: novel surfactant formulations and their efficacy to induce spontaneous imbibition. In *SPE EOR Conference at Oil and Gas West Asia*. Society of Petroleum Engineers.

135. Pavese, A., Catti, M., Parker, S.C. and Wall, A., **1996**. Modelling of the thermal dependence of structural and elastic properties of calcite, CaCO<sub>3</sub>. *Physics and chemistry of minerals*, 23(2), pp.89-93.
136. Penfold, J., Tucker, I., Thomas, R.K., Staples, E. and Schuermann, R., **2005**. Structure of mixed anionic/nonionic surfactant micelles: experimental observations relating to the role of headgroup electrostatic and steric effects and the effects of added electrolyte. *The Journal of Physical Chemistry B*, 109(21), pp.10760-10770.
137. Phan, T., Kazempour, M., Nguyen, D. and Champion, N., **2018**, February. Treating Liquid Banking Problem to Increase Shale Gas Wells Productivity. In *SPE International Conference and Exhibition on Formation Damage Control*. Society of Petroleum Engineers.
138. Plimpton, S., Thompson, A., Crozier, P. and Kohlmeyer, A., **2011**. LAMMPS molecular dynamics simulator. 2015-5-15]. <http://lammps.sandia.gov>.
139. Plimpton, S., **1995**. Fast parallel algorithms for short-range molecular dynamics. *Journal of computational physics*, 117(1), pp.1-19.
140. Portet, F., Desbene, P.L. and Treiner, C., **1997**. Adsorption isotherms at a silica/water interface of the oligomers of polydispersed nonionic surfactants of the alkylpolyoxyethylated series. *Journal of colloid and interface science*, 194(2), pp.379-391.
141. Portet, F., Desbene, P.L. and Treiner, C., **1996**. Nonideality of mixtures of pure nonionic surfactants both in solution and at silica/water interfaces. *Journal of colloid and interface science*, 184(1), pp.216-226.
142. Portet, F., Desbene, P.L. and Treiner, C., **1997**. Adsorption isotherms at a silica/water interface of the oligomers of polydispersed nonionic surfactants of the alkylpolyoxyethylated series. *Journal of colloid and interface science*, 194(2), pp.379-391.
143. Portet-Koltalo, F., Desbene, P.L. and Treiner, C., **2001**. Self-desorption of mixtures of anionic and nonionic surfactants from a silica/water interface. *Langmuir*, 17(13), pp.3858-3862.
144. Price, D.J. and Brooks III, C.L., **2004**. A modified TIP3P water potential for simulation with Ewald summation. *The Journal of chemical physics*, 121(20), pp.10096-10103.
145. Rigo, V.A., Metin, C.O., Nguyen, Q.P. and Miranda, C.R., **2012**. Hydrocarbon adsorption on carbonate mineral surfaces: a first-principles study with van der Waals interactions. *The Journal of Physical Chemistry C*, 116(46), pp.24538-24548.
146. Romanuka, J., Hofman, J., Ligthelm, D.J., Suijkerbuijk, B., Marcelis, F., Oedai, S., Brussee, N., van der Linde, H., Aksulu, H. and Austad, T., **2012**, January. Low salinity

EOR in carbonates. In *SPE Improved Oil Recovery Symposium*. Society of Petroleum Engineers.

147. Rosen, M.J. and Li, F., **2001**. The adsorption of gemini and conventional surfactants onto some soil solids and the removal of 2-naphthol by the soil surfaces. *Journal of colloid and interface science*, 234(2), pp.418-424.
148. Salathiel, R. A. Oil recovery by surface film drainage in mixed-wettability rocks. *Journal of Petroleum Technology*, **1973**, 25(10), 1-216.
149. Salehi, M., Johnson, S.J. and Liang, J.T., **2008**. Mechanistic study of wettability alteration using surfactants with applications in naturally fractured reservoirs. *Langmuir*, 24(24), pp.14099-14107.
150. Saputra, I.W.R., Park, K.H., Zhang, F., Adel, I.A. and Schechter, D.S., **2019**. Surfactant-Assisted Spontaneous Imbibition to Improve Oil Recovery on the Eagle Ford and Wolfcamp Shale Oil Reservoir: Laboratory to Field Analysis. *Energy & Fuels*, 33(8), pp.6904-6920.
151. Sarmoria, C., Puvvada, S. and Blankschtein, D., **1992**. Prediction of critical micelle concentrations of nonideal binary surfactant mixtures. *Langmuir*, 8(11), pp.2690-2697.
152. Schechter, D.S., Zhou, D. and Orr Jr, F.M., **1994**. Low IFT drainage and imbibition. *Journal of Petroleum Science and Engineering*, 11(4), pp.283-300.
153. Schlumberger Market Analysis, **2007**.
154. Schneider, M. H., & Tabeling, P. Lab-on-chip methodology in the energy industry: wettability patterns and their impact on fluid displacement in oil reservoir models. *American Journal of Applied Sciences*, **2011**, 8(10), 927.
155. Seethepalli, A., Adibhatla, B. and Mohanty, K.K., **2004**, January. Wettability alteration during surfactant flooding of carbonate reservoirs. In *SPE/DOE symposium on improved oil recovery*. Society of Petroleum Engineers.
156. Shah, K., Chiu, P., Jain, M., Fortes, J., Moudgil, B. and Sinnott, S., **2005**. Morphology and Mechanical Properties of Surfactant Aggregates at Water– Silica Interfaces: Molecular Dynamics Simulations. *Langmuir*, 21(12), pp.5337-5342.
157. Sharma, G. and Mohanty, K., **2013**. Wettability alteration in high-temperature and high-salinity carbonate reservoirs. *SPE Journal*, 18(04), pp.646-655.
158. Sharma, K.S., Rodgers, C., Palepu, R.M. and Rakshit, A.K., **2003**. Studies of mixed surfactant solutions of cationic dimeric (gemini) surfactant with nonionic surfactant C12E6 in aqueous medium. *Journal of colloid and interface science*, 268(2), pp.482-488.
159. Sharma, K.S., Hassan, P.A. and Rakshit, A.K., **2006**. Self aggregation of binary surfactant mixtures of a cationic dimeric (gemini) surfactant with nonionic surfactants



- in aqueous medium. *Colloids and Surfaces A: Physicochemical and Engineering Aspects*, 289(1-3), pp.17-24.
160. Shi, L., Ghezzi, M., Caminati, G., Lo Nostro, P., Grady, B.P. and Striolo, A., **2009**. Adsorption isotherms of aqueous C12E6 and cetyltrimethylammonium bromide surfactants on solid surfaces in the presence of low molecular weight coadsorbents. *Langmuir*, 25(10), pp.5536-5544.
  161. Shigeta, K., Olsson, U., & Kunieda, H. Correlation between micellar structure and cloud point in long poly (oxyethylene)<sub>n</sub> oleyl ether systems. *Langmuir*, **2001**, 17(16), 4717-4723.
  162. Sofla, S. J. D., Sharifi, M., & Sarapardeh, A. H. Toward mechanistic understanding of natural surfactant flooding in enhanced oil recovery processes: the role of salinity, surfactant concentration and rock type. *Journal of Molecular Liquids*, (**2016**), 222, 632-639.
  163. Somasundaran, P. and Zhang, L., **2006**. Adsorption of surfactants on minerals for wettability control in improved oil recovery processes. *Journal of Petroleum Science and Engineering*, 52(1-4), pp.198-212.
  164. Somasundaran, P. and Krishnakumar, S., **1997**. Adsorption of surfactants and polymers at the solid-liquid interface. *Colloids and Surfaces A: physicochemical and engineering aspects*, 123, pp.491-513.
  165. Somasundaran, P., Snell, E.D., Fu, E. and Xu, Q., **1992**. Effect of adsorption of non-ionic surfactant and non-ionic—anionic surfactant mixtures on silica—liquid interfacial properties. *Colloids and surfaces*, 63(1-2), pp.49-54.
  166. Somasundaran, P., Fu, E. and Xu, Q., **1992**. Coadsorption of anionic and nonionic surfactant mixtures at the alumina-water interface. *Langmuir*, 8(4), pp.1065-1069.
  167. Song, J., Zeng, Y., Wang, L., Duan, X., Puerto, M., Chapman, W.G., Biswal, S.L. and Hirasaki, G.J., **2017**. Surface complexation modeling of calcite zeta potential measurements in brines with mixed potential determining ions (Ca<sup>2+</sup>, CO<sub>3</sub><sup>2-</sup>, Mg<sup>2+</sup>, SO<sub>4</sub><sup>2-</sup>) for characterizing carbonate wettability. *Journal of colloid and interface science*, 506, pp.169-179.
  168. Spinler, E.A., Zornes, D.R., Tobola, D.P. and Moradi-Araghi, A. Enhancement of oil recovery using a low concentration of surfactant to improve spontaneous and forced imbibition in chalk. In *SPE/DOE Improved Oil Recovery Symposium*. Society of Petroleum Engineers, **2000**.
  169. Stålgren, J.J.R., Eriksson, J. and Boschkova, K., **2002**. A comparative study of surfactant adsorption on model surfaces using the quartz crystal microbalance and the ellipsometer. *Journal of colloid and interface science*, 253(1), pp.190-195.
  170. Standnes, D. C., & Austad, T. Wettability alteration in carbonates: Interaction between cationic surfactant and carboxylates as a key factor in wettability alteration from oil-

- wet to water-wet conditions. *Colloids and Surfaces A: Physicochemical and Engineering Aspects*, **2003**, 216(1-3), 243-259.
171. Standnes, D.C., Nogaret, L.A., Chen, H.L. and Austad, T. An evaluation of spontaneous imbibition of water into oil-wet carbonate reservoir cores using a nonionic and a cationic surfactant. *Energy & Fuels*, 16(6), **1997**, pp.1557-1564.
  172. Standnes, D.C. and Austad, T., **2000**. Wettability alteration in chalk: 2. Mechanism for wettability alteration from oil-wet to water-wet using surfactants. *Journal of Petroleum Science and Engineering*, 28(3), pp.123-143.
  173. Standnes, D.C. and Austad, T., **2000**. Wettability alteration in chalk: 1. Preparation of core material and oil properties. *Journal of Petroleum Science and Engineering*, 28(3), pp.111-121.
  174. Standnes, D.C., Nogaret, L.A., Chen, H.L. and Austad, T., **2002**. An evaluation of spontaneous imbibition of water into oil-wet carbonate reservoir cores using a nonionic and a cationic surfactant. *Energy & Fuels*, 16(6), pp.1557-1564.
  175. Standnes, D.C. and Austad, T., **2003**. Nontoxic low-cost amines as wettability alteration chemicals in carbonates. *Journal of Petroleum Science and Engineering*, 39(3-4), pp.431-446.
  176. Starov, V.M., Zhdanov, S.A. and Velarde, M.G., **2004**. Capillary imbibition of surfactant solutions in porous media and thin capillaries: partial wetting case. *Journal of colloid and interface science*, 273(2), pp.589-595.
  177. Starov, V.M., **2004**. Spontaneous rise of surfactant solutions into vertical hydrophobic capillaries. *Journal of colloid and interface science*, 270(1), pp.180-186.
  178. Steinby, K., Silveston, R., & Kronberg, B. The effect of temperature on the adsorption of a nonionic surfactant on a PMMA latex. *Journal of colloid and interface science*, **1993**, 155(1), 70-78.
  179. Strand, S., Standnes, D. C., & Austad, T. Spontaneous imbibition of aqueous surfactant solutions into neutral to oil-wet carbonate cores: Effects of brine salinity and composition. *Energy & fuels*, **2003**, 17(5), 1133-1144.
  180. Strand, S., Høgnesen, E. J., & Austad, T. Wettability alteration of carbonates—Effects of potential determining ions ( $\text{Ca}^{2+}$  and  $\text{SO}_4^{2-}$ ) and temperature. *Colloids and Surfaces A: Physicochemical and Engineering Aspects*, **2006**, 275(1-3), 1-10.
  181. Tagavifar, M., Jang, S.H., Sharma, H., Wang, D., Chang, L.Y., Mohanty, K. and Pope, G.A., **2018**. Effect of pH on adsorption of anionic surfactants on limestone: Experimental study and surface complexation modeling. *Colloids and Surfaces A: Physicochemical and Engineering Aspects*, 538, pp.549-558.
  182. Tanner, L. H. The spreading of silicone oil drops on horizontal surfaces. *Journal of Physics D: Applied Physics*, **1979**, 12(9), 1473.

183. Thibaut, A., Misselyn-Bauduin, A.M., Grandjean, J., Broze, G. and Jérôme, R., **2000**. Adsorption of an aqueous mixture of surfactants on silica. *Langmuir*, *16*(24), pp.9192-9198.
184. Thomas, H.G., Lomakin, A., Blankschtein, D. and Benedek, G.B., **1997**. Growth of mixed nonionic micelles. *Langmuir*, *13*(2), pp.209-218.
185. Thurston, G.M., Blankschtein, D., Fisch, M.R. and Benedek, G.B., **1986**. Theory of thermodynamic properties and phase separation of micellar solutions with lower consolute points. *The Journal of chemical physics*, *84*(8), pp.4558-4562.
186. Tiberg, F., Zhmud, B., Hallstenson, K. and Von Bahr, M., **2000**. Capillary rise of surfactant solutions. *Physical Chemistry Chemical Physics*, *2*(22), pp.5189-5196.
187. Tiberg, F., Joensson, B., Tang, J.A. and Lindman, B., **1994**. Ellipsometry studies of the self-assembly of nonionic surfactants at the silica-water interface: equilibrium aspects. *Langmuir*, *10*(7), pp.2294-2300.
188. Tiberg, F., Brinck, J. and Grant, L., **1999**. Adsorption and surface-induced self-assembly of surfactants at the solid–aqueous interface. *Current opinion in colloid & interface science*, *4*(6), pp.411-419.
189. Tiberg, F., **1996**. Physical characterization of nonionic surfactant layers adsorbed at hydrophilic and hydrophobic solid surfaces by time-resolved ellipsometry. *Journal of the Chemical Society, Faraday Transactions*, *92*(4), pp.531-538.
190. Torrie, G.M. and Valleau, J.P., **1977**. Nonphysical sampling distributions in Monte Carlo free-energy estimation: Umbrella sampling. *Journal of Computational Physics*, *23*(2), pp.187-199.
191. Totland, C. and Lewis, R.T., **2016**. Mechanism of calcite wettability alteration by alkyl polyglucoside. *Colloids and Surfaces A: Physicochemical and Engineering Aspects*, *488*, pp.129-137.
192. Tummala, N.R., Shi, L. and Striolo, A., **2011**. Molecular dynamics simulations of surfactants at the silica–water interface: Anionic vs nonionic headgroups. *Journal of colloid and interface science*, *362*(1), pp.135-143.
193. Unsal, E., Broens, M. and Armstrong, R.T., **2016**. Pore scale dynamics of microemulsion formation. *Langmuir*, *32*(28), pp.7096-7108.
194. Urbina-Villalba, G., Reif, I., Márquez, M.L. and Rogel, E., **1995**. Theoretical study on the structure and interfacial areas of nonyl phenol ethoxylated surfactants. *Colloids and Surfaces A: Physicochemical and Engineering Aspects*, *99*(2-3), pp.207-220.
195. Valiya Parambathu, A., Wang, L., Asthagiri, D. and Chapman, W.G., **2019**. Apolar behavior of hydrated calcite {1 0-1 4} surface assists in naphthenic acid adsorption. *Energy & Fuels*.

196. Vargo, J., Turner, J., Vergnani, B., Pitts, M.J., Wyatt, K., Surkalo, H. and Patterson, D., **1999**, January. Alkaline-surfactant-polymer flooding of the Cambridge Minnelusa field. In *SPE Rocky Mountain Regional Meeting*. Society of Petroleum Engineers.
197. Velinova, M., Sengupta, D., Tadjer, A.V. and Marrink, S.J., **2011**. Sphere-to-rod transitions of nonionic surfactant micelles in aqueous solution modeled by molecular dynamics simulations. *Langmuir*, 27(23), pp.14071-14077.
198. Viksund, B.G., Morrow, N.R., Ma, S., Wang, W. and Graue, A., **1998**, September. Initial water saturation and oil recovery from chalk and sandstone by spontaneous imbibition. In *Proceedings, 1998 International Symposium of Society of Core Analysts, The Hague*.
199. Viswanathan, K.V. and Somasundaran, P., **1987**. Adsorption of ethoxylated sulfonates on kaolinite and alumina. *Colloids and surfaces*, 26, pp.19-41.
200. Wang, J., Wolf, R.M., Caldwell, J.W., Kollman, P.A. and Case, D.A., **2004**. Development and testing of a general amber force field. *Journal of computational chemistry*, 25(9), pp.1157-1174.
201. Wang, L., Liu, R., Hu, Y., Liu, J. and Sun, W., **2016**. Adsorption behavior of mixed cationic/anionic surfactants and their depression mechanism on the flotation of quartz. *Powder Technology*, 302, pp.15-20.
202. Wang, L., Hu, Y., Liu, J., Sun, Y. and Sun, W., **2015**. Flotation and adsorption of muscovite using mixed cationic–nonionic surfactants as collector. *Powder technology*, 276, pp.26-33.
203. Wang, X., Wu, G., Yuan, C., Zhu, Q., Li, C., Sun, S. and Hu, S., **2018**. Molecular dynamics simulations of aggregation behavior of sodium dodecyl sulfate on SiO<sub>2</sub> and CaCO<sub>3</sub> surfaces. *Surface and Interface Analysis*, 50(3), pp.284-289.
204. Wu, Y., Shuler, P., Blanco, M., Tang, Y. and Goddard, W.A., **2006**. A Study of Wetting Behavior and Surfactant EOR in Carbonates With Model Components. Paper SPE 99612 presented at the SPE. In *DOE Symposium on Improved Oil Recovery, Tulsa*.
205. Xiao, J.X., Zhang, Y., Wang, C., Zhang, J., Wang, C.M., Bao, Y.X. and Zhao, Z.G., **2005**. Adsorption of cationic–anionic surfactant mixtures on activated carbon. *Carbon*, 43(5), pp.1032-1038.
206. Xie, X., Liu, Y., Sharma, M. and Weiss, W.W., **2009**. Wettability alteration to increase deliverability of gas production wells. *Journal of Natural Gas Science and Engineering*, 1(1-2), pp.39-45.
207. Xu, Z., Yang, X. and Yang, Z., **2008**. On the mechanism of surfactant adsorption on solid surfaces: Free-energy investigations. *The Journal of Physical Chemistry B*, 112(44), pp.13802-13811.

208. Yan, H. and Yuan, S., **2016**. Molecular dynamics simulation of the oil detachment process within silica nanopores. *The Journal of Physical Chemistry C*, 120(5), pp.2667-2674.
209. Yang, C. and Sun, H., **2014**. Surface–bulk partition of surfactants predicted by molecular dynamics simulations. *The Journal of Physical Chemistry B*, 118(36), pp.10695-10703.
210. Yin, D.Y. and Zhang, X.R., **2013**. Evaluation and research on performance of a blend surfactant system of alkyl polyglycoside in carbonate reservoir. *Journal of Petroleum Science and Engineering*, 111, pp.153-158.
211. Yousef, A.A., Al-Saleh, S.H., Al-Kaabi, A. and Al-Jawfi, M.S., **2011**. Laboratory investigation of the impact of injection-water salinity and ionic content on oil recovery from carbonate reservoirs. *SPE Reservoir Evaluation & Engineering*, 14(05), pp.578-593.
212. Yousef, A.A., Al-Saleh, S. and Al-Jawfi, M.S., **2012**, January. Improved/enhanced oil recovery from carbonate reservoirs by tuning injection water salinity and ionic content. In *SPE Improved Oil Recovery Symposium*. Society of Petroleum Engineers.
213. Yuan, S., Wang, S., Wang, X., Guo, M., Wang, Y. and Wang, D., **2016**. Molecular dynamics simulation of oil detachment from calcite surface in aqueous surfactant solution. *Computational and Theoretical Chemistry*, 1092, pp.82-89.
214. Zaeri, M.R., Hashemi, R., Shahverdi, H. and Sadeghi, M., **2018**. Enhanced oil recovery from carbonate reservoirs by spontaneous imbibition of low salinity water. *Petroleum Science*, 15(3), pp.564-576.
215. Zepa, L.E., Queipo, N.V., Pintos, S. and Salager, J.L., **2005**. An optimization methodology of alkaline–surfactant–polymer flooding processes using field scale numerical simulation and multiple surrogates. *Journal of Petroleum Science and Engineering*, 47(3-4), pp.197-208.
216. Zhang, J., Nguyen, Q. P., Flaaten, A., & Pope, G. A. Mechanisms of enhanced natural imbibition with novel chemicals. *SPE reservoir evaluation & engineering*, **2009**, 12(06), 912-920.
217. Zhang, L., Zhang, R. and Somasundaran, P., **2006**. Adsorption of mixtures of nonionic sugar-based surfactants with other surfactants at solid/liquid interfaces: II. Adsorption of n-dodecyl- $\beta$ -d-maltoside with a cationic surfactant and a nonionic ethoxylated surfactant on solids. *Journal of colloid and interface science*, 302(1), pp.25-31.
218. Zhang, P., & Austad, T. Wettability and oil recovery from carbonates: Effects of temperature and potential determining ions. *Colloids and Surfaces A: Physicochemical and Engineering Aspects*, **2006**, 279(1-3), 179-187.
219. Zhang, P., Tweheyo, M. T., & Austad, T. Wettability alteration and improved oil recovery by spontaneous imbibition of seawater into chalk: Impact of the potential

- determining ions  $\text{Ca}^{2+}$ ,  $\text{Mg}^{2+}$ , and  $\text{SO}_4^{2-}$ . *Colloids and Surfaces A: Physicochemical and Engineering Aspects*, **2007**, 301(1-3), 199-208.
220. Zhang, R. and Somasundaran, P., **2006**. Advances in adsorption of surfactants and their mixtures at solid/solution interfaces. *Advances in colloid and interface science*, *123*, pp.213-229.
221. Zhang, R., Qin, N., Peng, L., Tang, K., & Ye, Z. Wettability alteration by trimeric cationic surfactant at water-wet/oil-wet mica mineral surfaces. *Applied Surface Science*, **2012**, 258(20), 7943-7949.
222. Zhang, R. and Somasundaran, P., **2005**. Aggregate formation of binary nonionic surfactant mixtures on hydrophilic surfaces. *Langmuir*, *21*(11), pp.4868-4873.
223. Zhang, X., Morrow, N.R. and Ma, S., **1996**. Experimental verification of a modified scaling group for spontaneous imbibition. *SPE Reservoir Engineering*, *11*(04), pp.280-285.
224. Zhang, X., Morrow, N.R. and Ma, S., **1996**. Experimental verification of a modified scaling group for spontaneous imbibition. *SPE Reservoir Engineering*, *11*(04), pp.280-285.
225. Zhmud, B.V., Tiberg, F. and Hallstenson, K., **2000**. Dynamics of capillary rise. *Journal of colloid and interface science*, *228*(2), pp.263-269.
226. Zhou, X., Morrow, N.R. and Ma, S., **2000**. Interrelationship of wettability, initial water saturation, aging time, and oil recovery by spontaneous imbibition and waterflooding. *Spe Journal*, *5*(02), pp.199-207.

## Vita

Soumik Das grew up in India in his hometown of Andal, West Bengal. He finished his schooling in 2009 from DAV Model School, Durgapur, following which he joined Indian Institute of Technology, Kharagpur for his undergraduate studies in Chemical Engineering. During his undergraduate studies, he went to University of Alberta in Canada for summer research internship. Upon graduating in 2013, he worked in Oracle until 2014 as an Associate Applications Developer. He joined the PhD program in Chemical Engineering at the University of Texas in Austin in 2014.

Permanent email: [soumikdas123@gmail.com](mailto:soumikdas123@gmail.com)

This dissertation was typed by the author